



# **Genomics to Elucidate the Molecular Basis of Calcific Aortic Valve Disease**

**Thèse**

**Sandra Milena Guauque**

**Doctorat en biologie cellulaire et moléculaire**

Philosophiae doctor (Ph.D.)

Québec, Canada

© Sandra Milena Guauque, 2015



## Résumé

Le rétrécissement valvulaire aortique (RVA) est causé par une calcification et une fibrose progressive de la valve aortique. Le risque de développer la maladie augmente avec l'âge. À cause de l'augmentation de l'espérance de vie, le RVA est devenu un problème de santé publique. Le RVA est fatal en absence de traitement médical. Actuellement, la chirurgie est le seul traitement pour le stade sévère de la maladie, mais près de 50% des individus avec RVA n'y sont pas éligibles, principalement due à la présence de comorbidités. Plusieurs processus biologiques ont été associés à la maladie, mais les voies moléculaires spécifiques et les gènes impliqués dans le développement et la progression du RVA ne sont pas connus. Il est donc urgent de découvrir les gènes de susceptibilité pour le RVA afin d'identifier les personnes à risque ainsi que les biomarqueurs et les cibles thérapeutiques pouvant mener au développement de médicaments pour inverser ou limiter la progression de la maladie. L'objectif de cette thèse de doctorat était d'identifier la base moléculaire du RVA.

Des approches modernes en génomique, incluant l'étude de gènes candidats et le criblage génomique par association (GWAS), ont été réalisées à l'aide de collections d'ADN provenant d'un grand nombre de patients bien caractérisés pour le RVA. Des études complémentaires en transcriptomique ont comparé le profil d'expression global des gènes entre des valves calcifiées et non-calcifiées à l'aide de biopuces à ADN et de séquençage de l'ARN. Une première étude a identifié des variations dans le gène *NOTCH1* et suggère pour la première fois la présence d'un polymorphisme commun dans ce gène conférant une susceptibilité au RVA. La deuxième étude a combiné par méta-analyse deux GWAS de patients provenant de la ville de Québec et Paris (France) aux données transcriptomiques. Cette étude de génomique intégrative a confirmé le rôle de *RUNX2* dans le RVA et a permis l'identification d'un nouveau gène de susceptibilité, *CACNA1C*. Les troisième et quatrième études sur l'expression des gènes ont permis de mieux comprendre les bases moléculaires de la calcification des valves aortiques bicuspidées et ainsi d'identifier de nouvelles cibles thérapeutiques pour le RVA. Les données générées par ce projet sont la base de futures découvertes importantes qui permettront d'améliorer les options de traitement et la qualité de vie des patients atteints du RVA.



## Abstract

Calcific aortic valve disease (CAVD) is a common disease that causes the narrowing of the aortic valve due to fibrosis and calcification of the valve leaflets. The risk of CAVD increases with age. Due to the increase in life expectancy, CAVD is becoming a major public health problem. CAVD is fatal in the absence of medical treatment. Currently, surgery is the only treatment for severe stages of the disease, but nearly 50% of individual with CAVD are not eligible for surgery; mainly because of the presence of comorbidities. Several biological processes have been associated with the disease but the specific cell signaling pathways and genes implicated in CAVD development and progression are yet to be discovered. Thus, it is urgent to discover the susceptibility genes for CAVD, which will help identify individuals at risk as well as biomarkers and therapeutic targets for developing medication to reverse or limit disease progression. The objective of this thesis was to identify the molecular basis of CAVD.

Modern genomic approaches including candidate gene and genome-wide association studies (GWAS) were performed with large DNA collections of patients well-characterized for CAVD. Whole-genome gene expression studies were also performed to compare calcified bicuspid and tricuspid valves with normal aortic valves using microarrays and RNA-Sequencing. A GWAS meta-analysis was performed using two cohorts of patients with CAVD from Quebec City and Paris. The integration of different whole-genome approaches revealed a new gene associated with CAVD called *CACNA1C*. This work also confirmed the potential role of *NOTCH1* and *RUNX2* in CAVD. In addition, this work identified new genes differentially expressed in calcified compared to normal aortic valves that are implicated in biological processes involved in the disease. These new developments are important to better understand the pathophysiological processes implicated in aortic valve calcification. Several genes differentially expressed in calcified compared to normal valves are targets for existing and emerging drugs. In general, this work has increased the knowledge about the etiology of CAVD in patients with bicuspid and tricuspid aortic valves and has identified new susceptibility genes for the development of this disease. The data generated by this project are the base of future important discoveries that will improve treatment options and the quality of life of patients with CAVD.



# Table of contents

<b>Résumé</b> .....	<b>III</b>
<b>Abstract</b> .....	<b>V</b>
<b>Table of contents</b> .....	<b>VII</b>
<b>Table list</b> .....	<b>XI</b>
<b>Figure list</b> .....	<b>XIII</b>
<b>Abbreviations and acronyms</b> .....	<b>XIX</b>
<b>Acknowledgments</b> .....	<b>XXIII</b>
<b>Avant-propos</b> .....	<b>XXVII</b>
<b>Introduction</b> .....	<b>1</b>
<b>Chapter 1. Genetics and genomics: concepts</b> .....	<b>3</b>
1.1 Characteristics of the human genome .....	3
1.1.1 Flow of genetics information .....	3
1.1.2 Protein-coding and non-coding RNA .....	4
1.1.3 Single nucleotide polymorphisms.....	5
1.1.4 Consortia studying human genome variation and biology .....	9
1.2 Approach to genetic disease .....	11
1.2.1 Linkage studies .....	12
1.2.2 Association studies .....	13
1.2.3 Prioritization of GWAS results.....	22
1.3 Whole-genome gene expression .....	22
1.3.1 Microarrays .....	23
1.3.2 RNA Sequencing .....	25
1.4 Expression quantitative trait loci (eQTL) .....	27
<b>Chapter 2. Cardiac function and heart valves</b> .....	<b>29</b>
2.1 Cardiac function and heart structure .....	29
2.2 The cardiac cycle .....	30
2.3 The heart valves .....	31
2.3.1 The atrioventricular valves .....	32
2.3.2 The semilunar valves .....	33
2.4 The aortic valve macro- and microstructure .....	34

2.4.1	The aortic valve leaflets .....	35
2.5	Embriogenesis of the aortic valve .....	38
2.6	Aortic valve diseases .....	40
2.6.1	Causes of aortic valve disease .....	42
2.6.2	Congenital aortic valve disease .....	44
<b>Chapter 3.</b>	<b>Calcific aortic valve disease .....</b>	<b>51</b>
3.1	Epidemiology .....	51
3.2	Symptoms and complications.....	53
3.3	Diagnosis.....	53
3.4	Biomarkers .....	57
3.5	Natural history.....	60
3.6	Risk factors.....	61
3.6.1	Bicuspid valve calcification .....	62
3.7	Treatment .....	62
3.7.1	Aortic valve replacement surgery .....	63
3.7.2	Transcatheter aortic valve replacement.....	65
3.8	Medical treatment.....	67
3.8.1	Statins .....	68
3.8.2	Peroxisome proliferator-activated receptor $\gamma$ (PPAR- $\gamma$ ) .....	71
3.8.3	Lipoprotein(a) / oxidized phospholipids .....	71
3.8.4	Angiotensin system blocking .....	72
3.8.5	Bisphosphonates.....	73
3.8.6	Anti-RANKL monoclonal antibody.....	73
3.8.7	Vitamin K.....	74
<b>Chapter 4.</b>	<b>Genetics and molecular biology of CAVD .....</b>	<b>75</b>
4.1	Proposed molecular mechanisms of aortic valve calcification .....	75
4.1.1	miRNA and lncRNAs in AS .....	82
4.2	Animal models of CAVD.....	82
4.2.1	Mouse models .....	83
4.2.2	Rabbit models.....	86
4.2.3	Porcine models .....	87
4.3	Gene association studies on CAVD .....	87
4.4	Whole-genome approaches to study CAVD .....	95



4.4.1	GWAS.....	95
4.4.2	mRNA and miRNA whole-genome profiling.....	96
4.4.3	Proteomics .....	99
<b>Chapter 5.</b>	<b>Hypothesis and objectives .....</b>	<b>103</b>
5.1	Objectives .....	103
5.1.1	General objective .....	103
5.1.2	Specific objectives .....	103
5.2	Hypothesis .....	103
5.2.1	General hypothesis.....	103
5.2.2	Specific hypothesis .....	104
<b>Chapter 6.</b>	<b>Article 1: <i>NOTCH1</i> genetic variants in patients with tricuspid calcific aortic valve stenosis .....</b>	<b>105</b>
	Résumé.....	106
	Abstract.....	107
	Introduction.....	108
	Materials and methods .....	109
	Results.....	114
	Discussion.....	118
	Conflict of interest .....	121
	Acknowledgements.....	122
	References.....	123
	Tables and figures .....	126
<b>Chapter 7.</b>	<b>Article 2: Calcium signaling pathway genes <i>RUNX2</i> and <i>CACNA1C</i> are associated with calcific aortic valve disease.....</b>	<b>131</b>
	Résumé.....	132
	Abstract.....	133
	Author Summary.....	134
	Introduction.....	135
	Materials and methods .....	136
	Results.....	142
	Discussion.....	151
	Acknowledgments .....	154
	Funding Sources .....	155

Disclosures .....	156
References .....	157
S1 Supporting Information.....	162
<b>Chapter 8. Article 3: Whole-genome expression profile of calcified bicuspid and tricuspid aortic valves from patients with severe aortic stenosis.....</b>	<b>217</b>
Résumé .....	218
Abstract .....	219
Introduction .....	220
Methods.....	222
Results .....	225
Discussion .....	228
Acknowledgments.....	231
References .....	232
Tables and figures .....	237
Supplementary material.....	242
<b>Chapter 9. Article 4: RNA expression profile of calcified bicuspid, tricuspid and normal human aortic valves by RNA sequencing .....</b>	<b>257</b>
Résumé .....	258
Abstract .....	259
Introduction .....	260
Methods.....	262
Results .....	266
Discussion .....	270
References .....	273
Tables and figures .....	277
Supplemental information.....	289
<b>Chapter 10. Discussion, perspectives, and conclusion.....</b>	<b>315</b>
10.1 Discussion .....	315
10.2 Perspectives.....	325
10.3 Conclusion.....	328
<b>References .....</b>	<b>329</b>

# Table list

## Chapter 1

Table 1-1. Summary statistics of the human genome. ....	9
---	---

## Chapter 2

Table 2-1. Different types of VICs .....	38
--	----

Table 2-2. Causes of aortic valve stenosis. ....	43
--	----

## Chapter 3

Table 3-1. Classification of CAVD in adults .....	53
---	----

Table 3-2. Current biomarkers for CAVD .....	58
--	----

Table 3-3. Clinical factors associated with CAVD. ....	61
--	----

Table 3-4. Comparison of calcific aortic valve disease and atherosclerosis.....	68
---	----

Table 3-5. Large clinical trials of lipid lowering therapy in CAVD patients. ....	70
---	----

## Chapter 4

Table 4-1. Genes associated with aortic valve stenosis and CAVD. ....	93
---	----

## Chapter 6

Table 1. Clinical characteristics of case subjects (n = 457). ....	126
--	-----

Table 2. SNPs selected for genotyping <i>NOTCH1</i> ± 10 kilo bases. ....	127
---	-----

Table 3. Characteristics of common SNPs tested for association. ....	129
--	-----

## Chapter 8

<b>Table 1.</b> Clinical characteristics of the patients according to the three groups of aortic valves.....	237
<b>Table 2.</b> Number of genes differentially up- and down-regulated in each pairwise comparison. ....	239
<b>Table 3.</b> Genes differentially expressed in bicuspid compared to calcific tricuspid valves (Fold change $\geq 2$ ). ....	240

## Chapter 9

<b>Table 1.</b> Clinical characteristics of patients according to the three groups of valve. ....	277
<b>Table 2.</b> The number of differentially expressed genes in common between cuffdiff, DESeq, edgeR, and SAMSeq.....	279
<b>Table 3.</b> Top up- and down-regulated genes in the three pairwise comparisons.....	280
<b>Table 4.</b> Top 10 pathways enriched for differentially expressed genes in BAV compared to TAVn.....	285
<b>Table 5.</b> Top 10 pathways enriched for differentially expressed genes in TAVc compared to TAVn.....	287

# Figure list

## Chapter 1

<b>Figure 1-1.</b> Double helix structure of the DNA. ....	3
<b>Figure 1-2.</b> Contribution of coding vs. non-coding RNAs in the human genome. ....	5
<b>Figure 1-3.</b> Example of a SNP. ....	6
<b>Figure 1-4.</b> Diagram of a SNP in three individuals. ....	7
<b>Figure 1-5.</b> Classification of SNPs according to functional categories. ....	8
<b>Figure 1-6.</b> Approach to genetic disease. ....	12
<b>Figure 1-7.</b> Comparison of linkage and association studies ....	13
<b>Figure 1-8.</b> Indirect association of a genotyped SNP. ....	16
<b>Figure 1-9.</b> General steps in a GWAS. ....	17
<b>Figure 1-10.</b> Typical imputation scenario. ....	20
<b>Figure 1-11.</b> Steps involved in microarrays analysis. ....	24
<b>Figure 1-12.</b> Overview of RNA-Seq analysis. ....	26
<b>Figure 1-13.</b> eQTL mapping. ....	28

## Chapter 2

<b>Figure 2-1.</b> Gross anatomy of a normal heart. ....	30
<b>Figure 2-2.</b> The interior of the normal heart and direction of cardiac blood flow. ....	31
<b>Figure 2-3.</b> Structure of the atrioventricular valves. ....	32

<b>Figure 2-4.</b> Human pulmonary valve. ....	33
<b>Figure 2-5.</b> Aortic root components. ....	34
<b>Figure 2-6.</b> Aortic valve leaflet anatomy.....	35
<b>Figure 2-7.</b> Aortic valve layers and valvular cells.....	36
<b>Figure 2-8.</b> Overview of heart and valve development. ....	39
<b>Figure 2-9.</b> Semilunar valve maturation. ....	40
<b>Figure 2-10.</b> Prevalence of aortic stenosis according to age. ....	42
<b>Figure 2-11.</b> Representation of the developmental phenotypes of the aortic valve. ....	44
<b>Figure 2-12.</b> Phenotypes of aortic valves. ....	45
<b>Figure 2-13.</b> Valve morphology among patients undergoing aortic valve replacement. ....	46
 <b>Chapter 3</b>	
<b>Figure 3-1.</b> Tricuspid aortic valves.....	51
<b>Figure 3-2.</b> Average incidence rate of aortic valve calcium.....	52
<b>Figure 3-3.</b> Transesophageal echocardiograms of aortic valves. ....	54
<b>Figure 3-4.</b> Schematic diagram of the continuity equation. ....	56
<b>Figure 3-5.</b> The natural history of aortic stenosis.....	61
<b>Figure 3-6.</b> Bicuspid aortic valve with and without calcification. ....	62
<b>Figure 3-7.</b> Aortic valve replacement.....	64
<b>Figure 3-8.</b> Types of heart valve prosthesis for aortic valve replacement surgery. ....	65
<b>Figure 3-9.</b> TAVR procedure. ....	66

<b>Figure 3-10.</b> Similarities between aortic stenosis and other medical conditions and potential therapeutic strategies.....	67
---	----

#### **Chapter 4**

<b>Figure 4-1.</b> Molecular, cellular, and biomechanical mechanisms involved in CAVD. ....	76
---	----

<b>Figure 4-2.</b> Histology of early and late lesions of CAVD. ....	77
--	----

<b>Figure 4-3.</b> Potential mechanisms of aortic valve calcification by <i>NOTCH1</i> .....	80
--	----

#### **Chapter 6**

<b>Figure 1.</b> Triangular plot showing the genetic background of cases and controls.....	112
--	-----

<b>Figure 2.</b> LD-plot showing the $r^2$ values for the common <i>NOTCH1</i> SNPs in the case/control population. ....	114
--	-----

<b>Figure 3.</b> Genetic association of common SNPs in the <i>NOTCH1</i> gene with AS.....	115
--	-----

<b>Figure 4.</b> Disease severity assessed by aortic valve area, mean transvalvular gradient and age at surgery. ....	116
---	-----

<b>Figure 5.</b> Sequence chromatogram of the single heterozygote subject carrying the R1107X variant. ....	117
---	-----

#### **Chapter 7**

<b>Figure 1.</b> Flow chart showing the steps of the GWAS meta-analysis, pathway analysis, gene expression study of aortic valves, and valve eQTL mapping study.....	136
--	-----

<b>Figure 2.</b> Manhattan plot showing the results of the GWAS meta-analysis. ....	142
---	-----

<b>Figure 3.</b> Boxplots of GWAS <i>P</i> values for significant gene-sets. ....	143
---	-----

<b>Figure 4.</b> Venn diagrams showing the number of genes differentially expressed in aortic valves with and without AS using three RNA-Seq analysis tools. ....	144
---	-----

**Figure 5.** Integration of the GWAS and RNA-Seq results with known AS-related biological processes..... 145

**Figure 6.** Alterations of the calcium signaling pathway in AS. .... 146

**Figure 7.** eQTL-SNPs influencing the mRNA expression of *RUNX2* in aortic valves..... 147

**Figure 8.** eQTL-SNPs influencing the mRNA expression of *RUNX2* in aortic valves..... 148

**Figure 9.** *CACNA1C* a new susceptibility gene of AS. .... 150

## Chapter 8

**Figure 1.** Principal components plot of the 36 aortic valves. .... 225

**Figure 2.** Heat maps of the top genes differentially up- and down-regulated for the three pairwise comparisons. .... 226

## Chapter 9

**Figure 1.** Summary of the RNA sequencing pipeline. .... 265

**Figure 2.** Venn diagrams showing the number of genes differentially expressed in common among cuffdiff, DESeq, edgeR, and SAMSeq. .... 266

**Figure 3.** Volcano plots of the three pairwise comparisons based on the results of cuffdiff. .... 267

**Figure 4.** Heat maps presenting the gene expression of the top 10 up- and down-regulated annotated genes for each pairwise comparison. .... 267

## Chapter 10

**Figure 10-1.** The role of genome-based information across the continuum of health to disease. .... 315

**Figure 10-2.** Interaction between Ang II and the L-type calcium channels. .... 318



<b>Figure 10-3.</b> Ang II, <i>RUNX2</i> , and <i>NOTCH1</i> mediate aortic valve calcification. ....	319
<b>Figure 10-4.</b> Integration of the GWAS and RNA-Seq results with known CAVD-related biological processes. ....	320
<b>Figure 10-5.</b> Venn diagrams showing the number of genes up- and down-regulated in common between RNA-Seq and microarrays results. ....	323
<b>Figure 10-6.</b> Venn diagrams showing the number of genes up- and down-regulated in common between RNA-Seq and microarrays results from Bossé <i>et al.</i> , 2009.....	324
<b>Figure 10-7.</b> Gene discovery to clinical application. ....	327



## Abbreviations and acronyms

A	Adenine
ACE	Angiotensin-Converting Enzyme
AGES-RS	Age, Gene/Environment Susceptibility–Reykjavik Study
ALP	Alkaline phosphatase
ARB	Angiotensin receptor blocker
ARIC	Atherosclerosis Risk in Communities Study
ASTRONOMER	Aortic Stenosis Progression Observation: Measuring the Effects of Rosuvastatin
BNP	B-type natriuretic peptide
Bp	Basepair
C	Cytosine
CARDIA	Coronary Artery Risk Development in Young Adults
CAVD	Calcific aortic valve stenosis
CCHS	Copenhagen City Heart Study
CETP	Cholesterol ester transfer protein
CHARGE	Cohorts for Heart and Aging Research in Genome Epidemiology
CHS	Cardiovascular Health Study
dbGaP	Database of genotypes and phenotypes
dbSNP	Single nucleotide polymorphism database
DNA	Deoxyribonucleic acid
ECAC	Epidemiology of Coronary Artery Calcification
ECM	Extracellular matrix
EGFR	Epidermal growth factor receptor
eQTL	Expression quantitative trait loci
FHS	Framingham Heart Study
G	Guanine
GEO	Gene Expression Omnibus
GWAS	Genome-wide association study
HDL	High-density lipoprotein
HMG-CoA	3-hydroxy-3-methyl-glutaryl-CoA
HNR	Heinz Nixdorf Recall Studies
LD	Linkage disequilibrium
LDL	Low-density lipoprotein
lncRNAs	Long noncoding RNAs
Lp-PLA2	Lipoprotein-associated phospholipase A2
Lrp5	Low-density lipoprotein receptor-related protein 5
LVOT	LV outflow tract
MAF	Minor allele frequency
Mb	Megabasepair
MDCS	Malmö Diet and Cancer Study
MESA	Multi-Ethnic Study of Atherosclerosis
microRNA	miRNA
NCBI	National Center for Biotechnology Information
NICD	NOTCH1 intracellular domain

NIH	National Institutes of Health
OR	Odds ratio
PARTNER	Placement of Aortic Transcatheter Valves
Pi	Inorganic phosphate
PPi	Inorganic pyrophosphate
RAAVE	Rosuvastatin Affecting Aortic Valve Endothelium
RNA	Ribonucleic acid
RNA-Seq	RNA sequencing
rRNAs	Ribosomal RNAs
SALTIRE	Scottish Aortic Stenosis and Lipid Lowering Trial, Impact on Regression
SAM	Significance Analysis of Microarrays
SEAS	Simvastatin and Ezetimibe in Aortic Stenosis
SNP	Single nucleotide polymorphism
T	Thymine
TAVR	Transcatheter aortic valve replacement
tRNAs	Transfer RNAs
UTR	Untranslated region
VICs	Valve interstitial cells
$\alpha$ SMA	$\alpha$ -smooth muscle actin

*Para Carlitos, Beto y mi Familia, quienes  
inspiran cada paso que doy.*



## **Acknowledgments**

I want to acknowledge the people that contributed to my Ph.D. project with their knowledge, support, and friendship. I also want to thank all people that made me feel at home in Quebec

First, I want to thank the patients that participated in the studies and the collaborators of my project Drs. David Messika-Zeitoun, Arnaud Droit, Marie-Pierre Dubé, Jean-Claude Tardif, Jonathan G. Seidman, Catherine Boileau, and especially Simon C. Body for their important contribution in resources and intellectual guidance. I also want to thank Dr. Benoit J. Arsenault for his kindness and for sharing with me his experience in graduate studies since I arrived as a Master student at the CRIUCPQ. I also thank Joshua Gorham and Dr. Michael Parfenov for their assistance with the RNA-Seq experiment. I want to thank Fanny Therrien, Caroline Nadeau, and Christine Racine from the IUCPQ tissue bank and Stéphanie Dionne who managed the IUCPQ cardiac surgery database.

My most important acknowledgement is for Dr. Yohan Bossé for giving me the opportunity of being a member of his research group, for all his support and advices during the past six years. His dedication to research and his passion for genetics inspires me to be a better scientist. I am taking with me the tools for starting my own research path after seeing the group growing up in this short period of time.

My special acknowledgement to Drs. Patrick Mathieu and Philippe Pibarot for contributing intellectually to my project and improve the quality of my articles and abstracts with their advices. I admire their passion for research and their constant desire to acquire more knowledge. I also thank Dr. Pibarot for his career advices, sense of humour, and a kind “hola” when he sees me.

I want to thank the current and past members of Dr. Bossé’s team for all the good moments at the wet and dry laboratory. I thank Laura Sbarra and Cyndi Henry for their sympathy and unforgettable cakes, Josée Vézina, Jérôme Lane, Natasha Dargis and Jean-Christophe

Bérubé for their tenderness and the laughs we shared, and Joël Tremblay-Marchand for his kindness and support with the analysis of RNA-Seq. I thank Maxime Lamontagne for using his time to make important contributions to my project and Justin Nguyen who introduced me to the use of Bioinformatics tools.

I also thank from the bottom of my heart Nathalie Gaudreault for her friendship, her personal and professional support, advices, reviews, laughs, she offers me during my graduate studies journey and the good Colombian coffee we shared. You are the best teacher that someone might want. I give a very special acknowledgement to Emilie Lavoie-Charland for her friendship and her support in the good and bad times. You are the sweetest and more altruist person I met in Canada.

I want to thank all the members of the GRV especially Haifa Mahjoub and Wahiba Dhahri for their friendship and kindness. I thank Haifa, Marie-Annick Clavel and Romain Capoulade for introducing me to the world of echocardiography.

I want to thank the team of Dr. Mathieu, Rihab Bouchareb, Ahmed Fayez Hadji, Maihemuti Abulajiang, Elnur Elyar Shayhidin, Andrée Pépin, Audrey Audet, and specially Nancy Coté, and Valérie Ducharme for their tenderness.

I want to acknowledge very especially my friend Dominique Fournier. I will hold in my heart all the memories lived with you. Thank you for training me at the wet laboratory but especially for the good times at dinners and hockey games. For making me feel at home in Quebec. I also thank Diala El Husseini for her friendship, company, and advices.

I want to thank my friends who lived in Quebec that were a support during my Ph.D. journey, Julieta Caballero, Carly and her sons, Amélie Fauchon, Cristina Fürstenau, and Katherina Uribe and her family.



My special acknowledgement to my friends all around the world that supported me from far, Paola Cabal, Angela Fuentes-Pardo, Lina Gallego-Paez, Zuray Corredor, Ana Lucia Rivera, Laura Cifuentes, Dayana Salas, and Maria Fernanda Castillo.

I want to thank the Lopez and Acevedo families for making me feel like another family member. Thank you to Carlos Alberto Lopez and Maria Leonor Acevedo for their wise advices. Thank you to Maria del Mar Lopez and Olga Lopez for their career advices and support. Thank you to Maria Jimena Lopez for her kindness and support.

Finally but not least important, I thank my family for all their love and for believing in me. For making me feel everyday that they are always next to me. Thank you to Dagoberto Jr II, Angelita, Tia Transito, Mamá, Papá, Rafa, Jorge, and the Olarte Family. I want to thank my wonderful husband Carlos Andres Lopez for comforting me and making me see my strengths, this accomplishment is yours too.



## Avant-propos

The work presented in this doctoral thesis was performed at the “Institut universitaire de cardiologie et de pneumologie de Québec” (IUCPQ) research center under the supervision of Dr. Yohan Bossé. Several computations were made on the supercomputer Colosse from Laval University, managed by Calcul Québec and Compute Canada. The operation of this supercomputer is funded by the Canada Foundation for Innovation (CFI), NanoQuébec, RMGA and the Fonds de recherche du Québec - Nature et technologies (FRQ-NT).

For my work in research, I received two scholarships to support my Ph.D. studies: the doctoral research scholarship from the international research chair on cardiometabolic risk (effective from 01-09-2011 to 31-08-2012) and the doctoral research scholarship from the “IUCPQ” research center (effective from 05-01-2014 to 05-01-2015).

I am the first author of three articles in this thesis and the second author of a fourth article. The first article entitled “***NOTCH1* genetic variants in patients with tricuspid calcific aortic valve stenosis**” was published in the Journal of Heart Valve Disease in 2013. Guauque-Olarte (IUCPQ, Quebec, Canada) analyzed data and wrote the manuscript, Valerie Ducharme (IUCPQ, Quebec, Canada) analyzed sequencing data and wrote the manuscript, and Nathalie Gaudreault (IUCPQ, Quebec, Canada) performed DNA and RNA extractions. Dr. Philippe Pibarot (IUCPQ, Quebec, Canada) contributed with resources. Dr. Patrick Mathieu (IUCPQ, Quebec, Canada) conceived and designed the experiments, contributed to the interpretation of biological data, and provided resources. Dr. Yohan Bossé (IUCPQ, Quebec, Canada) conceived and designed the experiments, contributed with samples and resources, analyzed and interpreted the data, and wrote the manuscript. All authors contributed to the edition of the manuscript for intellectual content.

The second article entitled “**Calcium signaling pathway genes *RUNX2* and *CACNA1C* are associated with calcific aortic valve disease**” was submitted for publication in Circulation: Cardiovascular Genetics. The author contributions are as follows: Guauque-Olarte analyzed the data, participated in the biological interpretation of the data, and wrote

the manuscript. Dr. David Messika-Zeitoun (Bichat Hospital, Paris, France) contributed to sample collection and study design. Dr. Arnaud Droit (Centre de Recherche du CHU, Quebec, Canada) and Joël Tremblay-Marchand (IUCPQ, Quebec, Canada) provided support to analyze RNA-Sequencing data. Maxime Lamontagne (IUCPQ, Quebec, Canada) helped with quality controls and imputation of genome-wide association data. Emilie Lavoie-Charland (IUCPQ, Quebec, Canada) analyzed the eQTL data. Nathalie Gaudreault (IUCPQ, Quebec, Canada) performed DNA and RNA extractions. Benoit J. Arsenault (Montreal Heart Institute, Quebec, Canada) contributed to sample collection and data analysis. Marie-Pierre Dubé (Montreal Heart Institute, Quebec, Canada) provided resources and contributed to data analysis. Jean-Claude Tardif (Montreal Heart Institute, Quebec, Canada) provided resources. Drs. Simon C. Body and Jonathan G. Seidman (Harvard Medical School, Boston, USA) performed the RNA-Seq experiment. Catherine Boileau (INSERM U1148 and University Paris 7, Paris, France) provided resources. Drs. Patrick Mathieu and Philippe Pibarot (IUCPQ, Quebec, Canada) conceived and designed the experiments and provided resources. Dr. Patrick Mathieu also contributed to the interpretation of biological data. Dr. Yohan Bossé (IUCPQ, Quebec, Canada) conceived and designed the experiments, contributed with samples and resources, analyzed and interpreted the data, and wrote the manuscript. All authors contributed to the edition of the manuscript for intellectual content.

The third article “**Whole-genome expression profile of calcified bicuspid and tricuspid aortic valves from patients with severe aortic stenosis**” is in preparation for submission. Guauque-Olarte analyzed and interpreted data, and wrote the article. Fayez Hadji (IUCPQ, Quebec, Canada) and Nathalie Gaudreault (IUCPQ, Quebec, Canada) performed RNA extraction. Drs. Philippe Pibarot, Patrick Mathieu, and Yohan Bossé (IUCPQ, Quebec, Canada) conceived and designed the experiments, contributed samples, resources and interpretation of the data. Dr. Bossé also wrote the article. All authors contributed to the edition of the manuscript for intellectual content.

The fourth article entitled “**RNA expression profile of calcified bicuspid, tricuspid and normal human aortic valves by RNA sequencing**” is in preparation for submission.

Guauque-Olarte analyzed and interpreted data, and wrote the article. Dr. Arnaud Droit (Centre de Recherche du CHU, Quebec, Canada) and Joël Tremblay-Marchand (IUCPQ, Quebec, Canada) provided support to analyze RNA-Sequencing data. Nathalie Gaudreault (IUCPQ, Quebec, Canada) performed RNA extraction. Drs. Simon C. Body and Jonathan G. Seidman (Harvard Medical School, Boston, USA) performed the RNA-Seq experiment. Drs. Philippe Pibarot, Patrick Mathieu, and Yohan Bossé (IUCPQ, Quebec, Canada) conceived and designed the experiments, contributed samples, resources and interpretation of the data. Dr. Bossé also wrote the paper. All authors contributed to the edition of the manuscript for intellectual content.

I have contributed to three additional peer-reviewed articles during my Ph.D.:

- Evaluation of links between high-density lipoprotein genetics, functionality, and aortic valve stenosis risk in humans. Arsenault BJ, Dubé MP, Brodeur MR, de Oliveira Moraes AB, Lavoie V, Kernaléguen AE, **Guauque-Olarte S**, Mathieu P, Pibarot P, Messika-Zeitoun D, Bossé Y, Rhainds D, Rhéaume E, Tardif JC. *Arterioscler Thromb Vasc Biol.* 2014 Feb;34(2):457-62.
- ATP acts as a survival signal and prevents the mineralization of aortic valve. Côté N, El Husseini D, Pépin A, **Guauque-Olarte S**, Ducharme V, Bouchard-Cannon P, Audet A, Fournier D, Gaudreault N, Derbali H, McKee MD, Simard C, Després JP, Pibarot P, Bossé Y, Mathieu P. *J Mol Cell Cardiol.* 2012 May;52(5):1191-202.
- Replication of genetic association studies in aortic stenosis in adults. Gaudreault N, Ducharme V, Lamontagne M, **Guauque-Olarte S**, Mathieu P, Pibarot P, Bossé Y. *Am J Cardiol.* 2011 Nov 1;108(9):1305-10.



## Introduction

The aortic heart valve allows the flow of oxygenated blood from the left ventricle to the aorta, and from the aorta to the rest of the body. Calcific aortic valve disease (CAVD) is a fatal disease characterized by thickening, fibrosis, and calcification of the valve cusps causing stiffening, impaired motion, and the loss of valve functionality. CAVD is a disease mainly of the elderly population and affects 2% and 4% of people older than 65 and 85 years, respectively. The incidence of this disease rises with life expectancy and is a serious public health problem. CAVD prevalence is expected to double within the next 50 years<sup>1</sup>. Aortic valve replacement and transcatheter aortic valve replacement (TAVR) surgeries are the only treatments for symptomatic patients and no other medical treatment is available to stop or delay the progression of the disease. CAVD is a complex multifactorial disease with risk factors similar to those of atherosclerosis. Genetic factors, valve morphology, and shear stress also contribute to disease progression. In addition, for individuals with a bicuspid valve, having two leaflets instead of three, calcification is observed 10 to 20 years earlier than individuals with a tricuspid valve<sup>2</sup>.

In the present study, a candidate gene study on *NOTCH1* and a genome-wide association study (GWAS) were performed to identify susceptibility genes for CAVD. The whole-genome expression profiles of calcified bicuspid, tricuspid, and normal tricuspid valves were also compared by microarrays and RNA sequencing (RNA-Seq). The results presented in this research project have increased our understanding of CAVD and have led to the identification of new molecular targets to treat the disease.

This thesis is divided in ten chapters. In **Chapter 1**, the different methodologies used to achieve the objectives are explained, including GWAS, microarrays, and RNA-Seq. This chapter also includes definitions of key genetic terms to facilitate the comprehension of the results in next chapters. **Chapter 2** contains a short description of the heart structure and the normal functions of heart valves. **Chapter 3** describes the natural history of CAVD, the prevalence, diagnostic methods, and available treatments for the disease. **Chapter 4** is focused on CAVD, where the developmental stages, genetic and genomic studies on CAVD are described. **Chapter 5** describes the hypothesis and objectives of this thesis.

**Chapters 6 to 9** contain four scientific articles. A general discussion of the results, perspectives in the study of CAVD, and conclusions are presented in **Chapter 10**.



# Chapter 1. Genetics and genomics: concepts

## 1.1 Characteristics of the human genome

### 1.1.1 Flow of genetics information

DNA (deoxyribonucleic acid) is the heritable genetic material of a cell that provides instruction for cellular building, maintenance, and homeostasis regulation. The structure of a DNA strand forms a double helix in which two bases of a nucleotide (base + sugar + phosphate) are paired. Adenine (A) always pairs with a thymine (T) and cytosine (C) with a guanine (G) (Figure 1-1)<sup>3</sup>. The length of a DNA molecule is measured in base pairs (bp).

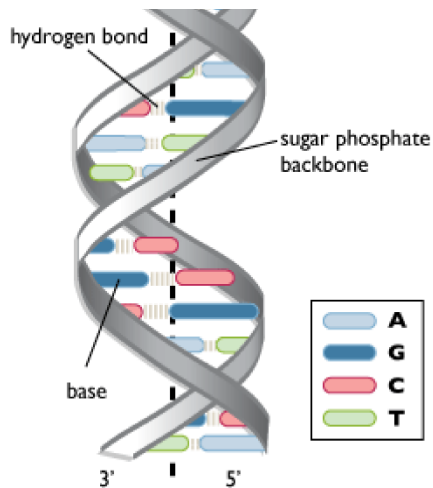


**Figure 1-1.** Double helix structure of the DNA. The DNA is built of repeated blocks or nucleotides. A nucleotide contains a nitrogenous base, a sugar (2-deoxyribose), and a phosphate. Complementary bases connect to one another by hydrogen bonds (<http://cyberbridge.mcb.harvard.edu/>).

The genome is the collection of the information contained in the DNA, and less than 3% of the genome codes for proteins<sup>4</sup>. During transcription, ribonucleic acid (RNA) is synthesized from DNA with the enzyme RNA polymerase. RNA composition is similar to DNA but RNA is single-stranded and contains uracil and 2-deoxyribose instead of thymine and deoxyribose, respectively. In eukaryotes there are three nuclear polymerase (I to III) enzymes to transcribe different RNAs<sup>5</sup>. Polymerase I transcribes ribosomal RNA (rRNA), Polymerase II transcribes all mRNAs and most regulatory non-coding RNAs, and Polymerase III synthesizes transfer RNAs (tRNAs) and 5S rRNA<sup>6</sup>. While DNA molecules

encode proteins, RNA molecules are translated into proteins. Before translation, mRNA is edited to eliminate introns (non coding regions of the mRNA), a 5' cap and a 3' tail of adenines (polyadenylinic acid tail) are added to protect it from premature degradation in the cytoplasm. Translation is mediated by tRNAs and an alphabet compound of 3 bases (codon), each codon coding for an amino acid or indicating the start or stop of the protein<sup>3</sup>. Proteins are the principal components of cell structure, signaling, and metabolism<sup>7</sup>. Some viruses can retro-transcribe RNA to DNA, using reverse transcriptase enzymes. These enzymes are very important in molecular biology for applications such as whole-genome expression microarrays and RNA sequencing<sup>8</sup>.

Transcriptional and post-transcriptional mechanisms modulate when and where (cellular type) the genetic information is expressed. Epigenetic mechanisms, such as DNA methylation, can act directly on the DNA strand or act through modifications in chromatin structure, changing the genomic structure of an individual<sup>8</sup>. This regulation of gene expression allows for the existence of different cellular types in an organism, even though every cell contains the same genetic material. Deregulation of this complex genetic structure through transcription, translation or gene expression can lead to diseases. Some modifications of the DNA sequence can also alter the same processes.

### **1.1.2 Protein-coding and non-coding RNA**

According to the most recent data of the Ensembl database v78.38 ([http://useast.ensembl.org/Homo\\_sapiens/](http://useast.ensembl.org/Homo_sapiens/)), the human genome, or collection of DNA in human cells, encodes 196,345 transcripts, including protein-coding and non-coding RNAs. A typical gene can express several RNA isoforms (up to 10-12) at the same time<sup>9</sup>, and 20,364 protein-coding genes are present in the human genome (this represents less than 3% of the genome). About 80% of the genome participates in at least one biochemical RNA- and/or chromatin-associated event and is considered to contain functional elements<sup>4</sup>. **Figure 1-2** summarizes the contribution of coding and non-coding DNA molecules in the human genome.

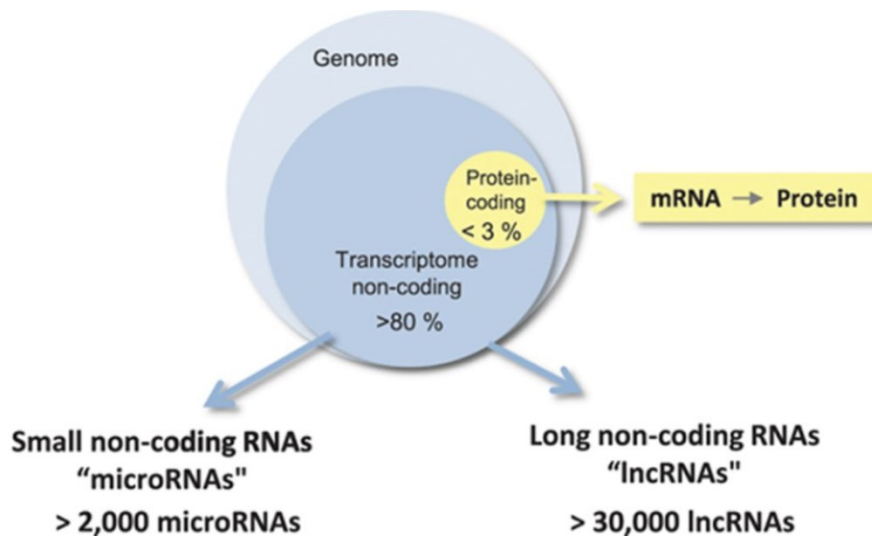


**Figure 1-2.** Contribution of coding vs. non-coding RNAs in the human genome. Less than 3% of the genome codes for proteins. Previously considered as junk DNA, nowadays it is known that the majority of non-coding DNA is transcribed and potentially functional. Figure taken from Uchida *et al*<sup>10</sup>, license number 3614881400449.

Non-coding RNAs are divided in two categories: small non-coding RNAs and long noncoding RNAs (lncRNAs, > 200 nucleotides). Small non-coding RNAs are part of the translational machinery [tRNAs and rRNAs], regulate other RNA molecules [small nucleolar and small nuclear RNAs], or regulate protein production [microRNAs (miRNAs)]<sup>9</sup>. Some known functions of lncRNAs are: enhancer activation, expression of a specific parental allele (imprinting), and scaffold of epigenetic and transcription factors<sup>9,10</sup>. The function of many non-coding RNAs is still unknown<sup>10</sup>.

### 1.1.3 Single nucleotide polymorphisms

The human genome has approximately 3 billion base pairs packaged in 23 chromosomes. From this total, 99.9% is identical between individuals even from different geographic populations<sup>8</sup>. 0.1% of DNA variations between individuals are responsible for individual phenotypic characteristics<sup>11</sup>. Many of these differences involve a single DNA nucleotide or single nucleotide polymorphism (SNP). Other differences are accounted by other types of variations including insertions, deletions, inversions, and repetitions.

A SNP is a nucleotide variation at one specific location on the genome, with a frequency higher than 1% in the population<sup>12</sup>. An example of a SNP is the presence of an A in one portion of the population and a G in the rest of the population for the same DNA location (**Figure 1-3**).

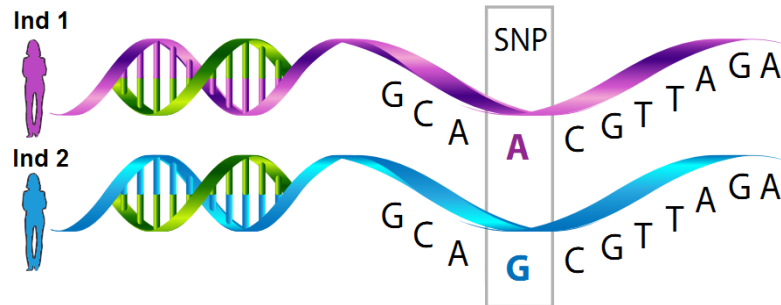


**Figure 1-3.** Example of a SNP. A SNP is a difference of one single nucleotide in a specific site of the DNA between two individuals. The alteration of the DNA sequence by the presence of a SNP can have repercussions on the phenotype. Figure derived from <http://biogeniq.ca/snp/>.

A human has 23 pairs of chromosome in each diploid cell and individual chromosomes in each pair are inherited from a different parent. In an individual, a SNP has two alleles, one in each homologous chromosome. The alleles can be identical or different between chromosomes. Individuals with two identical alleles are considered homozygous and individuals with different alleles in each chromosome are heterozygous<sup>12</sup>. In **Figure 1-3**, the alleles are A and G for this specific SNP. Individuals can be homozygous AA, heterozygous AG, or homozygous GG for that specific site (**Figure 1-4**). The possible genotypes for this SNP are thus AA, AG, and GG. A SNP can potentially have four alleles in a population because there are four nucleotides. The minor allele is the less frequent allele in the population under study. A SNP with a minor allele frequency (MAF) > 5% is considered to be common<sup>13</sup>. The genotype of SNPs can be measured using various sequencing technologies.

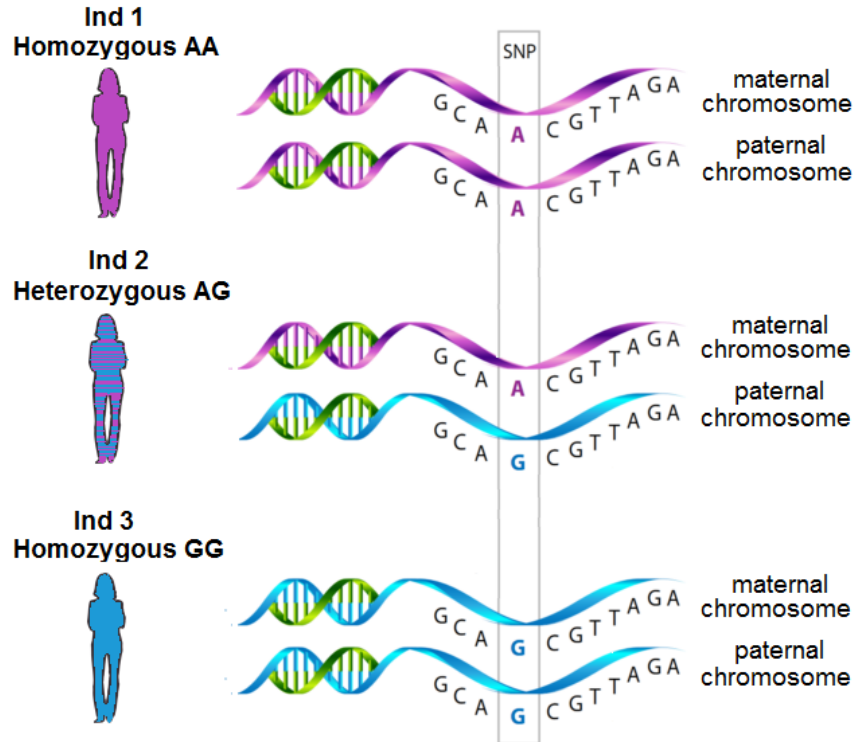


**Figure 1-4.** Diagram of a SNP in three individuals. An individual can be homozygous (top and bottom) or heterozygous (center) for a SNP. For simplicity only one strand of the DNA and the surrounding nucleotides of one SNP is presented. Figure derived from <http://biogeniq.ca/snp/>.

SNPs are the most common type of genetic variation occurring about 1 in every 100-300bp<sup>14</sup>. SNPs are generally clustered in certain chromosomal regions rather than randomly spaced, especially in the X chromosome. Greater susceptibility of local regions to mutation due to DNA packaging or errors during repair of DNA damage<sup>15</sup> could be the reason for this spacing. To better understand their functions, SNPs have been classified in several functional categories including non-synonymous, synonymous, splicing, 5'UTR (untranslated region), 3'UTR, intronic, and intergenic<sup>16</sup> (**Figure 1-5**).

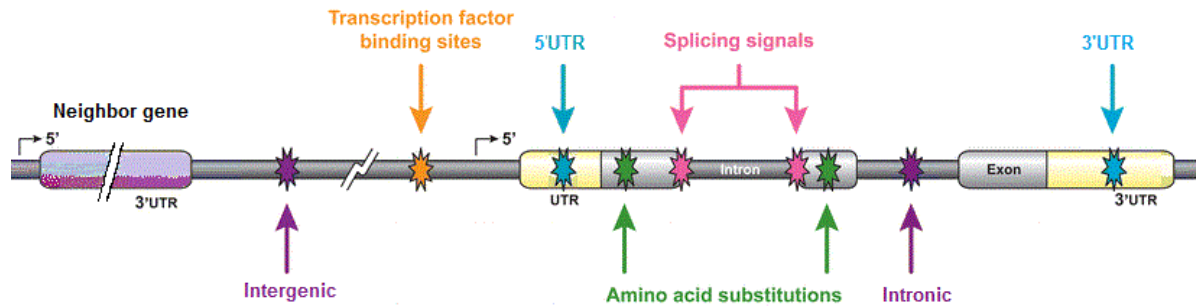


**Figure 1-5.** Classification of SNPs according to functional categories. The structure of a gene includes exons, introns, 5' and 3'UTRs and regulatory regions. The consequence of a SNP is related to its location in the genome. Figure derived from Lee *et al.*<sup>17</sup>, license number 3614890151334.

Synonymous SNPs do not alter the amino acid sequence of proteins and do not cause protein dysfunction. Non-synonymous mutations can cause a change of amino acids and their effects will depend on the amino acid chemical and physical properties in the protein. Other SNPs located in regulatory regions (e.g. promoter) or within the genes (e.g. 5'UTR, splicing sites) may affect RNA expression or protein function. Most SNPs are located outside coding regions (intergenic and intronic). Some intergenic and intronic SNPs can affect binding of transcription factors, regulatory RNA and proteins or alter chromatin structure. Other SNPs in this later group are useful as genetic markers of disease in linkage and association studies<sup>8,18</sup>.

Ke *et al.* in 2008 surveyed 8,876,160 SNPs from a public genetic database and found that 0.51% of them were non-synonymous, 0.46% were synonymous, 0.04% were in splicing sites, 0.2% were in 5'UTR, and 0.84% were in 3'UTR regions. Finally, 49.78% of the 8.9 million SNPs were located within introns and 46.83% in intergenic regions<sup>14</sup>. In 2012, 38 million SNPs in the genome were reported<sup>13</sup>. By 2014, 65.9 million SNPs and small variations were reported in the Ensembl database for annotation of genomes, variations, and regulatory data ([www.ensembl.org](http://www.ensembl.org)) and approximately 8.2 million variants have MAF > 0.05 (<http://www.ncbi.nlm.nih.gov/snp/>). **Table 1-1** summarizes some characteristics of the human genome.

**Table 1-1.** Summary statistics of the human genome.

Length of the human genome (bp)	3,381,944,086
Number of known protein-coding genes	20,364
Average gene density (number of genes/Mb)	6.0*
Number of non-coding RNA genes	24,490
Number of known SNPs and other small variants	65,897,584

Mb = megabasepair. \*Protein-coding genes only. Data from Ensembl database v78.38 ([http://useast.ensembl.org/Homo\\_sapiens/Info/Annotation#assembly](http://useast.ensembl.org/Homo_sapiens/Info/Annotation#assembly)).

#### 1.1.4 Consortia studying human genome variation and biology

After the completion of the human genome sequencing by the International Human Genome Sequencing Consortium ([www.genome.gov/11006939](http://www.genome.gov/11006939)) in 2003<sup>19</sup>, several other consortia have been created to analyze DNA variation and gene regulation. A goal of each consortium was to make the genome data publicly available. Several databases containing data of genetic variation and gene expression are also available. Some important projects and databases are listed below:

- **The International HapMap Consortium** created in 2003 aims to identify and understand the patterns of DNA variation by genotyping the DNA of 1,184 samples from eleven reference groups representative of larger populations with ancestry from Africa, Asia, and Europe including Yoruba in Ibadan, Nigeria; Japanese in Tokyo, Japan; Han Chinese in Beijing, China; and Utah residents with ancestry from northern and western Europe. The HapMap project identified genomic variants, their sequences and frequencies, and correlation between variations<sup>20,21</sup> (<http://hapmap.ncbi.nlm.nih.gov/>).
- **The 1000 Genomes Project Consortium** created in 2010 seeks to identify genome variation through DNA sequencing and dense SNP genotyping<sup>13</sup>. Up to 2014, the project has made public more than 79 million variants including SNPs, indels, and more. Data

from 2,535 individuals from 26 different populations worldwide were generated ([www.1000genomes.org](http://www.1000genomes.org)).

- Created in 2007, the **ENCODE** (Encyclopedia of DNA Elements) project had for objective to identify all functional elements (RNA transcripts, transcriptional regulator binding sites, and chromatin states) in the human genome in numerous cell types<sup>4</sup>. The data generated was published in 2012 ([www.genome.gov/10005107](http://www.genome.gov/10005107)).
- **National Institutes of Health (NIH) Roadmap Epigenomics Consortium** is generating the largest collection of human epigenome data (DNA methylation, histone modifications, chromatin accessibility, and small RNA transcripts) from stem cells and primary *ex vivo* tissues<sup>22</sup> ([www.roadmapepigenomics.org](http://www.roadmapepigenomics.org)).
- The NIH **Genotype-Tissue Expression (GTEx)** project, provides a publicly available catalog of tissue-specific gene expression profiles and expression quantitative trait loci (eQTL) which are regions of the genome harboring a genetic variant contributing to gene expression variation<sup>23</sup> ([www.gtexportal.org/home/](http://www.gtexportal.org/home/)).
- The **Single Nucleotide Polymorphism Database** (dbSNP) is a central repository of SNPs and other small variants in several populations and other organisms<sup>24</sup> ([www.ncbi.nlm.nih.gov/SNP/](http://www.ncbi.nlm.nih.gov/SNP/)).
- The **database of Genotypes and Phenotypes** (dbGaP) of the NIH compiles data on millions of SNPs in various human populations, as well as other organisms<sup>25</sup>. The database is a secure access repository of genetic information collected in studies such as GWAS, medical sequencing, molecular diagnostic assays, as well as association between genotype and non-clinical traits. Genotyping and sequencing data of cases and controls can be found at [www.ncbi.nlm.nih.gov/gap](http://www.ncbi.nlm.nih.gov/gap).



- The **Catalog of Published Genome-Wide Association Studies** is a collection of curated SNP-trait associations with  $P$  values  $< 1 \times 10^{-5}$  extracted from the literature<sup>26</sup>. Up to 2013, the catalog included 1,751 curated publications reporting on 11,912 SNPs. ([www.genome.gov/gwastudies](http://www.genome.gov/gwastudies)).
- The **Gene Expression Omnibus (GEO)** from the National Center for Biotechnology Information (NCBI) is a repository that archives and distributes published microarray, next-generation sequencing and other high-throughput functional genomic data<sup>27</sup> ([www.ncbi.nlm.nih.gov/geo](http://www.ncbi.nlm.nih.gov/geo)).

The work presented in this thesis took advantage of data from the 1000 genomes project and dbGaP. RNA sequencing and microarrays data from this project will be available in the GEO database. Genotyping data will be available in the dbGaP database.

## **1.2 Approach to genetic disease**

Some diseases, such as Huntington's disease<sup>28</sup> and cystic fibrosis<sup>29</sup>, show Mendelian segregation patterns which are caused by mutations in one gene (monogenic traits). In contrary, in complex diseases, such as cardiovascular disease, the disease risk is influenced by genetic and environmental factors and the genetic component involves several genes<sup>30</sup>. The most common strategies for identifying (mapping) variants and causal genes for simple and complex diseases are linkage and genetic association studies. Both types of studies can interrogate the entire genome or specific genes (candidate gene studies)<sup>31</sup>. A general approach to understand genetic disease is presented in **Figure 1-6**.

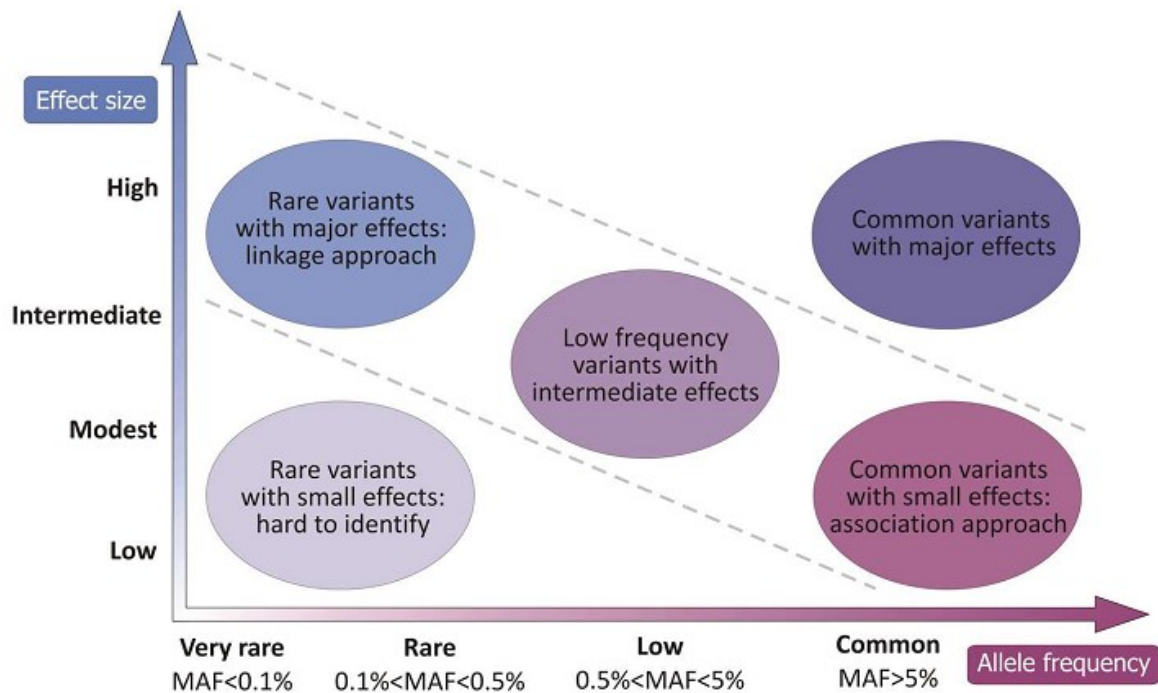


**Figure 1-6.** Approach to genetic disease. Linkage studies are useful to identify low-frequency alleles with large effect size (strength of association between variant and disease) typical of monogenic traits. Association study is the preferred method to analyze common complex diseases (www.intechopen.com, adapted from McCarthy *et al.*<sup>32</sup> and Manolio *et al.*<sup>30</sup>).

### 1.2.1 Linkage studies

Linkage studies are useful to analyze monogenic traits. This strategy involves individuals from several generations of a family, some of which are affected by a disease. In linkage studies, family pedigrees are built to identify the type of disease inheritance. Then, the co-segregation of a genetic marker (SNP or other kind of variation) with the disease is measured. A marker is a DNA segment for which the exact position is known. If affected individuals share a specific marker, the region where the marker is located is isolated for characterizing the genes responsible for the disease. For example, whole-genome linkage analysis associated the presence of mutations in the *NOTCH1* (notch 1) gene with aortic valve disease<sup>33</sup>. Although no control population is required, it can be difficult to collect large informative pedigrees and obtain sufficient statistical power to analyze complex traits<sup>34,35</sup>.

### 1.2.2 Association studies

In genetic association studies the frequency of the minor allele of a SNP is compared between a group of affected individuals (cases) and a group of unaffected individuals (controls). For example, if the allele frequency is statistically higher in cases than in controls, an association of the allele with increased risk for the disease is concluded. The associated SNP may affect risk of disease directly (causal) or may be a marker for another variant that affects risk of disease.

Candidate gene studies are suitable to detect susceptibility genes for common and complex diseases without the need for pedigrees (**Figure 1-7**). The phenotype or trait under study must be well characterized and measured. Some disadvantages of association studies are that they require a large sample size and that controls must be from the same population. There is an increase in false-positive results, if a control population with the same ancestry is not available. Family-based association studies use matched relative controls (e.g. unaffected parents or siblings) for the identification of susceptibility genes, insuring that cases and controls come from the same population. No large pedigree is necessary<sup>36</sup>.

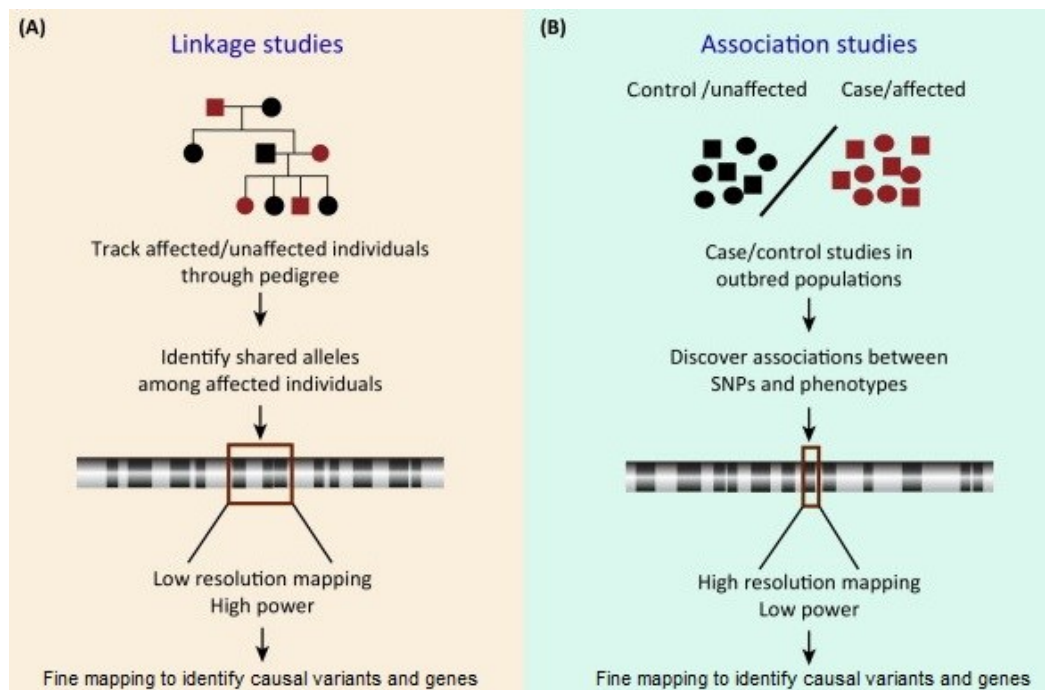


**Figure 1-7.** Comparison of linkage and association studies Figure derived from Kebede & Attie<sup>37</sup>, license number 3614890449956.

### **1.2.2.1 Candidate gene association studies**

Candidate gene studies are hypothesis-driven; potential candidate genes are selected from the most significant results of whole-genome screening or selected based on the knowledge of the pathophysiological mechanisms of the disease<sup>34</sup>. E.g. hypercholesterolemia has been associated with CAVD and polymorphisms in apolipoproteins AI (*APOA1*), B (*APOB*), and E (*APOE*) were interrogated in a gene association study for CAVD<sup>38</sup>. Therefore, candidate gene studies do not permit the detection of novel genes and pathways. Candidate gene studies offer the possibility to analyze a broader number of SNPs per gene, especially inside coding regions, mainly due to the low cost of these studies compared to whole-genome analysis<sup>34,35</sup>.

The design of gene association studies must be carefully addressed. However, many studies performed until now have been poorly planned in terms of phenotype definition, trait measurement, controls selection, genetic marker selection, and sample size, and cannot provide strong evidence for their conclusions<sup>31</sup>.

### **1.2.2.2 GWAS**

Genome-wide studies search for associations on the entire genome without any preconception of the function of specific genes; they are characterized as agnostic. The ultimate goal of GWAS is to identify genetic variants associated with disease or biological trait of interest. Whole-genome association studies are still relatively expensive<sup>35</sup> but they have been facilitated by the implementation of public sample databases such as dbGaP<sup>25</sup>, HapMap<sup>21</sup>, and the 1000 genomes projects<sup>13</sup>.

GWAS are useful to identify common variants with small effect sizes. Significant SNPs identified by GWAS have usually low associated risk and account for a small proportion of heritability<sup>30,39,40</sup>. The missing heritability may be found in rare variants or structural variants other than SNPs. Because complex diseases have an environmental component, gene-environment interactions can also explain part of the missing heritability<sup>30,41</sup>. Several susceptibility genes have been identified in cardiovascular disease, type-2 diabetes, hypertension, and other complex traits using GWAS<sup>32,41,42</sup>. These discoveries have given

insights into the molecular causes of diseases, narrowing the search for causal variants to smaller regions of the genome.

In GWAS, hundreds of thousand or even millions of SNPs are interrogated at the same time instead of genotyping SNPs in specific genes or regions of the genome. Several companies developed whole-genome genotyping arrays based on information from the HapMap and 1000 genomes projects that allow the selection of a proportion of SNPs (tag SNPs) that capture most of the variations in the genome. These tag SNPs are transmitted across generations in blocks<sup>8,15,41</sup>. Today the most powerful SNP array, HumanOmni5-Quad BeadChip, can interrogate up to 5 million variants with  $MAF \geq 1\%$  including ~500,000 functional exonic variants.

Particular combinations of SNPs (haplotypes) occur inside chromosomes. For SNPs located in close vicinity, meiotic recombination fails to separate alleles which results in linkage disequilibrium (LD). LD defines the non-random association of alleles of neighboring SNPs<sup>43,44</sup>. Statistics based on genotype allele counts are used to measure LD. The  $r^2$  is reported in GWAS studies as a measure of LD<sup>44,45</sup>. SNPs are in complete LD (not separated by recombination) when  $r^2 = 1$ , whereas they are independently transmitted when  $r^2 = 0$ <sup>46</sup>. If several SNPs are in strong LD, the entire haplotype can be interrogated by genotyping only one of the SNPs and that SNP is the “tag” SNP. The measurement of LD is important. First to facilitate the design of high-density SNP arrays by reducing the number of tested SNPs to cover genome variations and the cost of genotyping<sup>15</sup>. Second, if the significant SNPs identified in a GWAS are not causal, they are by definition in LD with the causal variants<sup>40</sup> (**Figure 1-8**). According to data from previous GWAS, a SNP associated with a trait is in moderate LD ( $r^2 > 0.5$ ) with an average of 51 SNPs<sup>13</sup>.

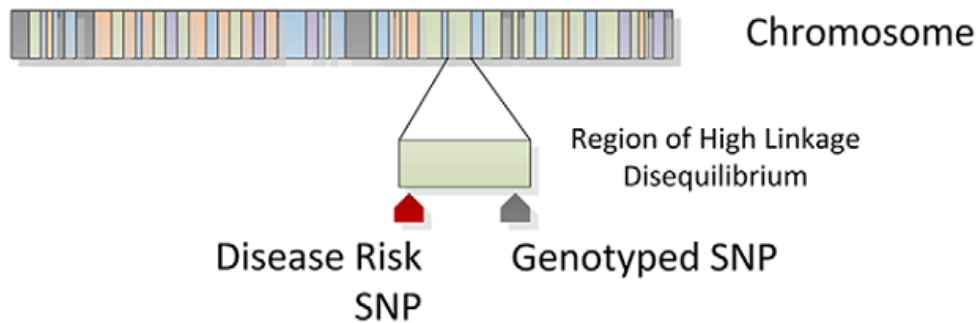


**Figure 1-8.** Indirect association of a genotyped SNP. If the causal variant was not genotyped, a significant genotyped SNP can be in LD and allow identification of disease causing SNP<sup>40</sup>. No permission is required from the authors or the publishers to reuse the figure.

GWAS generally test association of SNPs with quantitative [e.g. low-density lipoprotein (LDL) cholesterol levels] or categorical dichotomous traits (affected or unaffected). Quantitative traits are analyzed using linear regression models and dichotomous variables are analyzed using contingency table methods or logistic regression. Logistic regression is preferred because it permits the adjustment for confounding factors such as genetic background differences between cases and controls (population stratification) or clinical characteristics<sup>47</sup>.

Logistic regression tests the association between the probability of being affected and the genotype of a specific SNP. Genotypes can be grouped in four classes or models: dominant, recessive, multiplicative, and additive. Additive model is the most common model used in GWAS. Additive models are powerful enough for detecting additive and dominant effects, and to a lesser extent, recessive effects<sup>40,47</sup>. Additive models assume a linear increase of risk for each copy of the minor allele. Considering a SNP with genotypes AA, AG, and GG (A is the risk allele) (**Figure 1-4**), if the disease risk for genotype AG is 3-fold, then the risk for genotype AA is 6-fold. In addition to a *P* value for measuring significance of the results, adjusted odds ratio (OR) are also calculated to measure effect size. Odds ratio >1 means that the allele increase the risk of disease, and odds ratios < 1 means that the allele is protective<sup>40</sup>. In this thesis, the additive model for association tests was used.

Due to the large number of association tests performed in GWAS, at least one per SNP, the threshold for statistical significance needs to be adjusted. Usually, researchers use a threshold of  $5 \times 10^{-8}$  or a Bonferroni corrected threshold to avoid high numbers of false positive results<sup>41,48</sup>. SNP-disease association with  $P < 5 \times 10^{-8}$  are considered replicable. SNP-disease associations with  $P < 1 \times 10^{-7}$  can be also successfully replicated and a more liberal GWAS significant cutoff than  $5 \times 10^{-8}$  have been suggested<sup>48</sup>. When needed, significant SNPs can be replicated in a second independent set of cases and controls to identify true positive results and to minimize false negative associations. Meta-analysis combining results from several GWAS can also help improve statistical power<sup>41</sup>. The general steps in a GWAS are shown in **Figure 1-9**.

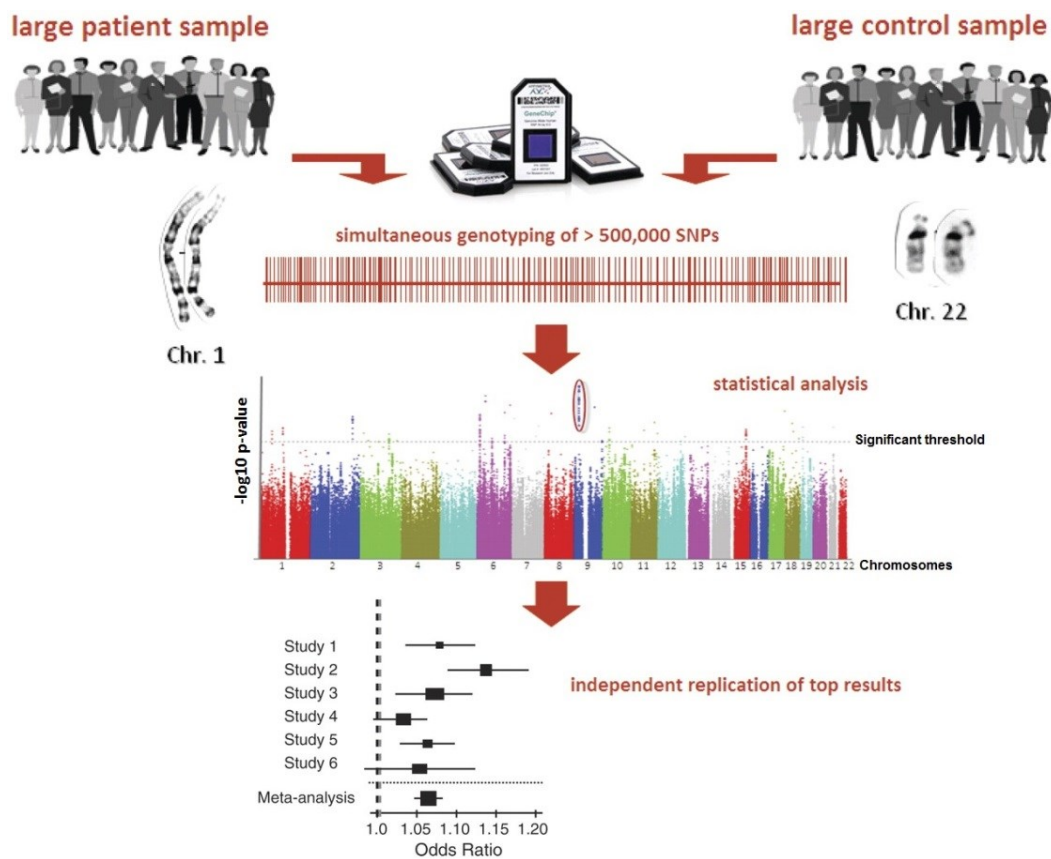


**Figure 1-9.** General steps in a GWAS. The frequency of SNPs is compared between cases and controls. Up to 5 million SNPs are interrogated in a current SNP genotyping array. The results of a GWAS are summarized in a Manhattan plot in which the  $-\log_{10} P$  values of association tests are plotted against the chromosomal position of the tested SNPs. Results of independent GWAS can be combined into a meta-analysis to increase power. Figure derived from Schunkert *et al.*<sup>49</sup>, license number 3614901209077.

Prior to data analysis, quality controls must be performed on SNPs and samples in order to avoid genotyping errors and other biases influencing the data. The list of SNP quality controls is presented below:

- **SNP genotyping efficiency.** SNPs are removed based on genotyping call rate (the proportion of genotypes per marker with non-missing data). SNPs that are not genotyped in at least 95-99% of samples (call rate < 95-99%) are removed<sup>46,50</sup>. This rate of failure indicates difficulties in the SNP genotyping process, e.g. other SNPs maybe located nearby, affecting probe hybridization.
- **Hardy-Weinberg equilibrium.** Allele frequencies should be equal from generation to generation, in large randomly mating populations. If allele frequencies in the population under study deviate from such expectation, SNPs are said not to be in Hardy-Weinberg equilibrium. A significant test usually indicates genotyping errors. The significant  $P$  value threshold for removing SNPs based on Hardy-Weinberg equilibrium is  $10^{-7}$  in GWAS, allowing control for multiple testing. Deviations from Hardy-Weinberg equilibrium can also indicate inbreeding and population stratification<sup>51</sup>.
- **MAF.** SNPs with  $MAF < 0.01$  are removed from analyzes<sup>46,50</sup>.
- **GenCall score.** Illumina has its own measurement for genotype or DNA sample failure called the GenCall score. Low-quality SNPs below the 10th percentile for the Illumina GenCall score ( $\leq 0.1$ ) must be removed ([www.illumina.com](http://www.illumina.com)).

Sample quality controls involve several steps that are listed below:

- **Sample genotyping call rate.** Samples with low quality usually have high genotyping rate failure. Individuals with missing genotypes > 3-7% are usually excluded<sup>50</sup>.



- **Gender inconsistencies.** SNPs on the X chromosome are analyzed to determine genotypic rate, which is then compared with phenotypic data. Men only have one X chromosome and cannot be heterozygous for SNPs outside the pseudoautosomal region on the Y chromosome (human X and Y chromosomes pair and recombine during meiosis in this region). Men and women are expected to have a homozygosity rate of  $\sim 1$  and  $< 0.2$ , respectively. Discrepancies in this rate may indicate samples mix-ups. If the homozygosity rate is between 0.2 and 0.8, the genotype data are inconclusive regarding the gender, and the samples must be excluded<sup>46,50</sup>.
- **Samples relatedness.** This analysis helps to identify duplicated samples, which is important if genotype data of controls is downloaded from public databases. In addition, the presence of related individuals (first- and second-degree) may increase the frequency of certain alleles, and these frequencies will not be representative of the ones in the general population<sup>46</sup>.
- **Population structure.** Most common human variations (85–90%) are shared among different populations and few are specific to a particular population. The comparison of variations in the cohort studied with variations in reference populations, such as HapMap, allows the identification of individuals with ancestries deviating from the cohort studied. If cases and controls are selected from different populations, a SNP can be significant due to differences in population frequencies under study, rather than by the true disease development influence. Well-designed GWAS select cases and controls from the same population, but fine-scale genetic substructure or unintentional inclusion of subjects from other populations can happen<sup>50,52</sup>. Ancestry can be measured using softwares such EIGENSTRAT, which compares allele frequencies of independent SNPs to those of HapMap individuals. EIGENSTRAT generates a number of principal components that can be utilized as covariates in association analysis to correct for population stratification<sup>40,53</sup>.

### 1.2.2.3 GWAS imputation

SNP arrays interrogate tag SNPs and attempt to cover most variations across the genome. However, there are SNPs that are not captured by tag SNPs. To increase genomic coverage, SNPs that were not genotyped are predicted from a reference panel, in this case, the 1000 genomes project<sup>54,55</sup>. Imputation is also useful when cases and controls are not genotyped with the same array platform and the number of common genotyped SNPs is low<sup>40,55</sup>. Another use for imputation is fine-mapping of regions where significant SNPs were identified<sup>55</sup>.

Briefly, imputation estimates haplotypes for the reference and the study samples, and aligns them (**Figure 1-10**). Haplotypes of the study samples will have missing data because only tag SNPs were genotyped. The haplotypes of the reference panel that are more similar to those of the study samples will be grouped, and the missing SNPs in the haplotype of the study sample will be filled with information from the reference panel. Different reference panel haplotypes can match the same study sample haplotype, so only haplotypes with the highest probability score (highest probability of being correct) are used for inferring SNPs. Popular algorithms for imputation are IMPUTE<sup>55</sup>, MaCH<sup>56</sup>, and Beagle<sup>57</sup>. After imputation, SNP quality controls are performed to ensure quality of the data.

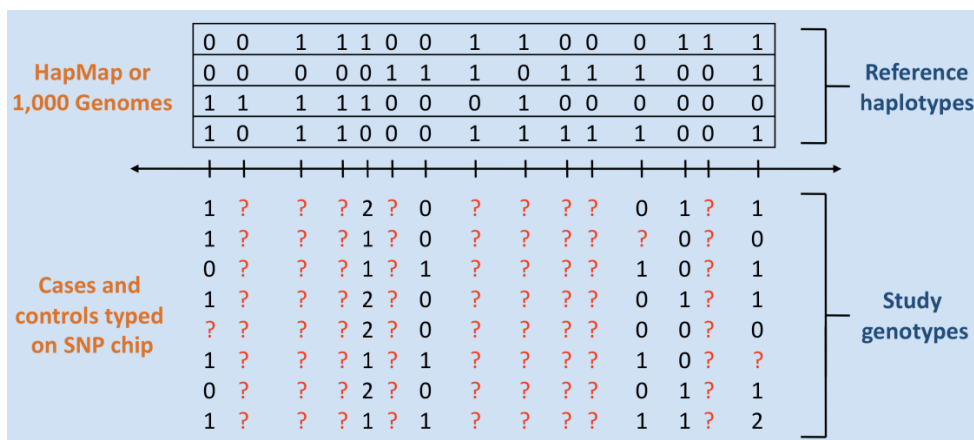


**Figure 1-10.** Typical imputation scenario. SNP genotypes are coded as 0, 1 (heterozygous), and 2. Non-genotyped SNPs (red question marks) in a set of individuals are imputed (or predicted) using a set of reference haplotypes from a reference panel ([https://mathgen.stats.ox.ac.uk/impute/impute\\_v2.html](https://mathgen.stats.ox.ac.uk/impute/impute_v2.html)).

#### **1.2.2.4 GWAS meta-analysis**

A disadvantage of GWAS is that to ensure enough power for the detection of significant SNP-disease associations, thousands of individuals in each group of cases and controls are required. The sample size required to identify significant associations increase with the number of SNPs tested. To test one polymorphism requires 248 cases and to test 1 million SNPs requires 1,255 cases, assuming an odds ratio of 2, 5% disease prevalence, 5% MAF, complete LD, 1:1 case/control ratio, and a 5% error rate in an allelic test<sup>58</sup>. These populations are not always available to researchers. However, the results of several independent GWAS can be summarized into a meta-analysis to increase power and reduce false positives<sup>32</sup>. Meta-analysis is the statistical synthesis of information from multiple independent studies<sup>59</sup>. Genotype data of each study, summary statistics or *P* values can be used for meta-analysis. Combining results of independent studies has limitations and is also associated with challenges including heterogeneity in the definition of the phenotype, different array platforms for genotyping, differences in the sampling methods, and ancestry differences between studies<sup>40</sup>.

Different statistical methods have been developed to perform meta-analyzes, among them there are the *P* value and *Z*-score, the fixed and random effects, the optimal weights and Bayesian methods<sup>59</sup>. The first method averages *P* values across studies. The second averages *Z*-scores and takes into account the effect size. Inverse variance weighting is the optimal method for a meta-analysis, weighting by the variance to give more importance to studies with more data<sup>60</sup>. Bayesian methods present results as posterior probabilities that the effect of a variant is null<sup>59</sup>.

The most popular and powerful approach is the fixed effects method complemented by the random effects method. The fixed effects method assumes that the risk allele has the same effect in each study. Inverse variance weighting can be applied in this method; each study is weighted by the inverse of its squared standard error. Random effects models are useful for measuring between-study heterogeneity in effect sizes<sup>59</sup>. Common heterogeneity metrics are Cochran's *Q* statistic and  $I^2$  (the most used).  $I^2$  represents the approximate proportion of

the variability that can be attributed to heterogeneity between studies<sup>40</sup>. PLINK and METAL are most commonly used to perform meta-analysis<sup>59</sup>.

### **1.2.3 Prioritization of GWAS results**

GWAS results can be confirmed by meta-analysis, replication studies, and ultimately with functional studies. Generally, variants with the smallest  $P$  values are selected for replication and the nearest genes are selected as candidate genes. However, GWAS results have a grey zone where nearly significant variants of modest effect size are located; those variants are likely to play a role in complex diseases. Combining the results of top SNPs with moderate association (not reaching strict genome-wide significance thresholds) and functional data can help to identify other true associations<sup>32,61</sup>.

Non-synonymous variants and variants located in the 5'UTR are good candidates for further studies. The variants can be annotated to a function using data from dbSNP and the UCSC genome browser website (<http://genome.ucsc.edu/>). Variants that belong to susceptibility genes and genes in biological pathways that have already been related to the disease are also good candidates for prioritization<sup>32,62</sup>. Pathway-based analysis evaluate if a group of genes that belong to the same pathway are jointly associated with the disease. The most significant biological pathways are the ones having the most genes with moderate to high SNP-disease associations. Commonly used pathway-based analysis software are GSA-SNP and VEGAS<sup>63,64</sup>.

## **1.3 Whole-genome gene expression**

Gene expression is a complex trait that is influenced by genetic variants, epigenetics, and environmental factors<sup>65</sup>. Whole-genome gene expression experiments allow the simultaneous quantification of the expression of all known genes in the human genome in specific cell types or tissues. Genes differentially expressed and their molecular pathways are likely to have an influence on disease development or to be part of a disease-compensatory mechanism. Those genes are potential candidates for development of drugs and diagnostic or prognostic methods, among others<sup>66</sup>. Two main approaches have been

utilized in this thesis to measure whole-genome expression based either on hybridization (microarrays) or sequencing (RNA-Seq)<sup>67</sup>.

### **1.3.1 Microarrays**

Hybridization-based approaches involve incubation of fluorescently labelled cDNA (RNA reverse transcribed to DNA) with high-density oligo microarray chips that contains thousands of probes (DNA fragments) that hybridizes with their complementary regions of cDNA. A microarray chip is a glass or silicone slide containing the microscopic probes. A chip provides genome-wide transcriptional coverage of well characterized genes, candidate genes, and splice variants selected bioinformatically.

Microarrays have been applied for the identification of diagnostic or prognostic biomarkers, the classification of disease stages, the monitoring of response to therapy, and the understanding of mechanisms involved in disease<sup>66</sup>. Some disadvantages of microarrays are that the probes are designed based on current knowledge of the genome sequence, thus discovery of new transcriptome features is limited. The probes may hybridize to regions where unknown SNPs are located, affecting measurement specificity. High background levels and saturation of signals can occur, leading to limited dynamic range of detection. Comparison of data between independent experiments is complex and less reliable<sup>67</sup>.

A microarray chip contains a thousand nucleotide fragments or probes that hybridize to a specific mRNA or transcript. The position of the probes on the chip as well as the mRNA that hybridize with each probe is predetermined. Other technologies such as Illumina use beads coated with probes with a unique barcode to identify each transcript. The level of gene expression is estimated from the raw intensities of the fluorescence emitted by the labeled cDNA hybridized with the probes. The Illumina chip utilized in this study is a single-channel array type in which one sample is hybridized on each line of the array. The chip has a capacity of 12 samples. In 2-channel arrays, two samples are hybridized simultaneously on a single array with two different fluorescent dyes<sup>68</sup>.

Significance Analysis of Microarrays (SAM)<sup>69</sup> is commonly used to determine the number of differentially expressed genes between sample groups. SAM applies a statistic similar to the t-statistic but takes into account the expression variability<sup>66</sup>. From these results, one can perform pathway analysis. Pathway analysis software tools include IPA (www.ingenuity.com/), DAVID<sup>70,71</sup>, and GSEA<sup>72</sup>. The goal of these tools is to identify biological pathways enriched with differentially expressed genes. The genes with the largest changes in expression between sample groups are considered of interest for further analysis, but genes with smaller changes that have a similar function or belong to the same pathway are also of interest. Significant pathways are likely to have implications in the disease. **Figure 1-11** summarizes the steps for microarrays analysis.

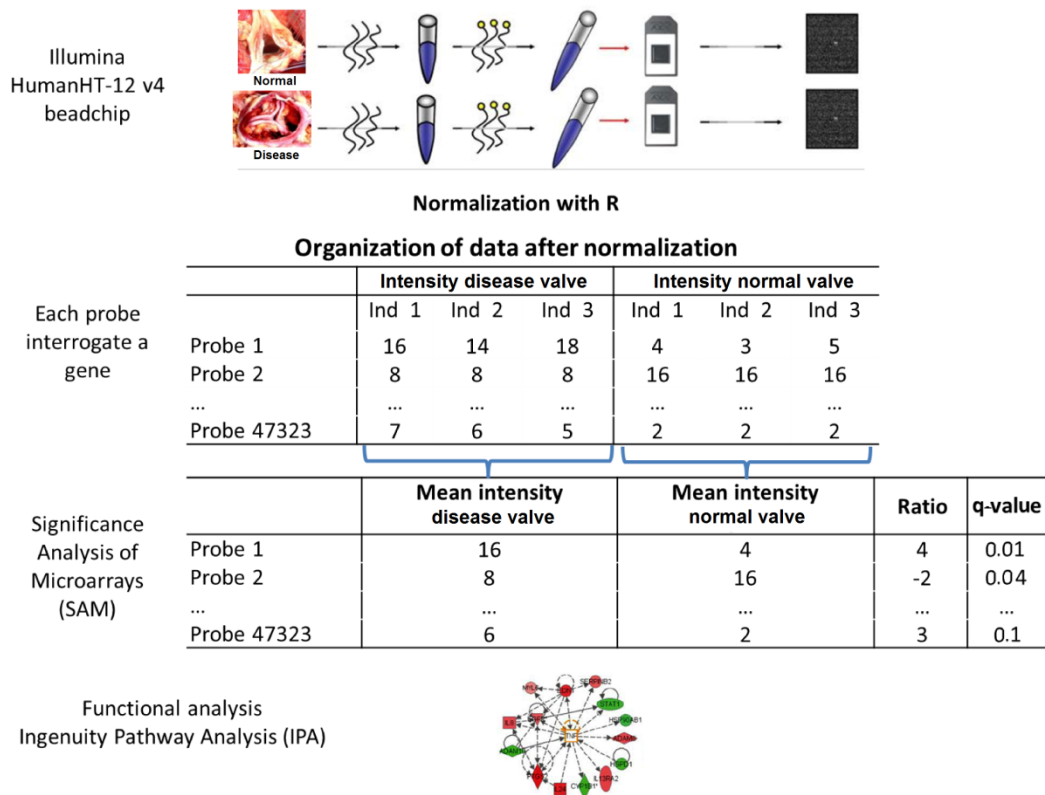


**Figure 1-11.** Steps involved in microarrays analysis. The upper panel illustrates the single channel technology utilized in this project to compare gene expression between normal and diseased valves. mRNA from each valve tissue is extracted and each sample is labeled with the same fluorescent dye, but independently hybridized on different arrays. Arrays are scanned and the intensity of hybridization is measured. The amount of fluorescence measured at each probe location (which contains several copies of the same probe) is directly proportional to the amount of mRNA that hybridizes that probe. Raw intensity data

are normalized. SAM determines the number of differentially expressed genes based on a specific ratio (fold change) and adjusted *P* value (q-value) thresholds. Pathway analysis can be performed with IPA. Figure by Guauque-Olarte.

### **1.3.2 RNA Sequencing**

RNA-Seq is a high-throughput DNA sequencing method to map and quantify transcriptomes. RNA sequencing directly determines the sequence of cDNA reverse transcribed from total cellular mRNA<sup>73</sup>. Compared to microarrays, RNA-Seq has some advantages. Novel transcripts can be detected because transcript-specific probes are not necessary. It is also possible to identify SNPs, gene fusions, and other variations. Gene expression measurement has a broader dynamic range because no background fluorescence is produced. RNA-Seq is more specific and sensitive than microarrays, and allows detection of rare and low-abundance transcripts.<sup>67,73</sup>

In this thesis, Illumina sequencing technology was used. Shortly, RNA is extracted and coding pre and mature RNAs are selected using oligo sequences complementary to the mRNA poly-adenine tails. mRNA is fragmented and reverse transcribed to cDNA which is then amplified. Deoxyadenosine triphosphate is added to the end of cDNA fragments to ligate adapters that hybridize to a flow cell array. Only fragments of specific lengths are selected for sequencing (e.g. 150-300 bases). cDNA is denatured and a new second strand is generated base-by-base. Each new nucleotide added is labeled which allows the system to determine it was included in the new cDNA strand, thus revealing the DNA sequence. Only the 50 bases at the start and the end of each cDNA molecule are sequenced. This is called paired-end sequencing because two reads of 50 bases are generated for each cDNA molecule. Thus, a read is a sequence of 50 nucleotides. The quality of raw reads is verified using bioinformatics tools such as FastQC ([www.bioinformatics.babraham.ac.uk/projects/fastqc](http://www.bioinformatics.babraham.ac.uk/projects/fastqc)). Subsequent steps are the alignment of the reads to a reference genome, mapping of reads to genes, and quantification of the transcriptome. These steps are performed for each sample (cases and controls). Reads are then normalized and differential expression analyzes can be performed.

Several methodologies can be followed to normalize raw data and compare gene expression between two conditions. Usually TopHat<sup>74</sup> is utilized for read alignment. Cufflinks<sup>74</sup> software contains several tools for quantification and normalization of reads, and for differential expression analysis. Up to date, there is no standard methodology for the analysis of RNA-Seq data. The logical approach is to compare the results of several algorithms to select the best candidate list of genes. Each program addresses the intra-group variability differently, some are too flexible and lead to a high number of differentially expressed genes and false positives while others are too stringent<sup>75,76</sup>. DESeq<sup>77</sup>, edgeR<sup>78</sup>, and SAMseq<sup>79</sup> use counts of the reads generated by HTSeq<sup>80</sup> software, normalize data, and perform differential expression analysis. Genes with adjusted *P* values < 0.05 in the three programs can be considered as differentially expressed. Pathway-based analysis can also be performed to prioritize results (**Figure 1-12**).

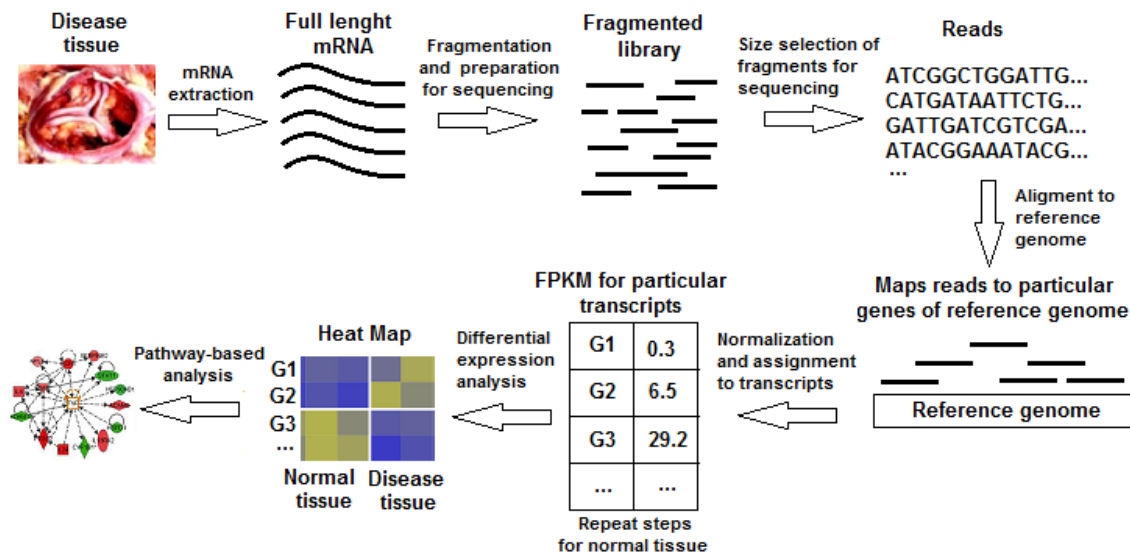


**Figure 1-12.** Overview of RNA-Seq analysis. For each sample, RNA is extracted and reverse transcribed to cDNA. cDNA is fragmented and sequenced to produce reads. Reads are aligned to a reference genome, quantified, and normalized. The amount of reads per gene depends on the number of cDNA molecules present in the sample at the beginning of the experiment and on the length of the gene. More cDNA is equal to more reads. Statistical analyzes are performed to identify differentially expressed genes between tissues. Pathway analysis can also be performed. FPKM: fragments per kilobase of transcript per million mapped reads. Figure by Guauque-Olarte.



## 1.4 Expression quantitative trait loci (eQTL)

Previous GWAS have come to the conclusion that complex diseases are influenced by several variations affecting the expression of several genes instead of being influenced by the alteration of a single gene. As stated above, variations in the DNA can affect gene expression depending on their localization. Specific variants that influence gene expression are called eQTL<sup>63</sup>. eQTL mapping studies aim to identify disease-associated SNPs also associated with gene expression. Not only SNPs but other kind of variations can be analyzed. Since the majority of GWAS-nominated variants are located in non-coding regions<sup>81,82</sup>, eQTLs are useful to identify the function of variations located in these regions.

eQTLs can be classified as local or distant according to their location in respect to the gene that they influence. Another classification is based on their mode of action (cis or trans). The distance between a local eQTL-SNP and a gene is selected arbitrarily<sup>83</sup>. eQTLs located up to 1Mb from the gene that they regulate are usually considered local eQTLs. Local eQTLs can act in cis or trans. cis-eQTLs regulates the gene near to them and are enriched in transcription sites, exons, and 5' regulatory regions. Trans-eQTLs alter the structure, function or expression of a diffusible factor or protein that binds to distant genes. Distant eQTLs are located outside cis-eQTL boundaries and are more difficult to identify due to lack of statistical power, a higher number of test have to be performed to identify trans-eQTLs and correction for multiple testing is more strict<sup>84</sup>. Distant eQTLs usually acts in trans. eQTL studies in lung<sup>85</sup>, heart left ventricle<sup>84</sup>, and other tissues have been performed<sup>86,87</sup> and it has been estimated that 50 to 80% of eQTLs are cell- and tissue-type dependent<sup>87,88</sup>. Measuring gene expression in a tissue relevant to the disease studied will thus improve the likely of positive and meaningful results.

In eQTL studies, whole-genome genotyping and gene expression are performed in the same individuals. DNA for genotyping is extracted from blood or from tissue and RNA expression is measured preferably in a relevant tissue for the disease using microarrays technology and/or, more recently, RNA-Seq. Statistical methods evaluate the association of each SNP with mRNA expression levels to detect eQTLs<sup>82</sup>. The PLINK software is commonly used to perform eQTL analysis, which is based on linear regression between

expression levels and genotypes. Significant eQTL-SNPs can be visualized in boxplots with the genotypes on the X axis and the level of expression of the eQTL-regulated gene on the Y axis. These plots help visualize whether the risk allele identified in a GWAS causes an increase or a decrease of gene expression levels, thus further refine the relationship between associated SNPs and the disease (**Figure 1-13**).

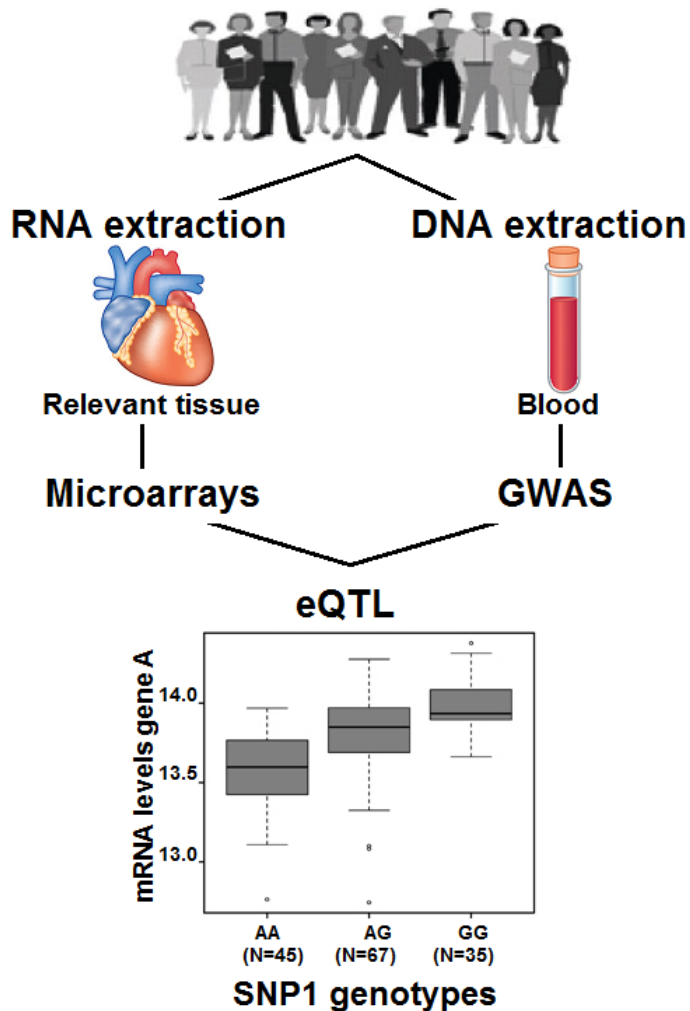


**Figure 1-13.** eQTL mapping. RNA and DNA are extracted from the same individuals. Whole-genome expression profiling and genotyping are performed. The strength of association between gene expression and specific SNPs is measured. In this example, SNP1 is significantly associated with mRNA levels of gene A. Individuals carrying the G allele express higher mRNA levels. Figure by Guauque-Olarte.

## Chapter 2. Cardiac function and heart valves

### 2.1 Cardiac function and heart structure

The main function of the cardiovascular system is to deliver oxygen and nutrients to metabolizing tissues and to remove carbon dioxide and wastes from body tissues<sup>89</sup>. It also contributes to homeostasis by regulating body temperature, humoral communication, and adjustment of oxygen and nutrients supplies. The cardiovascular system comprises the arteries, arterioles, capillaries, venules, veins, and the heart<sup>90</sup>.

The heart is contained within a fibrous layer called pericardium; this sac envelops and attaches the heart to the great vessels; the ascending aorta, the pulmonary artery, both vena cavae, and the four pulmonary veins<sup>89</sup>. The visceral pericardium or epicardium, which is the outermost layer of the heart, contains the epicardial coronary arteries and veins, autonomic nerves, lymphatics, and adipose tissue<sup>89,91</sup>. The thickest layer of the heart is the myocardium composed of cardiac muscle cells or myocytes. Myocytes are made of long chains of sarcomeres, which are responsible of cardiac contraction<sup>91</sup>. The endocardium, the inner cardiac layer, is the layer of endothelial cells that covers the interior surface of the cardiac chambers and the valves<sup>91</sup>.

The cardiac muscular chambers are the two atria and the two ventricles. The interventricular septum separates the left and right ventricles. The left ventricle wall is thicker because it does the hardest work, pump blood into the systemic circulation<sup>92</sup>. The atria and ventricles are separated by the atrioventricular grooves, the tricuspid, and the mitral valves<sup>89</sup>. On the right side, the ventricle is separated from the pulmonary artery by the pulmonic valve. On the left side, the aortic valve separates the ventricle from the aorta<sup>91</sup>. The valves are attached to the cardiac skeleton<sup>91</sup> by their annuli or valve rings<sup>89</sup>. The interior cardiac structures are shown in **Figure 2-1**.

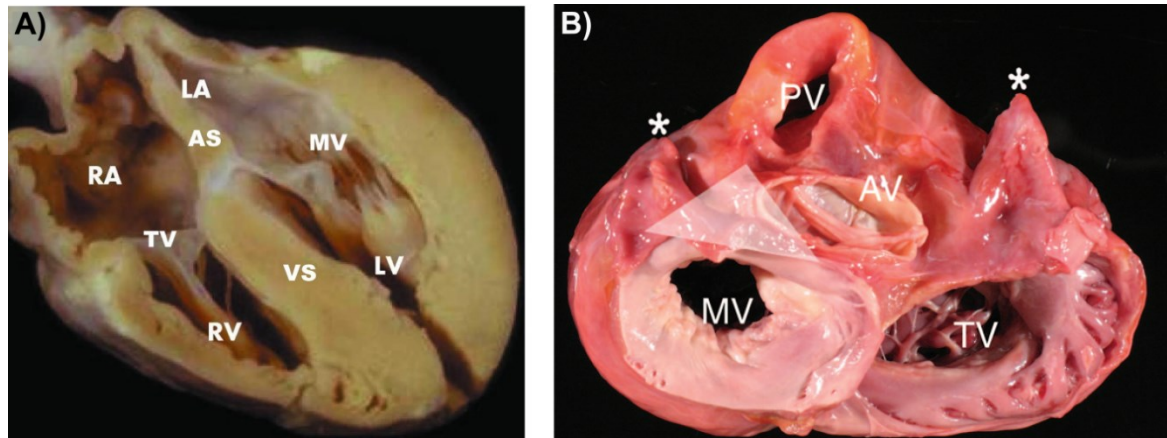


**Figure 2-1.** Gross anatomy of a normal heart. A) Four chamber view of the heart. The atria septum (AS) separates the left (LA) and right (RA) atria. The interventricular septum (VS) separates the left (LV) and right ventricle (RV). The atria and ventricles are separated by the atrioventricular grooves, the tricuspid (TV), and the mitral valves (MV). Taken from Ho & Nihoyannopoulos<sup>93</sup>. B) View from the atria toward the valvular apparatus showing the aortic valve (AV), MV, pulmonary valve (PV), and TV. Asterisks indicate the atrial appendages. Taken from Steven *et al.*<sup>94</sup>. Figure license numbers A) 3452801222505, B) 3553961348195.

## 2.2 The cardiac cycle

The right and left sections of the heart are independent pumps assuring the pulmonary and the systemic circulation, respectively<sup>92</sup>. In an average person, the heart beats about 100,000 times in one day and approximately 35 million times in a year. At rest, the heart beats about 60 to 90 times per minute and pumps 5 to 6 liters of blood through the body<sup>95,96</sup>. The heart pumps blood in a repeated sequence called the cardiac cycle.

The cardiac cycle consists of two periods called diastole (ventricular relaxation) and systole (ventricular contraction)<sup>89</sup>. During diastole the heart is relaxed, oxygenated blood is received into the left atrium and passively flows through the mitral valve to the left ventricle. Deoxygenated blood, coming from the body through the vena cavae, travels to the right atrium and flows to the right ventricle through the tricuspid valve. During systole, the filled left ventricle contracts and causes the closure of the mitral valve. When the ventricular pressure exceeds the systemic pressure, the aortic valve opens and the oxygenated blood is ejected through the aorta to other body tissues. In the right side of the heart, deoxygenated blood is sent toward the lungs through the pulmonary valve and artery.

In the lungs, the blood is oxygenated and sent to the left atrium through the four pulmonary veins<sup>89</sup>. Then, the cycle starts again (**Figure 2-2**).

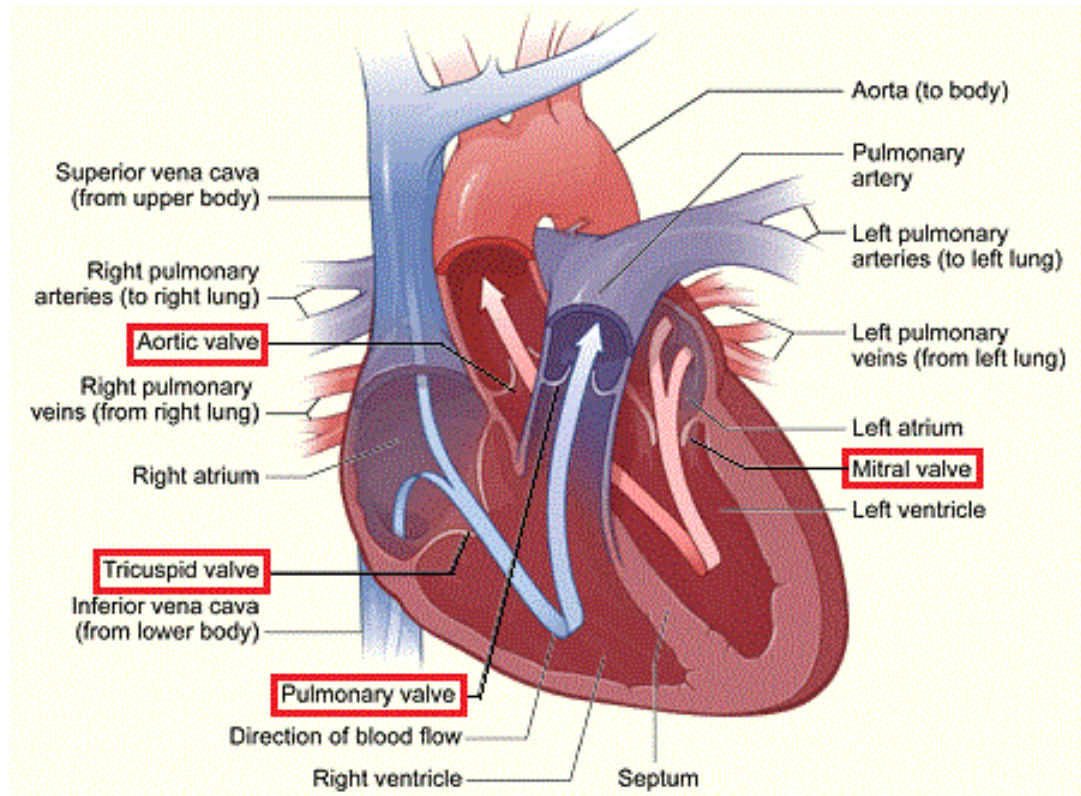


**Figure 2-2.** The interior of the normal heart and direction of cardiac blood flow. Oxygenated blood (red arrows) returns to the left atrium and flows to the left ventricle. Red blood is sent by the aorta across the body. Deoxygenated blood (blue arrows) returns to the right atrium and flows into the right ventricle. This blood is sent to the lungs via the pulmonary artery. [www.nhlbi.nih.gov/health/dci/Diseases/hhw/hhw\\_anatomy.html](http://www.nhlbi.nih.gov/health/dci/Diseases/hhw/hhw_anatomy.html).

### 2.3 The heart valves

The four valves of the heart (aortic, mitral, pulmonary, and tricuspid) direct the cardiac blood flow and prevent backward leakage. The valves open and close about 100,000 times a day, 3.7 billion times in an average life-span, and are constantly subject to mechanical stresses<sup>95</sup>. The right-sided valves, pulmonary and tricuspid, direct deoxygenated blood into the lungs at approximately 20 mmHg of transvalvular pressure. The left-sided valves, aortic and mitral, direct oxygenated blood out of the heart at a pressure of ~120 mmHg<sup>96</sup>. The heart valves can be classified in two groups, the atrioventricular and the semilunar valves<sup>92</sup>.

### 2.3.1 The atrioventricular valves

The mitral and tricuspid valves are located on the left and right side of the heart, respectively<sup>97</sup>. The atrioventricular valves control the flow of blood from the atria into the ventricles<sup>98</sup>. The valves comprise the annulus, leaflets, commissures, tendinous fiber (or *chordae tendinae*), and papillary muscles. The leaflets are attached to the papillary muscle by the tendinous fiber to the internal face of the left ventricle<sup>92</sup>. Contraction of the papillary muscles coapts the leaflets to one another, closing the valve during systole. The chordae helps to maintain the leaflets oriented towards the interior of the ventricle preventing them to prolapse backwards into the atrium during systole<sup>98</sup>. The mitral valve is the only valve with two leaflets instead of three<sup>89</sup>. The orifice of the tricuspid valve is bigger and the leaflets are thinner and more translucent<sup>99</sup> (Figure 2-3).

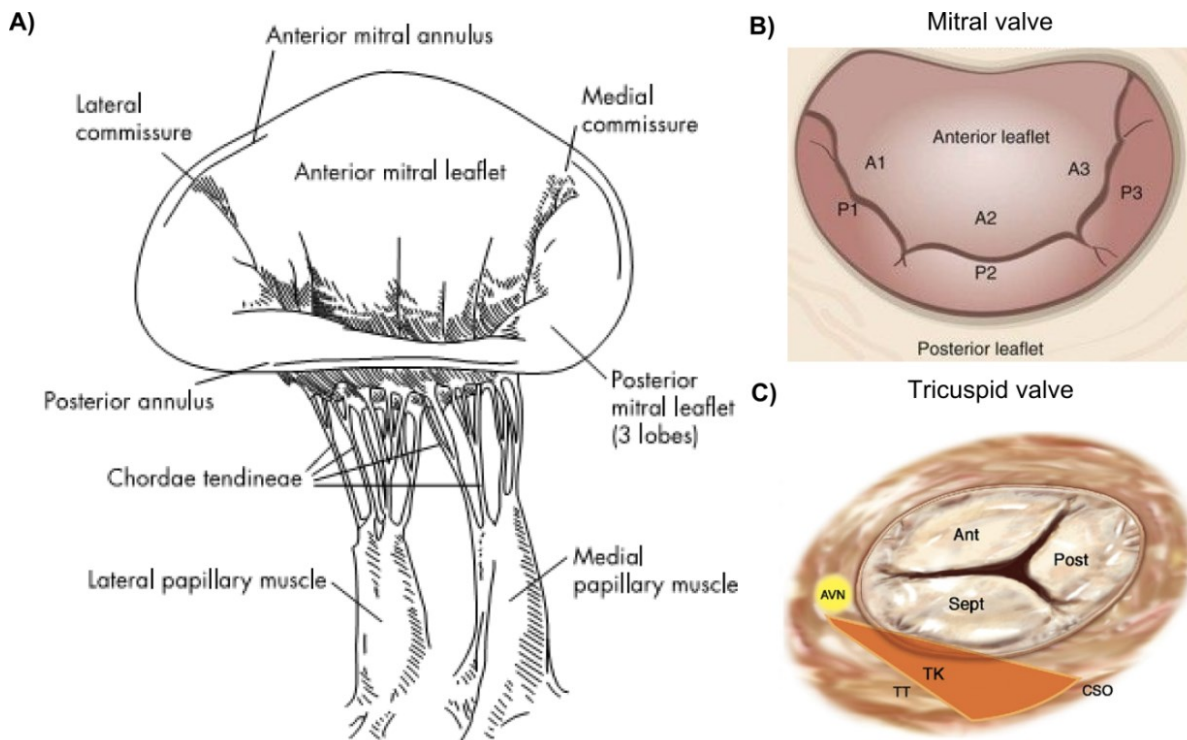


**Figure 2-3.** Structure of the atrioventricular valves. A) and B) The two leaflets of the mitral valve are attached to the ventricular wall by the tendinous fiber and papillary muscles. C) The tricuspid valve is anchored in a similar manner as the mitral valve but has three leaflets. Figures A and C were taken from Otto<sup>100</sup> and Taramasso *et al.*<sup>101</sup>, respectively. Figure license numbers A) 3614360423765 and C) 1982084. Figure B was taken from [www.mitralvalverepair.org/content/view/50/](http://www.mitralvalverepair.org/content/view/50/).

### 2.3.2 The semilunar valves

The semilunar valves, pulmonary and aortic, separate the ventricles from the arteries. The pulmonary valve is located on the right side of the heart and the aortic valve on the left side. They have no tensor apparatus such as the tendinous fiber and the papillary muscles<sup>89</sup>. The pulmonary valve (**Figure 2-4**) prevents the deoxygenated blood to flow backwards into the right ventricle during diastole<sup>99</sup>. This valve comprises the sinus (sinus trunci pulmonalis), the annulus, the commissures, the leaflets or cusps, and the sinotubular junction<sup>99</sup>. The leaflets are attached to the aortic root by a fibrous annulus<sup>97</sup> that separates the ventricle from the pulmonary artery. The pulmonary valve is similar in design to the aortic valve but the leaflets are thicker in the later. Due to the similarities between the pulmonary and aortic valves morphologies, the normal pulmonary valve can be used in the Ross procedure to replace a diseased aortic valve in a young patient<sup>102</sup>.



**Figure 2-4.** Human pulmonary valve. The pulmonic cusps are similar in appearance and size, with three radial, almost symmetric commissural lines ([http://www.e-heart.org/pages/01\\_cardiac\\_structure/01\\_Cardiac\\_Structure\\_PV\\_001.htm](http://www.e-heart.org/pages/01_cardiac_structure/01_Cardiac_Structure_PV_001.htm)).

The aortic valve connects the heart to the systemic circulation<sup>99</sup>. In the next section, the macro- and microstructure of the aortic valve is explained.

## 2.4 The aortic valve macro- and microstructure

The aortic valve allows the flow of oxygenated blood from the left ventricle to the rest of the body. It is located between the left ventricle and the ascending aorta<sup>99</sup>. The valve is attached to the aortic root, which comprises the annulus, commissures, interleaflet triangles, sinuses of Valsalva, sinotubular junction, and the valve leaflets<sup>102</sup> (**Figure 2-5**). The annulus is a crown-like fibrous structure that attaches the valve by the aortic root. The commissures separate two adjacent leaflets at the level of the aortic wall. The interleaflet triangles are the areas beneath the commissures<sup>103</sup>. The sinuses of Valsalva are pockets formed between the leaflets and the adjacent aortic wall<sup>99</sup>. When the blood fills these sinuses, the leaflets are pulled toward one another, closing the valve. At that moment, the leaflets overlap on several millimeters<sup>89,104</sup>. The sinotubular junction supports the peripheral attachments of the valve leaflets<sup>103</sup> and separates the aortic root from the ascending aorta<sup>105</sup>.

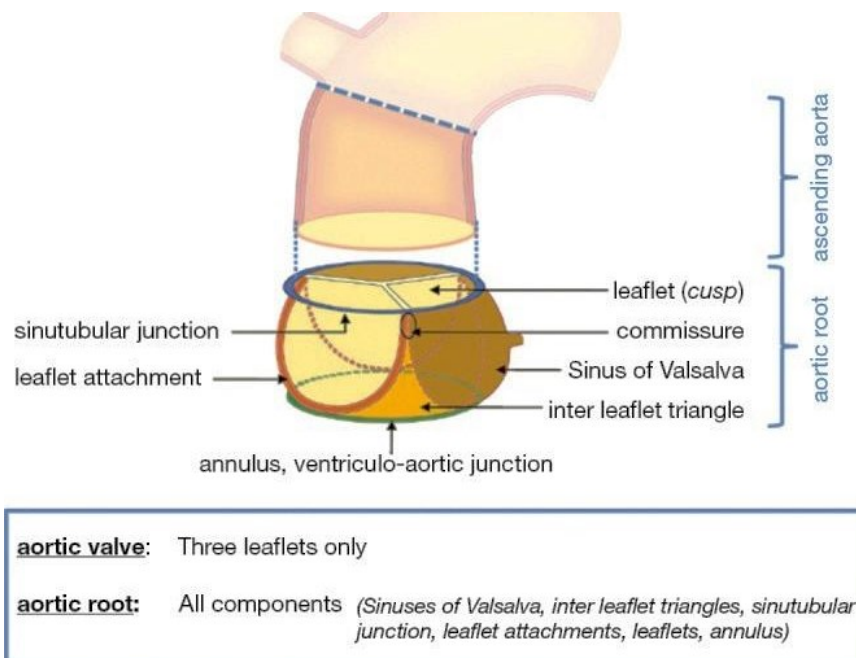


**Figure 2-5.** Aortic root components. The three leaflets of the aortic valve are attached to the aortic root. Figure taken from Charitos & Sievers<sup>105</sup> reused with permission by the publishers.



### 2.4.1 The aortic valve leaflets

The normal aortic valve has three leaflets named after the coronary artery originating from them, right and left coronary and noncoronary leaflets<sup>106</sup>. In normal condition, they are thin (< 1 mm thick<sup>107</sup>), flexible, and are attached to the aortic root in a semilunar fashion. The leaflets consist of the hinge or commissural region, the belly, the coapting surface, and the lunula with the noduli of Arantii<sup>99</sup>. The coapting surface is the region of the leaflet which overlaps with the other leaflets. The noduli of Arantii is located on the mid portion of the coapting surface. The lunula, which expands one-third of the leaflet height, is the region on each side of the nodule<sup>108</sup>. The leaflet is attached to the annulus by the hinge. This thick zone is made of collagen and transmits the stress of the leaflets to the aortic wall. The main part of the leaflet is the belly<sup>99</sup> (**Figure 2-6**).

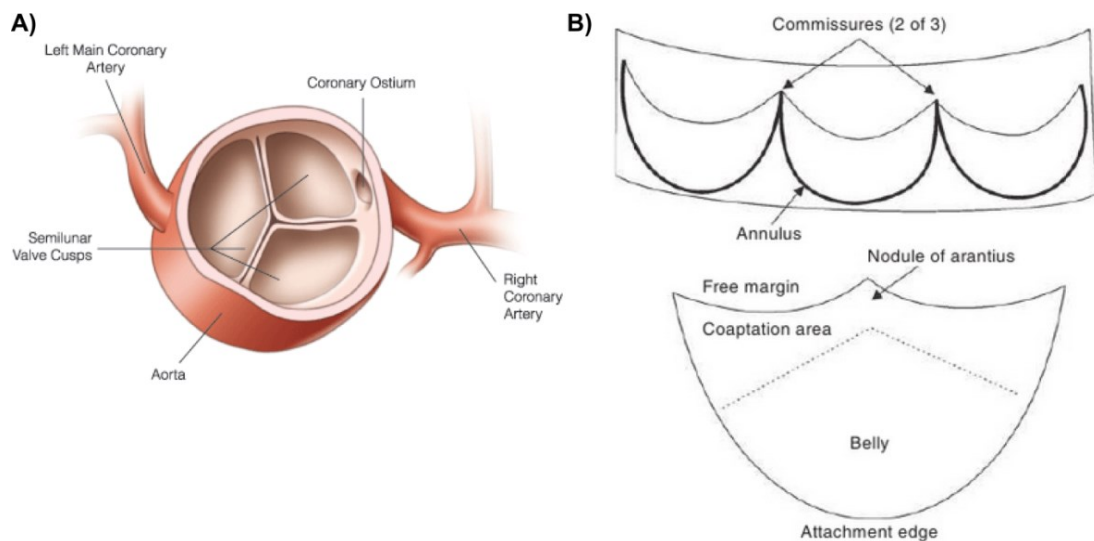


**Figure 2-6.** Aortic valve leaflet anatomy. A) Each leaflet is identified by its relationship to the coronary arteries as left and right coronary leaflets and noncoronary leaflet ([www.sciamsurgery.com](http://www.sciamsurgery.com)). B) Aortic valve leaflet within an open aortic root and parts of a valve leaflet (<http://www.slideshare.net/PZielinski/heart-velves-john-p-fisher>).

The two sides of the aortic valve support different types of mechanical stress. On the ventricular side, the valve is exposed to high-velocity and high-shear stress. On the aortic side, there is a pattern of interrupted low-velocity flow and low-shear stress<sup>109</sup>. For these reasons, the parts of the valve change in size, shape, and stiffness depending on the moment of the cardiac cycle through communication with the valvular cells and the extracellular

matrix<sup>110</sup>. The leaflets practically lack blood vessels and receive nutrients by hemodynamic convection and diffusion<sup>96</sup>. In the ventricular side, the leaflet is innervated except from the lunula and responds to neuromodulators, but the function of this innervation is not clear<sup>95</sup>.

The matrix of the aortic valve leaflet has three defined layers namely the fibrosa, spongiosa, and ventricularis<sup>107</sup> (**Figure 2-7**). The fibrosa is the thickest layer located in the valve's aortic side (the outflow surface) and is composed mainly of circumferentially aligned collagen type I fibers. The collagen fibers are surrounded by elastin, a highly elastic protein, which allows the valve to return to its resting position. The spongiosa is the loosely central layer that consists of mainly proteoglycans and hydrated glycosaminoglycans as well as some collagen and elastin. Its function is to resist compressive forces. The thinnest layer is the ventricularis (the layer at the inflow surface) and it is constituted of radially aligned elastin fiber sheets and a collagen network<sup>96,110,111</sup>.

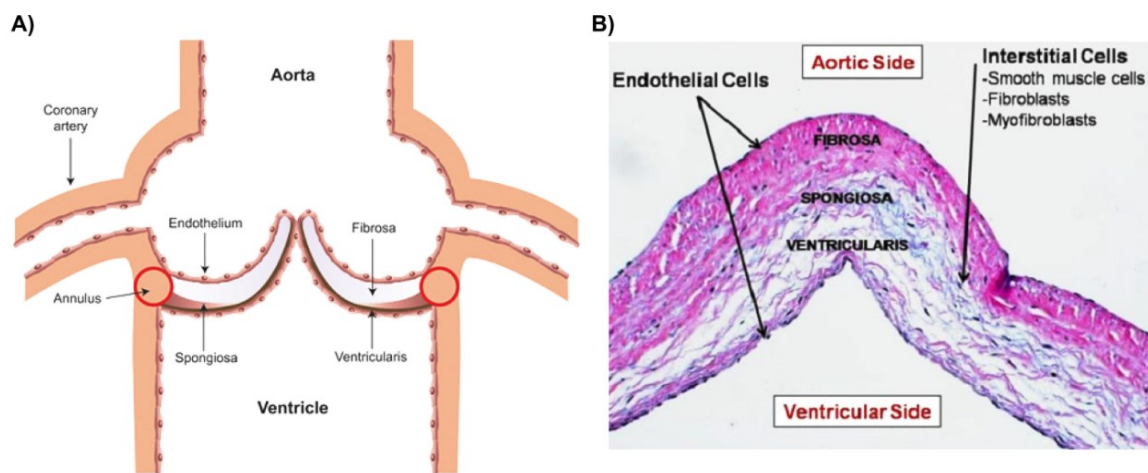


**Figure 2-7.** Aortic valve layers and valvular cells. A) The endothelium covers the ventricular and aortic side of the valve. Figure taken from Dweck *et al.*<sup>107</sup>, license number 3614371039473. B) Histology of a cross section of a valve leaflet showing the valvular cell composition and the three layers of the valve matrix: fibrosa, spongiosa, and ventricularis. Figure taken from Chester *et al.*<sup>109</sup>, no permission is required from the authors or the publishers.

Two types of cells constitute the aortic valve leaflets, the valve endothelial cells and the valve interstitial cells (VICs)<sup>95</sup>. A normal aortic valve is covered<sup>95</sup> with a layer of endothelium (**Figure 2-7**). Valve endothelial cells act as a barrier between the blood and

the VICs. On the side of the leaflets facing the aorta, the layer of valvular endothelial cells is crimped but on the side facing the ventricle, it is smooth<sup>108</sup>. The developmental source of the valve endothelial cells is different from that of the arterial endothelial or ventricular endocardial cells<sup>95,96</sup>. Valve endothelial cells originates from endocardial cells covering the myocardium<sup>112</sup>. Valve endothelial cells are perpendicularly aligned with the direction of the shear stress<sup>95</sup>. Valve endothelial cells transmit nutrients and biochemical signals to the VICs. They can secrete nitric oxide, prostacyclin, and endothelin 1<sup>109</sup>, and they express the von Willebrand factor<sup>96</sup>.

The matrix of a valve leaflet is composed of VICs. The VICs maintain and repair valve structure and are the main type of cells of the valve. Two populations of VICs can be distinguished: fibroblasts and  $\alpha$ -smooth muscle actin ( $\alpha$ SMA)-positive cells<sup>109</sup>, called myofibroblasts<sup>113</sup> (**Figure 2-7**). A healthy valve is composed mostly of normal fibroblasts<sup>113</sup>, which are different from dermal fibroblasts<sup>109</sup>. VICs can also synthesize extracellular matrix (ECM) components<sup>109</sup> such as collagen, proteoglycans, and elastin<sup>114</sup>. Five different VIC's phenotypes have been identified: embryonic progenitor endothelial/mesenchymal cells, quiescent VICs, activated VICs, progenitor VICs, and osteoblastic VICs<sup>115</sup> (**Table 2-1**). VICs communicate through cell-cell junction molecules including cadherins, desmosomal junctions, and gap-junction proteins or connexins<sup>109</sup>. Recently, another class of VICs called telocytes was identified in aortic, mitral, and tricuspid valves. Telocytes are interstitial cells with long and thin prolongations, named telopodes, that may help to increase flexibility and may serve as mechanical support for the valve<sup>114</sup>.

**Table 2-1.** Different types of VICs<sup>115,116</sup>.

<b>Cell type</b>	<b>Location</b>	<b>Function</b>
Embryonic progenitor endothelial/mesenchymal cells	Embryonic cardiac cushion	Give rise to resident VICs
qVICs	Heart valve leaflets	Maintain physiologic valve structure and function, inhibit angiogenesis in the leaflets
pVICs	Bone marrow, circulation and/or heart valve leaflets	Enter valves or reside in valves to provide aVICs to repair the heart valve
aVICs	Heart valve leaflets	$\alpha$ SMA positive cells that activate cellular repair processes including proliferation, migration, and matrix remodeling
obVICs	Heart valve leaflets	Calcification, chondrogenesis, and osteogenesis in the heart valve

qVICs: quiescent VICs, pVICs: progenitor VICs, aVICs: activated VICs, and obVICs: osteoblastic VICs.

## 2.5 Embriogenesis of the aortic valve

During the first trimester of gestation in human, the major organs are formed, starting with the heart: allowing the flow of blood and feeding of the embryo. Then, the organs mature and grow. The first cardiac structures appear at day 15 of gestation<sup>117</sup>. Atrioventricular valves are formed first, followed by semilunar valves from the atrioventricular cushion region of the heart tube. The outflow tract cushion region lead to aortic and pulmonary valve formation<sup>118</sup>. During weeks 6 and 7, the heart is divided in four chambers, plus the aorta and pulmonary arteries, establishing pulmonary and systemic circulations. At day 49, the aorta and pulmonary artery are septated and each has three leaflets<sup>117</sup>. When two of the leaflets remain fused in the aorta, a bicuspid aortic valve is formed (**Figure 2-8**).

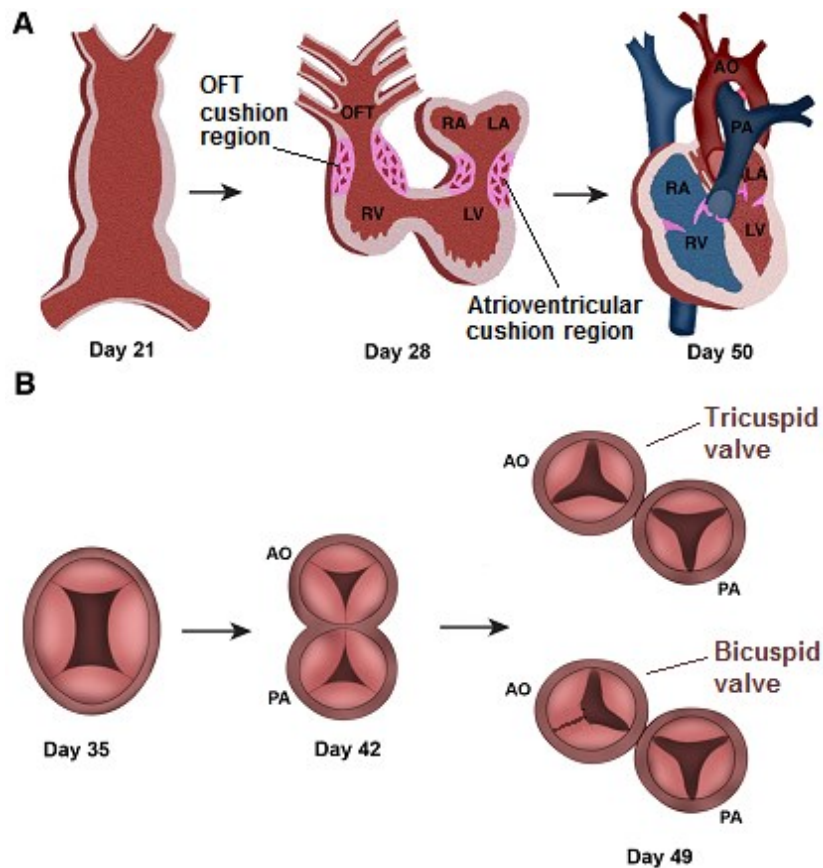


**Figure 2-8.** Overview of heart and valve development. A) At day 50 of gestation the heart is completely developed with partitioned systemic (red) and pulmonary circulations (blue). B) At day 49 the aorta (AO) and pulmonary (PA) artery are septated. When two of the leaflets remain fused in the aorta, a bicuspid aortic valve results<sup>117,118</sup>. LA: left atrium, LV: left ventricle, OFT: outflow tract, RA: right atrium, RV: right ventricle. Figure taken from La Haye *et al.*<sup>118</sup>, license number 3614440619568.

The formation of the valves begins around days 31-35 of gestation with the development of the endocardial cushions, while the heart is still a tube. The first stage involves the process of endothelial to mesenchymal transformation. The signals of this transformation come from the myocardium and the endocardial cells. A subset of endocardial cells loses cell-cell contacts, migrates to the cardiac jelly, a hyaluronic acid-rich ECM between the endocardial and myocardial cells, and is transformed to mesenchymal cells<sup>118,119</sup>. This valve primordia develops by a process of thinning, reshaping, elongation and remodeling of the ECM, finishing with the final tri-layer structure of the valve **Figure 2-9**<sup>118</sup>.

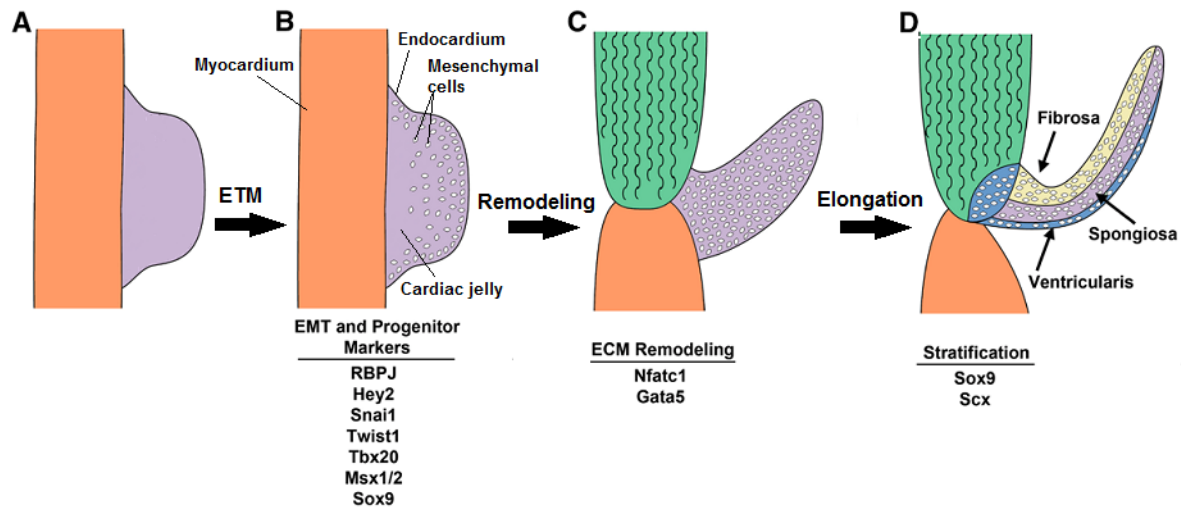


**Figure 2-9.** Semilunar valve maturation. Endocardial cells undergo epithelial-to-mesenchymal transformation (EMT) and generate mesenchymal cells that populate the cushions. The mesenchymal cushions then remodel and elongate to become thin valve leaflets. Some transcription factors active in aortic valve development are shown<sup>120,121</sup>. Figure modified from Wirrig & Yutzey<sup>121</sup>, license number 3614440927425.

Several lineage and cellular processes are involved in the process of outflow tract septation and semilunar valves development, which are controlled by several genetic programs that include signaling, transcription, epigenetics, and adhesion/migration factors. Some important molecules are *TGFBR1/2*, bone morphogenetic protein 2 (*BMP2*), and *NOTCH1*. Studies of heart and valve development have been performed mainly in mice and chicks<sup>120</sup>. Mutations in genes implicated in valve formation have been associated with congenital heart diseases.

## 2.6 Aortic valve diseases

Dysfunction of heart valves can be classified as either narrow (stenosis) or leaky (regurgitation)<sup>122</sup>. Stenosis leads to outflow obstruction, and regurgitation to backward flow. Diseases of the heart valves compromise the normal valvular functions, leading to more complications to the surrounding structures. Aging of the population and improvement of diagnosis of valvular diseases by echocardiography have caused an increase in the prevalence of these illnesses. CAVD prevalence is expected to double within the next 50 years<sup>1</sup>. In Scotland, the age- and sex-standardized incidence of patients hospitalized with a diagnosis of aortic stenosis increased from 246 per million in 1997 to

365 per million in 2005<sup>1</sup>. Valvular diseases have become a major public health burden causing 23,141 deaths in 2010<sup>123</sup> or 7 per 100,000 individuals per year<sup>124</sup> in United States (USA).

Survival rates are lower in patients with valvular diseases than in patients with healthy valves<sup>125</sup>. Survival rates of individuals with valvular diseases was 79% at 5 years and 68% at 8 years compared with 93% and 86% at 5 and 8 years, respectively, in individuals without valvular diseases<sup>125</sup>. In 2010, 106,000 valve procedures were performed in the USA, of which 64% were in men. In 2012, the mean hospital charge for valve procedures was \$190,194 USD<sup>123</sup>. In Canada, almost 9,000 heart valve surgeries were performed in 2005, representing an increase of approximately 38% since 1995<sup>126</sup>. In Canada the cost of an aortic valve replacement surgery is estimated at \$74,602 CAN<sup>127</sup>. In developed countries, the main cause of valvular disease is calcification, in contrast with developing countries where the main cause is rheumatic fever. In Brazil, among 174 patients with severe valvular disease (mean age  $56 \pm 17$  years and 54% female), the main causes of valvular disease were rheumatic (60%), degenerative aortic disease (15%), and mitral valve prolapse (13%)<sup>128</sup>.

In the USA, the prevalence of valvular diseases is 2.4% for men and 2.5% for women without statistical difference between genders<sup>125</sup>. However, a significantly higher prevalence of aortic stenosis was observed in men compared to women after adjustment for age ( $P = 0.04$ ). The most common valvular diseases are mitral regurgitation, aortic stenosis, aortic regurgitation, and mitral stenosis. In a combined study of the Atherosclerosis Risk in Communities Study (ARIC), the Coronary Artery Risk Development in Young Adults (CARDIA), and the Cardiovascular Health Study (CHS) population studies (combined  $n = 11,911$ ), the prevalence of these valvular diseases was 1.7% (95% CI 1.5–1.9) for mitral regurgitation, 0.5% (95% CI 0.3–0.6) for aortic regurgitation, 0.4% (95% CI 0.3–0.5) for aortic stenosis, and 0.1% (95% CI 0.02–0.2) for mitral stenosis. The overall prevalence of these valvular diseases increases with age from 0.7% in ages between 18 to 44 years to 11.7% in individuals older than 75 years. All

valvular diseases were also more frequent with age<sup>1,125,129</sup>, an example is shown for aortic stenosis in **Figure 2-10**.

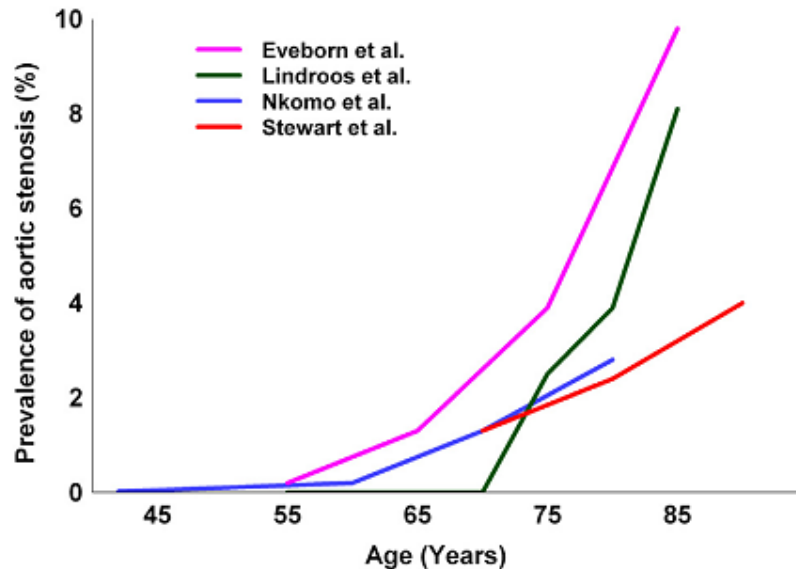


**Figure 2-10.** Prevalence of aortic stenosis according to age. Results based on four population-based studies from Norway in pink (Eveborn *et al.*<sup>130</sup>), Finland in green (Lindroos *et al.*<sup>129</sup>), and USA in blue and red (Nkomo *et al.*<sup>125</sup> and Stewart *et al.*<sup>131</sup>). Figure taken from Lung & Vahanian<sup>1</sup>, license number 3614911298078.

Diseases of the right-sided valves are less common as shown in the European Heart Survey where the incidence was of 1%<sup>132</sup>. Some degree of tricuspid regurgitation is considered to be physiological. Organic tricuspid disease is rare and is usually due to pulmonary hypertension and other diseases. Pulmonary valve diseases can be congenital or associated with other congenital diseases<sup>133</sup>. Multivalvular diseases, post-interventional valvular lesions, and valvular tumors also exist<sup>125</sup>.

### 2.6.1 Causes of aortic valve disease

Aortic stenosis is globally the third most frequent heart disease after hypertension and coronary artery disease. Aortic stenosis is also the most frequent heart disease in industrialized countries<sup>125</sup>. Although mitral regurgitation is more common than aortic stenosis, the latter is the most frequent single-valve disease (43%) in patients referred to hospitals<sup>1</sup>. Approximately 50% of patients with severe aortic stenosis are referred to cardiac



surgery and 40% undergo aortic valve replacement surgery<sup>123</sup>. Aortic stenosis is currently the principal indication for valve replacement surgery in North America and Europe<sup>134</sup> and the second most frequent cardiac surgery after coronary artery bypass grafting<sup>135</sup>. The main causes of aortic stenosis are: congenitally abnormal (often bicuspid) valve, CAVD, and rheumatic valve disease (**Table 2-2**)<sup>89</sup>.



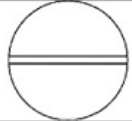


**Table 2-2.** Causes of aortic valve stenosis.

<b>Common</b>
Bicuspid aortic valve
CAVD
Rheumatic valve disease
<b>Uncommon</b>
Congenital aortic stenosis (unicommissural, quadricuspid, others)
Homozygous type II hyperlipoproteinemia
Metabolic infiltrative disorders (e.g. Fabry disease)
Systemic lupus erythematosus
Ochronosis with alkaptonuria
<b>Nonvalvular left ventricular outflow obstruction</b>
Subaortic membrane
Hypertrophic cardiomyopathy
Supravalvular aortic stenosis (e.g. Williams syndrome)

Causes of aortic regurgitation are: bicuspid aortic valve, rheumatic heart disease or infective endocarditis (which causes leaflet deformities), aortic root disease, aortic valve rupture or cusp perforation following chest trauma, and other<sup>133</sup>.

## 2.6.2 Congenital aortic valve disease

Four aortic valve configurations have been observed, unicuspid, bicuspid, tricuspid, and quadricuspid depending on the number of leaflets in the valve<sup>135-137</sup> (**Figure 2-11**). The tri-leaflet design offers the optimal solution for low resistance valve opening and is the most common in the population. With other valve configurations, there is always a co-existing degree of stenosis or valve dysfunction<sup>105</sup>.

Commonly used terms		quadricuspid	tricuspid	bicuspid		
Scheme of morphological appearance						
functional characteristics	No of cusps	4	3	2	2	2
	No of raphe	0	0	0	1	2
morphological characteristics	No of cusps	4	3	purely bicuspid*	potentially tricuspid*	
				2	3 anlagen, (2 under- and 1 fully developed)	3 anlagen, (2 under- and 1 fully developed)
	Size of cusps	non-equal	equal	equal	non-equal	non-equal
	No of commissures	4	3	2	1 under- and 2 fully developed	2 under- and 1 fully developed

**Figure 2-11.** Representation of the developmental phenotypes of the aortic valve. The type of valve configuration is based on the number of cusps or leaflets. The darker line in the schematic drawings of bicuspid valves represents a raphe, which defines the conjoint or sometimes called “fused” area of the two underdeveloped cusps extending into the commissural area. The unicuspid valve configuration is not shown. Figure taken from Sievers<sup>137</sup>, license number 3614920100141.

Roberts & Ko in 2005<sup>135</sup> analyzed the phenotypes of the excised aortic valves of 932 patients (26 to 91 years, mean age = 70 ± 12) with CAVD. The frequencies of the aortic valve phenotypes were 4.9% for unicuspid (n = 46, 42 unicommissural and 4 commissural), 49.1% for bicuspid (n = 458), 44.7% for tricuspid (n = 417 with absent or minimal commissural fusion), and 0% for quadricuspid. For 1.2% (n = 11) of valves, the configuration could not be determined. More men (59%) than women (46%) had unicuspid

or bicuspid valves, and this difference was significant. **Figure 2-12** shows calcified valves with different leaflet configurations. Calcified tricuspid valves can present slight ( $\leq 3\text{mm}$ ) fusion of one or more commissures<sup>135</sup>.

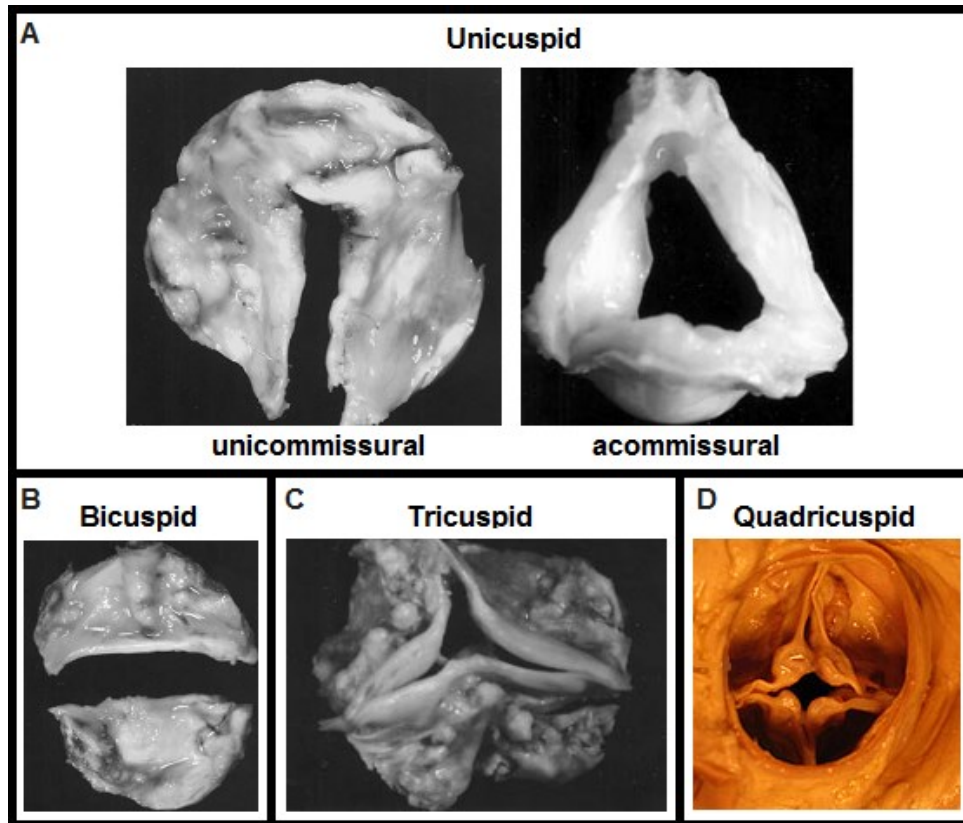


**Figure 2-12.** Phenotypes of aortic valves. A) Unicuspid valves with and without commissures. B) Purely bicuspid valve. C) Tricuspid valve. D) Quadricuspid valve is the rarer phenotype. Figures A to C are from Roberts & Ko<sup>135</sup>, license number 3614960340358. Figure D is from [https://apps.childrenshospital.org/clinical/mml/index.cfm?CAT = media&MEDIA\\_ID = 1575&OK](https://apps.childrenshospital.org/clinical/mml/index.cfm?CAT = media&MEDIA_ID = 1575&OK).

In the same study by Roberts & Ko, patients with fewer number of aortic valve leaflets, were the youngest<sup>135</sup>. Of the 46 patients with unicuspid valves, 24 (52.2%) were younger than 50 years, and 5 (10.9%) were older than 70 years. Of the 458 patients with bicuspid valves, 41 (9.0%) were younger than 50 years, and 188 (41%) were older than 70 years. Of the 417 patients with tricuspid valves, 2 (0.5%) were younger than 50 years, and 297 (71%) were older than 70 years (**Figure 2-13**). In another study on 85 autopsy patients, 75% of individuals between 15 to 65 years had unicuspid or bicuspid valves. 90% of patients with

aortic stenosis older than 65 years had tricuspid valves<sup>2</sup>. In summary, patients with unicuspid and bicuspid valves develop aortic stenosis younger than individuals with tricuspid valves.

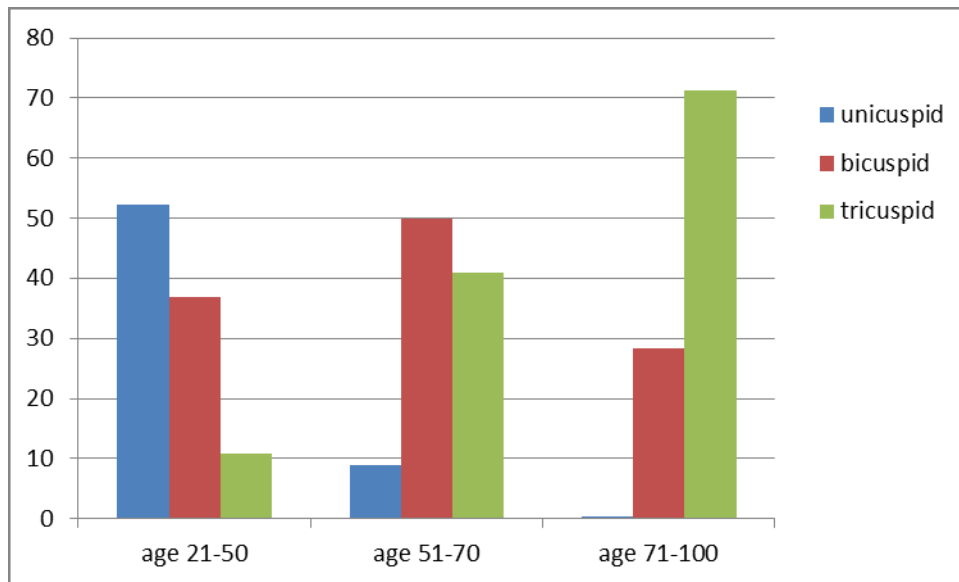


**Figure 2-13.** Valve morphology among patients undergoing aortic valve replacement. The fewer the number of aortic valve leaflets, the younger the patients. Figure by Guauque-Olarte using data from Roberts & Ko<sup>135</sup>.

### 2.6.2.1 Bicuspid aortic valve

0.6 to 2.0% of the population presents with a bicuspid valve, which is the most common congenital heart disease<sup>138</sup>. The annual prevalence of bicuspid aortic valve is 13.7 per 1,000 live births or approximately 54,800 cases per year in USA<sup>123</sup>. 70 to 80% of patients with a bicuspid valve are men<sup>137,139</sup>. Bicuspid valves present different combinations of leaflet fusion (**Figure 2-11**). The most common combinations are the fusion of the right- with left-coronary leaflets and the right-coronary with the non-coronary leaflet<sup>119,137</sup>. In a study including 304 patients (mean age  $53 \pm 15.4$  years) with bicuspid valves, 71% had right-with left-coronary leaflets fusion and 15% had right-coronary with the non-coronary fusion<sup>137</sup>. In a second study with younger patients ( $n = 1,135$ , 1 day to 17.9 years) with bicuspid valves, 70.4% had a right- with left-coronary leaflets fusion and 28.2% a right-coronary with the non-coronary fusion<sup>139</sup>.

### 2.6.2.2 *Genetics of bicuspid aortic valve*

There is strong evidence supporting the influence of genetic factors in bicuspid aortic valve disease<sup>140</sup>. Huntington *et al.*<sup>141</sup> evaluated the presence of a bicuspid aortic valve in 30 European-American families and suggested an autosomal-dominant inheritance pattern with reduce penetrance for this congenital defect. In that study, only 11 of the 30 families had more than one affected first-degree relative, which suggests that bicuspid valve may be a multifactorial disease with a single-major causative gene in a subset of patients. Specific polymorphisms in the signaling and transcriptional regulator *NOTCH1* were detected in families affected with bicuspid CAVD<sup>33,142</sup>. Garg *et al.*<sup>33</sup> performed a genome-wide linkage scan in a five-generation family with 11 cases of congenital heart disease. Nine affected individuals had aortic valve disease, including eight in which the only cardiac malformation was an abnormal aortic valve. Six affected individuals had a bicuspid aortic valve and seven presented CAVD including three individuals with a tricuspid aortic valve. The chromosomal region 9q34-35, where *NOTCH1* is located, was linked to the congenital heart disease phenotype. A nonsense mutation R1107X (rs41309764) in *NOTCH1* was only observed in affected subjects. The mutation was neither observed in unaffected family members nor in 1,136 unrelated subjects of diverse ethnicity, confirming the autosomal-dominant inheritance of the congenital disease. In addition, a frameshift mutation H1505del (rs4130976) in the gene was detected in three members from an independent Hispanic family with bicuspid aortic valve<sup>33</sup>.

Two other mutations [p.T596M (rs61755997) and p.P1797H] in *NOTCH1* were identified in patients with sporadic bicuspid aortic valve (non-familial type)<sup>143</sup>. In another cohort of patients with bicuspid valves and concomitant thoracic aortic aneurysms, two other mutations (p.A1343V and p.P1390T) in *NOTCH1* were identified<sup>144</sup>. Foffa *et al.*<sup>142</sup> performed a mutational screening by direct gene sequencing of 11 probands (mean age = 42 ± 19 years) from 11 independent Italian families with familial bicuspid aortic valve disease. The genes screened were *NOTCH1*, GATA binding protein 5 (*GATA5*), *TGFBR1*, and *TGFBR2*. A new missense and a nonsense mutation (p.P284L and p.Y1619X) plus three other variants were found in *NOTCH1* in two families. The mutations were not found in 100 ethnically matched controls. No mutation was found in the other three genes.

Bicuspid valve disease can occur with other congenital abnormalities such as aortic coarctation. Bicuspid valves have been observed in patients with Turner and other syndromes<sup>89,145</sup>. Bicuspid aortic valve was present in 4% and 7% of individuals with mutations in fibrillin 1 (*FBNI*) and *TGFBR2*, respectively<sup>146</sup>. The 4% of patients with bicuspid valves and *FBNI* mutations had Marfan syndrome, while all patients with a bicuspid valve and *TGFBR2* mutations also presented thoracic aortic aneurysm. Mutations in *TGFBR2* were also observed in 10 families presenting a syndrome with an autosomal-dominant inheritance characterized by perturbations in cardiovascular, craniofacial, neurocognitive, and skeletal development<sup>146</sup>. Two specific mutations (A355P and G357W) in *TGFBR2* were observed in the only two families with bicuspid aortic valve<sup>146</sup>.

A missense mutation (R67W) in potassium channel, inwardly rectifying subfamily J, member 2 (*KCNJ2*) was observed in individuals with the Anderson syndrome. One feature of this syndrome includes the presence of a bicuspid aortic valve. In addition, in a family-based genome-wide linkage analysis [n = 38 families (353 individuals)], chromosomal regions 18q, 5q15-21, and 13q33 (where *KCNJ2* is located) were associated with bicuspid aortic valve and/or associated with cardiovascular malformations<sup>147</sup>.

In the study of Guo *et al.*<sup>148</sup>, three individuals in six families with actin, alpha 2, smooth muscle, aorta (*ACTA2*) missense mutations had bicuspid aortic valves. The six families had thoracic aortic aneurysms and dissections. More recently, methionine adenosyltransferase II, alpha (*MAT2A*) variants, identified by whole-genome linkage analysis and exome sequencing, were identified in individuals with autosomal-dominant inheritance of thoracic aortic aneurysms and bicuspid aortic valve<sup>149</sup>.

Mouse models with mutations in *Gata5*<sup>150</sup>, homeobox A1 (*Hoxa1*)<sup>151</sup>, NK2 homeobox 5 (*Nkx2-5*)<sup>137</sup>, and nitric oxide synthase 3 (*NOS3*)<sup>152</sup> developed bicuspid aortic valves and other cardiovascular abnormalities. The prevalence of bicuspid valves was 41.6% for *NOS3* mutants, 25% for *Gata5* mutants, 23.5% for *Hoxa1* mutants, and 8.2% for *Nkx2-5* mutants.

In summary, mutations in *ACTA2*, *FBN1*, *KCNJ2*, *MAT2A*, *NOTCH1*, and *TGFBR2* have been observed in individuals with bicuspid aortic valves. Except for variants in *NOTCH1*, the other variations were identified in individuals with different syndromes without isolated bicuspid aortic valve disease. Mouse models that develop a bicuspid aortic valve presented other cardiac abnormalities. Thus, it is necessary to identify new variants and genes that can explain the development of the bicuspid phenotype in humans.





## Chapter 3. Calcific aortic valve disease

CAVD is an age-related degenerative disease of the aortic valve<sup>153</sup>. The obstruction of the blood flow through the aortic valve is due to the thickening, fibrosis, and calcification of the valve leaflets (**Figure 3-1**). CAVD causes stiffening, impaired motion, and the loss of valve functionality<sup>154</sup>. CAVD is caused by the deposition of calcium within the valve leaflets<sup>155</sup>.

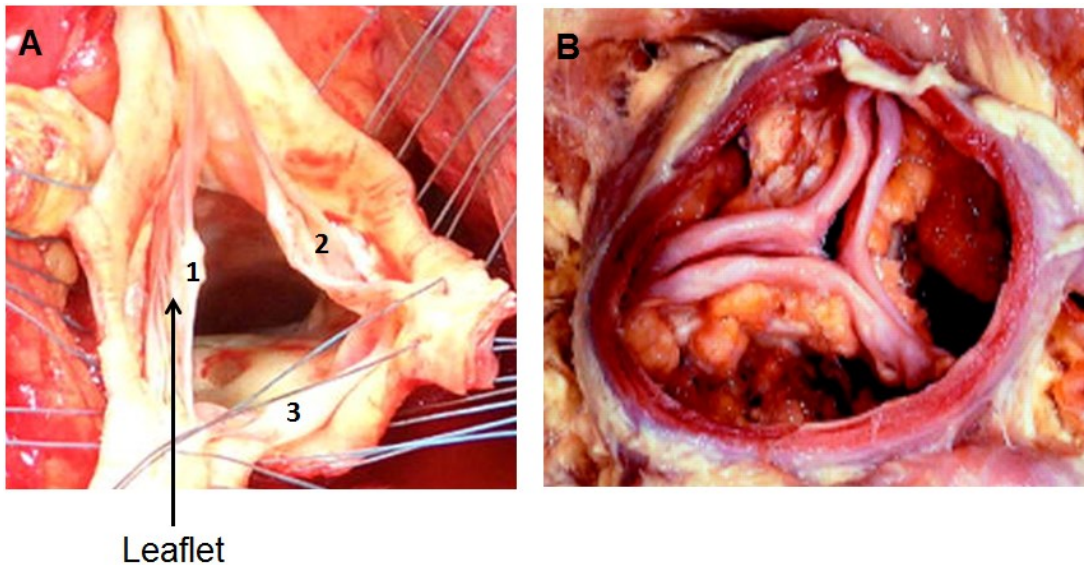


**Figure 3-1.** Tricuspid aortic valves. A) Normal aortic valve with each leaflet numbered. B) Tricuspid aortic valve with CAVD. Figures A and B were taken from Beckmann *et al.*<sup>156</sup> and Boon & Bloomfield<sup>157</sup>, respectively. Figure license B) 3614970820857.

### 3.1 Epidemiology

CAVD is the most frequent heart valve disease in developed countries<sup>132,155,158,159</sup>. In the Multi-Ethnic Study of Atherosclerosis (MESA, n = 5,880, mean age  $61.8 \pm 10.1$  years, 60% nonwhite), the prevalence of incident calcification, measured by CT scan, was 13%. The incidence rate increases significantly with age being 3.5% in patients between 70 to 79 years<sup>160</sup> (**Figure 3-2**). In the Epidemiology of Coronary Artery Calcification (ECAC) study<sup>161</sup> (n = 1,376, age  $\geq 60$  years), aortic valve calcium prevalence was 27% and also increased with age. Prevalence of aortic valve calcium was 19% between 60 and 69 years and 42% after 70 years. In the same study the prevalence of aortic valve calcium was significantly higher in men than in women.

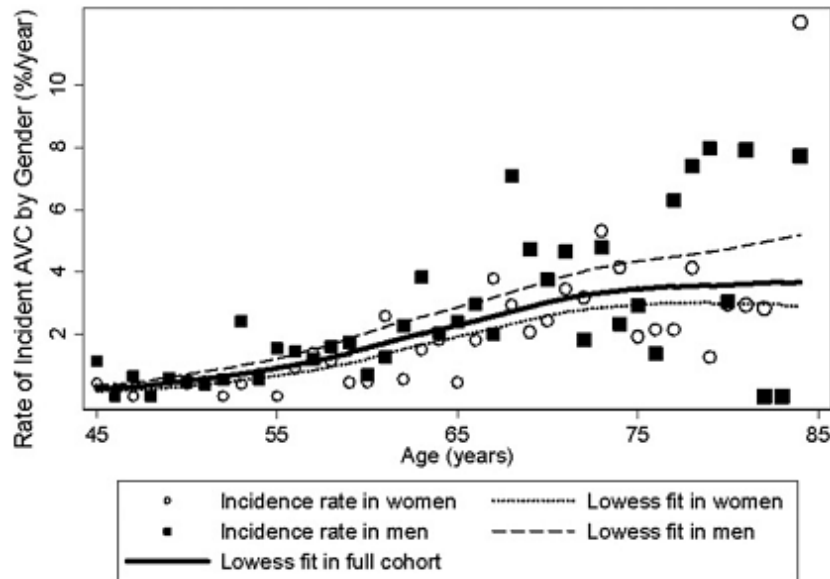


**Figure 3-2.** Average incidence rate of aortic valve calcium. Average incidence rate of aortic valve calcium (% per year) by yearly age increments among those free of aortic valve calcium at baseline. The size of the scatter points is weighted by the number at risk at each age category. A marked increase in aortic valve calcium incidence rate is seen with advancing age. Figure taken from Owens *et al.*<sup>160</sup>, license number 3614971001322.

In the MESA study, incidence of aortic valve calcium and rate of progression was not significantly different between individuals with European ancestry, African American, Chinese, and Hispanic populations<sup>160</sup>. However, the study by Patel *et al.*<sup>162</sup> indicates that African American have a significantly lower prevalence of aortic stenosis (by calcification or bicuspid etiology) compared to individuals with European ancestry. Patel *et al.* selected a sample of patients (mean age 45 years, 44% male) with echocardiography from the Synthetic Derivative at Vanderbilt University Medical Center, which is a database including medical records for 2.1 million patients. They concluded that 0.29% of African American (n = 36,681) have severe aortic stenosis compared with 0.91% of Caucasian (n = 222,976) (adjusted OR = 0.41, 95% CI [0.33, 0.50]). African Americans have also a smaller risk of developing CAVD (adjusted OR = 0.47, 95% CI [0.36, 0.61]) and valve calcification of bicuspid etiology (OR = 0.13, 95% CI [0.02, 0.80]). The lower prevalence of CAVD in African Americans could not be explained by the traditional risk factors such as male gender, age or hypertension, among others.

### 3.2 Symptoms and complications

Symptoms of CAVD include angina (chest pain), syncope, and heart failure (primarily dyspnea)<sup>89,155,163</sup>. Syncope is the transient loss of consciousness because of poor cerebral perfusion. Heart failure is the impaired ability of the heart to pump blood at a normal rate. Angina is developed by 35% of patients<sup>155</sup>. Angina is due to the poor filling of the coronary arteries and increased oxygen demands of a hypertrophic ventricle<sup>89</sup>. Patients with a valve orifice < 1.5 cm<sup>2</sup> develop left ventricular hypertrophy which is associated with increased mortality<sup>155</sup>. Left ventricular hypertrophy or thickening of the left ventricle wall is due to the increase in the pressure required for blood flow through the valve orifice, which can lead to ventricular arrhythmia and sudden death<sup>89</sup>. Sudden death also occurs because of ischemic changes, especially in patients treated conservatively<sup>124</sup>.

### 3.3 Diagnosis

CAVD has been divided in three degrees of severity (mild, moderate, and severe), but it develops as a disease continuum<sup>164</sup> (**Table 3-1**). This grading is based on hemodynamic and natural history data and it is determined using values of aortic jet velocity, mean gradient, and aortic valve area<sup>164</sup>. CAVD is initially identified during auscultation by changes in the typical crescendo-decrescendo systolic ejection murmur<sup>155</sup>. Depending on the degree of the murmur, patients are referred for further evaluation by Doppler echocardiography, which is the reference method for the diagnosis of CAVD.

**Table 3-1.** Classification of CAVD in adults<sup>164</sup>.

Degree of aortic stenosis	Peak jet Velocity (m/s)	Mean gradient (mmHg)	Aortic valve area (cm <sup>2</sup> )	Indexed aortic valve area (cm <sup>2</sup> /m <sup>2</sup> )
Mild	2 – < 3	< 25	> 1.5	-
Moderate	3 – 4	25 – 40	1.0 – 1.5	-
Severe	> 4	> 40	< 1.0	< 0.6

Echocardiography analysis can determine the severity of CAVD and its effect on the left ventricle by assessing left-ventricular function, degree of hypertrophy and calcification, transvalvular pressure gradient, and aortic valve area<sup>155,164</sup>(**Figure 3-3**).

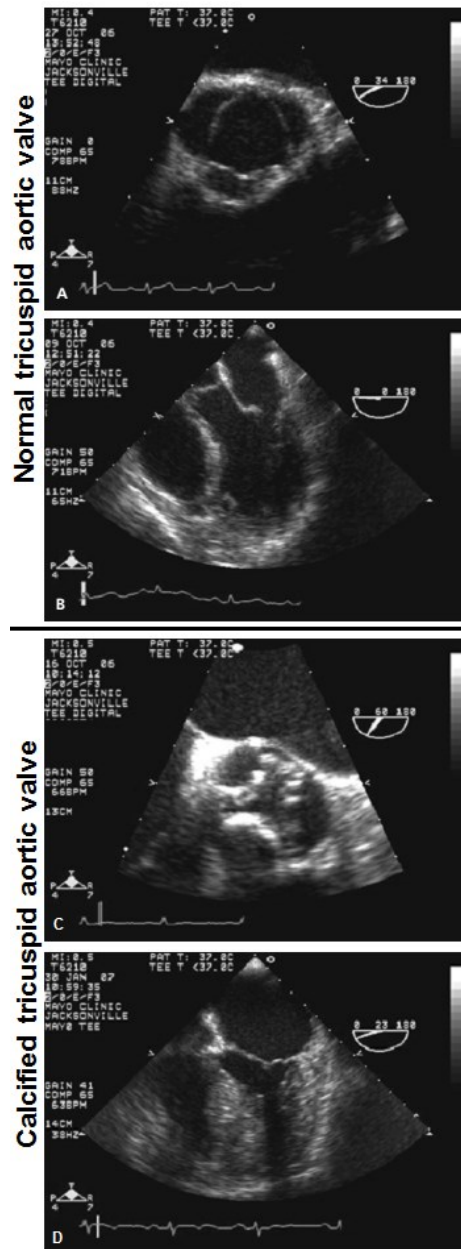


**Figure 3-3.** Transesophageal echocardiograms of aortic valves. A) Axial view of a normal tricuspid valve. (B) Horizontal four-chamber view of the same normal valve. C) Axial view of a severe stenotic valve, with diffusely thickened leaflets and a restricted opening motion. D) Horizontal four-chamber view of the calcified valve showing the resultant severe left ventricular hypertrophy and left atrial enlargement. Figure taken from Grimard & Larson<sup>165</sup> with permission of the author.

The degree of CAVD is based on the measurement of the following three parameters:

- **Peak jet velocity (or peak transvalvular flow velocity).** The aortic valve opens in systole during ventricular contraction and closes during diastole when the ventricle is relaxed. Normally, blood flows through the aortic valve, accelerating to a peak value of  $1.35 \pm 0.35$  m/s. This peak jet velocity is increased in patients with CAVD<sup>166</sup>.
- **Mean pressure gradient.** The pressure gradient is the pressure difference between the ventricular and the aortic side of the valve. The speed of the blood flow through the valve is used to calculate the pressure gradient through the valve using a modification of the Bernoulli equation,  $G = 4V^2$ , where G is the gradient and V is the peak jet velocity. The average difference over the duration of blood flow is the mean gradient<sup>167</sup>. The mean gradient increases in severe CAVD.
- **Aortic valve area** is the area between the leaflets during left ventricular systole. The measurement of the aortic valve area directly (geometric or anatomic valve area) is not reliable. The effective aortic valve area is measured in clinic using the continuity equation. The principle of the equation is that the stroke volume proximal to the valve (LVOT or left ventricle outflow track) is equal to the stroke volume through the stenotic valve<sup>106,167,168</sup>. The stroke volume is the volume of blood pumped from the left ventricle at each heartbeat. The stroke volume is equal to the product of the cross-sectional area (of the LVOT or stenotic valve) by the velocity inside this area. The LVOT area and the velocity are obtained by echocardiography, thus the aortic valve area can be extrapolated<sup>168</sup> (**Figure 3-4**). The normal aortic valve area is usually 3 to 4 cm<sup>2</sup><sup>169</sup>. The aortic valve area can be indexed to the body surface to adjust the valve area to the hemodynamic necessities of each patient<sup>155</sup>. An aortic valve area of 0.9 cm<sup>2</sup> can indicate mild stenosis in a small person and severe stenosis in a larger person.

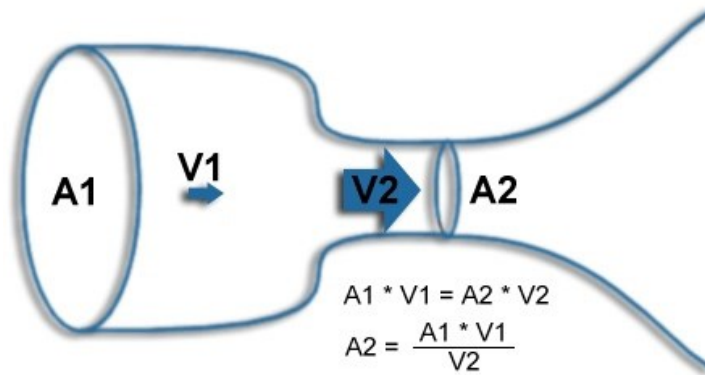


**Figure 3-4.** Schematic diagram of the continuity equation. Aortic valve area is calculated based on the continuity equation concept that the stroke volume (SV) ejected through the LVOT passes completely the stenotic orifice and thus SV is equal on both sides:  $SV_{AV} = SV_{LVOT}$ .  $A1$  = LVOT area.  $V1$  = LVOT velocity time integral.  $A2$  = aortic valve area.  $V2$  = aortic valve velocity time integral ([www.echobasics.de/klappen-en.html](http://www.echobasics.de/klappen-en.html)).

Severe CAVD with a normal cardiac output is associated with a mean transvalvular pressure gradient greater than 40 mmHg. However, some patients with low cardiac output can present severe stenosis with a lower transvalvular gradient and velocity<sup>164</sup>. When inconsistencies exist between the patient history, physical examination, and echocardiographic results, the degree of severity cannot be established and cardiac catheterization and coronary angiography may be required<sup>155,164</sup>.

Clinical imaging techniques can complement the use of echocardiography for the diagnosis and follow up of CAVD patients. Multidetector computed tomography accurately measures the mineralization of leaflets<sup>170</sup>. Magnetic resonance imaging is not commonly used in clinics for the diagnosis of aortic stenosis but a recent study by Le Ven *et al.*<sup>171</sup> showed that magnetic resonance imaging can quantify the tissue components within the valve leaflet, not only calcium but also lipids and fibrous constituents. This is an advantage over multidetector computed tomography that can only quantify mineralization.

### **3.4 Biomarkers**

Biomarkers are used in research and clinical practice because they provide information about current status or future risk of disease. They should be objective laboratory measurements. Several biomarkers have been studied for their use in the prediction of CAVD risk and disease status<sup>156</sup>. CAVD is a disease developing in several stages (as explained in the next section), and the symptoms do not appear in the first stage. Various biomarkers that may help to identify each stage of CAVD development have been studied<sup>156</sup>.

Although biomarkers could be useful to identify patients who may benefit from valve replacement surgery, they have been associated with other diseases that are usually comorbidities of CAVD. Thus, their application in CAVD might lack specificity<sup>155,172</sup>. **Table 3-2** summarizes the current biomarkers for CAVD.

**Table 3-2.** Current biomarkers for CAVD<sup>156,172-175</sup>.

Stage	Biomarkers	Description
Mechanical stress Endothelial dysfunction	ADMA (Asymmetric dimethylarginine)	Inhibitor of nitric oxide synthase. Increased plasma ADMA was associated with CAVD. <b>Cons:</b> Study performed only in moderate and severe CAVD. <b>Use:</b> Severity <b>Other diseases:</b> Homocysteinemia, diabetes mellitus, chronic kidney disease and cardiovascular diseases.
	Homocysteine	Associated with severity of CAVD. Increased levels in CAVD patients compared to controls. <b>Cons:</b> Contradictory results may be due to statistical power. <b>Other diseases:</b> Homocysteinemia, diabetes mellitus, chronic kidney disease and cardiovascular diseases.
	tPA (Tissue plasminogen activator)	Secreted by endothelial cells. Catalyzes the conversion of plasminogen to plasmin, resulting in fibrinolysis. Increased plasma levels in severe CAVD patients compared to controls. <b>Cons:</b> Study performed only in moderate and severe CAVD. <b>Use:</b> Severity <b>Other diseases:</b> To treat myocardial infarction, ischemic stroke, deep venous thrombosis and pulmonary embolism.
Lipid deposition	LDL	Oxidized LDL was associated with worse fibrocalcific remodeling of valve tissue of patients suffering from AS. LDL-cholesterol predicts CAVD development. LDL-cholesterol was associated with presence of aortic valve calcium and incidence of aortic stenosis. <b>Use:</b> Severity
	Leptin	Hormone produced by adipocytes that acts in energy balance. Increased plasma levels in CAVD patients compared to controls. <b>Cons:</b> Role in CAVD is unclear. Study only in moderate and severe CAVD. <b>Other diseases:</b> Myocardial infarction
	Lp-PLA2 (lipoprotein-associated phospholipase A2)	Used oxidized LDL to produce free fatty acids and lysophosphatidylcholine (LPC), a proinflammatory and procalcifying factor. Associated with a faster stenosis progression rate in the subset of patients with mild AS. <b>Use:</b> Prognosis <b>Other diseases:</b> Coronary artery disease, Alzheimer's disease.
Inflammation	CRP (C-reactive protein)	Increased plasma levels in severe CAVD patients compared to controls. CAVD progress faster in patients with higher levels of CRP. <b>Cons:</b> Weak association with aortic sclerosis. Contradictory results. <b>Use:</b> Prognosis <b>Other diseases:</b> Infections, atherosclerosis, auto-immune disease.



Stage	Biomarkers	Description
ECM remodeling	-	There is no biomarker yet.
Calcification	Fetuin-A	Glycoprotein produced by the liver. Inversely correlated with vascular calcification in patient with and without renal disease, and in patients with diabetes. <b>Cons:</b> Unclear results <b>Use:</b> Severity
	CaxP (calcium-phosphorus product)	Predictor of calcification in nephrology. Inversely related to aortic valve area. Directly related to peak and mean transvalvular gradients. <b>Cons:</b> Influenced by other diseases <b>Use:</b> Presence, severity
	Osteopontin	Glycophosphoprotein with regulatory function in bone remodeling. Related with biomineralization of dystrophic and ectopic sites, including aortic valve tissue. Increased plasma levels in severe CAVD patients compared to mild CAVD and controls. <b>Cons:</b> Little number of patients studied <b>Use:</b> Severity <b>Other diseases:</b> Chronic inflammatory diseases
	dpMGP [desphosphorylated matrix g-carboxyglutamate (Gla) protein]	Inhibitor of vascular calcification. Higher plasma levels of total dpMGP was associated with faster progression of CAVD in younger patients. <b>Cons:</b> Correlation is weak <b>Use:</b> Prognosis <b>Other diseases:</b> Heart failure, chronic kidney disease
Clinical symptoms	BNP (B-type natriuretic peptide) and Pro-BNP	Released from myocytes in volume-loaded and pressure-loaded conditions such as CAVD. Patients who present symptoms have higher BNP levels than patients who never develop symptoms. High BNP levels at baseline are a predictor of poor outcome after aortic valve replacement. <b>Cons:</b> It has not been possible to determine the specific range of BNP and pro-BNP levels to identify CAVD patients. That problem can be solved by comparing BNP levels at baseline and during follow up for each patient. <b>Use:</b> Severity, prognosis <b>Other diseases:</b> Renal disease, pulmonary hypertension, and obesity
	GGT (Gamma-glutamyl transferase)	Liver enzyme. Counteracts oxidative stress. Correlation with severe CAVD. <b>Cons:</b> Study only in moderate and severe CAVD. <b>Other diseases:</b> Hepatic disease and alcohol intake.

### 3.5 Natural history

CAVD has a long period of latency before the onset of symptoms. Severe stenosis of the aortic valve is preceded by aortic sclerosis, the thickening of the valve without significant obstruction. In the CHS study (n = 5,201, age > 65 years), 26% of individuals had aortic sclerosis and 2% had aortic stenosis<sup>131</sup>. Thus, not every individual with aortic valve sclerosis progresses to CAVD.

Cosmi *et al.*<sup>176</sup> studied 2,131 patients with aortic sclerosis. In those patients, the rate of progression from aortic sclerosis to mild CAVD was 10.5%, to moderate CAVD was 2.9%, to severe CAVD was 2.5% during a mean follow-up of 7 years. Most patients developed moderate CAVD after 6 years and severe CAVD after 8 years of follow-up. Other studies indicate that when moderate stenosis is present, jet velocity increases 0.3 m/s per year, mean pressure gradient increases 7 mmHg per year, and valve area decreases 0.1 cm<sup>2</sup> per year<sup>164,177</sup>. In the MESA study the mean incidence rate of progression was 1.7% per year<sup>160</sup>. In a meta-analysis that summarized the results of 22 studies about aortic sclerosis, the rate of progression to severe CAVD was 1.8% to 1.9% per year<sup>178</sup>. In the same meta-analysis, patients with aortic sclerosis had 68% risk of coronary events, 27% risk of stroke, and 69% increased risk of cardiovascular mortality.

Most patients develop symptoms of CAVD between the seventh and ninth decades of life<sup>179</sup> (**Figure 3-5**). After the onset of the symptoms, patients have a 5-year risk of about 80% of aortic valve replacement or death<sup>177</sup>. In the absence of aortic valve replacement, the mortality rate is about 25% per year<sup>155</sup>. The average survival time depends on the symptoms and is five years after angina, three years after syncope, and two years after heart failure<sup>180</sup>. On average, 50% of individuals who develop symptoms and do not undergo aortic valve replacement surgery will die 2-3 years after the onset of symptoms<sup>179,180</sup>.

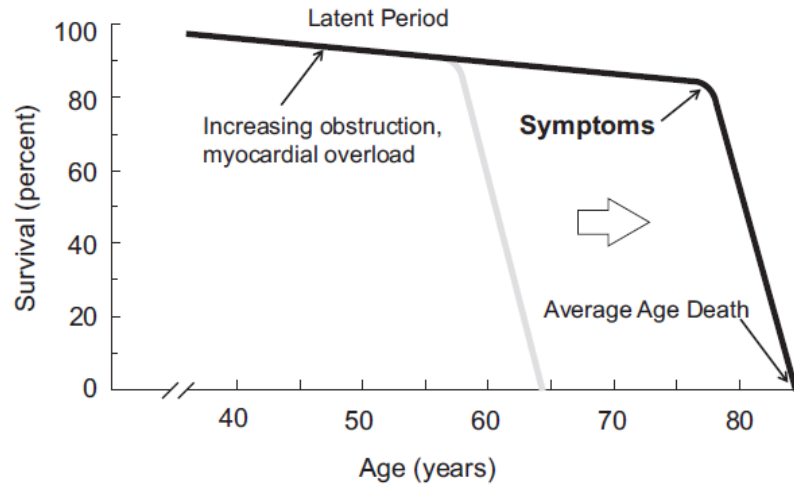


**Figure 3-5.** The natural history of aortic stenosis. Valvular stenosis and left ventricular hypertrophy gradually increase over time. Ross & Braunwald in 1968 hypothesized the onset of symptoms between the fifth and sixth decade of life (light gray curve). Nowadays, the natural history curve often shifts to the right with patients presenting symptomatic CAVD in the seventh through ninth decades. The poor survival rate after the onset of the symptoms in the absence of aortic valve replacement have been confirmed<sup>155,180</sup>. Figure taken from Bonow & Greenland<sup>179</sup>, license number 3615031247814.

### 3.6 Risk factors

The strongest risk factor for CAVD is a congenitally bicuspid valve<sup>89</sup>. The classical risk factors of cardiovascular disease have been associated with increased risk of CAVD including age, male gender, body mass index, and smoking (**Table 3-3**).

**Table 3-3.** Clinical factors associated with CAVD.

<b>Clinical Factors</b>	
Age <sup>125,131,160,162,181</sup>	Lipoprotein(a) [Lp(a)] <sup>131,182</sup>
Body mass index <sup>160,181</sup>	Male gender <sup>131,160,162,181</sup>
Calcium baseline score <sup>160</sup>	Metabolic syndrome <sup>183</sup>
Diabetes <sup>160,162,183</sup>	Phosphorous <sup>184</sup>
Height <sup>131</sup>	Renal dysfunction <sup>106,160</sup>
Hypertension <sup>131,183</sup>	Smoking <sup>131,160,181</sup>
LDL cholesterol <sup>131,175,183</sup>	Total cholesterol <sup>160,181</sup>

### 3.6.1 Bicuspid valve calcification

Bicuspid aortic valve (**Figure 3-6**) causes severe aortic stenosis in childhood and increases the risk of aortic stenosis in adults. CAVD progresses faster in patients with bicuspid valves than in patients with tricuspid aortic valves. In bicuspid valve patients, fibrosis starts at the second decade of life, while calcification starts at the fourth decade<sup>2</sup>. In the Olmsted County community based study<sup>185</sup> (n = 212 asymptomatic individuals, baseline mean age  $32 \pm 20$  years; 65% male), aortic valve replacement was performed at a mean age of  $49 \pm 20$  years in individuals with a bicuspid aortic valve and mean age  $67 \pm 16$  years in patients with a tricuspid aortic valve; this difference was significant. If calcification is present, it may be difficult to identify the number of leaflets on clinical imaging, specially echocardiography, but surgeons, during aortic valve replacement, can identify the type of valve<sup>89</sup>. Other cardiovascular surgeries also occurred at a significantly age in patients with bicuspid valves than in the general population. Twenty years after diagnosis, individuals developed symptoms of heart failure ( $7\% \pm 2\%$ ) and cardiovascular medical events ( $33\% \pm 5\%$ )<sup>185</sup>.

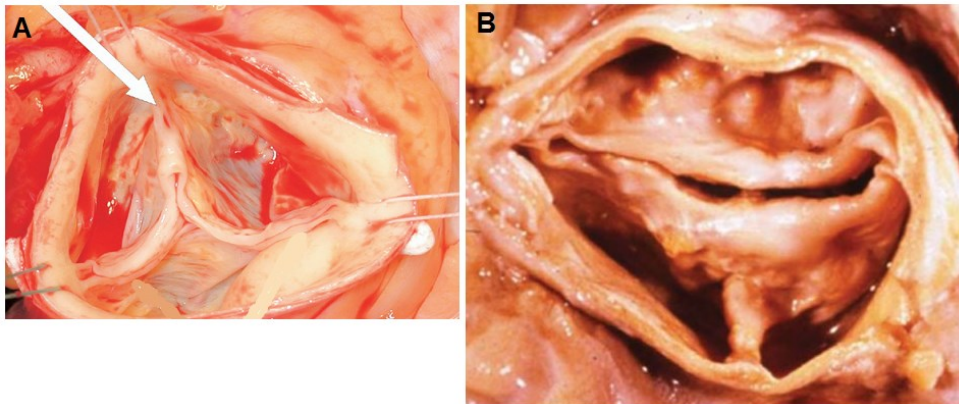


**Figure 3-6.** Bicuspid aortic valve with and without calcification. A) Non-calcified bicuspid aortic valve. A raphe between the underdeveloped left and right leaflets is indicated by a white arrow. B) Calcified bicuspid valve. Figure A and B were taken from Sievers<sup>137</sup> and Bax<sup>170</sup>, respectively. Figure license number A) 3614920100141 and B) 3614920371931.

### 3.7 Treatment

Aortic valve replacement surgery and TAVR are the only clinical treatments available for severe and/or symptomatic CAVD<sup>136</sup>. No medical therapy is currently available to slow the

progression or to reverse aortic valve calcification<sup>138,186</sup>. Aortic valve replacement surgery has been performed since 1960<sup>187</sup>. However, 50% of patients with severe CAVD are not referred to valve replacement surgery. Reasons not to operate patients are high perioperative risk, comorbidities (e.g. pulmonary disease, renal dysfunction, hepatic disease, and hematologic abnormalities), absence of symptoms, advanced age or short life expectancy, and patient/family refusal<sup>89,188</sup>. In the European Heart Survey, surgery was denied to 32% of patients with symptoms of CAVD. Among 153 unoperated CAVD patients in The University of Michigan echocardiography database (year 2005), 33% symptomatic patients did not undergo valve replacement surgery. TAVR is an alternative treatment option for CAVD in patients with high perioperative risk.

Coronary artery disease is present in more than 50% of patients with CAVD younger than 70 years and more than 65% of patients older than 80 years<sup>135,189</sup>. Patients with severe CAVD with and without symptoms, who undergo coronary artery bypass grafting, mitral valve replacement or aortic root surgeries may also undergo aortic valve replacement. In patients with moderate CAVD who undergo cardiac surgeries, aortic valve replacement is also recommended<sup>164</sup>.

### **3.7.1 Aortic valve replacement surgery**

An aortic valve replacement consists of the removal of the stenotic aortic valve and the installation of a prosthetic valve (**Figure 3-7**). Prosthetic valves can be biological or mechanical. The type of valve to be implanted depends on age, life expectancy, preference, indication/contraindication for warfarin therapy, and comorbidities<sup>190</sup>.

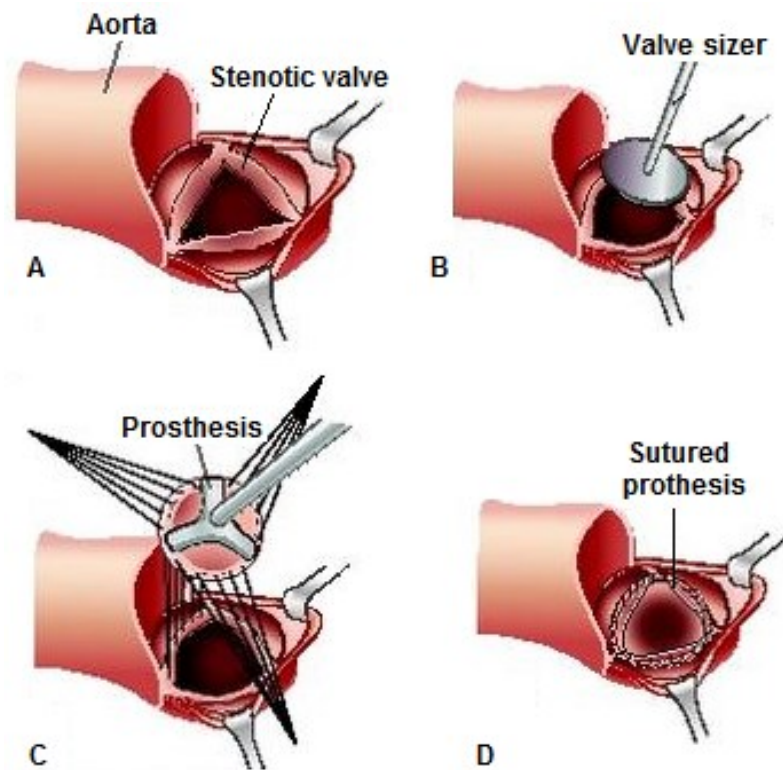


**Figure 3-7.** Aortic valve replacement. A) An incision is performed in the aorta to expose the stenotic valve. The stenotic valve is excised. Calcium in the annulus is removed. B) The annulus is measured to select the size of the prosthesis. C) Sutures are placed into the aortic valve annulus D) and subsequently through the sewing ring of the prosthetic valve ([www.surgeryencyclopedia.com/A-Ce/Aortic-Valve-Replacement.html](http://www.surgeryencyclopedia.com/A-Ce/Aortic-Valve-Replacement.html)).

Bioprosthetic valves can have animal origin (xenografts), such as porcine and bovine pericardial valves, or can be homografts from human donors. Bioprosthetic valves have a limited life expectancy and a second valve replacement may be necessary. Mechanical valves have longer lifespan but are associated with increased risk of clots formation and require anti-coagulation treatment for life. For women in childbearing age, mechanical valves are not suggested because anticoagulant agents such as warfarin increase fetal anomalies. Mechanical valves are preferred in young patients to avoid future valve replacement surgeries since the risk of degeneration of a bioprosthesis is higher in those patients<sup>190</sup> (**Figure 3-8**).

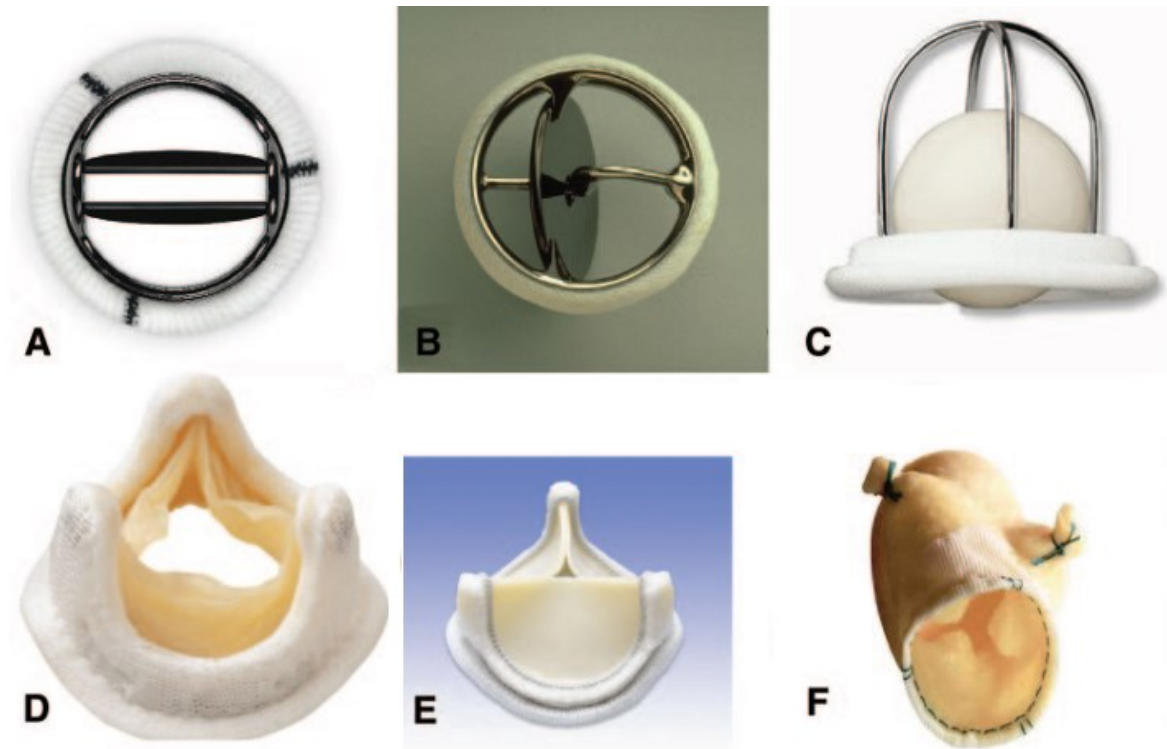


**Figure 3-8.** Types of heart valve prosthesis for aortic valve replacement surgery. A) Bileaflet mechanical valve (St Jude). B) Monoleaflet mechanical valve (Medtronic Hall). C) Caged ball valve (Starr-Edwards). D) Stented porcine bioprosthesis (Medtronic Mosaic). E) Stented pericardial bioprosthesis (Carpentier-Edwards Magna). F) Stentless porcine bioprosthesis (Medtronic Freestyle). Figure taken from Pibarot & Dumesnil<sup>190</sup>, license number 3614920682665.

### 3.7.2 Transcatheter aortic valve replacement

TAVR consists of the insertion of a new valve on top of the existing one (**Figure 3-9**). Multidetector computed tomography is used before TAVR to measure the valve annulus and to select the right size of the valve that is going to be implanted. Note that 2D-echocardiography is not reliable enough to measure annulus, especially in the presence of a bicuspid valve<sup>191</sup>. TAVR avoids an open heart surgery and is the suggested treatment for CAVD in patients with high perioperative risk. Approximately 100,000 TAVRs were performed between 2002 and 2013 in USA<sup>191</sup>.

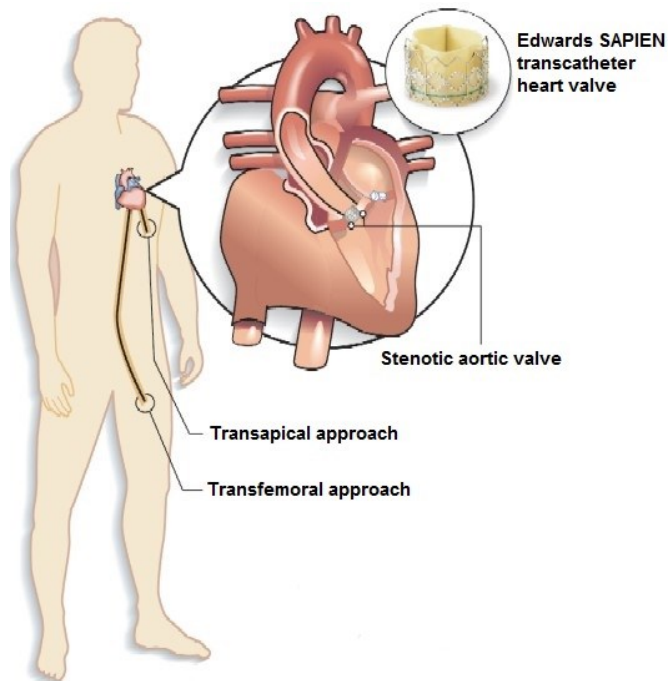


**Figure 3-9.** TAVR procedure. A replacement valve is folded and inserted via catheter into the femoral artery (transfemoral approach) in the upper thigh or in the chest between the ribs directly to the heart (transapical). Once the new valve is placed to the site of the stenotic valve, the new valve is expanded with a balloon and starts working ([www.nhcs.com.sg/patientcare/ConditionsAndTreatments/Pages/tavi.aspx](http://www.nhcs.com.sg/patientcare/ConditionsAndTreatments/Pages/tavi.aspx)).

The Placement of Aortic Transcatheter Valves (PARTNER) trial was a multicenter (including 21 centers worldwide), randomized study. PARTNER A involved 699 high-risk surgical patients that were assigned to the TAVR group or to the valve replacement surgery group<sup>192</sup>. PARTNER B involved 358 patients (mean age = 83 years) with severe symptomatic CAVD who were not considered good candidates for surgery. Patients were assigned to the TAVR group or medical therapy, including balloon aortic valvuloplasty<sup>193</sup>.

The 2-year mortality rate in the PARTNER A trial was 34% for TAVR compared to 35% for valve replacement surgery, but this difference was not significant<sup>192</sup>. PARTNER B compared TAVR with medical therapy, in unoperated patients with CAVD. The 2-year mortality rate was 43% for TAVR and 68% for medical therapy<sup>193</sup>. Stroke and transient ischemic attack were significantly more common in TAVR than in unoperated patients and patients undergoing valve replacement surgery. However, TAVR reduced death and hospitalization rates and improved symptoms and valve hemodynamics<sup>192,193</sup>.



### 3.8 Medical treatment

As stated before, there is currently no medical therapy to slow or reverse the progression of CAVD. Conventional therapy for CAVD is focused on the management of comorbidities and risk factors to decrease the possibility of undergoing valve replacement surgery or TAVR or to decrease symptoms in patients considered unoperable. Treatment of hypertension and dyslipidemia are often prescribed. Short term infusion of the nitric oxide donor sodium nitroprusside can ameliorate left-ventricular dysfunction. Perhexiline may ameliorate myocardial oxygenation and inflammation<sup>194</sup>. Similarities between CAVD and other medical conditions led to propose some potential therapies for CAVD (**Figure 3-10**).

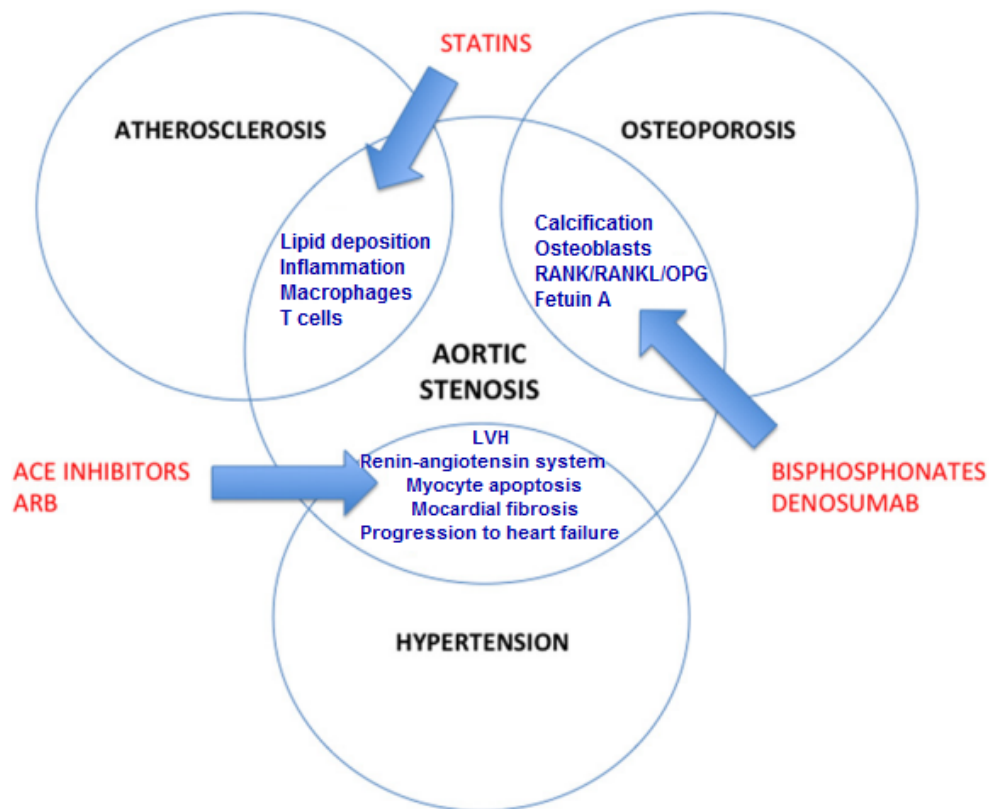


**Figure 3-10.** Similarities between aortic stenosis and other medical conditions and potential therapeutic strategies. ACE: angiotensin-converting enzyme. ARB: angiotensin receptor blocker. LVH: left ventricular hypertrophy. OPG: osteoprotegerin. RANK: receptor activator of nuclear factor kappa  $\beta$ . RANKL: receptor activator of nuclear factor kappa  $\beta$  ligand. Figure derived from Dweck et al.<sup>107</sup>, license number 3614371039473.

### 3.8.1 Statins

CAVD shared the classical risk factors with coronary artery disease. Cellular processes related to atherosclerotic plaques formation are also implicated in valvular calcification such as inflammation and lipid infiltration<sup>163</sup> (Table 3-4). Statins reduce plasma LDL levels and reduce mortality in patients with atherosclerotic diseases<sup>195</sup>. For this reason, lowering lipid therapy was hypothesized to slow or reverse progression of CAVD.

**Table 3-4.** Comparison of calcific aortic valve disease and atherosclerosis<sup>163</sup>

	CAVD	Atherosclerosis
<b>Histopathologic features</b>		
Lipoprotein accumulation	++++	++++
Lipid oxidation	++++	++++
Calcification	+++++	++
Inflammatory changes	++++	++++
Systemic inflammatory markers	+	++
<i>C. pneumoniae</i> and other infectious agents	+	+
Genetic polymorphisms	++	+++
Prominent cell type	Fibroblast	Smooth muscle
<b>Clinical risk factors</b>		
Renal dysfunction	++++	++++
Smoking	+++	++++
Hypertension	++	++++
Elevated serum lipoprotein levels	+++	++++
Diabetes mellitus	+	+++++
Endothelial dysfunction	++	++++

Statins are 3-hydroxy-3-methyl-glutaryl-CoA reductase (HMG-CoA reductase) inhibitors. HMG-CoA reductase is the rate-limiting enzyme in cholesterol biosynthesis. The drug also has an effect on inflammation by reducing the C-reactive protein and depressing leukocyte cell surface molecules required for monocyte adhesion and initiation of inflammation<sup>195,196</sup>. In cellular and animal models, atorvastatin reduced the expression of bone morphogenic proteins. Watanabe heritable hyperlipidaemic rabbits develop aortic valve lesions. In those rabbits atorvastatin decreases atrioventricular valve lesions through down-regulation of

Lrp5 (low-density lipoprotein receptor-related protein 5), which is a critical LDL co-receptor associated with skeletal bone formation<sup>197</sup>.

Retrospectives studies (n between 65 and 211 and average follow-up between 15 months and 3.7 years) have shown that patients taking statin have significantly lower median aortic valve calcium, peak gradient, and peak jet velocity, and higher aortic valve area compared to non-statin patients<sup>163</sup>.

Despite the positive results of retrospective studies, three prospective studies, specifically designed to analyze the progression of aortic stenosis in patients treated or not with statin reported that statin therapy did not prevent CAVD progression (**Table 3-5**). The latter results were confirmed by Teo *et al.*<sup>198</sup> who performed a meta-analysis of four clinical trials that included three negative trials on the effects of statins in CAVD. The positive trial showed a slower rate of progression in patients with moderate-to-severe CAVD, but in that study, patients with low LDL levels were not treated with statin<sup>199</sup>. The lack of efficiency of statin may be explained by the absence of effect on LDL particle size<sup>200,201</sup>. In the 2014 AHA/ACC guideline for the management of patients with valvular heart disease, statin therapy was not recommended to treat patients with mild-to-moderate CAVD<sup>202</sup>. However, CAVD patients with hypercholesterolemia may benefit from lipid-lowering therapy to reduce risk of cardiovascular events.

**Table 3-5.** Large clinical trials of lipid lowering therapy in CAVD patients. Modified from Freeman & Otto<sup>163</sup>.

Study, n (year)	Type, mean follow-up (years)	Assessment of valvular stenosis	Treatment Group (n)	Serum LDL (% change from baseline in treatment group)	Decrease in AVA (cm <sup>2</sup> /y) treatment, placebo	Conclusion
SALTIRE <sup>203</sup> , 134 (2005), Scotland	Randomized, double-blind, placebo controlled (2.1)	Mild to severe CAVD. Echocardiography and computed tomography	Atorvastatin 80 mg/d (77)	↓53%	-0.08 ± 0.11, -0.08 ± 0.11 (NS)	No effect on the rate of change in aortic-jet velocity or valvular calcification.
RAAVE <sup>199</sup> , 121 (2007), Portugal	Open-label, prospective (1.4)	Moderate to severe CAVD. Echocardiography	Rosuvastatin 20 mg/d (61)	↓42%	-0.05 ± 0.12, -0.1 ± 0.09 (P = 0.041)	The rate of progression of CAVD in hypercholesterolemic patients treated with rosuvastatin is slower than in those untreated patients with lower lipid levels.
ASTRONOMER <sup>204</sup> , 296 (2010), Canada	Randomized, double-blind, placebo controlled (3.5)	Mild to moderate CAVD. Echocardiography	Rosuvastatin 40 mg/d (134)	↓54%	-0.08 ± 0.21, -0.07 ± 0.15 (NS)	Intensive lipid lowering with rosuvastatin did not reduce the rate of progression of CAVD in patients with mild to moderate CAVD.
SEAS <sup>205</sup> , 1,837 (2008), 7 European Countries	Randomized, double-blind, placebo controlled (5.4)	Mild to moderate CAVD. Echocardiography	Simvastatin 40 mg plus ezetimibe 10 mg/d (944)	↓61%	-0.03 ± 0.01, -0.03 ± 0.01 (NS)	Statin reduced the incidence of ischemic cardiovascular events but not events related to CAVD.

AVA: Aortic valve area. ASTRONOMER: Aortic Stenosis Progression Observation: Measuring the Effects of Rosuvastatin. RAAVE: Rosuvastatin Affecting Aortic Valve Endothelium. SEAS: Simvastatin and Ezetimibe in Aortic Stenosis. SALTIRE: Scottish Aortic Stenosis and Lipid Lowering Trial, Impact on Regression. NS: Not significant.

### 3.8.2 Peroxisome proliferator-activated receptor $\gamma$ (PPAR- $\gamma$ )

PPAR- $\gamma$  is involved in glucose and lipid metabolism<sup>206</sup>. Hypercholesterolemic rabbits treated with vitamin D developed aortic valve calcification. The treatment of rabbits with pioglitazone, a PPAR- $\gamma$  agonist, reduced expression of the receptor for advanced glycation end products (RAGE) in aortic valves. This observation was confirmed in porcine VICs. RAGE has pro-inflammatory properties and mediates osteoblastic differentiation of VICs. Treatment with pioglitazone also decreases  $\beta$ -catenin levels, oxidative stress, inflammation, and osteoblastic markers [runt-related transcription factor 2 (*RUNX2*), osteopontin (*SPPI/OPN*), and alkaline phosphatase (*ALP*)], thus attenuating the progression of aortic valve calcification<sup>207</sup>. Similarly, in hypercholesterolemic mice treated with pioglitazone lipid deposition, calcification, and apoptosis in aortic valves was attenuated while improving aortic valve function. The use of another thiazolidinedione called rosiglitazone, used for treatment of diabetes, has been related with increased risk of cardiovascular disease. Whether pioglitazone is beneficial for patients with CAVD needs to be clarified with additional studies<sup>208</sup>.

### 3.8.3 Lipoprotein(a) / oxidized phospholipids

Lowering plasma levels of Lp(a) has recently emerged as a new therapeutic approach for treating CAVD. The kringle IV (KIV) polymorphism of *LPA* explains 20 to 80% of the variability of Lp(a) plasma concentrations depending on ethnicity<sup>209</sup>. A variant in *LPA*, the gene coding for Lp(a), was significantly associated with aortic valve calcium and aortic stenosis<sup>210</sup>. Elevated Lp(a) levels were also associated with CAVD<sup>211</sup>. Lp(a) particles are atherogenic and thrombogenic<sup>212</sup>. Lp(a) promotes inflammation because in addition to apolipoprotein B100 (APOB100), it also contains oxidized lipids. Lp(a) is cleaved by Lp-PLA2 to release free oxidized fatty acids. Lp-PLA2 levels are increased by 4.2-fold in calcified aortic valves probably by inflammatory cells<sup>213</sup>.

Some approaches for Lp(a) lowering include the use of oligonucleotides specifically directed to apo(a) of Lp(a), inhibitors of Lp-PLA2 such as darapladib, and agents to prevent oxidation of lipoproteins or minimize their adverse effects, e.g. antioxidants and oxidation-specific antibodies targeting free oxidized fatty acids<sup>214</sup>. Lp(a) levels can be reduced using

high-dose niacin, omega-3 fatty acid supplements, fenofibrate, hormone/estrogen replacement therapy, aspirin, and other therapies<sup>212</sup>. A pilot randomized controlled-trial [Early Aortic Valve Lipoprotein(a) Lowering Trial (EAVaLL)] in patients with aortic sclerosis and mild CAVD (age = 50 to 85 years) is ongoing in Canada (clinicaltrials.gov). The endpoint will measure calcium score progression by cardiac CT in individuals randomized to niacin as compared to placebo.

### **3.8.4 Angiotensin system blocking**

One risk factor of CAVD is hypertension, which was associated with reduced survival and faster progression of CAVD<sup>215</sup>. The main treatments for hypertension are drugs acting on the renin-angiotensin-aldosterone system, such as Angiotensin-Converting Enzyme (ACE) inhibitors and angiotensin II receptor blockers<sup>216</sup>. ACE and angiotensin II are expressed in calcified aortic valves and possibly contribute to valve inflammation, calcification, and disease progression<sup>217</sup>. ACE inhibitors decrease systolic and diastolic blood pressure, which reduce pressure overload and decelerate left ventricular hypertrophy; this can reduce mechanical stress on the aortic valve<sup>216</sup>. Retrospective studies on the effect of ACE inhibitors in CAVD are contradictory. A prospective clinical trial is ongoing in Finland<sup>218</sup>.

In the study of Capoulade *et al.*<sup>215</sup>, angiotensin II receptor blockers but not ACE inhibitors decrease risk of mortality associated with hypertension in CAVD patients. Other studies showed that angiotensin II levels are increased in calcified aortic valves and these levels correlate with levels of inflammatory markers<sup>217</sup>. Furthermore, angiotensin II receptor blockers were associated with lower aortic valve weight and remodeling score. Aortic valve weight is significantly associated with increased peak transvalvular gradient<sup>219</sup>. In cardiac ventricles, 80% of angiotensin II is produced by the chymase pathway<sup>220</sup>. Angiotensin II receptor blockers inhibit this pathway but not ACE inhibitors<sup>186,220</sup>; this may explain why angiotensin II receptor blockers have a beneficial effect in CAVD, but not ACE inhibitors. Thus, angiotensin II receptor blockers have potential therapeutic use in CAVD.

### 3.8.5 Bisphosphonates

Calcification is a feature of severe CAVD. Molher *et al.*<sup>221</sup> analyzed 347 surgically excised heart valves and found that 83% had dystrophic calcification. Active bone remodeling was observed in 13% of the valves with dystrophic calcification, and valves also expressed *BMP2* and *BMP4*. Bisphosphonates, which are used for treating osteoporosis, inhibit bone turnover and like statins, reduce production of cholesterol by inhibiting HMG-CoA reductase pathway. The effect of bisphosphonates in CAVD has been studied. In a retrospective study, the annual change on aortic valve area was compared between CAVD patients taking a treatment for osteoporosis (12 on bisphosphonates, 4 on calcitonin, and 2 on estrogen receptor modulators) with patients not receiving osteoporosis treatment (n = 37). Patients under osteoporosis treatment had slower reduction of aortic valve area compared to untreated patients after a mean follow-up of  $2.4 \pm 1$  years<sup>222</sup>. A second study comparing only CAVD patients treated (n = 8) or not (n = 68) with bisphosphonates also showed a slower rate of aortic valve area reduction in treated patients<sup>223</sup>. These results must be confirmed in larger studies.

### 3.8.6 Anti-RANKL monoclonal antibody

The ventricularis layer of the valve, which does not calcify, expresses OPG that inhibits differentiation of VICs and calcification by blocking the action of RANKL<sup>224</sup>. RANKL is overexpressed in human aortic valves from CAVD patients compared with controls. The expression of OPG and RANKL in mineralized valves is inversely correlated<sup>225</sup>. RANKL expression is enhanced by tumor necrosis factor (TNF- $\alpha$ ) and interleukin (IL) 1<sup>226</sup>. In myofibroblasts treated with RANKL, the expression levels of matrix metalloproteinases such as matrix metalloproteinase (MMP) 1 and 2, and pro-osteogenic proteins are increased<sup>225,227</sup>.

In osteoporosis, there is also an increased expression of RANKL and reduced levels of OPG, which lead to the development of the anti-RANKL monoclonal antibody denosumab, a potent and well-tolerated osteoporosis treatment<sup>107</sup>. Thus, denosumab may have potential beneficial effects for CAVD patients.

### **3.8.7 Vitamin K**

Vitamin K antagonists such as warfarin have been associated with calcification and faster progression of CAVD. These pathological events are mediated through failure of  $\gamma$ -carboxylative activation of MGP via the vitamin K cycle. Paracetamol that also intervening in the vitamin K cycle maybe avoid. Several other anticoagulants available on the market do not intervening in this cycle and may represent a therapeutic option for CAVD<sup>194</sup>.



## Chapter 4. Genetics and molecular biology of CAVD

### 4.1 Proposed molecular mechanisms of aortic valve calcification

In the past, CAVD was thought to be the cause of aging and degeneration of the valve as well as passive accumulation of calcium in the leaflets due to mechanical stresses accumulated during life. However, aortic stenosis is not observed among all the elderly; about 25% to 45% of octogenarians have no evidence of aortic valve calcification<sup>131</sup>. This observation along with the increased susceptibility to CAVD in individuals with bicuspid aortic valves and their relatives, and the geographical clustering of CAVD patients with tricuspid valves<sup>228</sup> have led to the hypothesis that CAVD development has a genetic component. In the region of Finisterra (France) the disease is clustered and thus more common in specific geographic areas with a frequency between 0 to 52 cases per 10,000 inhabitants depending of the area<sup>228</sup>. CAVD is a disease with multiple stages in which the dysfunction of different cellular mechanisms is involved.

Several histological, *in vivo*, and *in vitro* studies have identified biological processes that contribute to the development of the disease<sup>200,229,230</sup>. Inflammation, lipid deposition, extracellular matrix remodeling, angiogenesis, apoptosis, and calcification are among those processes<sup>134,230,231</sup>. **Figure 4-1** summarizes the molecular and cellular mechanisms implicated in CAVD.

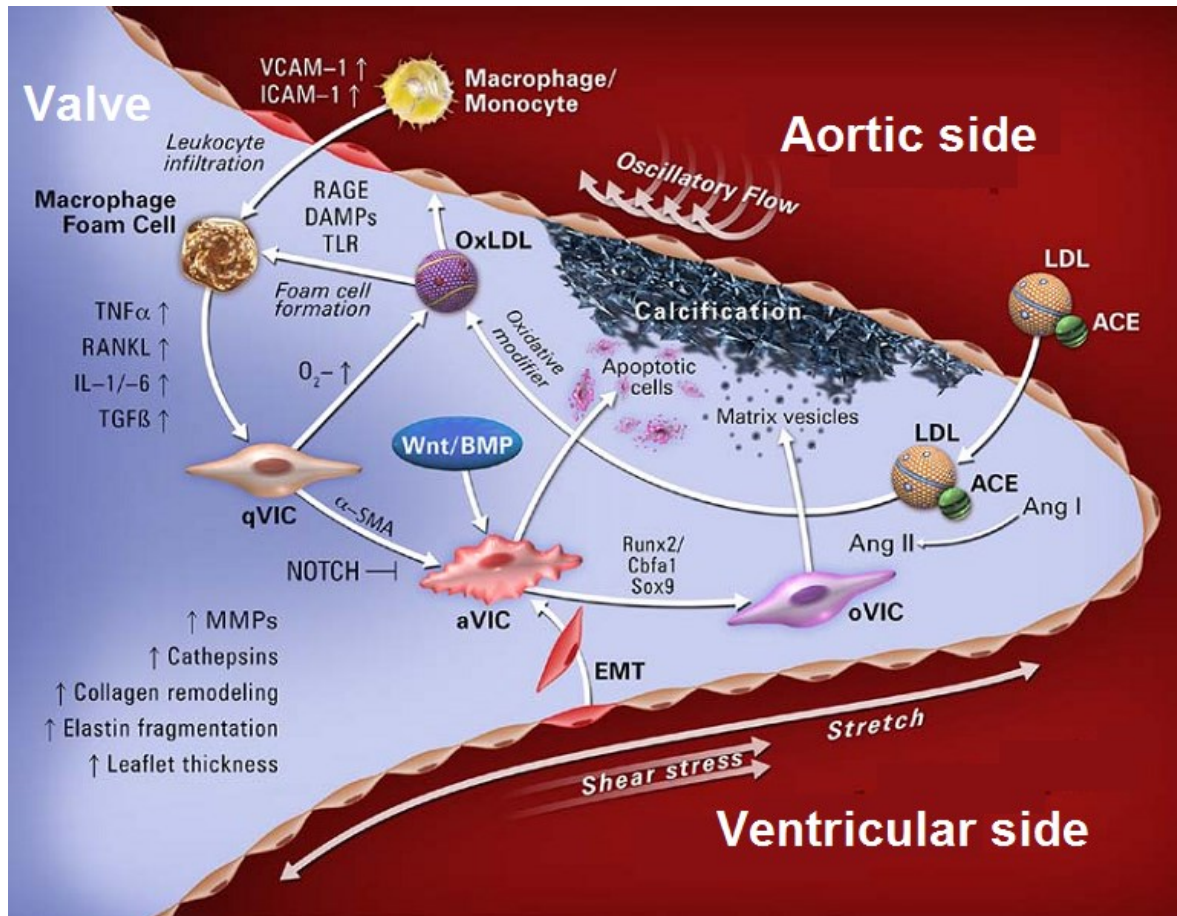


**Figure 4-1.** Molecular, cellular, and biomechanical mechanisms involved in CAVD. ACE: angiotensin-converting enzyme. AngI/II: angiotensin I/II. aVIC: activated valve interstitial cell. BMP: bone morphogenetic protein. EMT: endothelial-to-mesenchymal transition. ICAM-1: intracellular adhesion molecule-1. IL-1/-6: interleukin-1/-6. LDL: low-density lipoprotein. MV: matrix vesicles. oVI: osteogenic valve interstitial cell. qVIC: quiescent valve interstitial cell. RAGE: receptor for advanced glycation end products. RANKL: receptor activator of nuclear factor- $\kappa$ B ligand. Runx2: runt-related transcription factor 2. TGF- $\beta$ : transforming growth factor- $\beta$ . TNF- $\alpha$ : tumor necrosis factor- $\alpha$ . VCAM-1: vascular adhesion molecule-1. Modified from Yutzey *et al.*<sup>232</sup>, license number 3614920968199.

The first aortic valve lesions appear in the aortic side of the valve, in the subendothelium, then affect the fibrosa layer (**Figure 4-2**), the region with the highest turbulence<sup>156</sup>. This mechanical stress has been associated with mineralization of aortic valves and may be one of the reasons why bicuspid valves calcify earlier than tricuspid valves<sup>233</sup>. Bouchared *et al.* isolated VICs from patients with CAVD to measure the effect of mechanical stress in aortic valve calcification. In 24 hours VIC cultures submitted to a strain of 15% (which represent hypertension) shown increased mineralization by 120-fold compared to control VICs not

under strain condition. Due to the two leaflet configurations, bicuspid valves have to endure higher mechanical stress than tricuspid valves<sup>105</sup>. In addition, VICs from the aortic and ventricular side of the valve present different miRNA expression profiles<sup>234</sup>. Those differences may arise as a protective mechanism or as a consequence of mechanical stress.

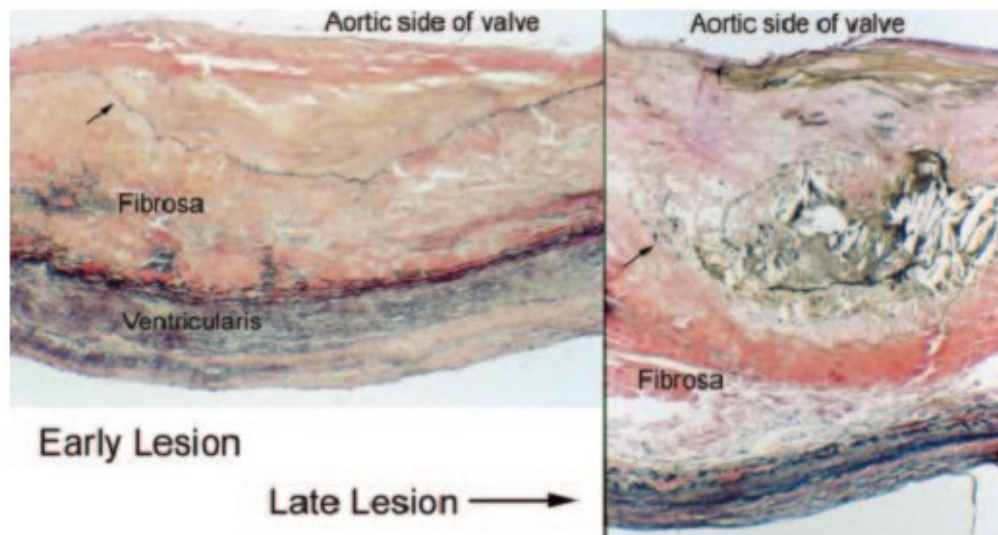


**Figure 4-2.** Histology of early and late lesions of CAVD. Early lesions (left) present accumulation of cells and extracellular lipids and matrix in the aortic side of the leaflet, with displacement of normal subendothelial elastic lamina (arrow). In the late lesion (right), there is a more prominent accumulation of lipids, cells, and extracellular matrix. Elastic lamina is displaced and fragmented (arrow). The disease processes extend into adjacent fibrosa. Figure taking from Freeman<sup>163</sup>, license number 3614921149707.

Mechanical stress causes damage of the valve endothelium, allowing the infiltration of lipids and inflammatory mediators into the valve. This was confirmed by the study of aortic valve leaflets in early stage of stenosis. The first lesions contain oxidized LDL (oxLDL), macrophages, and T lymphocytes<sup>235,236</sup>. Furthermore, in mouse and rabbit models of CAVD, a high-fat diet promotes valve calcification and increases expression of inflammatory markers, suggesting an important role of lipids in the development of the disease<sup>235,237</sup>. In patients with the metabolic syndrome, which is a risk factor of CAVD<sup>183</sup>, and normal plasma LDL levels, the size of the LDL particles was small, suggesting that small LDL particles can easily infiltrate the valve endothelium and trigger CAVD development<sup>200,238</sup>.

Dysfunction of the endothelium allows lipids to accumulate in the subendothelial space and the fibrosa. Lp(a), lipoprotein lipase (LPL), APOA, APOB, and APOE that mostly comes from plasma<sup>229,239</sup> have been observed in the aortic valve. Lp(a) and APOAI have been found near calcified areas of the valve<sup>239</sup>. Increased oxidative stress has also been related to CAVD, and antioxidant enzymes such as superoxide dismutase are decreased in mineralized valves. Superoxide anion and hydrogen peroxide levels are increased in calcified parts of aortic valves when compared to the non-calcified parts of the same valves or when compared to normal valves. This increase of reactive oxygen species is due to the uncoupling of nitric oxide synthase, which is due to a deficiency of its substrate L-arginine. Oxidation of lipids is mediated by reactive oxygen species<sup>240</sup>.

Levels of oxLDL in valves explanted from CAVD patients correlates with the presence of inflammatory markers such as leukocytes, macrophages, and TNF- $\alpha$ . OxLDL levels were also associated with a valve remodeling score<sup>200</sup>. Valves with higher levels of remodeling presented higher circulating oxLDL levels<sup>241</sup>. OxLDL colocalizes with biglycan which promotes retention of lipids within the aortic valve by increasing expression of phospholipid transfer protein (*PLTP*) through the action of toll-like receptor 2 (*TLR2*)<sup>242</sup>. OxLDL activates peroxisome proliferator-activated receptor  $\gamma$  (PPAR- $\gamma$ ) in macrophages<sup>206</sup>, which is pro-inflammatory and enhance proliferation of VICs<sup>206,207</sup>.

Circulating macrophages also infiltrate the aortic valve. A proportion of them expresses ACE which may contribute to valve inflammation, calcification, and disease progression<sup>217</sup>. Macrophages that uptake lipids are transformed to foam cells<sup>235</sup>. Foam cells enhance inflammation by expressing monocyte chemoattractant protein-1 (*MCP-1/CCL2*), triggering infiltration of more inflammatory mediators and lipids<sup>236</sup>. Cytokines and chemokines can recruit bone-marrow-derived cells<sup>236</sup>. Aortic valves from CAVD patients overexpress cytokines (e.g., IL-1 $\beta$ , IL-6, and TGFB1)<sup>236</sup>. IL-6 is involved in the translocation of the p65 subunit of nuclear factor kappa-light-chain-enhancer of activated B cells (NF $\kappa$ B) to the nucleus and acts on the BMP2 pathway<sup>243</sup>. TGFB1 is increased in mineralized valves and increases affinity of proteoglycans such as biglycan to lipids by adding sulfates to the proteoglycans<sup>244</sup>. Calcified aortic valves also express chemokines

such as chemokine (C-C motif) ligand 5 (*CCL5*) and chemokine (C-X-C motif) ligand 12 (*CXCL12*)<sup>236</sup>.

Mechanical stress and inflammation lead to valve extracellular matrix remodeling<sup>245</sup> and neovascularization<sup>236,246</sup>. *TGFB1* and *IL-1B* cause increased production of matrix metalloproteinases, specifically *MMP1* and *MMP2*, enhancing extracellular matrix remodeling and fibrosis<sup>247</sup>. Matrix metalloproteinases are produced by VICs, monocytes, macrophages, lymphocytes, and endothelial cells<sup>248,249</sup>. In the study of Bossé *et al.*, the expression of *MMP1*, *MMP9*, and *MMP12* were upregulated<sup>231</sup>.

Valve leaflets are avascular. Aortic valves explanted from CAVD patients expressed platelet-derived growth factor subunit B (*PDGF-BB*), vascular endothelial growth factor (*VEGF*), *VEGFR2*, and *TEK* tyrosine kinase, endothelial (*TEK/Tie-2*) genes that enhance angiogenesis and endothelial proliferation<sup>236,250</sup>. Osteonectin/SPARC colocalized with *MMP9* in mature blood vessels and macrophages of aortic valves explanted from CAVD patients. The latter suggests a role of SPARC in valve neovascularization<sup>248</sup>. The presence of blood vessels in the aortic valve facilitates the infiltration of circulatory inflammatory cells and promotes inflammation and calcification. In fact, angiogenesis was associated with increased levels of inflammation in CAVD patients<sup>246</sup>.

The final stages of CAVD are calcification<sup>235</sup> and apoptosis<sup>236</sup>. Calcification begins with the formation of calcium nodules, which contain hydroxyapatite embedded on a matrix of collagen similar to bone. This matrix also contains *SPP1/OPN* and BMPs<sup>107</sup>. The observation of VICs in cultures suggests that a cause of valve calcification can be the transdifferentiation of a subset of myofibroblasts into osteoblast-like cells. Osteoblast-like cells from valves overexpress genes involved in pro-osteogenic pathways such as *OPN*, osterix, *BMP2*, and *RUNX2*. The overexpression of these proteins leads to fibrosis, cartilage, and bone formation<sup>245,251,252</sup>. *RUNX2* is the master osteogenic regulator for which overexpression can be mediated by the dysfunction of the *NOTCH1* pathway.

*NOTCH1* is a repressor of pro-osteogenic pathways and may prevent osteoblastogenic differentiation<sup>253</sup>. *NOTCH1* is a transmembrane receptor activated by its agonists, Delta-like and Jagged proteins. Activation of *NOTCH1* causes the cleavage of its intracellular domain (NICD) by an  $\alpha$ -secretase and a presilin. The domain is translocated to the nucleus and binds to its coactivator: the recombining binding protein suppressor of hairless (RBPJK). The complex NICD-RBPJK binds to the promoter of the hairy family of repressors, hairy enhancer of split (HES) or the hairy-related transcription factor (HRT/Hey), to promote their transcription. Then, HES and HRT/Hey inhibits *BMP2* and *RUNX2*<sup>254</sup> (Figure 4-3). Thus, inhibition of *NOTCH1* promotes activation of *RUNX2*<sup>33</sup> and *BMP2* in aortic valves<sup>254</sup>. Increased expression of *BMP2* is associated with calcium nodules formation in VICs<sup>254</sup>.

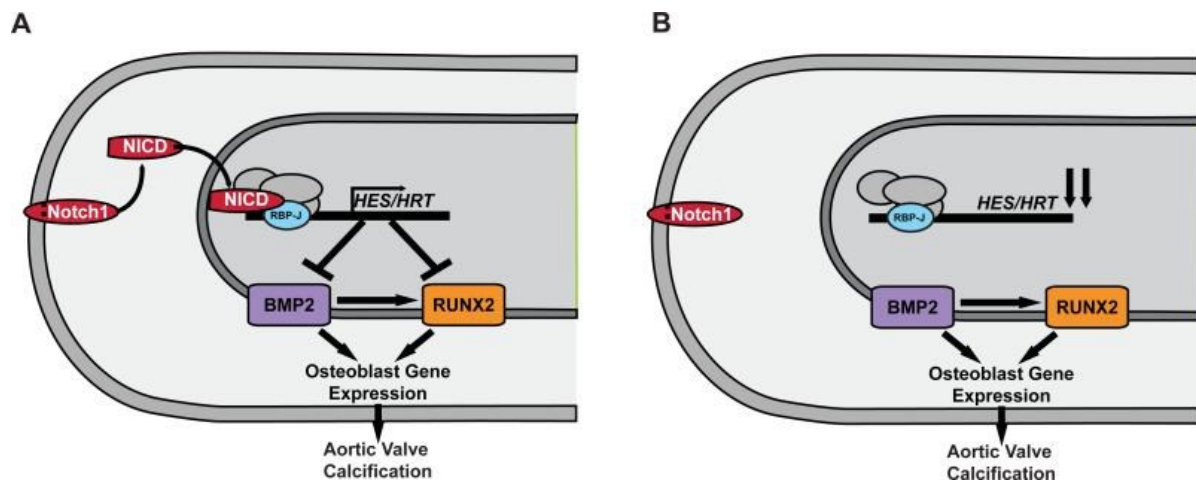


**Figure 4-3.** Potential mechanisms of aortic valve calcification by *NOTCH1*. A) After activation of *NOTCH1*, the NICD is cleaved and translocated to the nucleus where it binds the coactivator RBPJ and activates expression of HES and or HRT/Hey, which are repressors of *BMP2* and *RUNX2*. B) Inactivation of *NOTCH1* causes reduced expression of HES or HRT/Hey and activation of pro-osteogenic genes. Figure taken from Nigam & Srivastava<sup>254</sup>, license number 3614921318572.

Furthermore, *NOTCH1* inhibition in rat VICs prevents the expression of *SOX9*, a chondriogenic transcription factor regulated by *BMP2*. *SOX9* is necessary for valve development. *SOX9* inhibition in VICs downregulates expression of extracellular matrix genes such as collagen types II, IX, and XI, causing extracellular matrix remodeling<sup>255</sup>.

The pro-osteogenic Lrp5/Wnt/ $\beta$ -catenin signaling pathway is also activated in calcified valves<sup>256</sup>. The Lrp5/Wnt/ $\beta$ -catenin pathway interacts with *NOTCH1* signaling and its function in bone formation is well known. Lrp5/6 interacts with APOE, reducing lipid clearance and activating Wnt. Increased Wnt leads to translocation of  $\beta$ -catenin to the nucleus and activation of *BMP2*<sup>257,258</sup>. *TGFBI* stabilizes  $\beta$ -catenin and promotes transdifferentiation of VICs into myofibroblast with a pro-osteogenic profile<sup>259</sup>. However, Liu & Gotlieb associated the expression of *TGFBI* with valve repair through modulation of  $\alpha$ SMA expression<sup>260</sup>.

Apoptosis causes the release of cell calcium content into the extracellular matrix and causes the formation of calcium nodules. Serum phosphate levels are associated with aortic valve sclerosis<sup>184</sup>. Ectonucleotidases such as *ALP* and ectonucleotide pyrophosphatase/phosphodiesterase 1 (*ENPP1*) regulate the ratio between inorganic phosphate (Pi) and inorganic pyrophosphate (PPi). Pi promotes calcification whereas PPi is a strong inhibitor of calcification. The allele A of rs9402349 located in intron 9 of *ENPP1* was significantly associated with CAVD, increased levels of *ENPP1* and calcium in aortic valves<sup>261</sup>. Overexpression of *ENPP1* causes an imbalance in the ratio Pi/PPi in the extracellular matrix, favoring the entrance of Pi into the VICs, through the inorganic phosphate transporter Pit1 (*SLC20A1*)<sup>261</sup>. Pit1 levels are increased in calcified valves. The imbalance in Pi/PPi ratio is created because *ENPP1* hydrolyzes ATP to produce AMP+PPi and ADP+Pi. In addition, ADP is used to produce more AMP+Pi. Elevated levels of the ectonucleotidase deplete extracellular levels of nucleotides and contribute to reduce purinergic signaling through P2Y2R/PI3K/Akt promoting apoptosis and caspase-3 calcification<sup>261</sup>. P2Y2R is the purinergic receptor P2Y, G-protein coupled, 2 and PI3K is phosphatidylinositol kinase. Depression of P2Y2R/PI3K/Akt results in the phosphorylation of IKK and I $\kappa$ B, and the translocation of NF $\kappa$ B to the nucleus through IL-6. In turn, IL-6 promotes, by autocrine/paracrine effect, the expression of *BMP2* and osteogenic transition of VICs<sup>243</sup>.

Apoptosis of VICs is also mediated by TNF-related apoptosis-inducing ligand (TNFSF10/TRAIL). TRAIL, produced by macrophages and T-cells, activates a pro-

apoptotic pathway mediated by recruitment of caspase-8. TRAIL is overexpressed in VICs and plasma from CAVD patients compared to normal patients<sup>262</sup>.

#### 4.1.1 miRNA and lncRNAs in AS

miRNA have been related to cardiovascular pathologies including left ventricular hypertrophy and cardiac fibrosis. They can also regulate cardiac vessel density and cardiac metabolism<sup>263</sup>. miRNA-30b is a repressor of *BMP2* in human VICs through direct targeting of *RUNX2*, SMAD family member 1 (*SMAD1*), and caspase-3<sup>264</sup>. In mice, another miRNA, miR-23, inhibited the TGF $\beta$ -induced endothelial-to-mesenchymal transition necessary for heart valve development. miR-23 targets hyaluronic acid synthase 2 (*Has2*), catenin, beta interacting protein 1 (*Icat/CTNNBIP1*), and transmembrane protein 2 (*Tmem2*)<sup>265</sup>. In another study, nine miRNAs, (miR-let-7c, miR-125b, miR-127, miR-199a-3p, miR-204, miR-320, miR-99b, miR-328 and miR-744) were highly enriched in the cardiac valves of three species, *Rattus norvegicus*, *Canis familiaris*, and *Macaca fascicularis*<sup>266</sup>. In porcine VICs stimulated with TGF $\beta$ , miRNA-141 induced myofibroblastic transformation, activated BMP2 signaling, and as a consequence increased calcification<sup>267</sup>.

LncRNAs have been involved in the control of pluripotency and lineage specification during development. They are also regulated in myocardial infarction (Novlnc6) and heart failure (Mhrt)<sup>10</sup>. They are highly expressed in endothelial cells and human smooth muscle cells from coronary arteries<sup>10</sup>. The expression of HOTAIR (a LncRNA) is decreased in aortic valves from patients with bicuspid valve leaflets and in human VICs exposed to cycle stretch. This decreased expression of HOTAIR led to the increased expression of *BMP2* and alkaline phosphatase, liver/bone/kidney (*ALPL*) and subsequent valve calcification. HOTAIR may be repressed by  $\beta$ -catenin<sup>268</sup>.

## 4.2 Animal models of CAVD

Animal models of CAVD include mice, rabbits and pigs. All these animals naturally present a tricuspid aortic valve as in humans<sup>269</sup>. Most of these models have been already used to study the mechanisms leading to atherosclerosis and hypercholesterolemia. In pigs a high-fat diet is used to accelerate CAVD. Rabbits develop CAVD when fed with high-fat



diet and the Watanabe strain develops atherosclerosis spontaneously. Mice develop CAVD faster than pigs and rabbits but genetic modifications must be performed. The mouse strain C57Bl/6J is sensitive to atherogenic changes if fed with specific diets. Typically, LDL receptor or APOE deficient mice have been used to study CAVD development and progression. In mice, assessment of aortic valve inflammation by echocardiography is difficult due to their small size and aortic stenosis can be under- or overestimated<sup>270</sup>.

The use of animal models has limitations. Pigs develop aortic stenosis with age akin to humans but they are big and difficult to maintain in research facilities. Humans and pigs share similar lipid profiles, but rabbits and mice present differences in lipid metabolism compared to humans<sup>271</sup>. These differences may be reflected in the way that the disease develops or progresses in animal models. Most animal models develop either pathological changes in the aortic valve or hemodynamic changes (e.g. increased jet velocity) but not both as in humans. However, animal models have allowed the study of potential pharmacological treatments for the disease. Common animal models to study CAVD are listed below.

#### **4.2.1 Mouse models**

- C57Bl/6J mice are genetically prone to develop diet-induced obesity and atherosclerotic lesions<sup>235</sup>. C57BL/6 adult male mice under high-fat diet developed modest calcification and lipid deposition in the aortic valves, but not the hemodynamic changes normally observed in CAVD<sup>235</sup>.
- ApoE<sup>-/-</sup> is a hypercholesterolemic mouse model, widely used to study atherosclerosis. ApoE<sup>-/-</sup> mice have increased cholesterol levels due to the accumulation of very low density lipoprotein remnants and develop severe atherosclerotic lesions<sup>272</sup>. ApoE<sup>-/-</sup> (apolipoprotein E deficient) senile mice under chow diet presented lipid deposition, calcification and macrophages and T cell infiltration in the aortic valves<sup>236</sup>.

Under high-fat/high-carbohydrate diet, ApoE<sup>-/-</sup> mice presented lipid deposition and macrophage infiltration in the aortic valves and thick leaflets. Even in the absence of

calcific nodules, aortic valves expressed SPP1/OPN, osteocalcin, Runx2, osterix, and Notch1. In valve myofibroblast, expression of *MMP2* and *MMP9* was observed<sup>252</sup>.

- LDLr<sup>-/-</sup> (LDL receptor-deficient) mice fed with chow diet had a slight increase in plasma cholesterol levels from an accumulation of LDL<sup>272</sup>. LDLr<sup>-/-</sup> mice under high-fat/high carbohydrate diet had smaller aortic valve area. Aortic valve leaflets were thicker and shown macrophages and foam cell infiltration<sup>229</sup>.
- ApoB<sup>100</sup> homozygous genotype worsen hypercholesterolemia in the presence of LDLr<sup>-/-</sup> deficiency (LDLr<sup>-/-</sup> homozygous for the ApoB<sup>100</sup>) in mice<sup>272</sup>. LDLr<sup>-/-</sup>/apoB<sup>100/100</sup> old mice under a chow diet presented lipid deposition, calcification, and superoxide levels in aortic valves. 30% of mice showed reduced aortic valve area<sup>251</sup>.

Under high-fat/high-carbohydrate diet, mice develop aortic valve calcification, and myofibroblast activation<sup>256</sup>. Mice aortic valves expressed smooth muscle actin, and had increased levels of superoxide levels, Runx2, and  $\beta$ -catenin.

- LDLr<sup>-/-</sup>/ApoB<sup>100/100</sup>/IGF-II mice fed with a high-fat/sucrose/cholesterol diet have an increased susceptibility to type-2 diabetes, atherosclerosis, and to the development of the metabolic syndrome. These mice develop aortic stenosis faster than other animal models for CAVD. They have increased left ventricular weight, peak aortic jet velocity, and mean transvalvular pressure gradient. Calcification, fibrosis, and inflammation were also observed in the aortic side of the valve of LDLr<sup>-/-</sup>/ApoB<sup>100/100</sup>/IGF-II mice but not in control mice<sup>245</sup>.
- Epidermal growth factor receptor (EGFR) belongs to a family of protein kinase receptors. It is involved in cell proliferation, differentiation, and/or survival. Egfr<sup>-/-</sup> mice die in the uterus. The EGFR allele waved 2 (wa2) carries a point mutation in the kinase domain leading to a reduction of 10–20% of the normal kinase activity<sup>273</sup>. EGFR<sup>Wa2/Wa2</sup> mice (homozygous for the hypomorphic EGFR allele wa2) under chow

diet develop fibrosis, calcification and inflammatory cell infiltration in the aortic valve. C57BL/6J mice developed hemodynamic changes of CAVD but not 129S1/SvImJ mice in this model. 129S1/SvImJ mice had higher plasma high-density lipoprotein (HDL) levels and some resistance to atherosclerosis<sup>274</sup>.

- Nitric oxide is a vasodilator released by the endothelium. eNOS/NOS3 uses L-arginine as a substrate to generate nitric oxide. eNOS<sup>-/-</sup> mouse is a model of endothelial dysfunction; they present increased platelet aggregation, leukocyte-endothelial adhesion, increased vascular, and smooth muscle cell proliferation. eNOS<sup>-/-</sup> mice are also prone to thrombosis, develop hypertension, stroke, and atherosclerosis<sup>275</sup>. 40% of eNOS<sup>-/-</sup> mice under chow diet developed bicuspid aortic valves<sup>152</sup>.
- Notch1<sup>+/-</sup> (Notch1 heterozygous knockout) mice under high-fat/high-carbohydrate diet had 5-fold more aortic valve calcification than wild type. All mice presented tricuspid aortic valves. Bmp2 expression was 3-fold greater<sup>254</sup>.
- RBPJK/CSL mice<sup>+/-</sup> (haploinsufficient for the Notch pathway effector RBPJK/CSL) fed with high-fat diet supplemented with vitamin D develop valve thickening and calcification. Valve leaflets from these mice express pro-osteogenic proteins, present macrophage infiltration and enhanced collagen deposition<sup>276</sup>.
- Periostin (*POSTN*) is expressed in the heart, the outflow tract, and the atrioventricular canal, thus it is important for valve formation<sup>277</sup>. Periostin<sup>-/-</sup> mice under chow diet developed calcification, fibrosis, and a bicuspid aortic valve phenotype<sup>277</sup>.

Under high-fat/high-carbohydrate diet, mice presented increased valve thickening, fibrosis, but not hemodynamic changes<sup>278</sup>.

- MGP<sup>m1/m1</sup> mice. MGP is a mineral-binding Gla protein that belongs to the family of the coagulation factors VII and VIII and the osteocalcin, an inhibitor of bone formation<sup>279</sup>.

MGP is expressed in smooth muscle cells of aortic valves<sup>279</sup> and inhibits valvular calcification<sup>174</sup>. MGP<sup>-/-</sup> are not viable but MGP<sup>m1/m1</sup> mice with a deficiency of MGP develop to term and die within two months of birth. When fed with chow diet, MGP<sup>m1/m1</sup> mice developed calcification of the aortic valve, aorta, and coronary artery<sup>279</sup>.

- Chondromodulin-I (*Chm1*) is a glycoprotein that stimulates chondrocyte growth. Null *Chm1* mice presented increase in bone mineral density with reduced bone resorption<sup>280</sup>. *Chm1*<sup>-/-</sup> mice under chow diet developed neoangiogenesis, lipid deposition, and calcification in aortic valve of senile mice. Aortic valve leaflets of *Chm1*<sup>-/-</sup> mice at 32 weeks were 1.8 times thicker compared to wild-type mice at 90 weeks<sup>281</sup>.

#### 4.2.2 Rabbit models

- New Zealand White rabbits fed with chow diet and treated with vitamin D2 developed lipid deposition, calcification, and inflammatory cell infiltration in aortic valves. They also had small increases in transvalvular velocity and transvalvular pressure gradient<sup>237</sup>.

New Zealand White hypertensive rabbits induced by one-kidney/one-clip Goldblatt model (chow diet) had increased aortic valve thickness, transvalvular mean gradient, and transvalvular maximal gradient<sup>282</sup>.

- The Watanabe rabbit has been a model of familial hypercholesterolemia for the last 40 years. The Watanabe rabbit strain spontaneously develops atherosclerosis due to a deficiency in LDL receptors and accumulation of LDL, apoB-editing enzyme in the liver and cholesterol ester transfer protein (CETP) activity in plasma<sup>283</sup>. Watanabe rabbits under high-fat diet develop thicker leaflets, increased SPP1/OPN, Lrp5,  $\beta$ -catenin and collagen deposition in the aortic valve, and myofibroblast activation<sup>197</sup>.

### 4.2.3 Porcine models

- Pigs are models of atherosclerosis and recently CAVD. Swine share similar systemic hemodynamic variables and heart anatomy with humans<sup>269</sup>. Yorkshire Landrace adult pigs under high-fat/high-carbohydrate diet develop lipid deposition but do not show hemodynamic changes or signs of inflammation in aortic valve tissue<sup>284,285</sup>.

### 4.3 Gene association studies on CAVD

Few gene association studies have been conducted to uncover the genetic architecture of CAVD and these studies have limitations. They used small sample sizes or genotyped few genetic variants per gene. The definition of CAVD and the characteristics of cases and controls vary among studies, which make them difficult to compare. Candidate genes were selected based on their implication in cellular processes and molecular pathways implicated in the pathobiology of CAVD or were associated with risk factors of the disease<sup>286,287</sup>.

Knez and collaborators compared the allele frequencies of three polymorphisms in three genes between 75 individuals (mean age  $\pm$  SD = 64  $\pm$  9.1 years, 57.3% males) with symptomatic CAVD and 21 (mean age  $\pm$  SD = 55.8  $\pm$  8.9 years, 76.2% males) with aortic regurgitation, which were used as controls<sup>288</sup>. The cases had class I indication for aortic valve replacement. The polymorphisms genotyped were ACE 16 insertion/deletion, angiotensinogen (AGT) Met235Thr, and angiotensin II receptor, type 1 (*AGTRI*) A+86C. Only the ACE 16 ins/del variant was significantly ( $P = 0.007$ ) less frequent in CAVD patients compared to controls (0.79 versus 0.28,  $P = 0.0002$ ).

Avakian *et al.* studied the *APOA1* A/G mutation, *APOB* signal peptide insertion/deletion, *APOB* XbaI restriction fragment length, and *APOE* polymorphisms in 62 males individuals with isolated severe CAVD and 62 males controls<sup>38</sup>. Severe CAVD was defined by an aortic valve gradient  $\geq$  60 mmHg. The mean age  $\pm$  SD of cases and controls was 62.3  $\pm$  12.1 years. *APOE* genotypes were defined by the presence of an arginine–cysteine interchange at positions 112 and 158, which generates three protein isoforms [APOE2 (cys112/cys158), E3 (cys112/arg158), and E4 (arg112/arg158)]. In the ApoB protein, the substitution of cytosine by thymine (2,488th nucleotide of gene) does not change the amino

sequence but creates an Xba I restriction site that characterizes the X+ allele. Only the APOE2 ( $P = 0.034$ ) and XbaI X+X+ ( $P = 0.007$ ) polymorphism of *APOB* were significantly associated with CAVD.

In 2001, Ortlepp *et al.* compared the frequency of one polymorphism (BsmI B/b) in the vitamin D receptor (*VDR*) gene between 100 individuals with CAVD (mean age  $\pm$  SD =  $69.4 \pm 9.3$  years, 55% males) and 100 controls (mean age  $\pm$  SD =  $67.1 \pm 6.7$  years, 55% males) without CAVD<sup>289</sup>. CAVD was defined by visible calcification of the aortic valve visible by fluoroscopy and aortic valve area  $< 1.0 \text{ cm}^2$  or mean transvalvar gradient  $> 40$  mmHg. The BsmI polymorphism (rs1544410) was significantly associated with CAVD ( $P = 0.001$ ).

Novaro *et al.* genotyped variants that generate the three isoforms of the ApoE protein<sup>290</sup>. A total of 43 cases (mean age  $\pm$  SD =  $68 \pm 10$  years, 67% males) and 759 controls (mean age  $\pm$  SD =  $60 \pm 12$  years, 64% males) were included in the study. CAVD was defined as thickened and/or calcified aortic valve leaflets with restricted systolic motion, aortic valve area  $\leq 1.8 \text{ cm}^2$  and a transaortic mean pressure gradient  $\geq 10$  mmHg. The frequency of the APOE4 allele was significantly higher in cases than in controls (0.4 versus 0.27 in controls,  $P = 0.01$ ). The APOE2/4 and APOE3/4 variants were more prevalent in CAVD patients compared to controls, 2% vs. 9% and 23% vs. 28%, respectively.

Nordstrom and collaborators, genotyped polymorphisms in the estrogen receptor 1 (*ESR1*) and transforming growth factor, beta 1 (*TGFBI*) genes<sup>291</sup>. The polymorphisms in *ESR1* were defined by the restriction enzymes PvuII and XbaI, and in *TGFBI* by the restriction enzyme AocI. The cases consisted of 41 postmenopausal women (mean age  $\pm$  SD =  $72 \pm 9$  years) with moderate to severe CAVD and the controls comprised 41 women (mean age  $\pm$  SD =  $26.6 \pm 21.2$  years). Moderate CAVD was defined by an aortic valve area between  $1.0$  and  $1.3 \text{ cm}^2$  and severe CAVD was defined by an aortic valve area  $< 1 \text{ cm}^2$ . The PvuII was associated with CAVD ( $P = 0.03$ ). The combination of polymorphisms in PvuII and AocI increased even more the risk for CAVD ( $P = 0.003$ ).

In 2004, Ortlepp *et al.* evaluated the association of *CCR5*, connective tissue growth factor (*CTGF*), and *IL10* genes with calcification and fibrosis of aortic valves from CAVD patients<sup>292</sup>. The study included 187 individuals (mean age  $\pm$  SD = 70  $\pm$  9, 54% males). Valve calcification was measured by atomic absorption analysis. Three polymorphisms in *IL10* (-1082G/A, -819C/T, and -592C/A;  $P \leq 0.028$ ) were significantly associated with the degree of calcification. Homozygous for the major alleles of -1082C/T and homozygous for the minor allele for -819C/T, and -592C/A had a smaller percentage of calcium mass. The combination of rare variations in *CCR5* ( $\Delta 32$  bp) or *CTGF* (-447 G/C) was also associated with the degree of valvular calcification ( $P = 0.037$ ). The combination of polymorphisms in *IL10*, *CCR5*, and *CTGF* had a higher association ( $P < 0.001$ ) with the degree of valvular calcification.

Schmitz and collaborators analyzed three variants in *VDR* (rs1544410 and rs1073810) and parathyroid hormone (*PTH*, rs6524) genes<sup>293</sup>. They compared the allele frequencies of the SNPs between 538 patients with severe CAVD (mean age  $\pm$  SD = 72  $\pm$  6 years, 54.3% males) and 536 individuals (mean age  $\pm$  SD = 71  $\pm$  5 years, 40.1% males) without any heart disease. Severe CAVD was defined by a mean gradient  $> 40$  mmHg or aortic valve area  $< 0.1$ . Only the SNP rs6524 in *PTH* was associated with CAVD ( $P = 0.007$ , AA frequency was 0.21 in cases and 0.13 in controls).

Turkmen *et al.* studied the association of two variations (A990G and C1011G) in the calcium-sensing receptor (*CASR*) gene<sup>294</sup>. The cases consisted of 41 chronic hemodialysis patients (mean age  $\pm$  SD = 47.23  $\pm$  11.36 years, 63% males, 51.2% presented aortic and/or mitral valve calcification) and the controls were 15 women (mean age  $\pm$  SD = 48.1  $\pm$  14.7). Valvular calcification was defined as thickening of valves and increased echogenicity. The A990G polymorphism had a borderline significant association ( $P = 0.05$ ).

In 2011, our group tested 43 SNPs in seven genes (*APOB*, *APOE*, *CTGF*, *IL10*, *PTH*, *TGFBI*, and *VDR*) previously associated with CAVD in 450 patients with severe disease (mean age  $\pm$  SD = 72.3  $\pm$  8.5 years, 57% males) from Quebec city and 3,294 controls (mean age  $\pm$  SD = 26.6  $\pm$  21.2 years, 38% males) from a public genetic database<sup>295</sup>. All

patients underwent aortic valve replacement for severe CAVD. Ten SNPs surrounding *IL10* were associated with CAVD, including one SNP, rs1800872, with a  $P = 6.2 \times 10^{-11}$ . The missense mutation rs1042031 (E4181K,  $P = 1.0 \times 10^{-5}$ ) and a variation (rs6725189,  $P = 1.3 \times 10^{-5}$ ) causing a stop codon in *APOB* were significantly associated with CAVD. Four other polymorphisms in *PTH* (rs6254,  $P = 0.024$ ), *TGFBI* (rs6957  $P = 0.019$ ), and *VDR* [rs4328262 ( $P = 8.75 \times 10^{-3}$ ) and rs2254210 ( $P = 0.048$ )] had  $P$  values lower than 0.05.

Moura and collaborators performed a gene association test for two variants (Q192R and L55M) in the paraoxonase 1 (*PON1*) gene<sup>296</sup>. They included participants of the RAAVE study, 57 with moderate CAVD (mean age  $\pm$  SD =  $73.4 \pm 8.9$ , 62.7% males) and 251 healthy controls (mean age  $\pm$  SD =  $73.8 \pm 9.1$  years, 49.0%). The cases were asymptomatic with an aortic valve area between 1.0 and 1.5 cm<sup>2</sup>. Both polymorphisms were significantly associated with CAVD (Q192R  $P = 0.03$  and L55M  $P = 0.01$ ). The *PON1* enzyme activity was significantly associated with the variant Q192R and with CAVD progression (reduction in aortic valve area and increase of peak aortic valve velocity). The variants Q192R and L55M were not associated with the levels of HDL and LDL.

Ellis *et al.*<sup>297</sup> analyzed almost 660 SNPs in 265 patients with tricuspid aortic valves and at least mild CAVD (mean age  $\pm$  SD =  $73 \pm 7$  years, 72.7% men) and 961 controls (mean age  $\pm$  SD =  $69 \pm 6$  years, 69.8% men). Cases and controls were divided into two training cohorts [n1 = 364 (20.9% with at least mild CAVD); n2 = 303 (20.1% with at least mild CAVD)] and two validation cohorts [n1 = 361 (24.7% with at least mild CAVD); n2 = 303 (15.5% with at least mild CAVD)]. Some patients overlapped between the cohorts. Candidate SNPs were selected based on their possible association with coronary artery disease and propensity toward plaque rupture. Twenty-nine SNPs located in eight genes already associate with CAVD (*APOB*, *APOE*, IL10 receptor- $\alpha$ , IL10 receptor- $\beta$ , *TGFBI*, TGF- $\beta$  receptor-1, TGF- $\beta$  receptor-2, and TGF- $\beta$  receptor-3) were also genotyped. They did not include the significant SNPs in *IL10* found by Gaudreault *et al.*<sup>295</sup>. Three SNPs, rs2276288 ( $P = 0.001$ ), rs5194 ( $P = 0.004$ ), and rs207 ( $P = 0.005$ ) were significantly associated with CAVD. The SNPs are located in myosin VIIA (*MYO7A*), *AGTRI*, and elastin (*ELN*) genes, respectively.



Arsenault and collaborators confirmed the association of rs10455872 located in the *LPA* gene (found in a GWAS, see section 4.4.1) with CAVD in a cohort of 118 cases (mean age  $\pm$  SD = 65.9  $\pm$  6.8 years, 60.2% men) and 17,453 controls (mean age  $\pm$  SD = 59.1  $\pm$  9.2 years, 43.9% men) from the European Prospective Investigation into Cancer (EPIC)-Norfolk study<sup>211</sup>. Patients hospitalized for CAVD or which cause of death was reported as CAVD were considered as cases. rs10455872 was significantly associated with CAVD risk ( $P < 0.001$ ). In a second cohort from the Montreal Heart Institute Biobank, the association of rs10455872 was less strong ( $P = 0.01$ ) but nine other SNPs in the *LPA* gene region had  $P$  values lower than  $1 \times 10^{-3}$ . The Montreal cohort consisted of relatively older individuals, 405 with CAVD (mean age  $\pm$  SD = 72.4  $\pm$  7.6 years, 65.7% men) and 415 without CAVD (mean age  $\pm$  SD = 69.2  $\pm$  7.1 years, 65.8% males). In this cohort, CAVD was defined by an aortic jet velocity  $> 2.5$  m/s. Higher levels of Lp(a) were also associated with increased risk of CAVD ( $P < 0.001$ ).

In another study, Arsenault *et al.* analyzed 1,435 SNPs associated with HDL cholesterol levels surrounding 11 genes [polypeptide N-acetylgalactosaminyltransferase (*GALNT2*), *LPL*, ATP-binding cassette, sub-family A, member 1 (*ABCA1*), *APOA5*, scavenger receptor class B, member 1 (*SCARB1*), hepatic lipase (*LIPC*), *CETP*, lecithin-cholesterol acyltransferase (*LCAT*), endothelial lipase (*LIPG*), *APOC4*, and *PLTP*)] and their association with the risk of CAVD<sup>298</sup>. The disease was defined by an aortic jet velocity  $> 2.5$  m/s. The cases and controls consisted of 382 and 401 individuals, respectively, from the Montreal Heart Institute Biobank. None of the SNPs was significantly associated with CAVD or HDL levels, which suggest that HDL-associated genetic variants are not good predictors of CAVD risk. They confirmed this lack of association in our cohorts of CAVD patients from Quebec and Paris.

Kamstrup *et al.* studied the association of genetic polymorphisms (rs10455872, rs3798220, and kringle IV type 2 repeat) in *LPA*<sup>182</sup>. The study involved 10,803 individuals from the Copenhagen City Heart Study (CCHS) and 66,877 from the Copenhagen General Population Study. These individuals were followed up during 20 years and 454 developed CAVD. Information of diagnoses of CAVD was obtained from the national Danish patient

registry and the national Danish causes of death registry. The SNP rs10455872 was significantly associated with CAVD ( $P < 0.001$ ), but not rs3798220. In individuals carrying the minor allele of rs10455872 and rs3798220 or with a small number of KIV-2 repeats, the plasma levels of Lp(a) were increased ( $P < 0.001$ ). Additionally, increased levels of Lp(a) were significantly associated with CAVD ( $P < 0.001$ ). Rs10455872, the KIV-2 genotype, and rs3798220 explained 28%, 24%, and 5% respectively, of the total variation in plasma Lp(a) levels.

In summary, genetic variants in the *ACE* and *AGTR1* genes have been evaluated for association with CAVD<sup>288,297</sup>. Both genes are members of the renin-angiotensin pathway and are involved in hypertension and atherosclerosis. Variants in genes involved in lipid metabolism were also part of gene association studies, i.e. the apolipoproteins *APOA1*, *APOB*, *APOE*, *LPA*, and *PONI*<sup>38,182,290,295-297</sup>. The hallmark of CAVD is the accumulation of calcium in the valve leaflets, thus, genes involved in bone metabolism, i.e. *ESR1*, *MYO7A*, *PTH*, and *VDR*, have been targets of interest<sup>289,291-293,297</sup>. Inflammation is also critical in the first stages of the disease and polymorphisms in *IL10* and *CCR5* were associated with increased calcification of aortic valves<sup>292,295</sup>. Tissue remodeling genes were also considered. Polymorphisms in *CTGF*, *ELN* and *TGFBI*<sup>291,292,295,297</sup> were associated with CAVD.

In general, some significant associations did not pass correction for multiple testing and deserve to be verified in studies of larger sample size. Several gene association studies were performed to replicate the results of previous studies<sup>295,297</sup>. Result for *APOB*, *APOE*, *PTH*, *TGFBI*, and *VDR* were supported for at least two studies. Despite their limitations, these studies provided a better understanding of the molecular mechanisms implicated in CAVD and suggested that some individuals are more susceptible to suffer from this disease. **Table 4-1** summarizes the significant gene association studies performed on CAVD.

**Table 4-1.** Genes associated with aortic valve stenosis and CAVD.

<b>Symbol</b>	<b>Population (n cases/n controls)</b>	<b>Phenotype cases/controls</b>	<b>Associated variations</b>	<b>Reference</b>
<i>ACE</i>	Caucasian, Germany (75/21)	Symptomatic AVS/AR	ACE 16 ins/del	Knez <i>et al.</i> <sup>288</sup>
<i>AGTRI</i>	American, USA (265/961)	≥ mild AVS	rs5194	Ellis <i>et al.</i> <sup>297</sup>
<i>APOA1</i>	Brasilian (62/62)	Isolated severe AVS	A/G	Avakian <i>et al.</i> <sup>38</sup>
<i>APOB</i>	Brasilian (62/62)	Isolated severe AVS	Ins/del XbaI X+X+	Avakian <i>et al.</i> <sup>38</sup>
	Caucasian, Quebec (450/3,294)	Severe CAVD/public	rs1042031 (E4181K) rs6725189	Gaudreault <i>et al.</i> <sup>295</sup>
<i>APOE</i>	Brasilian (62/62)	Isolated severe AVS	APOE2 (cys112/cys158)	Avakian <i>et al.</i> <sup>38</sup>
	Caucasian, USA (43/759)	≥ mild AVS	APOE 2/4 APOE 3/4	Novaro <i>et al.</i> <sup>290</sup>
<i>CCR5</i>	Caucasian, Germany (187)	CAVD (endpoint = degree of calcification)	D32 bp additive effect with -447 G/C of <i>CTGF</i>	Ortlepp <i>et al.</i> <sup>292</sup>
<i>CTGF</i>	Caucasian, Germany (187)	CAVD (endpoint = degree of calcification)	-447 G/C additive effect with D32 bp of <i>CCR5</i>	Ortlepp <i>et al.</i> <sup>292</sup>
<i>ELN</i>	Caucasian, USA (265/961)	≥ mild AVS	rs2071307	Ellis <i>et al.</i> <sup>297</sup>
<i>ESR1</i>	Caucasian, Sweden (41/41)	≥ moderate AVS, all post-menopausal women	PVuII (918 T/C)	Nordström <i>et al.</i> <sup>291</sup>
<i>IL10</i>	Caucasian, Quebec (450/3,294)	Severe CAVD/public	rs1800872 (-592 C/A) rs3021094 (intron1) rs1554286 (intron 3) rs1800896 (promoter) rs3024491 (intron 1) rs3024498 (3'UTR)	Gaudreault <i>et al.</i> <sup>295</sup>

<b>Symbol</b>	<b>Population (n cases/n controls)</b>	<b>Phenotype cases/controls</b>	<b>Associated variations</b>	<b>Reference</b>
	Caucasian, Germany (187)	CAVD (endpoint = degree of calcification)	-1082 G/A -819 C/T 592 C/A	Ortlepp <i>et al.</i> <sup>292</sup>
<i>LPA</i>	Caucasian, Denmark (454/77,226)	AVS with and without valve replacement surgery	rs10455872	Kamstrup <i>et al.</i> <sup>182</sup>
	Caucasian, United Kingdom (118/17,453)	CAVD	rs10455872	Arsenault <i>et al.</i> <sup>211</sup>
<i>MYO7A</i>	Caucasian, USA (265/961)	≥ mild AVS	rs2276288	Ellis <i>et al.</i> <sup>297</sup>
<i>PONI</i>	Portuguese (67/251)	Moderate CAVD	rs662 (Q192R)	Moura <i>et al.</i> <sup>296</sup>
<i>PTH</i>	Caucasian, Germany (538/536)	Severe CAVD	rs6254 (intron 2)	Schmitz <i>et al.</i> <sup>293</sup>
	Caucasian, Quebec (450/3,294)	Severe CAVD/public	rs6254	Gaudreault <i>et al.</i> <sup>295</sup>
<i>TGFBI</i>	Caucasian, Sweden (41/41)	≥ moderate AVS, post-menopausal women	-509 C/T (AocI) additive effect with PVuII of <i>ESRI</i>	Nordström <i>et al.</i> <sup>291</sup>
	Caucasian, Quebec (450/3,294)	Severe CAVD/public	rs6957 (3'UTR)	Gaudreault <i>et al.</i> <sup>295</sup>
<i>VDR</i>	Caucasian, Germany (100/100)	CAVD	rs1544410 (BsmI)	Ortlepp <i>et al.</i> <sup>289</sup>
	Caucasian, Quebec (450/3,294)	Severe CAVD/public	rs4328262 (intron 1) rs2254210 (intron 2)	Gaudreault <i>et al.</i> <sup>295</sup>

AR: Aortic valve regurgitation. AVS: aortic valve stenosis.

## 4.4 Whole-genome approaches to study CAVD

Genomics and transcriptomics are being used to unveil the genetic components of CAVD and identify biomarkers and drug targets to treat the disease.

### 4.4.1 GWAS

In 2013, Thanassoulis *et al.* presented the results of a genome-wide association study on aortic-valve calcification and mitral annular calcification<sup>210</sup>. They first analyzed 6,942 individuals from three cohorts of the Cohorts for Heart and Aging Research in Genome Epidemiology (CHARGE) study: Age, Gene/Environment Susceptibility–Reykjavik Study (AGES-RS), Framingham Heart Study (FHS), and MESA. Mean age was  $76 \pm 5$  (42% male),  $60 \pm 9$  (53% male), and  $63 \pm 10$  (48% male), respectively. A total of 2,245 individuals presented aortic valve calcium. CT scan was used to measure aortic valve calcium. They also analyzed mitral valve calcification. The SNP rs10455872 located in *LPA* was associated with the presence of aortic valve calcification (OR = 2.05,  $P = 9.0 \times 10^{-10}$ ). The association of this SNP was replicated in 6,043 individuals (10.8% presented aortic valve calcium) with different ancestry selected from the MESA and Heinz Nixdorf Recall Studies (HNR). These individuals were white European (mean age =  $60 \pm 8$ , 49% male), African American (mean age =  $61 \pm 10$ , 44% male), Chinese (mean age =  $62 \pm 10$ , 49% male), and Hispanic-American (mean age =  $61 \pm 10$ , 46% male) and 91, 263, 67, and 243 of them presented aortic valve calcium, respectively. Lp(a) levels were also associated with aortic valve calcification.

Additionally, in two independent cohorts from Sweden [ $n = 28,193$  (308 with CAVD); mean age =  $58 \pm 8$ , 40% male] and Denmark [ $N = 10,400$  (192 with CAVD); mean age =  $56 \pm 16$ , 44% male], rs10455872 was associated with incidence of aortic stenosis ( $P = 3 \times 10^{-5}$  and  $P = 0.008$ , respectively). The association was less strong or not significant in patients who underwent aortic valve replacement ( $P = 0.03$  in Swedish and  $P = 0.13$  in Danish). The later cohorts were from the Malmö Diet and Cancer Study (MDCS) and the CCHS. The prevalence of aortic stenosis was 1.1% for Swedish and 1.8% of Danish.

#### 4.4.2 mRNA and miRNA whole-genome profiling

Few microarrays studies have been performed to identify mRNAs differentially expressed in human and porcine aortic valve tissues under different conditions.

Bossé *et al.* compared the transcriptome of tricuspid aortic valves explanted from male patients with ( $n = 5$ , mean age =  $67.4 \pm 5.5$ ) and without ( $n = 5$ , mean age =  $64.3 \pm 7.8$ ) CAVD<sup>231</sup>. Calcified valves were explanted from patients undergoing aortic valve replacement and normal valves were explanted at the time of heart transplantation. Microarrays were performed using an Affymetrix chip interrogating more than 47,000 transcripts. The experience was performed twice using a different set of samples. Two provide technical validation of the microarrays experiments, the mRNA expression of seven up-regulated genes (absolute fold change  $> 2$ , false discovery rate  $< 5\%$ ) from the first microarrays experience was measured by quantitative-PCR using the same RNAs. The biological validation of the two most highly up-regulated genes *MMP12* and chitinase 3-like 1 (*CHI3L1*) was performed by quantitative PCR in 38 additional valves ( $n$  cases = 26 and  $n$  controls = 12).

A total of 409 unique genes were upregulated and 306 genes were downregulated in CAVD valves compared to normal valves. From this total, 223 genes were replicated in the second microarrays experiment. The two most highly upregulated genes, *MMP12* and chitinase 3-like 1 (*CHI3L1*), were validated by qPCR. *MMP12* is known to be expressed by macrophages and to degrade elastin, the main component of elastic fibers. *CHI3L1* is secreted by activated macrophages, chondrocytes, neutrophils and synovial cells. The activity of *CHI3L1* may be mediated by *SOX9* and may play a role in the process of inflammation and tissue remodeling. The top genes deregulated in CAVD also included genes involved in bone formation and calcium regulation, several matrix metalloproteinase, chemokines, and collagen genes. Based on the results of Bossé *et al.* and subsequent studies, *PLA2G7* (which codes for Lp-PLA2) and *ENPP1*, are now considered as a potential biomarker and a potential drug target for CAVD, respectively<sup>213,261</sup>.

Male gender is a risk factor for CAVD and McCoy *et al.* performed a microarrays experiment using VICs from male (n = 3) and female (n = 3) healthy pigs (*Sus Scrofa*)<sup>299</sup>. The arrays interrogated 20,201 genes and 183 of these genes were differentially expressed (fold change > 2,  $P < 0.05$ ) in male compared to female VICs. These genes belong to the following biological processes: calcification, cell proliferation, angiogenesis, ECM remodeling, cell adhesion, cell migration, and inflammation. Results of nine genes were selected for validation by qPCR in 11 pigs (including the six of the microarrays experiment). The increased expression was validated for calcitonin receptor-like (*CALCRL*) that increased proliferation, stanniocalcin 1 (*STCI*) and natriuretic peptide C (*NPPC*) which increased calcification, *APOE* that enhanced lipid metabolism, dipeptidyl-peptidase 4 (*DPP4*) which increased ECM remodeling, and insulin-like growth factor binding protein 5 (*IGFBP5*) that increased migration. Decreased expression was validated for angiotensin-like 4 (*ANGPTL4*) that decreased inhibition of angiogenesis and aggrecan (*ACAN*), which increased ECM remodeling.

In CAVD, subendothelial lesions and calcification appear on the aortic side of the leaflets and extend into the fibrosa<sup>89</sup>. Holliday *et al.* compared the mRNA and the miRNA profiles of human aortic valvular endothelial cells from the fibrosa and ventricularis isolated from noncalcified aortic valves<sup>234</sup>. Valves were obtained during heart transplantation (n = 6). Human aortic valvular endothelial cells were isolated by collagenase digestion and subjected to shear and oscillatory stress. They used the Illumina Human miRNA BeadChips (n probes = 1,145) and the Illumina Human HT-12 Expression BeadChips (n probes = 47,231).

A total of 1,032 genes were differentially expressed between fibrosa under oscillatory stress and ventricularis under shear stress (most physiologically relevant conditions). The top molecular and cellular functions enriched with significant genes were cell movement, cell death, and cellular growth and proliferation. Results of 28 selected mRNAs were validated by quantitative-PCR. Genes for validation were selected based on the following criteria: 1) higher absolute fold changes, 2) were transcription regulators, 3) were well-known, shear - sensitive genes, or 4) were novel targets that may be involved in CAVD. Twenty-six out of

28 were successfully validated including *BMP4*, *NOS3*, and FBJ murine osteosarcoma viral oncogene homolog B (*FOSB*). Western blot confirmed up-regulation of BMP4 protein expression and decrease I $\kappa$ B- $\alpha$  and eNOS protein expressions under oscillatory shear compared with laminar shear. The researchers identified 30 shear-sensitive miRNAs and 3 side-dependent miRNAs. Four of 17 miRNA selected for validation using qPCR were confirmed (miRNA-139-3p, miRNA-187, miRNA-192, and miRNA-486-5p) and one side-dependent miRNA (miRNA-370).

Nigam *et al.* studied the miRNA profile of bicuspid aortic valves with fusions of the right and left coronary leaflets collected from 9 male patients (mean age  $44.9 \pm 13.8$  years) who underwent aortic valve replacement<sup>300</sup>. The profile of 1,421 miRNA of bicuspid aortic valve leaflets from CAVD patients were compared with that of patients with aortic insufficiency. Seven miRNA were differentially expressed between aortic stenosis and aortic insufficiency, including miRNA-26a, miRNA-30b, and miRNA-195. MiR-26a and miR-30b levels were reduced in CAVD patients, which represses calcification-related genes such as Smad1/3, *RUNX2*, and *BMP2*.

Yanagawa *et al.* compared the miRNA profiles of aortic valve leaflets obtained from patients with congenital bicuspid aortic valve (n = 19, mean age =  $59.2 \pm 10.6$ , 47.4% males) and with tricuspid aortic valve (n = 17, mean age =  $77.4 \pm 6.2$ , 35.3% males) who underwent aortic valve replacement<sup>267</sup>. They used the GenoExplorer microRNA human array containing 1,583 human miRNA probes. Thirty-five miRNAs were differentially expressed between bicuspid and tricuspid aortic valves. Eight miRNAs were upregulated and 27 were downregulated including miRNA-141. Those miRNA are key elements for the identification of the molecular basis of CAVD in patients with bicuspid valves.

In addition to mRNA expression analysis, the study of the expression profile of miRNA has emerged as a new experimental option to identify drug targets for CAVD and improve the knowledge of the molecular mechanisms implicated in the disease<sup>267,301</sup>.



#### 4.4.3 Proteomics

Proteome analyzes are valuable to identify biomarker proteins released by the disease tissue that can be measured in the plasma and improve the knowledge about the pathophysiological mechanisms of a disease.

Martin-Rojas *et al.* performed a proteomic analysis comparing valves from patients with severe CAVD to healthy aortic valves by quantitative differential electrophoresis (2D-DIGE) combined with mass spectrometry<sup>302</sup>. The study included 20 patients (mean age =  $74 \pm 3.9$ , 55% male) who underwent aortic valve replacement of which three patients showed calcification. Control valves were obtained from necropsies (n = 20, mean age  $69 \pm 7$ , 40% male). Extracts of proteins from cases and controls were labeled with different dyes, each to measure differences in proteins abundance between groups. The results were validated by immunohistochemistry and western blot.

Seventeen unique proteins were differentially expressed in diseased valves compared to controls. These proteins correspond to antioxidant enzymes (superoxide dismutase [Cu-Zn]), glutathione s-transferase P, glutathione peroxidase 3, haptoglobin), structural and contractile proteins (lumican, transgelin, vimentin), proteins involved in inflammation (serum amyloid P-component, alpha-1-antitrypsin, fibrinogen gamma chain), transport [transthyretin, APOA1, fatty acid-binding protein (FABP)], chaperones (HSP27, calreticulin), and alpha-1B-glycoprotein. Six of these proteins were downregulated (transgelin, haptoglobin, glutathione peroxidase 3, HSP27, calreticulin, and superoxide dismutase [Cu-Zn]).

More recently, Alvarez-Llamas *et al.* studied the secretome of aortic valves by labeling proteins to discriminate proteins secreted by the valves from plasma contaminants<sup>303</sup>. The proteome of 20 valves from patients (age =  $74 \pm 4$ , 55% male) with CAVD who underwent aortic valve replacement and 20 macroscopically normal valves from nonaffected individuals (age =  $69 \pm 7$ , 40% male, from autopsies) was analyzed by liquid chromatography mass spectrometry. The results were validated by Western blot using

plasma samples from independent cases and controls using mass spectrometry applying the selective reaction monitoring method.

To eliminate serum contaminants 1 mm<sup>3</sup> pieces of each valve from three cases and three controls were cultivated with the labeled aminoacids L-lysine 2HCl (U-<sup>13</sup>C<sup>6</sup>) and L-Arginine HCl (U-<sup>13</sup>C<sup>6</sup>). This approach is useful to differentiate proteins synthesized by the aortic valves (labeled) and contaminating proteins from the blood (unlabeled). Sixty-one proteins were labeled and 82% of them incorporated the label in a unique tissue group (cases or controls). The labeled proteins were classified in groups according to their molecular function: ECM/cytoskeletal, immune response, degradation, transport/metabolic processes, regulatory functions, and other functions. Proteins included AGT, EGF containing fibulin, gelsolin, and prostaglandin D2 synthase. The most significant pathways enriched with labeled proteins were the “Cardiovascular System Development and Function” and the “Tissue Development” pathways. The actin binding protein gelsolin, coded by the *GELS* gene, was selected as a high sensitivity biomarker for CAVD because its secretion in plasma from atherosclerotic arteries is inversely, and can differentiate between the two diseases. Gelsolin is involved in cytoskeletal remodeling and ion channel regulation; its up-regulation in disease aortic valves may be the tissue response to flow-induced endothelium damage<sup>303</sup>.

The same research group also performed a proteomic analysis of plasma from individuals with (n = 12, mean age = 74.9, 42% male) and without (n = 12, mean age = 64.6, 42% male) CAVD<sup>304</sup>. They used 2D-DIGE and mass spectrophotometry. Differentially expressed proteins were classified as proteases and protease inhibitors (~19.5%), blood homeostasis and coagulation (~16.6%), inflammation and immune response (~36.2%), lipid metabolism and transport (~16.6%), and others (~11.1%). The expression levels of five proteins were confirmed by 1D and 2D western blots, i.e. APOAI, APOE, PON1, complement C3 (CO3), and alpha 2 HS glycoprotein (FETUA).

Proteins in the five groups were:

- Proteinase inhibitors and proteases: inter- $\alpha$ -trypsin inhibitor H4, protein AMBP,  $\alpha$ 1-antichymotrypsin,  $\alpha$ 1-antitrypsin, kininogen-1, hemopexin, and vitronectin.
- Blood coagulation and homeostasis:  $\alpha$ ,  $\beta$  and  $\gamma$  fibrinogens, prothrombin, antithrombin III, and plasma protease C1 inhibitor.
- Inflammation and immune response: antigen CD 5-like, ficolin-2, Ig kappa chain, Ig lambda chain, Ig mu chain, complement C4B, complement C9, complement factor B, complement factor H, complement factor I, complement C3, complement Factor H-related protein, and mannose binding protein C.
- Lipid metabolism and transport: APOAI, APOAIV, APOE, clusterin, apolipoprotein CIII, and other related proteins.
- Others: hemoglobin, ceruloplasmin, alpha 2 HS glycoprotein, and leucin-rich  $\alpha$ 2 glycoprotein.

Another proteomic study was performed in bovine aortic VICs acquiring a pro-calcific phenotype following treatment with lipopolysaccharide<sup>305</sup>. The proteome of these calcified valves was compared with the proteome of VICs not treated with lipopolysaccharide (non-calcified). Thirty-four unique proteins from the cytosolic fraction and 10 of the membrane fraction were identified. Significantly differentially expressed proteins had functions in protein synthesis, assembly, metabolism and transport [e.g. heat shock proteins, 78 kDa glucose-regulated protein (GRP78), reticulocalbin, calumenin, calreticulin, FABP, elongation factor 1-beta (EF-1-beta), and other], energy metabolism [phosphoglycerate kinase 1 (PGK1), R-enolase, triosephosphate isomerase], cytoskeletal organization (including vimentin,  $\alpha$ -actin-4, fascin, profilin-1), and cell redox/nitric oxide (NO) homeostasis such as superoxide dismutase [Cu-Zn] and thioredoxin.

Matsumoto *et al.* performed a proteomic analysis comparing cells of calcified aortic valve tissue with adjacent normal valvular tissues<sup>306</sup>. Calcified and healthy valve tissues were taken from eight patients who underwent aortic valve replacement (mean age = 78.1, 62.5% males). The results were confirmed by Western blot using calcified and healthy valve tissue from six other patients (mean age = 76.5, 17.7% males). A total of 105 proteins were differentially expressed in calcified valve tissues compared to normal adjacent valve tissue. From them, 34 downregulated proteins and 39 upregulated had absolute fold changes > 1.3. These proteins included  $\alpha$ -2-HS-glycoprotein and tenascin-X, as well as extracellular matrix proteins such as collagens.

Since the expression of an mRNA does not guarantee protein expression in the same cell type, proteomic studies are important to identify proteins expressed in aortic valve leaflets in physiologic and pathological conditions. Proteomic studies have confirmed the expression at the level of proteins of CAVD-related genes such as *APOA1*, *APOE* and the downregulation of antioxidant enzymes such as superoxide dismutase [Cu-Zn] in aortic valves. Differentially expressed proteins in these studies included proteins involved in inflammation, ECM remodeling, and lipid deposition in aortic valves. However, none of the proteome studies integrated the results from genomics and/or transcriptomic studies, which will be important to perform in the future.

## **Chapter 5. Hypothesis and objectives**

### **5.1 Objectives**

#### **5.1.1 General objective**

Identify susceptibility genes of CAVD in order to better understand the development and progression of this disease, in patients with bicuspid and tricuspid aortic valves, and to discover molecular targets for treatment and diagnosis.

#### **5.1.2 Specific objectives**

- 1) Identify rare and common polymorphisms in the *NOTCH1* gene associated with CAVD.
- 2) Conduct the first GWAS on CAVD to identify new susceptibility genes.
- 3) Perform the first valvular eQTL mapping study to identify eQTL-SNPs associated with the mRNA expression of genes expressed in human aortic valves.
- 4) Identify genes differentially expressed between tricuspid aortic valves with and without calcification using RNA-Seq.
- 5) Integrate GWAS, eQTL, and RNA-Seq results to identify the best candidate genes and molecular pathways underpinning CAVD.
- 6) Identify genes differentially expressed between calcified bicuspid and tricuspid aortic valves with and without calcification using microarrays and RNA-Seq.

### **5.2 Hypothesis**

#### **5.2.1 General hypothesis**

Susceptibility genes and molecular pathways driving the development of CAVD will be identified using genomic and transcriptomic approaches.

### 5.2.2 Specific hypothesis

- 1) Rare and common genetic variants in the *NOTCH1* gene are present in CAVD patients with tricuspid aortic valves and are associated with the disease.
- 2) GWAS will identify new susceptibility genes and molecular pathways for CAVD.
- 3) Valvular eQTLs and transcriptome analyzes in human aortic valves will refine and facilitate the interpretation of susceptibility variants for CAVD identified by GWAS.
- 4) A number of genes are differentially expressed in the transcriptome of tricuspid aortic valves with and without calcification.
- 5) Several genes and molecular pathways interact in the development of CAVD and integrative genomic approaches are needed to elucidate the most promising molecular targets for future therapeutic interventions.
- 6) A large number of genes are differentially expressed in the transcriptome of calcified bicuspid and tricuspid aortic valves compared to non-calcified tricuspid aortic valves.

## **Chapter 6. Article 1: *NOTCH1* genetic variants in patients with tricuspid calcific aortic valve stenosis**

**Variations génétiques dans *NOTCH1* chez des patients avec rétrécissement valvulaire aortique et valves tricuspides**

Valérie Ducharme, BSc1, Sandra Guauque-Olarte, MSc 1, Nathalie Gaudreault, BSc 1, Philippe Pibarot, DVM, PhD1, Patrick Mathieu, MD1,2, Yohan Bossé, PhD1,3

1) Centre de recherche Institut universitaire de cardiologie et de pneumologie de Québec, Laval University, Quebec, Canada.

2) Laboratoire d'Études Moléculaires des Valvulopathies (LEMV), Groupe de Recherche en Valvulopathies (GRV), Quebec Heart and Lung Institute/Research Center, Department of Surgery, Laval University, Quebec, Canada.

3) Department of Molecular Medicine, Laval University, Quebec, Canada.

**Short running head:** *NOTCH1* and aortic valve stenosis

**Address all correspondence to:**

Yohan Bossé, Ph.D.

Assistant Professor, Laval University

Institut universitaire de cardiologie et de pneumologie de Québec

Pavillon Marguerite-d'Youville, Y4190

2725, chemin Sainte-Foy

Quebec (Quebec)

Canada, G1V 4G5

Tel: 418-656-8711 ext. 3725

Fax: 418-656-4602

email: yohan.bosse@crhl.ulaval.ca

## Résumé

**Objectif-** Le rétrécissement valvulaire aortique (RVA) affecte 2-5% de la population âgée de plus de 65 ans. Les variations génétiques du gène *NOTCH1* ont été identifiées chez des patients avec une valve aortique bicuspide et une calcification valvulaire sévère. La contribution de ces variations au RVA chez les individus avec des valves aortiques tricuspides (TAV) n'est pas encore connue.

**Méthodes-** Quatorze variations génétiques dans le gène *NOTCH1* ont été genotypées, incluant certaines variations rares et communes déjà rapportées. Quatre cent cinquante sept patients canadiens-français avec des valves aortiques tricuspides et un RVA sévère ont été recrutés. Le génotypage a été réalisé avec la plateforme BeadXpress d'Illumina. Les fréquences alléliques des SNP communs ont été comparées entre les patients atteints et 3 294 contrôles d'origine européenne. Quatre-vingt-huit marqueurs informatifs de l'ascendance ont été utilisés afin de corriger pour la stratification des populations.

**Résultats-** La mutation p.R1107X, précédemment associée à la bicuspide et à la calcification valvulaire sévère, a été identifiée chez un individu de 58 ans. Les mutations p.R1279H et p.V2285I ont été détectées chez 18 et 14 hétérozygotes, respectivement. Un polymorphisme commun (rs13290979) localisé dans l'intron 2 de *NOTCH1* a été associé avec le RVA ( $P = 0.003$ ), même après correction pour tests multiples. Cette association n'était plus significative après correction pour la stratification des populations ( $P = 0.088$ ).

**Conclusion-** Cette étude a identifié des variations fonctionnelles rares dans le gène *NOTCH1* chez une population canadienne-française de patients souffrant de RVA avec une valve tricuspide. L'étude suggère pour la première fois la présence d'un polymorphisme commun dans ce gène conférant une susceptibilité au RVA.



## **Abstract**

**Background-** Calcific aortic valve stenosis (AS) affects 2-5% of the population older than age 65 years. Functional DNA variants at the *NOTCH1* locus result in bicuspid aortic valves (BAV) and severe valve calcification. The contribution of these variants to AS in the population with tricuspid aortic valves (TAV) still remains to be determined.

**Methods-** 14 genetic variants surrounding the *NOTCH1* gene were genotyped, including rare mutations previously reported and common polymorphisms. The study involved 457 French Canadian patients with severe tricuspid AS. Genotyping was carried out using the Illumina® BeadXpress platform. Allele frequencies of common SNPs for patients with AS were compared to a shared control group of European ancestry (n = 3,294). Eighty-eight ancestry-informative markers were used to correct for population stratification.

**Results-** The mutation p.R1107X, previously associated with AS and BAV, was identified in a relatively young patient (58 years). The mutations p.R1279H and p.V2285I were detected in 18 and 14 heterozygotes, respectively. A common polymorphism (rs13290979) located in intron 2 was significantly associated with AS ( $P = 0.003$ ), which remained significant after correction for multiple testing. However, this association was no longer significant after accounting for population stratification ( $P = 0.088$ ).

**Conclusion-** This study found rare functional variants in the *NOTCH1* gene in a French Canadian population of patients with severe tricuspid AS and suggests for the first time the presence of a common polymorphism in this gene conferring susceptibility to AS.

**Keywords:** Calcific aortic valve stenosis / candidate gene / genetic association study / genetics / NOTCH

## Introduction

Calcific aortic valve stenosis (AS) is the most frequent valvular heart disease. AS affects 2% of the population over 65 years old (1). AS shares many clinical risk factors with atherosclerosis including age, hypertension, and dyslipidemia (2). Nowadays, AS is known as a disease implicating many cellular processes such as inflammation, lipids deposition, and calcification (3,4). There is no treatment available other than aortic valve replacement surgery or transcatheter valve implantation (5).

A number of genetic studies were performed to identify genes associated with AS (6). For most genes investigated so far, replication in larger populations is needed and functional causality remains to be established. The most compelling evidence of genetic predisposition to AS was observed with the *NOTCH1* gene. Two mutations that have functional consequences on the Notch1 protein have been identified. A mutation labelled R1107X was identified in a five-generation family affected with aortic valve diseases and results in a premature stop codon (7). The mutation (H1505del) identified in a smaller Hispanic family characterized by bicuspid aortic valve (BAV) cause a frameshift that alters 74 amino acids of the protein before ending its translation prematurely. The absence of these functional mutations in unaffected family members and healthy controls strongly suggested that *NOTCH1* was the causal gene. These specific mutations have not been reported in other populations. Another group has reported two different likely pathogenic missense mutations (p.T596M and p.P1797H) in two sporadic cases of BAV (8). Whether these mutations are private or restrict to a few families in isolated geographic regions remained to be confirmed. In this study, we hypothesized that known mutations in the *NOTCH1* gene are found among patients undergoing aortic valve replacement surgery for tricuspid calcific AS. We also hypothesized that more subtle but common (Minor allele frequency [MAF] > 0.05) polymorphisms in the *NOTCH1* gene influence susceptibility to AS.

## **Materials and methods**

### **Patients**

A total of 457 patients with severe AS undergoing aortic valve replacement surgery were recruited at the Institut universitaire de cardiologie et de pneumologie de Québec (Quebec City, Canada). All patients provided written informed consent. The study was approved by the local ethics committee. The patients are French Canadians, which are known as a homogenous population of European ancestry (9). Only subjects with tricuspid nonrheumatic AS were considered. All patients had moderate to severe AS and an aortic regurgitation grade  $\leq$  mild. Patients with a history of rheumatic disease, endocarditis or an inflammatory disease were excluded. Clinical data included diagnoses of hypertension (patients receiving antihypertensive medications or having known, but untreated, elevated blood pressure [ $\geq$  140/90 mmHg]), and diabetes (patients with established diagnoses currently receiving oral hypoglycemic medication or insulin). Every patient underwent a coronary angiogram. A significant coronary artery disease (CAD) was considered to be present when at least one coronary artery had a lesion  $\geq$  50%. All patients underwent a comprehensive Doppler echocardiographic examination pre-operatively. Doppler echocardiographic measurements included transvalvular gradients calculated using the modified Bernoulli equation (10) and the aortic valve area calculated with the continuity equation. Table 1 shows the clinical characteristics of patients.

### **Control population**

Genotype data for 3,294 white control subjects typed on the HumanHap550 BeadChip were obtained from the Illumina Genotyping Control Database ([www.illumina.com/science/icontrolldb.ilmn](http://www.illumina.com/science/icontrolldb.ilmn)). Cardiovascular phenotypes are not available for this share control group, which consists of 2,034 women (61.7%) and 1,260 men (38.3%) with a mean age of  $32.2 \pm 21.5$  and  $20.9 \pm 20.8$  years, respectively. In addition, DNAs for this control population are not available, so no additional genotyping can be carried out.

## **DNA extraction in patients with AS**

Genomic DNA was isolated from Buffy coat using QIAmp® DNA Blood Midi Kit (Qiagen). DNA quality was assessed by UV A260/A280 ratio. DNA quantification was assessed by PicoGreen® assay (Invitrogen™, Carlsbad, CA, USA) using a Synergy™ HT fluorometer (Biotek®, Winooski, VT, USA). Every sample was diluted to a final concentration of 50 ng/μL.

## **SNP selection**

To facilitate genetic association testing Illumina controls, we selected 12 SNPs genotyped on the HumanHap550 BeadChip located within 20 kilobases up- and downstream of *NOTCH1*. Nine of these SNPs were identified as tagging SNPs and 3 as singletons using the European-derived (CEU) genotype data from the HapMap project (11) and a pairwise tagging algorithm implemented in Haploview 4.2 (12). MAF and  $r^2$  thresholds were set at 0.05 and 0.8, respectively. Seven additional SNPs were selected from the literature and known to alter Notch1 protein (nonsense, missense or frameshift) even if they were not present on the HumanHap550 array. Using Illumina's Assay Design tool, we designed a first panel containing 19 SNPs in the *NOTCH1* locus. Four tagging SNPs failed Hardy-Weinberg equilibrium in the controls and were excluded. One tagging SNP with an assay design final score of 0, reflecting a low designability of the assay for this locus, was excluded. Accordingly, a total of 14 SNPs were selected and a multiplex assay was manufactured by Illumina to interrogate them. Table 2 provides a list of SNPs genotyped in this study and the reason for their selection.

## **Genotyping**

Genotyping of the 457 patients was performed using the VeraCode GoldenGate genotyping assay. Microbeads were read on the Illumina BeadXpress Platform (Illumina, San Diego, CA, USA). The results were analyzed and genotype reports were produced with the Illumina GenomeStudioV2010.1 Genotyping Module 1.6.3. DNAs from one Coriell trio (Camden, NJ,

USA) were included as positive controls. In order to monitor repeatability, one AS sample and a single Coriell subject were included in all five 96-well genotyping plates.

### **Quality control of genotyping data**

Clustering of genotyping data was performed using the Illumina GenomeStudio software. One singleton SNP (rs7849014) failed the genotyping assay. A rare variant rs35136134 failed Hardy-Weinberg equilibrium ( $P = 5.44E-18$ ) and was excluded from further analysis. Seven samples with a call rate  $\leq 0.90$  were excluded. No replicate or parent-parent-child errors were found from the Coriell trio and replicates tested. The software STRUCTURE version 2.3.2.1 (13) was used to identify population outliers using 88 ancestry-informative markers (AIMs) (14). Cases, controls and four reference populations from HapMap (11) (CEU, CHB, JPT, and YRI) were used. As shown in Figure 1, the majority of cases, controls and CEU individuals were contained in a major cluster. Three cases and 82 controls located outside the major cluster were removed. One sample for which AIMs genotyping data were not available was excluded.

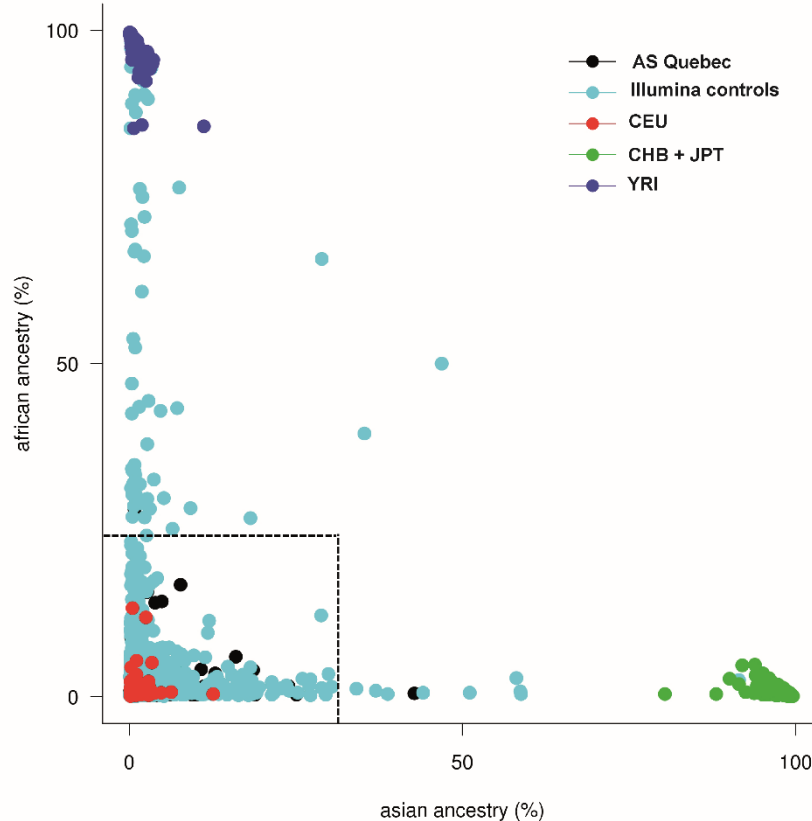


**Figure 1.** Triangular plot showing the genetic background of cases and controls. The plot was generated using STRUCTURE version 2.3.2.1 with HapMap subjects as internal controls. Black, AS (calcific aortic valve stenosis) cases; Cyan, Illumina controls; Red, CEU population (Utah residents with ancestry from northern and western Europe); Green, CHB + JPT population (Han Chinese in Beijing, China + Japanese in Tokyo, Japan); Violet, YRI population (Yoruba in Ibadan, Nigeria). The dotted lines delimited our boundaries for European ancestry.

## Sequencing

The single heterozygote patient carrying the R1107X mutation was confirmed by sequencing. A 357 bp fragment of the NOTCH1 gene was amplified with the sense primer 5'-GTCCACCAGGTCCTCACAGT-3' and the antisense primer 5'-TGTGCACTGGTGTGACTCCT-3'. PCR was performed in a final volume of 20  $\mu$ l containing 30 ng of genomic DNA, 2 U of HotStar Taq DNA polymerase (Qiagen), PCR buffer 1X, 200  $\mu$ M of each dNTP and 0.2  $\mu$ M of each primer. The PCR reaction was carried out on the GeneAmp® PCR system 9700 (Applied Biosystems) with the following cycling conditions: 15 minutes at

95oC, 35 PCR amplification cycles (15 seconds at 94oC, 30 seconds at 56oC, and 30 seconds at 72oC), and 7 minutes at 72oC. The sequencing reaction was then performed using standard procedures and the product was run on the ABI 3730xl DNA Analyzer (Applied Biosystems). Sequencing files were assembled and analyzed using the Phred/Phrap/Consed System.

## **Statistical analyzes**

Allele frequencies of common SNPs between 446 cases and 3212 controls that passed quality controls were compared using chi square tests in PLINK version 1.06 (15). The method of Nyholt was used to correct for multiple testing (16), leading to a *P* value threshold of 0.0085 or lower to consider polymorphisms statistically significant. The AIMs were further used to calculate the genomic inflation factor in order to correct for population stratification (17). Population stratification can exist when the populations under study consist of subpopulations with different marker allele frequencies and disease prevalence, caused by different ancestry, which may increase the rate of false positives in case-controls studies (18). Linkage disequilibrium (LD) was calculated using Haploview. The influence of SNPs on disease severity, as assessed with aortic valve area and mean transvalvular gradient, was tested using linear regression models adjusted for age and body surface area. Age of surgery was additionally analyzed using linear models adjusted for body surface area. Disease severity was also analyzed between carriers and non-carriers of nonsynonymous sequence variants. Disease severity analyzes were performed with R software version 2.8.1. The population-attributable risk was calculated as  $PAR\% = 100\% \times P \times (OR - 1) / [P \times (OR - 1) + 1]$ , where *P* is the frequency of the risk allele associated with AS in the control group, and the OR is the odds ratio calculated in the case-control cohort.

## Results

The assay conversion rate was 93% (13 out of 14 SNPs). Call rates for the remaining SNPs were above 95% with a mean of  $99.8 \pm 0.3$ . Table 3 shows the 6 common SNPs tested for association in the case-control cohort. Figure 2 shows the LD plot for the common SNPs in the case-control cohort.

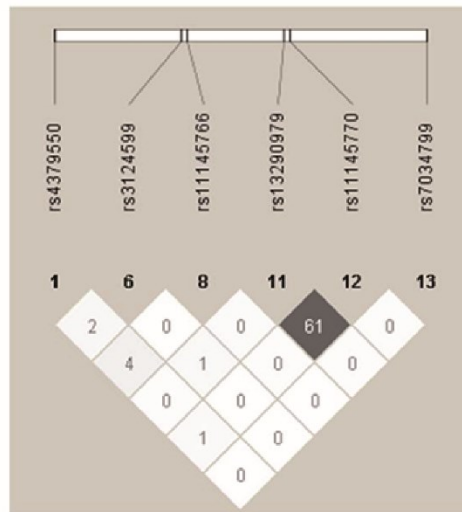


**Figure 2.** LD-plot showing the  $r^2$  values for the common *NOTCH1* SNPs in the case/control population.

### A common SNP is associated with the disease

A common polymorphism (rs13290979) in the intron 2 of the *NOTCH1* gene was significantly associated with AS (Figure 3 and Table 3). The minor allele frequency was 32.6% in cases and 37.7% in controls ( $P = 0.0034$ ). The risk allele is the common allele (common:rare allele counts were 601:291 in cases and 3999:2417 in controls) with an odds ratio of 1.25 (95% confidence interval [1.08-1.45]). The association remained significant after correction for multiple testing. The estimated population attributable risk was 14.3%. A genomic inflation factor of 2.9 was calculated using AIMs between cases and controls. After accounting for population stratification, the association between rs13290979 and AS was no longer significant ( $P = 0.087$ ). Among cases,



no association was found between rs13290979 and disease severity. The aortic valve area, the mean transvalvular gradient, and age at surgery were not different between genotyping groups (Figure 4A). We searched for SNPs in LD  $\pm$  100 kilobases up and downstream of rs13290979 using the CEU 1000 genomes (19) genotyping dataset. The SNP rs13290840 also located in the second intron of *NOTCH1* was in moderate LD ( $r^2 = 0.759$ ) with rs13290979. The other five common variants tested in the cases-controls cohort were not significantly associated with AS (Figure 3 and Table 3).

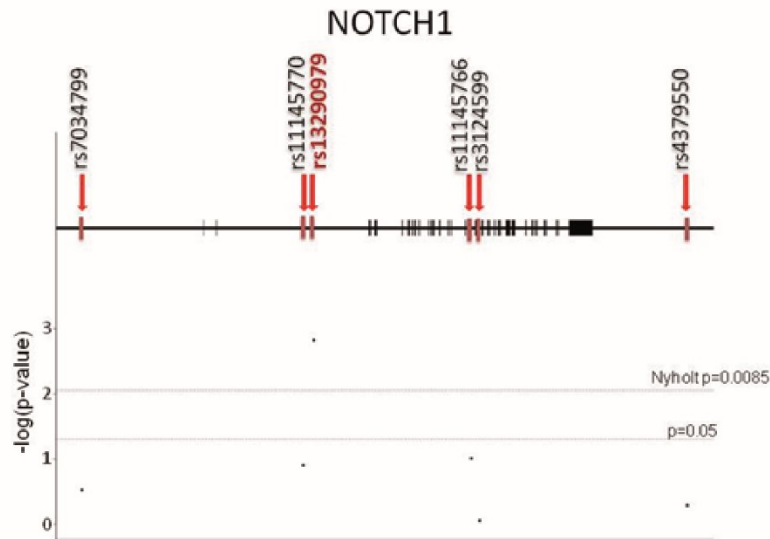


**Figure 3.** Genetic association of common SNPs in the *NOTCH1* gene with AS. The upper part of the figure shows the intron-exon structure of the gene and the localization of the genotyped SNPs. The lower part of the figure shows the genetic association results. The x-axis shows the localization of the SNPs relative to the upper part of the figure. The y-axis shows the  $P$  values on a  $-\log_{10}$  scale. The horizontal lines represent  $P$  value thresholds of 0.05 and 0.0085.

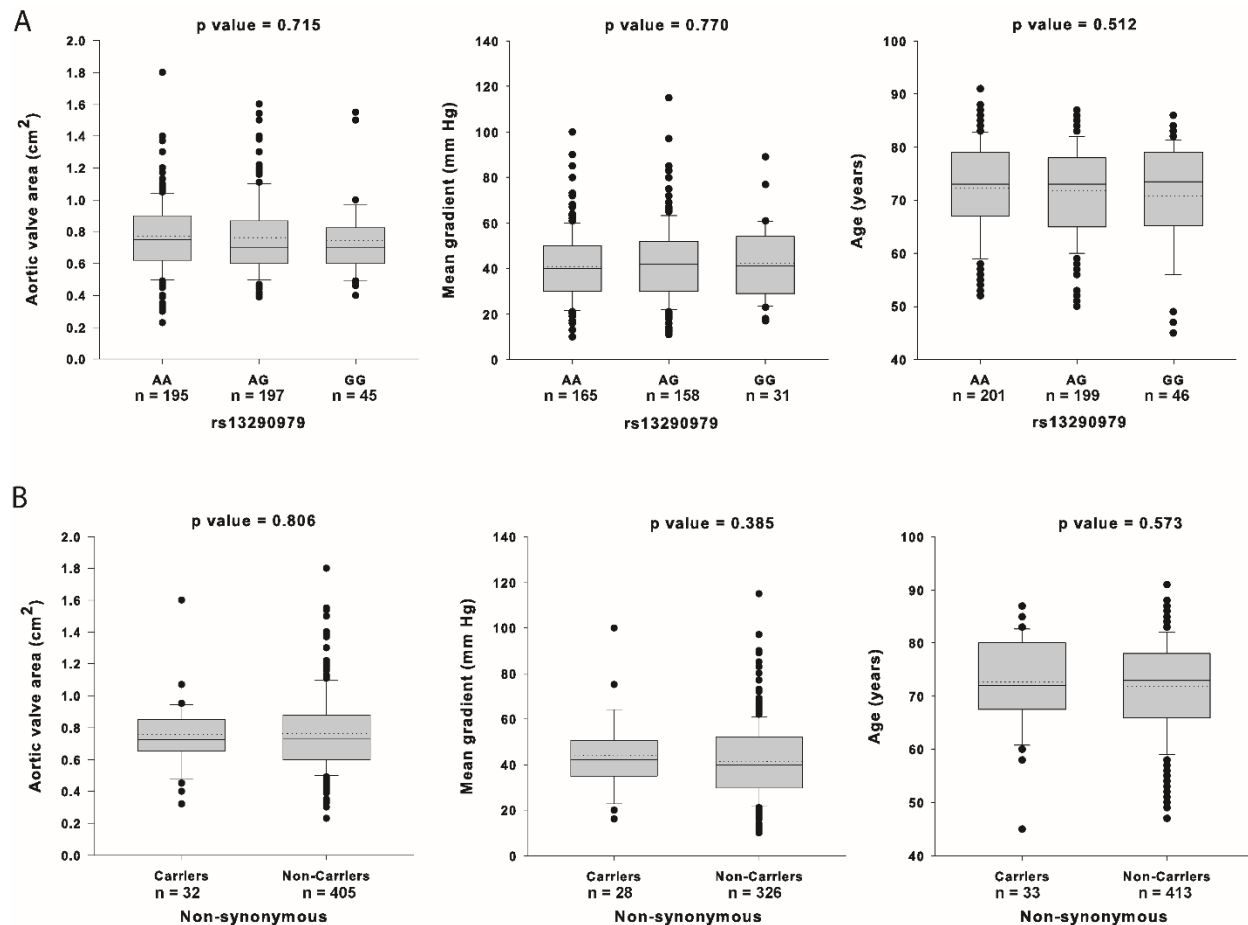


**Figure 4.** Disease severity assessed by aortic valve area, mean transvalvular gradient and age at surgery. A) Association between disease severity and the common SNP rs13290979. Box plots show the median, 25<sup>th</sup> and 75<sup>th</sup> percentiles. The dotted line inside the box represents the mean. Whiskers above and below the box indicate the 90<sup>th</sup> and 10<sup>th</sup> percentiles. B) Association between disease severity and carrier status for rare non-synonymous SNPs (rs41309764, rs61751489, and rs61751543). Patients included those with clinical and genotypic data available.

### Three rare variants were found in patients with AS

Among cases, 33 carry one single rare mutation. The mutations R1107X, R1279H and V2285I were found in 1, 18 and 14 patients, respectively. The single carrier of the R1107X variant was confirmed by sequencing (Figure 5). Despite of the presence of these variants in our cohort, there was no difference in disease severity or age of surgery between AS patients with or without these

mutations (Figure 4B). The other mutations, T596M, R938Q or H1504del, were not found among cases.

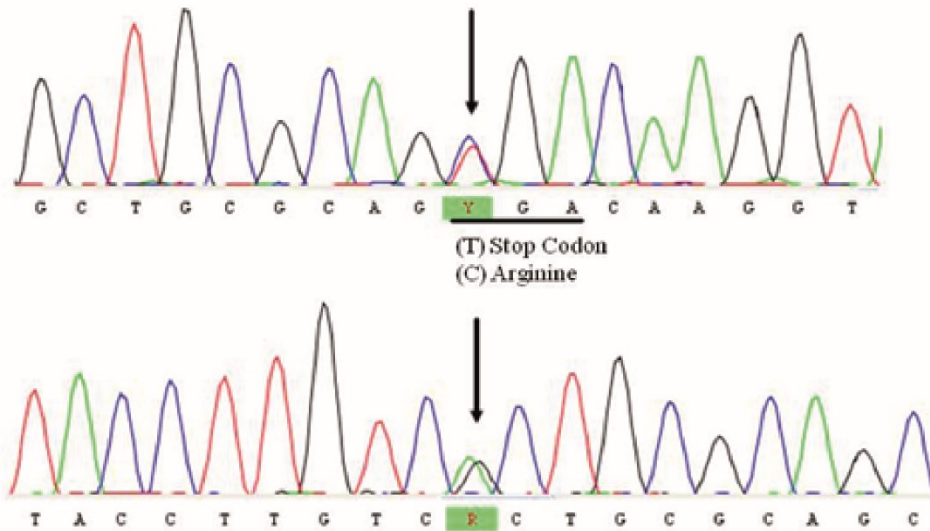


**Figure 5.** Sequence chromatogram of the single heterozygote subject carrying the R1107X variant. The sequence was obtained on both strands (top and bottom panels). R = A or G.

## Discussion

A previous study suggested that rare mutations in the *NOTCH1* gene caused aortic valve diseases (7). The frequency of these mutations in the general population and in patients with valve diseases is unclear. It is also unclear whether common polymorphisms in the *NOTCH1* gene confer susceptibility to AS. In the current study we typed previously rare mutations associated with AS and common polymorphisms in *NOTCH1* in a cohort of 457 patients with severe AS. Briefly, we show for the first time an association between a common SNP in the *NOTCH1* gene and AS that will require further validation in an independent cohort. We also detected multiple rare variants in our case population including one carrier of the R1107X mutation.

Previous *NOTCH1* gene association studies found that rare variants may have a role in the pathobiology of AS (7,8). Garg et al. reported a nonsense mutation to cause developmental valves anomalies and severe valve calcification (7). They described a five-generation family of European-American descent with 11 cases of congenital heart disease (nine with aortic valve disease). Members of this family had bicuspid or tricuspid valves. Seven developed calcific AS and 4 of them underwent aortic valve replacement. Every affected family member carried the mutation R1107X, while unaffected members were noncarriers, suggesting an autosomal-dominant mutation with a complete penetrance (7). Interestingly, and for the first time since Garg et al., we found one male patient carrying this mutation. This patient was 58 years of age at surgery. He had a grade 3 calcification based on the Warren and Yong scoring system (20) and light fibrosis. He had an index aortic valve area of  $0.47 \text{ cm}^2/\text{m}^2$ , waist circumference of 107.4 cm and body mass index of  $29.5 \text{ kg}/\text{m}^2$ . This individual has multiple cardiovascular risk factors. He suffers from the metabolic syndrome, dyslipidemia, hypertension, and CAD. He takes angiotensin-converting enzyme inhibitor and statin medications. He underwent aortic valve replacement for severe AS at a young age, suggesting that the presence of this variation might be associated with premature development of AS. No family history of calcific aortic valve stenosis was found in the patient's medical chart. We do not have DNA or echocardiography exams for relatives of this patient. No family history of AS exist in the patient's family. Nevertheless, our study confirms that this mutation is found in the French Canadian population and may be more widely spread than previously suggested.

In this study we provide suggestive evidence that a common polymorphism in the *NOTCH1* gene is associated with AS. Although the odds ratio (1.25) of this polymorphism is modest, the population attributable risk indicates that more than 14.3% of AS cases could be attributed to this common variant. This polymorphism is in moderate LD with a second variation in the same intron. The genotyping of the latter variation in a cohort of AS patients and controls will be needed to know if it is also associated with the disease. Accordingly, in addition to several rare penetrant variants, there is a common risk allele that seems to modulate the risk of suffering from AS. Our data do not support the concept that multiple rare variants collectively contribute to disease severity among AS cases. However, combined with previous literature (7), our study suggests that the *NOTCH1* locus contains multiple polymorphisms covering a range of allele frequency and penetrance associated with AS. Functional studies will be required to prove causality of the common rs13290979 polymorphism.

This study has limitations. Validation in independent populations will be required. Although, we detect three known and potentially deleterious mutations in patients with AS, the frequency of these rare mutations will need to be evaluated in large populations with and without valve diseases in order to demonstrate their clinical relevance. Finally we used a set of control subjects publically available to perform our case-control analysis. Detailed phenotyping of the cardiovascular system and other traits of interest were not available in this control group. One consequence of such strategy relates to the potential for misclassification: a proportion of the controls is likely to have AS and some others will develop this disease in the future. However, it was demonstrated that the effect of this misclassification in the control population on statistical power is minimal unless the extent of misclassification bias is substantial. For example, if 5% of controls would meet the definition of cases, the loss of power is approximately the same as that due to a reduction of the sample size by 10% (21). In the general population, the prevalence of all valve diseases is estimated at 2.5% (22). Accordingly, the effect of misclassification is likely to be low in our proposed control group.

This study further supports *NOTCH1* as a potentially important gene involved in AS. An autosomal-dominant mutation with complete penetrance (R1107X) originally identified in a single pedigree was found in one of our patients with AS. The clinical condition and age of this

patient at surgery support this mutation as being penetrant. Although additional rare variants were found, they were not associated with disease severity among cases. The frequency of these nonsynonymous sequence variants in healthy controls is required. Finally, we found some evidence that a common variant in the *NOTCH1* gene was associated with AS, suggesting that more subtle but frequent polymorphisms at this locus might predispose to the disease. Replication in an independent cohort is needed.

**Conflict of interest**

The authors declare no conflict of interest.

## **Acknowledgements**

The authors would like to thank Fanny Therrien, Caroline Nadeau, and the research team at the cardiovascular biobank of the Institut universitaire de cardiologie et de pneumologie de Québec for their valuable assistance. We are also thankful to Dominique Fournier and Stéphanie Dionne for assistance with clinical data and the cardiac surgical database. This study was supported by Canadian Institutes of Health Research grants MOP 102481 (Y. Bossé) and MOP 79342 (P. Pibarot and P. Mathieu). This study was also funded by grants from the Heart and Stroke Foundation of Canada and the Fondation Institut universitaire de cardiologie et de pneumologie de Québec. V. Ducharme is the recipient of a Frederick Banting and Charles Best Canada Graduate scholarship from the Canadian Institutes of Health Research. Y. Bossé is a research scholar from the Heart and Stroke Foundation of Canada. P. Mathieu is a research scholar from the Fonds de Recherche en Santé du Québec. P. Pibarot holds the Canada Research Chair in Valvular Heart Diseases.



## References

1. Lindroos M, Kupari M, Heikkila J, Tilvis R. Prevalence of aortic valve abnormalities in the elderly: an echocardiographic study of a random population sample. *J Am Coll Cardiol* 1993;21:1220-1225
2. Stewart BF, Siscovick D, Lind BK, Gardin JM, Gottdiener JS, Smith VE, et al. Clinical factors associated with calcific aortic valve disease. Cardiovascular Health Study. *J Am Coll Cardiol* 1997;29:630-634
3. Freeman RV, Otto CM. Spectrum of calcific aortic valve disease: pathogenesis, disease progression, and treatment strategies. *Circulation* 2005;111:3316-3326
4. Rajamannan NM. Calcific aortic stenosis: lessons learned from experimental and clinical studies. *Arterioscler Thromb Vasc Biol* 2009;29:162-168
5. Bonow RO, Carabello BA, Kanu C, de Leon ACJ, Faxon DP, Freed MD, et al. ACC/AHA 2006 guidelines for the management of patients with valvular heart disease: a report of the American College of Cardiology/American Heart Association Task Force on Practice Guidelines (writing committee to revise the 1998 Guidelines for the Management of Patients With Valvular Heart Disease): developed in collaboration with the Society of Cardiovascular Anesthesiologists: endorsed by the Society for Cardiovascular Angiography and Interventions and the Society of Thoracic Surgeons. *Circulation* 2006;114:e84-231
6. Bosse Y, Mathieu P, Pibarot P. Genomics: the next step to elucidate the etiology of calcific aortic valve stenosis. *J Am Coll Cardiol* 2008;51:1327-1336
7. Garg V, Muth AN, Ransom JF, Schluterman MK, Barnes R, King IN, et al. Mutations in NOTCH1 cause aortic valve disease. *Nature* 2005;437:270-274
8. Mohamed SA, Aherrahrou Z, Liptau H, Erasmi AW, Hagemann C, Wrobel S, et al. Novel missense mutations (p.T596M and p.P1797H) in NOTCH1 in patients with bicuspid aortic valve. *Biochem Biophys Res Commun* 2006;345:1460-1465
9. Roy-Gagnon MH, Moreau C, Bherer C, St-Onge P, Sinnett D, Laprise C, et al. Genomic and genealogical investigation of the French Canadian founder population structure. *Hum Genet* 2011;129:521-531

10. Baumgartner H, Hung J, Bermejo J, Chambers JB, Evangelista A, Griffin BP, et al. Echocardiographic assessment of valve stenosis: EAE/ASE recommendations for clinical practice. *Eur J Echocardiogr* 2009;10:1-25
11. Frazer KA, Ballinger DG, Cox DR, Hinds DA, Stuve LL, Gibbs RA, et al. A second generation human haplotype map of over 3.1 million SNPs. *Nature* 2007;449:851-861
12. Barrett JC, Fry B, Maller J, Daly MJ. Haploview: analysis and visualization of LD and haplotype maps. *Bioinformatics* 2005;21:263-265
13. Pritchard JK, Stephens M, Donnelly P. Inference of population structure using multilocus genotype data. *Genetics* 2000;155:945-959
14. Price AL, Butler J, Patterson N, Capelli C, Pascali VL, Scarnicci F, et al. Discerning the ancestry of European Americans in genetic association studies. *PLoS Genet* 2008;4:e236
15. Purcell S, Neale B, Todd-Brown K, Thomas L, Ferreira MA, Bender D, et al. PLINK: a tool set for whole-genome association and population-based linkage analyses. *Am J Hum Genet* 2007;81:559-575
16. Nyholt DR. A simple correction for multiple testing for single-nucleotide polymorphisms in linkage disequilibrium with each other. *Am J Hum Genet* 2004;74:765-769
17. Devlin B, Roeder K. Genomic control for association studies. *Biometrics* 1999;55:997-1004
18. Shmulewitz D, Zhang J, Greenberg DA. Case-control association studies in mixed populations: correcting using genomic control. *Hum Hered* 2004;58:145-153
19. The 1000 Genomes Project Consortium. A map of human genome variation from population-scale sequencing. *Nature* 2010;467:1061-1073
20. Warren BA, Yong JL. Calcification of the aortic valve: its progression and grading. *Pathology* 1997;29:360-368
21. Colhoun HM, McKeigue PM, Davey SG. Problems of reporting genetic associations with complex outcomes. *Lancet* 2003;361:865-872

22. Nkomo VT, Gardin JM, Skelton TN, Gottdiener JS, Scott CG, Enriquez-Sarano M. Burden of valvular heart diseases: a population-based study. *Lancet* 2006;368:1005-1011
23. Srivastava D, Garg V, inventors; NOTCH1 variants associated with cardiovascular disease. U.S. patent 7,629,121. 2009 Aug 12.

## Tables and figures

**Table 1.** Clinical characteristics of case subjects (n = 457).

	Male	Female
Sex	57% (259)	43% (198)
Age (years)	70.7 ± 9.0	73.8 ± 7.9
Weight (kg)	78.6 ± 13.5	68.6 ± 4.9
Waist circumference (cm) <sup>a</sup>	102.5 ± 12.0	98.5 ± 14.8
Body surface area (m <sup>2</sup> )	1.9 ± 0.2	1.7 ± 0.2
Body mass index (kg/m <sup>2</sup> )	27.7 ± 4.3	28.7 ± 6.1
Mean transvalvular gradient (mmHg) <sup>b</sup>	40.8 ± 16.5	42.5 ± 16.1
Aortic valve area (cm <sup>2</sup> )	0.82 ± 0.24	0.68 ± 0.20
Coronary artery disease	62.4% (161)	41.1% (81)
Hypolipemic drugs	81.4% (210)	76.1% (150)
Hypertension	66.3% (171)	75.1% (148)
Diabetes	26.3% (68)	31.5% (62)

<sup>a</sup>n = 393 patients. <sup>b</sup>n = 362 patients. Continuous variables are expressed as mean ± SD.

Dichotomous variables are expressed as percentage (n).

**Table 2.** SNPs selected for genotyping *NOTCH1*  $\pm$  10 kilo bases.

<b>rs number</b>	<b>Function</b>	<b>Location*</b>	<b>Reason for selection</b>	<b>Genotyped on Illumina HumanHap550 BeadChip</b>
rs4379550	3' region	chr9:138,496,247	Present on Hap550 BeadChip	X
rs61751489	Exon 33	chr9:138,511,159	Srivastava et al.(23), Missense, p.V2286I	
rs41309766	Exon 25	chr9:138,519,657	Garg et al. (7), frameshift, H1505del	
rs61751543	Exon 23	chr9:138,521,054	Srivastava et al.(23), Missense, p.R1280H	
rs41309764	Exon 20	chr9:138,522,511	Garg et al.(7), nonsense p.R1108X	
rs3124599	Intron 18	chr9:138,523,591	Tag	X
rs35962301	Exon 18	chr9:138,524,162	Srivastava et al.(23), Missense, p.R939Q	
rs11145766	Intron 17	chr9:138,524,716	Tag	X

rs35136134	Exon 16	chr9:138,525,470	Srivastava et al.(23), Missense, p.E848K	
rs61755997	Exon 11	chr9:138,529,872	Mohamed et al.(8), missense, p.T596M	
rs13290979	Intron 2	chr9:138,545,455	Tag	X
rs11145770	Intron 2	chr9:138,546,887	Tag	X
rs7034799	5' region	chr9:138,576,033	Present on Hap550 BeadChip	X
rs7849014	5' region	chr9:138,577,327	Present on Hap550 BeadChip	X

---

\* NCBI36/hg18

**Table 3.** Characteristics of common SNPs tested for association.

SNP	Call rate	MAF*	HW pvalue*	Frequency cases	Frequency controls	Association <i>P</i> value	<i>P</i> value genomic control	Risk allele	Odds ratio	95% confidence interval
rs4379550	99.97	0.4333	0.0593	0.442	0.432	0.5942	0.7557	G	1.039	0.903 - 1.197
rs3124599	99.95	0.0514	0.6100	0.053	0.051	0.8548	0.9149	A	1.03	0.752 - 1.41
rs11145766	98.03	0.1088	0.7959	0.128	0.106	0.0509	0.2542	A	1.235	0.999 - 1.527
<b>rs13290979</b>	99.89	0.3706	0.3385	0.326	0.377	<b>0.0034</b>	0.0876	<b>A</b>	<b>1.248</b>	1.076 - 1.449
rs11145770	99.70	0.3591	0.7192	0.343	0.361	0.2873	0.5344	G	1.083	0.935 - 1.255
rs7034799	99.75	0.0554	1.0000	0.051	0.056	0.5043	0.6966	A	1.114	0.811 - 1.532

MAF: minor allele frequency. HW: Hardy-Weinberg. \* Calculated from combined cases and controls.





## **Chapter 7. Article 2: Calcium signaling pathway genes *RUNX2* and *CACNA1C* are associated with calcific aortic valve disease**

***RUNX2* et *CACNA1C* sont associés au rétrécissement valvulaire aortique**

Sandra Guauque-Olarte<sup>1</sup>; David Messika-Zeitoun<sup>2,3</sup>; Arnaud Droit<sup>4,5</sup>; Maxime Lamontagne<sup>1</sup>; Joël Tremblay-Marchand<sup>1</sup>; Emilie Lavoie-Charland<sup>1</sup>; Nathalie Gaudreault<sup>1</sup>; Benoit J. Arsenault<sup>6</sup>; Marie-Pierre Dubé<sup>6</sup>; Jean-Claude Tardif<sup>6</sup>; Simon C. Body<sup>7</sup>; Jonathan G. Seidman<sup>8</sup>; Catherine Boileau<sup>9</sup>; Patrick Mathieu<sup>1</sup>; Philippe Pibarot<sup>1</sup>; Yohan Bosse<sup>1,4\*</sup>

<sup>1</sup> Centre de recherche Institut universitaire de cardiologie et de pneumologie de Québec, Laval University, Quebec, Canada;

<sup>2</sup> Cardiology Department, AP-HP, Bichat Hospital, Paris, France;

<sup>3</sup> INSERM U698 and University Paris 7, Paris, France;

<sup>4</sup> Department of Molecular Medicine, Laval University, Quebec, Canada;

<sup>5</sup> Centre de Recherche du CHUQ, Quebec, Canada;

<sup>6</sup> Montreal Heart Institute, Université de Montréal, Quebec, Canada;

<sup>7</sup> Department of Anesthesiology, Perioperative and Pain Medicine, Brigham and Women's Hospital, Harvard Medical School, Boston, Massachusetts, USA;

<sup>8</sup> Department of Genetics, Harvard Medical School, Boston, Massachusetts, USA;

<sup>9</sup> INSERM U1148 and University Paris 7, Paris, France.

**Short Title:** Susceptibility Genes to Aortic Valve Stenosis

**\*Corresponding author:**

E-mail: [yohan.bosse@criucpq.ulaval.ca](mailto:yohan.bosse@criucpq.ulaval.ca) (YB)

## Résumé

**Objectif-** Le rétrécissement valvulaire aortique (RVA) est une maladie mortelle et sans traitement médical. Les mécanismes moléculaires impliqués dans le développement de la maladie ne sont pas connus. Cette étude combine les résultats de deux criblages génomiques par association (GWAS), l'expression des gènes et la cartographie des eQTL dans des tissus valvulaires humains afin d'identifier les gènes de susceptibilité au RVA.

**Méthodes et résultats-** Une méta-analyse combinant deux GWAS dans deux cohortes indépendantes de patients provenant de Québec (n = 474) et de la France (n = 486) a été réalisée. La fréquence des polymorphismes dans chaque cohorte a été comparée à deux groupes de 2 988 et 1 864 témoins, respectivement, d'origine européenne et provenant de la base de données dbGaP. L'expression des gènes dans les valves aortiques normales et calcifiées a été mesurée par le séquençage de l'ARN. Les résultats ont été intégrés aux eQTL valvulaires obtenus à partir de 22 valves aortiques provenant de patients avec RVA. Vingt-cinq SNPs ont démontré une valeur  $P < 5 \times 10^{-6}$  dans le GWAS. La voie de signalisation du calcium s'est avérée être le groupe de gènes le plus enrichi en SNP associés au RVA. Certains de ces gènes étaient différentiellement exprimés dans les valves avec ou sans RVA. Deux SNP dans le gène *RUNX2*, codant pour un facteur de transcription ostéogénique, étaient associés au RVA ( $P_{\text{GWAS}} = 5.33 \times 10^{-5}$ ). Les niveaux d'expression de *RUNX2* étaient plus élevés dans les valves calcifiées et étaient associés avec des eQTL-SNP. Les niveaux d'expression du gène *CACNA1C* codant pour une sous-unité du canal calcique de la voie de signalisation du calcium étaient plus élevés dans les valves calcifiées et étaient également associés à des eQTL-SNP. L'eQTL-SNP le plus fortement associé avec le RVA (rs2239118), localisé dans un intron du *CACNA1C*, était associé avec des niveaux d'expression plus élevés de ce gène (eQTL  $P < 0.030$ ). Ce résultat suggère que l'allèle de risque pour rs2239118 agit en augmentant les niveaux d'expression de *CACNA1C* dans le tissu valvulaire.

**Conclusion-** Cette étude génomique intégrative a confirmé le rôle de *RUNX2* dans le RVA et a permis l'identification d'un nouveau gène de susceptibilité, *CACNA1C*, pour le RVA.

## Abstract

**Background-** Calcific aortic valve stenosis (AS) is a frequent and life-threatening disease with no medical therapy. The genetic architecture of this disease remains elusive. This study combines genome-wide association studies (GWAS), gene expression and eQTL mapping in human valve tissues to identify susceptibility genes of AS.

**Methods and Results-** A meta-analysis was performed combining the results of two independent GWAS in 474 and 486 cases from Quebec City (Canada) and Paris (France), respectively. The controls consisted of 2,988 and 1,864 individuals with European ancestry, both from dbGaP. mRNA expression levels were evaluated in calcified and normal aortic valves by RNA sequencing. The results were integrated with valve eQTL data obtained from 22 AS patients. Twenty-five SNPs had  $P < 5 \times 10^{-6}$  in the GWAS meta-analysis. The calcium signaling pathway was the top gene set enriched for genes mapped to AS-associated SNPs. Genes in this pathway were found differentially expressed in valves with and without AS. Two SNPs located in intron 1 of *RUNX2*, encoding an osteogenic transcription factor, were associated with AS (GWAS  $P = 5.33 \times 10^{-5}$ ). The mRNA expression levels of *RUNX2* were up-regulated in calcified valves and associated with eQTL-SNPs. *CACNA1C* in the calcium signaling pathway encoding the alpha-1C subunit of a voltage-dependent calcium channel was also up-regulated in calcified valve and regulated by eQTL-SNPs. The eQTL-SNP with the most significant association with AS (rs2239118, GWAS  $P < 9.38 \times 10^{-4}$ ), located in intron 10 of *CACNA1C*, was associated with higher expression of the gene (eQTL  $P < 0.030$ ) suggesting that the risk allele for rs2239118 mediates its effect by increasing the mRNA expression of *CACNA1C* in valve tissue.

**Conclusions-** This integrative genomic study confirmed the role of *RUNX2* as a potential driver of AS and identified a new AS susceptibility gene, *CACNA1C*, belonging to the calcium signaling pathway.

**Key words:** aortic valve, aortic stenosis, genomics, GWAS, RNA-Seq, valve eQTL

## Author Summary

Calcific aortic valve stenosis (AS) is a frequent and fatal disease with no medical therapy. Symptomatic patients are currently treated with costly surgical interventions. AS runs in families, but the heritable predisposition factors and molecular mechanisms that drive the development of this disease are largely unknown. Here, we used an integrative genomic approach to identify susceptibility genes of AS and extend their functional meaning to gene expression levels in human aortic valves. We identified coordinated genetic associations with AS for genes involved in the calcium signaling pathway. Many genes in this pathway were differentially expressed in calcified compared to normal aortic valves. The risk alleles for genetic variants located in the *RUNX2* and *CACNA1C* genes were found to mediate their effect by increasing expression levels of *RUNX2* and *CACNA1C* in valve tissues. This study confirms the role of *RUNX2* as a potential driver of AS and identifies *CACNA1C* as a new calcium signaling pathway gene associated with AS. This study is also important as it provides unique information about the possible function of the newly discovered susceptibility variants leading to abnormal expression of the genes in a disease-relevant tissue, which in turn promotes the development of this disorder.

## Introduction

AS is the most frequent acquired heart valve disease in developed countries affecting 2% and 4% of people older than 65 and 85 years, respectively[1]. The actual increase of life expectancy will raise the incidence of AS and amplify this public health problem[2]. The risk of death, valve replacement or progression to heart failure is increased by 80% over a period of five years in patients with AS[3]. No pharmacological treatments are available and conventional cardiovascular drugs such as statin have failed to prevent the development of AS[4, 5]. Open heart surgery (aortic valve replacement) and more recently transcatheter aortic valve implantation (TAVI) are the only treatments available for symptomatic and severe cases. AS is the principal indication for valve replacement surgery in North America and Europe[6]. In Canada and USA, the cost of an aortic valve replacement surgery is estimated at \$74,602 CAN[7] and \$171,270 USD[8], respectively. New treatment strategies for this growing disease are urgently needed.

AS is a biologically active process involving pathways and cellular processes such as inflammation, extracellular matrix remodeling, and calcification[6, 9]. A genetic component to AS is demonstrated[10, 11], and candidate gene studies have identified polymorphisms associated with AS or AS-related phenotypes[12] (**S1 Table**). Rare mutations in *NOTCH1* have been associated with bicuspid aortic valve disease and severe valve calcification[13, 14]. A recent genome-wide association study (GWAS) identified the lipoprotein(a) (*LPA*) gene associated with aortic valve calcification[15].

We performed a GWAS meta-analysis using patients with AS from Quebec and France to identify new susceptibility genes for AS. Gene expression of susceptibility genes was evaluated by RNA sequencing (RNA-Seq) in human aortic valves with and without AS. Finally, the functional meanings of the newly identified AS-associated SNPs located in differentially regulated genes were extended by carrying out the first expression quantitative trait loci (eQTL) mapping study in human valve tissues. This integrative genomic study confirmed the role of *RUNX2* as a potential driver of AS development and identified a new AS susceptibility gene, namely *CACNA1C*, belonging to the calcium signaling pathway.

## Materials and methods

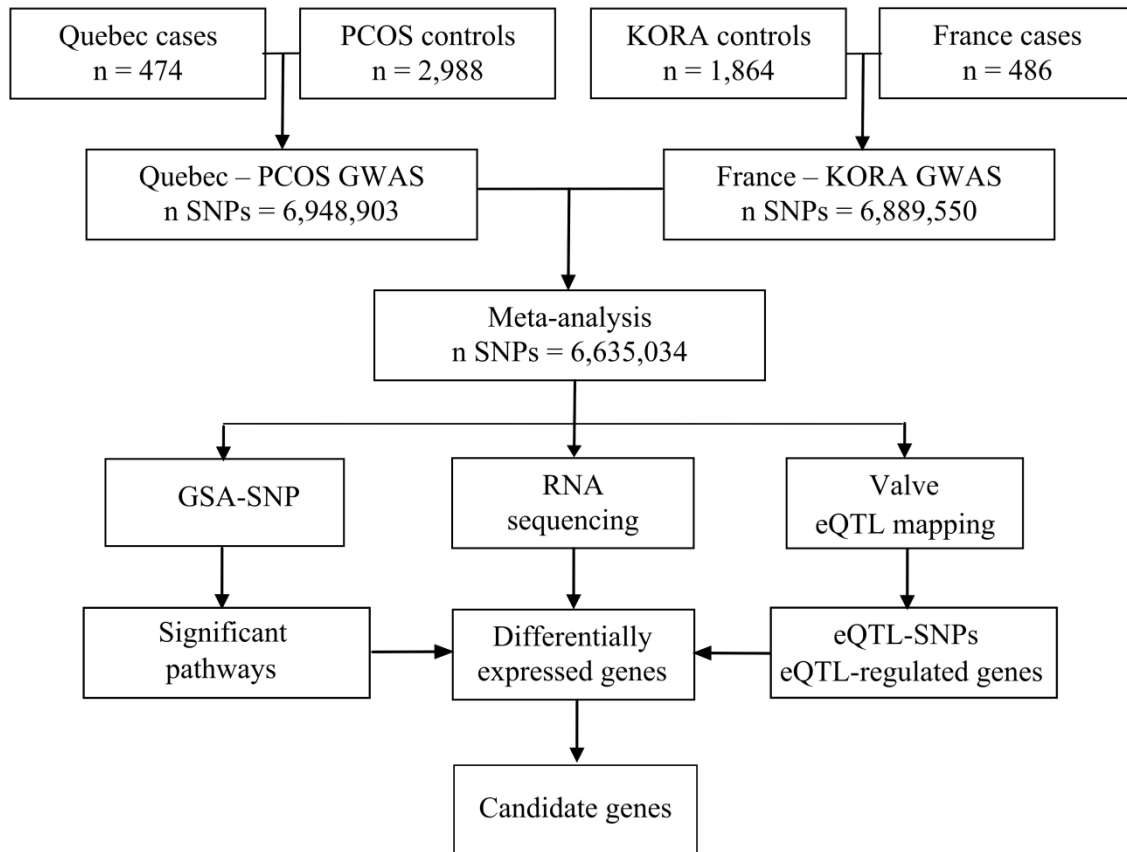


**Figure 1.** Flow chart showing the steps of the GWAS meta-analysis, pathway analysis, gene expression study of aortic valves, and valve eQTL mapping study.

## Populations

Written informed consent was obtained from all study participants after institutional Review Board approval. The Quebec cohort consisted of 494 French Canadian patients who underwent aortic valve replacement for severe tricuspid non-rheumatic AS at the “Institut universitaire de cardiologie et de pneumologie de Québec” (IUCPQ). Patients with moderate or severe aortic regurgitation, other valve diseases, or previous cardiac surgery were excluded. The France cohort consisted of 505 patients with degenerative AS from the COFRASA and GENERAC studies. Inclusion criteria were at least mild AS (mean pressure gradient  $\geq 10$  mmHg) and aortic valve structural changes (thickening/calcification). Exclusion criteria were AS due to rheumatic

disease or radiotherapy, previous aortic endocarditis, coexisting aortic regurgitation, other valvular disease and severe respiratory or renal insufficiency (creatinine clearance  $\leq 30$  ml/min). **S2 Table** summarizes the clinical characteristics of individuals from Quebec and Paris.

Control cohorts were obtained from the database of Genotypes and Phenotypes[16] (dbGAP). Proper control groups were selected based on genetic ancestry, genotyping data available, and sample size (S1 Supporting Information). For cases from Quebec, the Polycystic Ovary Syndrome Genetics-NUgene (PCOS, phs000368) cohort from United States was selected. This cohort is a control group of individuals recruited at the Northwestern University Medical Center for performing a GWAS on PCOS susceptibility. For cases from France, one European cohort was selected, namely the Genetic Epidemiology of Refractive Error in the Kooperative Gesundheitsforschung in der Region Augsburg Study (KORA, phs000303). KORA is a population based study of adults randomly selected from 430,000 individuals in Augsburg and 16 surrounding counties in Germany. **S3 Table** presents the characteristics of the dbGaP cohorts.

### **Whole-genome genotyping, quality controls and imputation**

DNA was extracted from whole blood or buffy coat (S1 Supporting Information). Whole-genome genotyping for the Quebec and France cohorts was performed at the McGill University and Genome Quebec Innovation Center (<http://gqinnovationcenter.com>) using the Illumina HumanOmniExpress-12v1.0 BeadChip testing 733,202 SNPs. Standard genotyping quality controls were performed independently in the Quebec, France, and dbGaP cohorts. Details are provided and summarized in **S4** and **S5 Tables**. For the Quebec cohort, 639,052 SNPs and 474 patients remained after quality controls. For the France cohort, 654,363 SNPs and 486 samples remained. The PCOS cohort was also genotyped using the Illumina HumanOmniExpress-12v1.0 platform. The KORA cohort was genotyped using the Illumina HumanOmni2.5 platform testing 2,443,179 SNPs. For the PCOS cohort, 645,438 SNPs and 2,988 individuals passed quality controls. For the KORA cohort, 1,492,728 SNPs and 1,864 individuals passed quality controls. To increase whole-genome coverage, additional SNPs were inferred using the SHAPEIT[17] / IMPUTE2[18] pipeline (S1 Supporting Information).

## **Association tests and meta-analysis**

To account for differences in clinical characteristics between AS cases from Quebec and France, genetic association tests were performed independently and then combined into a meta-analysis. Association tests were performed with additive logistic regression models. Seven significant principal components derived from EIGENSTRAT[19] were used as covariates to adjust for potential population stratification. After adjustment, the genomic inflation factors for the Quebec-PCOS and the France-KORA comparisons were both 1.0. The meta-analysis was performed using the inverse variance method with fixed and random effect models. The meta-analysis included 6,635,034 SNPs after the exclusion of polymorphisms with alternate risk alleles ( $n = 36,590$ ). The significant  $P$  value cutoff was set to  $5 \times 10^{-8}$ . Association tests, meta-analysis, and linkage disequilibrium (LD) calculation were performed with PLINK[20]. Regional plots were created with LocusZoom[21]. SNPs with GWAS  $P$  lower than  $1 \times 10^{-4}$  were mapped 1,000 kb up- or downstream of UCSC hg19 genes using PLINK to generate a list of possible susceptibility genes for further analysis.

## **Biological, functional, and disease analysis**

We performed pathway analysis enrichment of the 6,635,034 SNPs included in the meta-analysis using the default procedure in the GSA-SNP software[22]. Instead of relying on individual marker analysis, GSA-SNP tests pre-defined gene-sets or pathways for association with disease, and thus the contribution of multiple genes. GSA-SNP allows detecting subtle effects of multiple SNPs in the same gene-set that might be missed when assessed individually. The software assigned the most significant SNPs located 10 kb up- and downstream to each gene (i.e. padding size of 10,000 bps and  $k = 1$ ) in KEGG gene-sets. The genes were used to calculate pathway enrichment. The expression levels of genes in significant pathways were verified using the RNA-Seq data. Ingenuity<sup>®</sup> Pathway Analysis system (IPA, QIAGEN) was used to identify the connections among these genes and their associated biological functions. The effects of differentially expressed genes in pathways were predicted with the IPA Molecule Activity Predictor tool.



IPA was used to integrate susceptibility genes in biological processes known to be implicated in AS development and progression[9]. A SNP was considered within a gene if it was located in the exon-intron structure or 10 kb up- or downstream of the gene. Gene previously associated with AS were extracted from Phenopedia[23] and curated manually (**S1 Table**).

### **Gene expression analysis in human aortic valves**

Gene expression levels were evaluated in human aortic valve tissues (n = 10) explanted from patients undergoing aortic valve replacement at the IUCPQ (**S2 Table**). Stenotic valves were selected to have the same degree of fibro-calcific remodeling (i.e. Warren score of 3)[24]. To further decrease heterogeneity of expression, only valves taken from white male non-smoking, non-diabetic subjects without renal insufficiency (creatinine levels > 150  $\mu\text{mol/L}$ ), significant aortic regurgitation (grade > 2) and/or ascending aorta aneurysm undergoing a concomitant Bentall procedure or replacement of the ascending aorta were selected. Normal non-calcified valves (n = 10) were collected from hearts harvested during cardiac transplantation. Control valves had no evidence of disease at post-explant examination. Stenotic and control groups were matched for age ( $\pm 10$  years).

Valve leaflets of each individual were conserved at  $-80^{\circ}\text{C}$  and one leaflet per valve was used for RNA extraction using a modified TRIzol protocol[25] followed by RNA cleanup using the RNeasy Mini Kit (QIAGEN). RNA was extracted from 45 to 192 mg of valve tissue. cDNA fragments of 150 to 300 nucleotides were selected and gene expression evaluated by 50 bp length paired-end RNA-Seq using the Illumina HiSeq2000 platform. One calcified valve sample failed library preparation and was discarded. The quality of fastq data was verified using the FastQC application. TopHat[26] was used to align reads of each sample to the UCSC hg19 reference using these parameters: -r150 and --mate-std-dev 100. The reads were then assembled by Cufflinks[26] and Cuffdiff was utilized to quantify the transcriptomes and compare gene expression levels between calcified and normal valves. Genes with FPKM < 1 in more than 80% of the samples were excluded. In addition, HTSeq[27] was used to count reads aligned by TopHat. Count tables were used in DESeq[28] and edgeR[29] to compare gene expression between the two groups of valves. Multidimensional scaling (MDS) plots generated with

cummeRbund and edgeR showed two normal valve samples outside the main cluster of normal valves and were excluded. The function nbinomTest in DESeq and exactTest in edgeR were applied. Genes with adjusted  $P$  values  $< 0.05$  using the three softwares (i.e. cuffdiff, DESeq and edgeR) were considered as differentially expressed. The RNA-Seq data have been deposited in NCBI's Gene Expression Omnibus[30] (accession number GSE55492).

### **Valve expression quantitative trait loci (eQTL)**

Genome-wide genotyping and gene expression profiling was performed on an independent set of 24 human aortic valves. Aortic valves were explanted from 24 white male patients under 67 years of age who underwent aortic valve replacement at the IUCPQ from February 2005 to October 2013. Only tricuspid nonrheumatic aortic valve with a Warren score of 3[24] were selected. Patients that were undergoing concomitant coronary artery bypass grafting were included. Patients with other valve diseases, previous cardiac surgery, and moderate or severe aortic regurgitation were excluded. The clinical characteristics of these patients are shown in **S6 Table**.

Whole-genome genotyping and gene expression were performed at the McGill University and Genome Quebec Innovation Center. DNA was extracted from 60-80 mg of frozen aortic valve tissue. The genotyping was carried out using the Illumina® Infinium HumanOmni2.5-8 BeadChip testing 2,379,855 SNPs throughout the human genome. SNPs were excluded based on Hardy-Weinberg ( $P$  value  $> 0.01$ ), minor allele frequency smaller than 0.01 or call rates lower than 0.97. DNA samples were removed based on completion rate lower than 0.95, gender discrepancies, duplicates and genetic background. 1,474,616 SNPs and 24 patients passed all quality controls and were available for analysis. To increase whole-genome coverage, additional SNPs were inferred using the SHAPEIT / IMPUTE2 pipeline (S1 Supporting Information). Total RNA was extracted from 100 mg of aortic valve tissue using the RNeasy Plus Universal Mini Kit (QIAGEN) according to manufacturer's protocol. Gene expression was measured on the Illumina HumanHT-12 v4 Expression BeadChip. Samples were removed based on outliers in pairwise correlation, principal components analysis (PCA), and hierarchical clustering. After quality controls, 22 samples were available for analysis. mRNA expression data were log<sub>2</sub> transformed

and quantile normalized prior to analysis using R 3.0.0 statistical software and the Bioconductor[31] package lumi[32]. Due to sample size and patient selection, no adjustment was applied to the mRNA expression datasets. mRNA transcripts were selected for valve eQTL analysis if they were within 1Mb of the top GWAS meta-analysis SNPs. Valve eQTLs were also evaluated in genes differentially expressed between calcified and normal aortic valves in the RNA-Seq experiment and with SNPs with GWAS  $P < 1 \times 10^{-4}$ . Association testing between genotypes and mRNA expression levels were performed in PLINK v1.07 using the --assoc command.

## Results

### GWAS results

The meta-analysis of the two independent GWAS is summarized in **Fig. 2**. No SNP reached genome-wide significance. However, 25 SNPs had  $P < 5 \times 10^{-6}$  under the fixed-effects model (**S7 Table**). Using a more liberal significant threshold ( $P < 1 \times 10^{-4}$ ), 646 SNPs were associated with AS and mapped to or near 130 unique genes. Among those SNPs, rs9371549 was located 3.8 kb downstream of *ESR1* (estrogen receptor 1), and rs4708867 mapped 109 kb downstream of *LPA* (**S1 Fig**). *ESR1* and *LPA* were previously associated with AS[15, 33] (**S1 Table**).

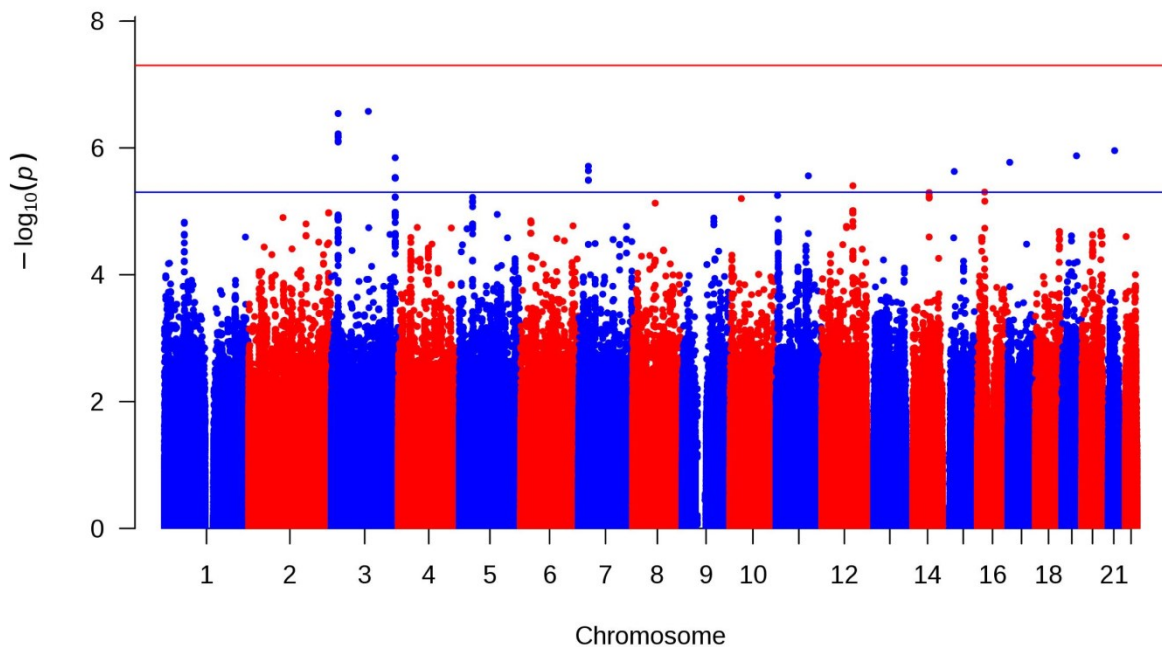


**Figure 2.** Manhattan plot showing the results of the GWAS meta-analysis. The y-axis represents  $P$  in  $-\log_{10}$  scale combining the results of the two independent GWAS. The horizontal red line indicates the genome-wide significance cutoff ( $P = 5 \times 10^{-8}$ ). The horizontal blue line indicates the  $P$  cutoff of  $5 \times 10^{-6}$ .

Considering the modest evidence of association from single marker analysis in the GWAS, we performed gene-set association analysis. GSA-SNP revealed 25 pathways significantly enriched (Benjamini-Hochberg corrected  $P < 0.05$ ) among genes mapped to disease-associated SNPs in

the meta-analysis. **Fig. 3** shows the distributions of  $P$  values for these pathways. The most significant KEGG gene-set was the calcium signaling pathway (corrected  $P = 7.27 \times 10^{-5}$ ). The median  $P$  for this gene-set was 0.031, suggesting that GSA-SNP identified moderate but coordinated association for this group of genes. A schematic representation of the calcium signaling pathway and members of this pathway that are drug targets is illustrated in **S2 Fig**.

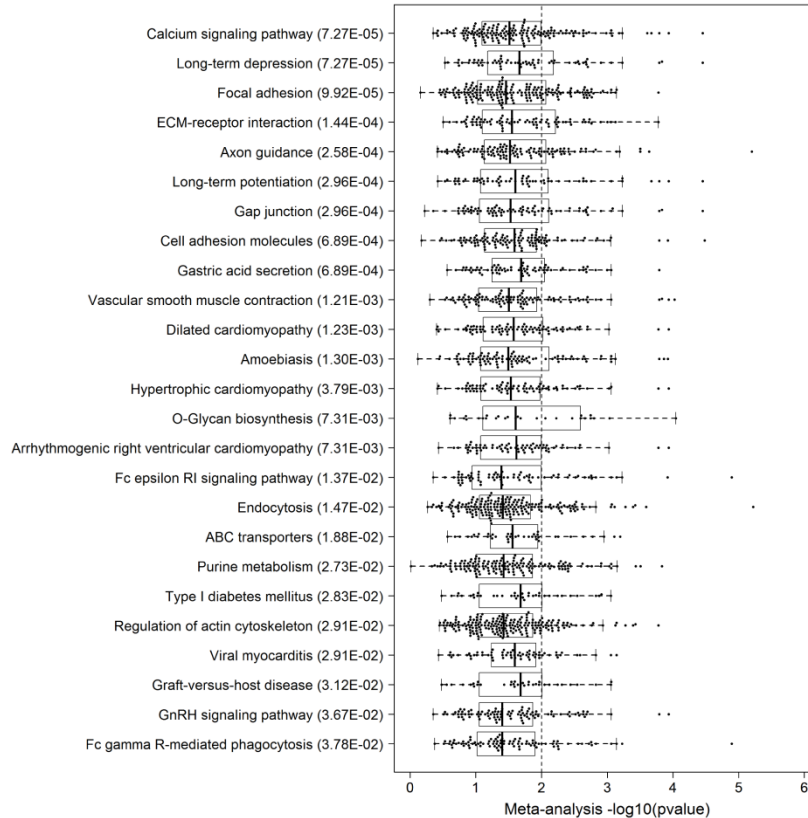


**Figure 3.** Boxplots of GWAS  $P$  values for significant gene-sets. Corrected  $P$  values for each pathway are shown in parentheses. The vertical dashed line indicates  $P = 0.01$ . ECM: extracellular matrix; GnRH: Gonadotropin-releasing hormone.

### Integration with RNA-Seq

We then extended the functional assessment of SNPs associated with AS in this study to gene expression in human aortic valves. Combining the results of three RNA-Seq analysis tools, 518

genes were found consistently differentially expressed between calcified and normal aortic valves (**Fig. 4**). A total of 332 and 186 genes were up- and down-regulated in calcified valves, respectively. All genes had absolute fold-changes of at least 1.52 and higher. Among the differentially expressed genes, 46 were located 1Mb up- or down-stream of SNPs with  $P < 1 \times 10^{-4}$  in the GWAS meta-analysis (**S8 Table**). Twenty-six of these 46 genes (56.5%) were linked to genes in molecular pathways known to be altered in the development and progression of AS, such as inflammation, lipid deposition and oxidation, angiogenesis, calcification, and extracellular matrix remodeling[9] (**Fig. 5, S9 Table**). Interestingly, eleven genes in the calcium signaling pathway identified above were differentially expressed in calcified compared to non-calcified aortic valves in the RNA-Seq experiment (**Fig. 6**).

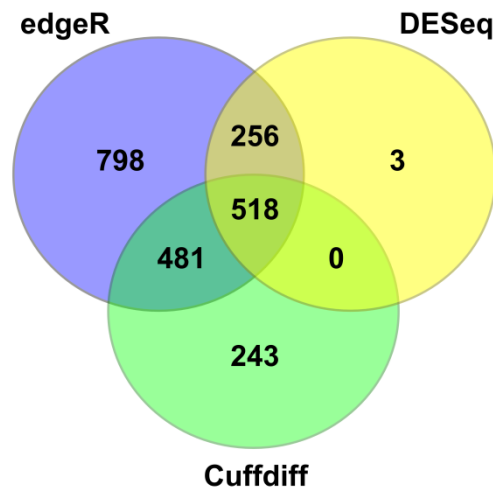


**Figure 4.** Venn diagrams showing the number of genes differentially expressed in aortic valves with and without AS using three RNA-Seq analysis tools.

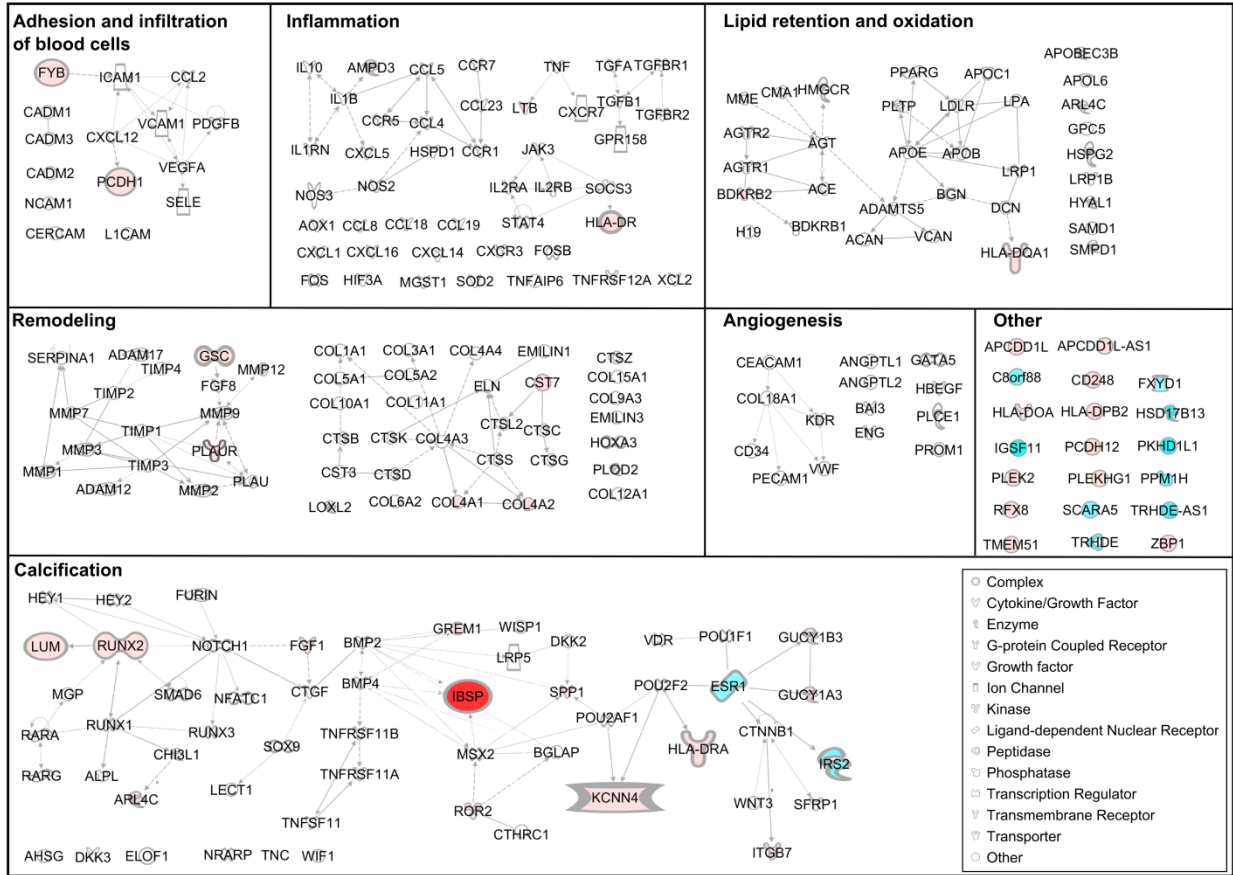


**Figure 5.** Integration of the GWAS and RNA-Seq results with known AS-related biological processes. Integration of genes differentially expressed between calcified and normal valves and with/near SNPs with  $P < 1 \times 10^{-4}$  in biological processes known to be implicated in AS development and progression. Cyan: down-regulated gene. Red: up-regulated genes. Some genes can belong to more than one biological process. This figure was modified from Bossé et al.[9]. Name of all genes are provided in **S9 Table**.

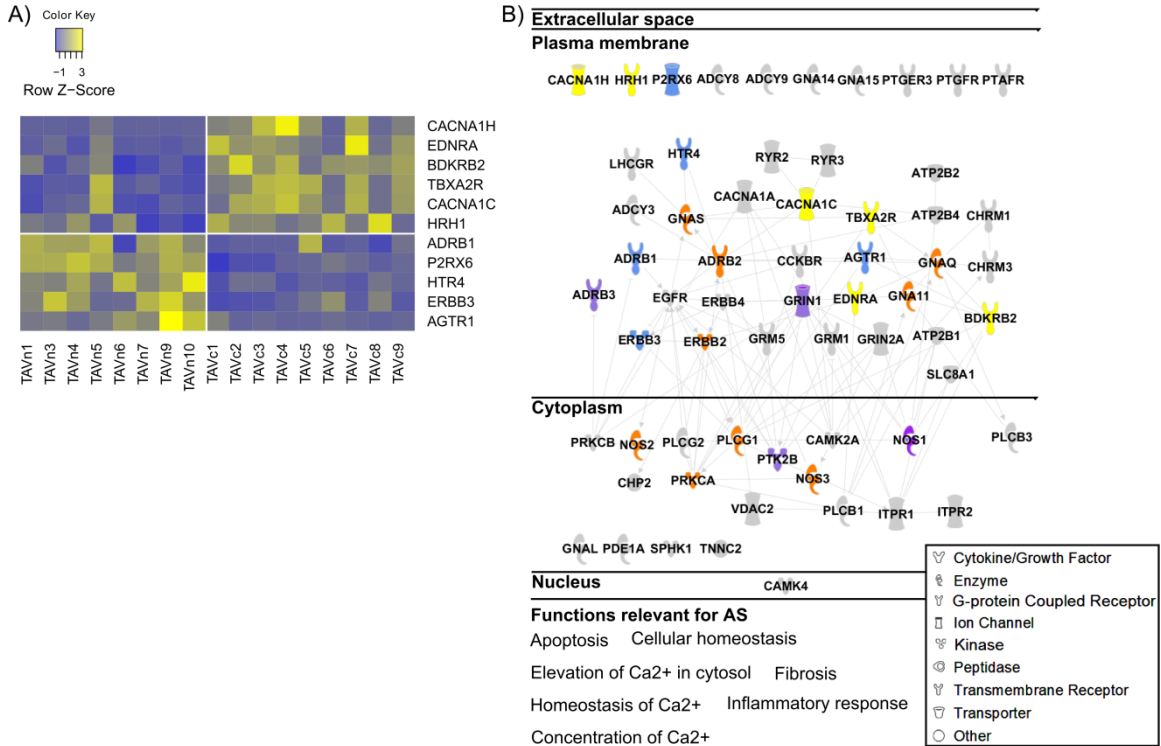


**Figure 6.** Alterations of the calcium signaling pathway in AS. A) Heat map of genes differentially expressed in the RNA-Seq experiment that belong to the calcium signaling pathway. Genes in yellow are up-regulated and genes in blue are down-regulated in calcified valves (TAVc) compared to normal valves (TAVn). The vertical white line separates the two groups. Each row represents a different gene indicated at the right. The calcium signaling pathway genes are: *ADRB1* (adrenoceptor beta 1), *AGTR1* (angiotensin II receptor, type 1), *BDKRB2* (bradykinin receptor B2), *CACNA1C* (calcium channel, voltage-dependent, L type, alpha 1C subunit), *CACNA1H* (calcium channel, voltage-dependent, T type, alpha 1H subunit), *EDNRA* (endothelin receptor type A), *ERBB3* (v-erb-b2 avian erythroblastic leukemia viral oncogene homolog 3), *HRH1* (histamine receptor H1), *HTR4* [5-hydroxytryptamine (serotonin) receptor 4, G protein-coupled], *P2RX6* (purinergic receptor P2X, ligand-gated ion channel, 6), and *TBXA2R* (thromboxane A2 receptor). B) IPA of the calcium pathway showing only genes that are altered (SNPs with  $P < 0.01$  or genes differentially expressed) or regulated as predicted by the Molecule Activity Predictor (MAP). Symbol indicates gene function (see legend). Genes in yellow are up-regulated and genes in blue are down-regulated in TAVc. Predicted activation and inhibition of genes due to the differential expression in TAVc are shown in orange and violet, respectively.



## Integration with valve eQTL mapping

Of the 646 SNPs with GWAS  $P < 1 \times 10^{-4}$ , 363 were genotyped or imputed in the valve eQTL dataset. Association between genotypes and gene expression levels in valve tissues had  $P < 0.05$  for 2,783 SNP-probe pairs, including 230 unique genes and 223 unique SNPs. These eQTL-SNPs and eQTL-regulated genes were overlaid to genes differentially expressed in the RNA-Seq experiment and SNPs associated with AS in the GWAS. Data integration revealed *RUNX2* (runt-related transcription factor 2) as a potential driver of AS development. Two SNPs located in intron 1 of this gene, rs114193529 and rs144071310 ( $r^2 = 1$ ), were associated with AS (GWAS  $P = 5.33 \times 10^{-5}$ , odds ratio = 3.49) (Fig. 7). *RUNX2* was differentially expressed between calcified and normal aortic valves (fold change = 2.68,  $P$  adjusted =  $1.47 \times 10^{-3}$ ) (Fig. 7).

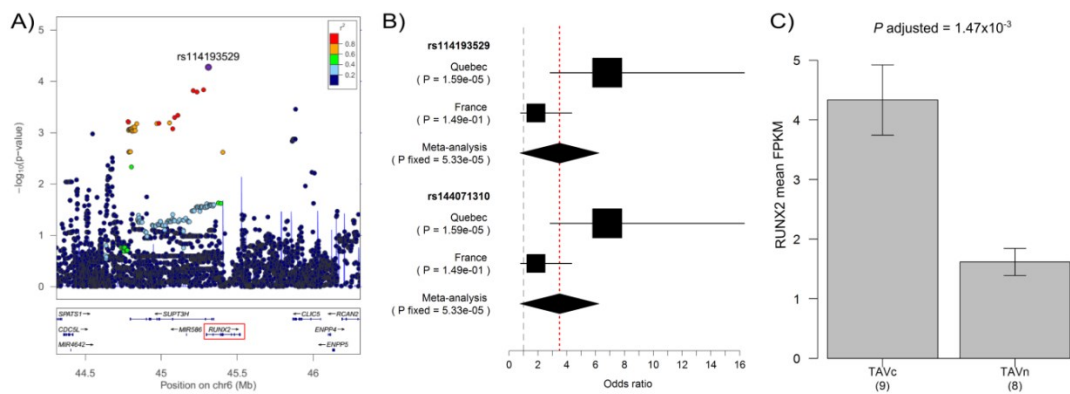


**Figure 7.** eQTL-SNPs influencing the mRNA expression of *RUNX2* in aortic valves. A) Regional plots showing SNP rs114193529 located in *RUNX2*. The y-axis shows the  $P$  values in  $-\log_{10}$  scale for SNPs 1 Mb up- and down-stream of the sentinel SNP (purple dot). The extent of LD ( $r^2$  values) for all SNPs with the sentinel SNP is indicated by colors. The location of genes is shown at the bottom. *RUNX2* is framed in red. SNPs are plotted based on their chromosomal position on build hg19. B) Forest plot of overall effect size for rs114193529 and rs144071310 ( $r^2 = 1$ ) in the two independent GWAS and meta-analysis. The black filled squares represent the odds ratio (OR) for each cohort, and are proportional to the study size. The horizontal lines represent the 95% confidence intervals of the OR. The dashed grey and the dotted red vertical lines represent an OR of 1.0 and the OR of the meta-analysis, respectively. C) Gene expression levels of *RUNX2* in human aortic valves with and without AS measured by RNA-Seq and expressed as mean FPKM (fragments per kilobase of exon per million fragments mapped). The number of valves assessed per group is indicated in parenthesis. Error bars represent the standard error. TAVc: calcified tricuspid aortic valve; TAVn: normal tricuspid valve.

The two AS-associated SNPs in *RUNX2* were not genotyped or imputed in the eQTL project. However, three other SNPs, rs1200428 (eQTL  $P = 5.54 \times 10^{-5}$ ), rs12209785 (eQTL  $P = 4.35 \times 10^{-3}$ ), and rs35565233 (eQTL  $P = 8.83 \times 10^{-3}$ ) were significantly associated with the mRNA expression of *RUNX2* (**Fig. 8**). These three SNPs were independent of the AS-associated SNPs ( $r^2 < 0.015$ ). The minor alleles for rs1200428, rs12209785, and rs35565233 were associated with lower mRNA expression levels of *RUNX2* in valve tissues. Although these eQTL-SNPs were not significantly associated with AS, rs35565233 had an odds ratio below 1 in both GWAS and OR of 0.68 (95%CI = 0.44-1.05) in the meta-analysis (**S3 Fig.**). In addition, the protective allele T for rs35565233 was associated with lower mRNA expression levels of *RUNX2* (**S3 Fig.**), suggesting that the SNP decreases susceptibility to AS through down-regulation of *RUNX2* in valve tissue.

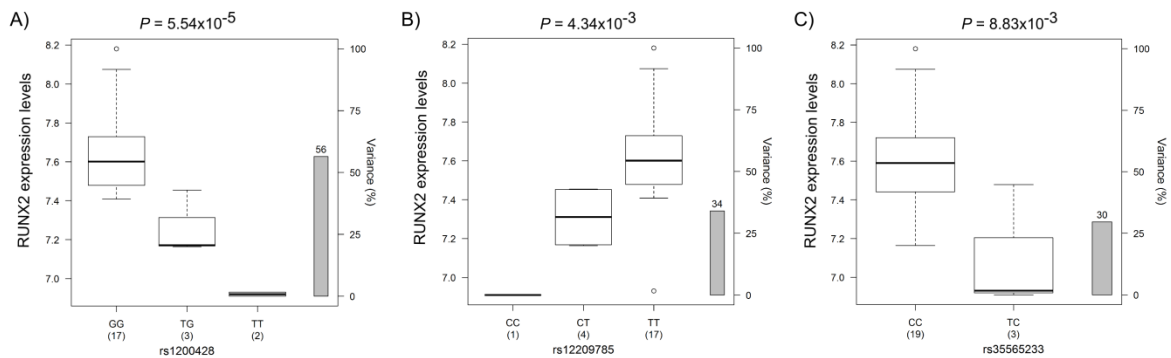


**Figure 8.** eQTL-SNPs influencing the mRNA expression of *RUNX2* in aortic valves. Boxplots of mRNA expression levels for *RUNX2* in human aortic valves according to genotyping groups for SNPs A) rs1200428, B) rs12209785, and C) rs35565233. The left y-axis presents the expression levels and the right y-axis presents the percent variance in expression levels explained by the genotype. The x axis represents the three genotyping groups for each SNP, with the number of subjects in parenthesis.

Valve eQTL data were further studied for genes differentially expressed in the calcium signaling pathway. A total of 460 significant eQTL-SNPs in eleven of these differentially expressed genes (*ADRB1*, *AGTR1*, *BDKRB2*, *CACNA1C*, *CACNA1H*, *EDNRA*, *ERBB3*, *HRH1*, *HTR4*, *P2RX6*, and *TBXA2R*) in this pathway were identified. From these eQTL-SNPs, 268 were associated with the expression levels of *CACNA1C*. Rs2239118 located in intron 10 of *CACNA1C* is the eQTL-SNP with the strongest genetic association signal (GWAS  $P = 4.09 \times 10^{-4}$ ) in the meta-analysis. The risk allele G of rs2239118 was associated with increased mRNA levels of *CACNA1C* (eQTL

$P = 0.030$ ), and *CACNA1C* is increased 1.8 times in calcified compared to normal aortic valves ( $P = 1.47 \times 10^{-3}$ ) (**Fig. 9**). The observed direction of effect of a second eQTL-SNP, rs1034936 (GWAS  $P = 9.38 \times 10^{-4}$ ), was also concordant with the expected direction of effect based on GWAS and RNA-Seq results (**S4 Fig.**). These results suggest that risk alleles for rs2239118 and rs1034936 mediate their effects by increasing the mRNA expression levels of *CACNA1C* in valve tissue. Sixteen additional significant eQTL-SNPs with GWAS  $P < 0.01$  were also associated with the expression levels of *CACNA1C*.

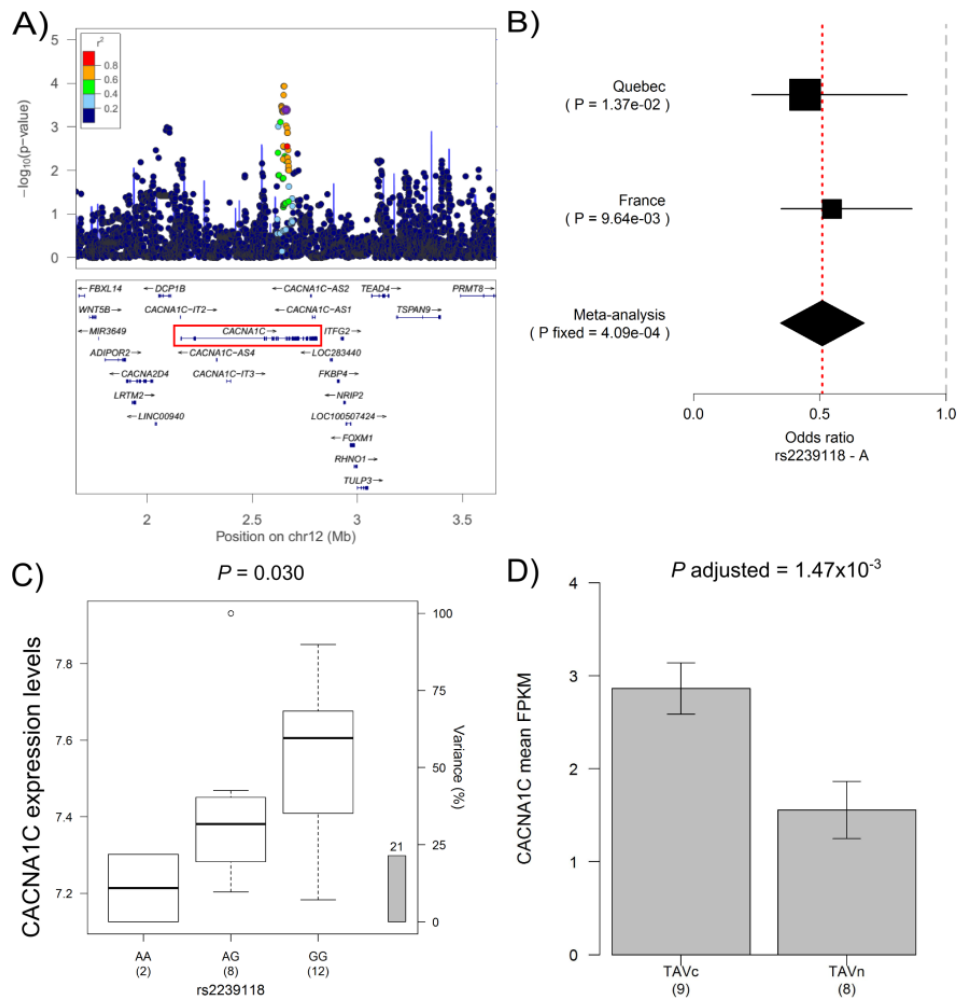


**Figure 9.** *CACNA1C* a new susceptibility gene of AS. A) Regional plot showing SNP rs2239118 located in *CACNA1C*. The y-axis shows the  $P$  values in  $-\log_{10}$  scale for SNPs 1 Mb up- and down-stream of the sentinel SNP (purple dot). The extent of LD ( $r^2$  values) for all SNPs with the sentinel SNP is indicated by colors. The location of genes is shown at the bottom. *CACNA1C* is framed in red. SNPs are plotted based on their chromosomal position on build hg19. B) Forest plot of overall effect size for rs2239118 in the two independent GWAS and meta-analysis. The black filled squares represent the odds ratio (OR) for each cohort, and are proportional to the study size. The horizontal lines represent the 95% confidence intervals of the OR. The dashed grey and the dotted red vertical lines represent an OR of 1.0 and the OR of the meta-analysis, respectively. C) Boxplot of gene expression levels in human aortic valves for *CACNA1C* according to genotyping groups of rs2239118. The left y-axis presents the mRNA expression levels and the right y-axis presents the percent variance in gene expression explained by the genotype. Number of patients per genotype is presented in parenthesis. D) Gene expression levels of *CACNA1C* in human aortic valves measured by RNA-Seq and expressed as mean FPKM (fragments per kilobase of exon per million fragments mapped). The number of valves assessed per group is indicated in parenthesis. Error bars represent the standard error. TAVc: calcified tricuspid aortic valve; TAVn: normal tricuspid valve.

## Discussion

We performed a meta-analysis of two independent GWAS in white individuals with diagnosis of AS from Quebec and France. By traditional single marker analysis, no SNP reached stringent GWAS significance, however, 25 SNPs located in or near biologically relevant genes were moderately significant ( $P < 5 \times 10^{-6}$ ). Gene-set association analysis was carried out to identify coordinated association patterns for genes involved in the same biological pathway. Twenty-five pathways were significantly enriched for genes mapping to moderate disease-associated SNPs. This is consistent with the small to moderate effect sizes observed for individual SNPs in GWAS that collectively acting on a common pathway may reveal the underlying biological mechanisms underpinning AS. The most significant gene-set was the calcium signaling pathway. Eleven genes in this pathway were differentially expressed in calcified compared to normal aortic valves. AS-associated variants in *RUNX2* and *CACNA1C* were found to regulate mRNA expression levels of their respective gene in valve tissues. This is concordant with the overexpression of *RUNX2* and *CACNA1C* observed in calcified valves and suggest that newly discovered AS-associated variants increase the risk of AS by increasing the mRNA expression levels of *RUNX2* and *CACNA1C* in valve tissue.

In a typical GWAS, each SNP is tested individually for association with the disease or trait of interest. A wealth of empirical data shows that this approach is successful to identify some robust genetic variants associated with complex diseases, but the effect sizes of risk variants is small to modest. Many polymorphisms are found in the “grey zone” of GWA studies, an area where the statistical signals are below the stringent threshold used to control for multiple SNP-disease tests, but are likely to contain true positive associations[34] with only moderate effect sizes. Many strategies are being pursued to alleviate the large burden of multiple testing encountered in GWA studies in order to find true-positive signals in the grey zone[35]. In this study, we used gene-set association analysis[22] and found coordinated association patterns for genes involved in the calcium signaling pathway. Most SNPs located near or within genes in this gene-set were not individually associated with AS in our meta-analysis. However, considered together, members of this gene-set showed an enrichment of small  $P$  values beyond what is expected by chance. The functional meaning of this discovery was extended to gene expression in aortic valve specimens. Eleven gene members of the calcium signaling pathway were differentially expressed between

patients with and without AS. The differential expression of these genes could lead to AS by altering normal homeostasis of calcium, apoptosis or enhancing fibrosis (**Fig. 6**). Valve eQTL-SNPs in differentially expressed genes were also assessed leading to the identification of *CACNA1C* as a new AS susceptibility gene.

*CACNA1C* was overexpressed in calcified valves compared to normal valve. In addition, its mRNA expression levels were modulated by two moderately AS-associated SNPs located in intron 10 of the gene. *CACNA1C* encodes the alpha-1C subunit of the voltage-dependent calcium channel[36]. Polymorphisms in this gene have been associated with systolic and diastolic blood pressure and hypertension[37]. Angiotensin II was shown to up-regulate the expression and activity of *CACNA1C* in cultured arteries[38]. Further studies will be needed to elucidate the role of *CACNA1C* in AS, but a crosstalk with the renin-angiotensin is possible[39, 40]. Several commercial calcium channel inhibitors/blockers are available for treating hypertension, arrhythmias, and chronic angina pectoris. Whether calcium channel blockers can be used to treat patients with AS is currently unknown. In short terms, functional studies in valve interstitial cells[41] and mouse models of AS[42] are needed to investigate *CACNA1C* as a potential target to treat AS.

Twenty-six candidate genes differentially expressed in this study, including *RUNX2*, were overlaid on known biological processes involved in AS (**Fig. 5**). *RUNX2* is an osteogenic transcription factor repressed by the action of Notch1 and the Hairy family of repressors[43]. *RUNX2* regulates the expression of osteopontin and is up-regulated in mouse and rabbit models of AS[14]. Circulating and valve tissue levels of *RUNX2* significantly correlated with valve stenosis severity[44]. In this study, we demonstrated that two SNPs, rs114193529 and rs144071310, located in intron 1 of *RUNX2* were associated with AS. In addition, the mRNA expression of *RUNX2* was up-regulated in calcified valves and associated with valve eQTL-SNPs. Together these results further support the role of *RUNX2* as a potential driver of AS development.

In this study, two polymorphisms near *ESR1* and *LPA* shown evidence of association with AS. Both genes have already been associated with the disease[15, 33] (**S1 Table**). Interestingly,

estrogen was shown to reduce L-type calcium channel activity *in vitro* and protects mice from the consequences of increased intracellular  $\text{Ca}^{2+}$ [45]. A molecular interaction with the newly discovered AS gene *CACNA1C* is thus possible. A recent GWAS reported the association of rs10455872 with aortic valve calcification [15]. A subsequent study demonstrated that this polymorphism is associated with circulating lipoprotein(a) levels and the risk of AS[46]. This SNP, located in the *LPA* gene, was not present in our genotyping array and was excluded after imputation based on call rate < 90%. In the current GWAS meta-analysis, the SNP rs4708867 located in exon 5 of *SLC22A3* and 109 kb of the *LPA* gene was found modestly associated with AS (**S1 Fig**). This modest genetic association signal is independent from the previous rs10455872 finding. A large-scale meta-analysis of the *LPA* locus is needed to understand its contribution in aortic valve calcification and AS.

This study has limitations. This study represents the largest collection of well-phenotyped patients for AS, but the sample size is still relatively small for a GWAS. Heterogeneity, due to differences in clinical characteristics of cases from Quebec and France, may attenuate genetic associations in the meta-analysis. In addition, genotypes of control individuals were obtained from a younger cohort of individuals. A proportion of these controls is likely to later develop AS, causing a misclassification of a small subset of controls. However, this is not likely to be a major bias as the prevalence of all valve diseases is estimated at 2.5%[2]. It was demonstrated that if 5% of controls would meet the definition of cases, thus misclassified, the loss of power is approximately the same as that due to a reduction of the sample size by 10%[47]. Further work is needed to determine whether the identified eQTL-SNPs associated with AS are tagging non-genotyped/imputed functional variants. Although the sample size to detect valve eQTLs is small ( $n = 22$ ), the eQTL mapping study is conducted in the most relevant tissue to study AS. eQTLs are known to be cell type and tissue specific[48, 49]. Human aortic valve specimens are challenging to obtain and here we reported the first valve eQTL mapping study. To alleviate the power limitation, we have restricted the eQTL analysis to AS-associated SNPs and genes differentially expressed in calcified compared to normal valves.

Several genes implicated in AS development and progression have been documented[9]. However, the key molecules that will allow the development of drugs to treat AS are still

unknown. This GWAS confirmed that AS is not due to one causal gene but the action of several genes with subtle individual risk effects that are acting in concert to modulate higher-order biological processes leading to AS. One of the most important discoveries of this study is the identification of new plausible candidate genes moderately associated with AS and differentially expressed in calcified compared to normal aortic valves. Gene-set association analysis coupled with RNA-Seq and valve eQTL data revealed *CACNA1C* as a new gene in the calcium signaling pathway associated with AS and confirm the role of *RUNX2* as a potential driver of AS development.

### **Acknowledgments**

The authors thank the research team at the cardiac surgical database and biobank of the IUCPQ for their valuable assistance. We also thank the team of the Centre d'Investigation Clinique and the Centre de Ressources Biologiques of Bichat Hospital for their help as well as the clinical and research staff at the Montreal Heart Institute. We thank the patients at all sites for participating in this study. Complete acknowledgements for the dbGaP cohorts are available in S1 Supporting Information.



## **Funding Sources**

This study was supported by the Heart and Stroke Foundation of Canada, the IUCPQ Foundation, and the Canadian Institutes of Health Research grants MOP 102481 (Y.B.), MOP – 137058 (Y.B.), MOP 79342 (P.P. and P.M.), MOP 245048 (P.M. and P.P). The COFRASA and GENERAC studies are supported by grants from the Assistance Publique-Hôpitaux de Paris [PHRC National 2005 and 2010, and PHRC regional 2007 (D.M.Z)]. S.G. was a recipient of a studentship from the International Chair on Cardiometabolic Risk and a doctoral scholarship from the “Centre de recherche de l’IUCPQ”. M.L. is the recipient of a doctoral studentship from the Fonds de recherche Québec - Santé (FRQS) and was a recipient of doctoral studentships from the “Centre de recherche de l’IUCPQ” and the Faculty of medicine of Laval University. B.J.A was a recipient of a post-doctoral fellowship of the Canadian Institutes of Health Research and is now recipient of a Junior 1 Research Scholar award from the FRQS. J.C.T holds the Canada Research Chair in translational and personalized medicine and the University of Montreal endowed research chair in atherosclerosis. S.C.B. received funding from the National Institutes of Health (R01HL114823). P.M. is a research scholar from the FRQS. P.P. holds the Canada Research Chair in Valvular Heart Diseases. Y.B. was a research scholar from the Heart and Stroke Foundation of Canada and is now recipient of a Junior 2 Research Scholar award from the Fonds de recherche Québec-Santé (FRQS).

## **Disclosures**

None.

## References

1. Carabello BA, Paulus WJ. Aortic stenosis. *Lancet*. 2009 Mar 14;373(9667):956-66.
2. Nkomo VT, Gardin JM, Skelton TN, Gottdiener JS, Scott CG, Enriquez-Sarano M. Burden of valvular heart diseases: a population-based study. *Lancet*. 2006 Sep 16;368(9540):1005-11.
3. Otto CM, Burwash IG, Legget ME, Munt BI, Fujioka M, Healy NL, et al. Prospective study of asymptomatic valvular aortic stenosis. Clinical, echocardiographic, and exercise predictors of outcome. *Circulation*. 1997 May 6;95(9):2262-70.
4. Cowell SJ, Newby DE, Prescott RJ, Bloomfield P, Reid J, Northridge DB, et al. A randomized trial of intensive lipid-lowering therapy in calcific aortic stenosis. *N Engl J Med*. 2005 Jun 9;352(23):2389-97.
5. Rossebo AB, Pedersen TR, Boman K, Brudi P, Chambers JB, Egstrup K, et al. Intensive lipid lowering with simvastatin and ezetimibe in aortic stenosis. *N Engl J Med*. 2008 Sep 25;359(13):1343-56.
6. Rajamannan NM, Bonow RO, Rahimtoola SH. Calcific aortic stenosis: an update. *Nat Clin Pract Cardiovasc Med*. 2007 May;4(5):254-62.
7. Sehatzadeh S, Doble B, Xie F, Blackhouse G, Campbell K, Kaulback K, et al. Transcatheter aortic valve implantation (TAVI) for treatment of aortic valve stenosis: an evidence update. *Ont Health Technol Assess Ser*. 2013;13(1):1-40.
8. Paradis JM, George I, Kodali S. Management of significant left main coronary disease before and after trans-apical transcatheter aortic valve replacement in a patient with severe and complex arterial disease. *Catheter Cardiovasc Interv*. 2013 Sep 1;82(3):E262-5.
9. Bosse Y, Miqdad A, Fournier D, Pepin A, Pibarot P, Mathieu P. Refining molecular pathways leading to calcific aortic valve stenosis by studying gene expression profile of normal and calcified stenotic human aortic valves. *Circ Cardiovasc Genet*. 2009 Oct;2(5):489-98.
10. Horne BD, Camp NJ, Muhlestein JB, Cannon-Albright LA. Evidence for a heritable component in death resulting from aortic and mitral valve diseases. *Circulation*. 2004 Nov 9;110(19):3143-8.

11. Probst V, Le Scouarnec S, Legendre A, Jousseau V, Jaafar P, Nguyen JM, et al. Familial aggregation of calcific aortic valve stenosis in the western part of France. *Circulation*. 2006 Feb 14;113(6):856-60.
12. Gaudreault N, Ducharme V, Lamontagne M, Guauque-Olarte S, Mathieu P, Pibarot P, et al. Replication of genetic association studies in aortic stenosis in adults. *Am J Cardiol*. 2011 Nov 1;108(9):1305-10.
13. Ducharme V, Guauque-Olarte S, Gaudreault N, Pibarot P, Mathieu P, Bosse Y. NOTCH1 Genetic Variants in Patients with Tricuspid Calcific Aortic Valve Stenosis. *J Heart Valve Dis*. 2013;22(2):142-9.
14. Garg V, Muth AN, Ransom JF, Schluterman MK, Barnes R, King IN, et al. Mutations in NOTCH1 cause aortic valve disease. *Nature*. 2005 Sep 8;437(7056):270-4.
15. Thanassoulis G, Campbell CY, Owens DS, Smith JG, Smith AV, Peloso GM, et al. Genetic associations with valvular calcification and aortic stenosis. *N Engl J Med*. 2013 Feb 7;368(6):503-12.
16. Mailman MD, Feolo M, Jin Y, Kimura M, Tryka K, Bagoutdinov R, et al. The NCBI dbGaP database of genotypes and phenotypes. *Nat Genet*. 2007 Oct;39(10):1181-6.
17. Delaneau O, Marchini J, Zagury JF. A linear complexity phasing method for thousands of genomes. *Nat Methods*. 2012 Feb;9(2):179-81.
18. Howie BN, Donnelly P, Marchini J. A flexible and accurate genotype imputation method for the next generation of genome-wide association studies. *PLoS Genet*. 2009 Jun;5(6):e1000529.
19. Patterson N, Price AL, Reich D. Population structure and eigenanalysis. *PLoS Genet*. 2006 Dec;2(12):e190.
20. Purcell S, Neale B, Todd-Brown K, Thomas L, Ferreira MA, Bender D, et al. PLINK: a tool set for whole-genome association and population-based linkage analyses. *Am J Hum Genet*. 2007 Sep;81(3):559-75.
21. Pruim RJ, Welch RP, Sanna S, Teslovich TM, Chines PS, Gliedt TP, et al. LocusZoom: regional visualization of genome-wide association scan results. *Bioinformatics*. 2010 Sep 15;26(18):2336-7.

22. Nam D, Kim J, Kim SY, Kim S. GSA-SNP: a general approach for gene set analysis of polymorphisms. *Nucleic Acids Res.* 2010 Jul;38(Web Server issue):W749-54.
23. Yu W, Clyne M, Khoury MJ, Gwinn M. Phenopedia and Genopedia: disease-centered and gene-centered views of the evolving knowledge of human genetic associations. *Bioinformatics.* 2010 Jan 1;26(1):145-6.
24. Warren BA, Yong JL. Calcification of the aortic valve: its progression and grading. *Pathology (Phila).* 1997 Nov;29(4):360-8.
25. Lee JTY, Tsang WH, Chow KL. Simple Modifications to Standard TRIzol® Protocol Allow High-Yield RNA Extraction from Cells on Resorbable Materials. *J Biomater Nanobiotechnol.* 2011;2(1):41-8.
26. Trapnell C, Hendrickson DG, Sauvageau M, Goff L, Rinn JL, Pachter L. Differential analysis of gene regulation at transcript resolution with RNA-Seq. *Nat Biotechnol.* 2013 Jan;31(1):46-53.
27. Anders S, Pyl PT, Huber W. HTSeq-a Python framework to work with high-throughput sequencing data. *Bioinformatics.* 2014 Sep 25.
28. Anders S, Huber W. Differential expression analysis for sequence count data. *Genome Biol.* 2010;11(10):R106.
29. Robinson MD, McCarthy DJ, Smyth GK. edgeR: a Bioconductor package for differential expression analysis of digital gene expression data. *Bioinformatics.* 2010 Jan 1;26(1):139-40.
30. Edgar R, Domrachev M, Lash AE. Gene Expression Omnibus: NCBI gene expression and hybridization array data repository. *Nucleic Acids Res.* 2002 Jan 1;30(1):207-10.
31. Gentleman RC, Carey VJ, Bates DM, Bolstad B, Dettling M, Dudoit S, et al. Bioconductor: open software development for computational biology and bioinformatics. *Genome Biol.* 2004;5(10):R80.
32. Du P, Kibbe WA, Lin SM. lumi: a pipeline for processing Illumina microarray. *Bioinformatics.* 2008 Jul 1;24(13):1547-8.

33. Nordstrom P, Glader CA, Dahlen G, Birgander LS, Lorentzon R, Waldenstrom A, et al. Oestrogen receptor alpha gene polymorphism is related to aortic valve sclerosis in postmenopausal women. *J Intern Med*. 2003 Aug;254(2):140-6.
34. Panagiotou OA, Ioannidis JP. What should the genome-wide significance threshold be? Empirical replication of borderline genetic associations. *Int J Epidemiol*. 2012 Feb;41(1):273-86.
35. Manolio TA. Bringing genome-wide association findings into clinical use. *Nat Rev Genet*. 2013 Aug;14(8):549-58.
36. Hennessey JA, Boczek NJ, Jiang YH, Miller JD, Patrick W, Pfeiffer R, et al. A CACNA1C variant associated with reduced voltage-dependent inactivation, increased CaV1.2 channel window current, and arrhythmogenesis. *PLoS One*. 2014;9(9):e106982.
37. Johnson AD, Newton-Cheh C, Chasman DI, Ehret GB, Johnson T, Rose L, et al. Association of hypertension drug target genes with blood pressure and hypertension in 86,588 individuals. *Hypertension*. 2011 May;57(5):903-10.
38. Wang W, Pang L, Palade P. Angiotensin II upregulates Ca(V)1.2 protein expression in cultured arteries via endothelial H(2)O(2) production. *J Vasc Res*. 2011;48(1):67-78.
39. Helske S, Lindstedt KA, Laine M, Mayranpaa M, Werkkala K, Lommi J, et al. Induction of local angiotensin II-producing systems in stenotic aortic valves. *J Am Coll Cardiol*. 2004 Nov 2;44(9):1859-66.
40. O'Brien KD, Shavelle DM, Caulfield MT, McDonald TO, Olin-Lewis K, Otto CM, et al. Association of angiotensin-converting enzyme with low-density lipoprotein in aortic valvular lesions and in human plasma. *Circulation*. 2002 Oct 22;106(17):2224-30.
41. El Husseini D, Boulanger MC, Mahmut A, Bouchareb R, Laflamme MH, Fournier D, et al. P2Y2 receptor represses IL-6 expression by valve interstitial cells through Akt: implication for calcific aortic valve disease. *J Mol Cell Cardiol*. 2014 Jul;72:146-56.
42. Le Quang K, Bouchareb R, Lachance D, Laplante MA, El Husseini D, Boulanger MC, et al. Early development of calcific aortic valve disease and left ventricular hypertrophy in a mouse model of combined dyslipidemia and type 2 diabetes mellitus. *Arterioscler Thromb Vasc Biol*. 2014 Oct;34(10):2283-91.

43. Towler DA. Molecular and cellular aspects of calcific aortic valve disease. *Circ Res*. 2013 Jul 5;113(2):198-208.
44. Nagy E, Eriksson P, Yousry M, Caidahl K, Ingelsson E, Hansson GK, et al. Valvular osteoclasts in calcification and aortic valve stenosis severity. *Int J Cardiol*. 2013 Oct 3;168(3):2264-71.
45. Nordmeyer J, Eder S, Mahmoodzadeh S, Martus P, Fielitz J, Bass J, et al. Upregulation of myocardial estrogen receptors in human aortic stenosis. *Circulation*. 2004 Nov 16;110(20):3270-5.
46. Arsenault BJ, Boekholdt SM, Dube MP, Rheume E, Wareham NJ, Khaw KT, et al. Lipoprotein(a) levels, genotype, and incident aortic valve stenosis: a prospective mendelian randomization study and replication in a case-control cohort. *Circ Cardiovasc Genet*. 2014 Jun;7(3):304-10.
47. Colhoun HM, McKeigue PM, Davey Smith G. Problems of reporting genetic associations with complex outcomes. *Lancet*. 2003 Mar 8;361(9360):865-72.
48. Dimas AS, Deutsch S, Stranger BE, Montgomery SB, Borel C, Attar-Cohen H, et al. Common regulatory variation impacts gene expression in a cell type-dependent manner. *Science*. 2009 Sep 4;325(5945):1246-50.
49. Fu J, Wolfs MG, Deelen P, Westra HJ, Fehrmann RS, Te Meerman GJ, et al. Unraveling the regulatory mechanisms underlying tissue-dependent genetic variation of gene expression. *PLoS Genet*. 2012 Jan;8(1):e1002431.

## **S1 Supporting Information**

### **Selection of the dbGaP control cohorts**

The genotype data of four control cohorts were obtained from the database of Genotypes and Phenotypes[1] (dbGaP). Three cohorts are from United States including the SNP Typing for Association with Multiple Phenotypes from Existing Epidemiologic Data (STAMPEED, phs000226), the Electronic Medical Records and Genomics (eMERGE, phs000381), and the Polycystic Ovary Syndrome Genetics-NUgene (PCOS, phs000368). After standard SNP quality controls, the ancestry of each sample in the control cohorts was measured using STRUCTURE v2.3.4 and three HapMap populations. The STAMPEED cohort comprised 99.5% of individuals with African ancestry and was not used. The genomic inflation factor and size of the PCOS and eMERGE cohorts were evaluated to select the best control group for AS cases from Quebec. After quality controls and adjustment for population stratification, the genomic inflation factor was 1.0 for both Quebec-PCOS and Quebec-eMERGE GWAS. A total of 2,988 and 1,175 individuals with European ancestry passed all quality controls in the PCOS and eMERGE cohorts, respectively. On the basis of samples size, the PCOS cohort was selected. One European cohort was selected as a control group for the France cases, namely the Genetic Epidemiology of Refractive Error in the Kooperative Gesundheitsforschung in der Region Augsburg Study (KORA, phs000303). KORA is a population based study of adults randomly selected from 430,000 individuals in Augsburg and 16 surrounding counties in Germany.

### **DNA extraction and quality assessment**

DNA of the Quebec cohort was extracted from either frozen whole blood or buffy coat using QIAamp® DNA Blood Midi kit (QIAGEN, Mississauga, ON, Canada). DNA of 72 subjects was extracted using in-house method based on Lahiri et al.[2]. The DNA quality and concentration was assessed by the UV ratio 260 nm/280 nm and fluorescence determination using Quant-iT PicoGreen® dsDNA Assay (Invitrogen™- Life Technologies, Grand Island, NY, USA), respectively. Fourteen samples having UV ratio < 1.7 and/or DNA concentration < 45 ng/μL were excluded.



DNA of the France cohort was extracted from frozen buffy coat using the QIAamp® DNA Blood Maxi kit (QIAGEN). DNA concentration of all samples was assessed using the Nanodrop system (Thermo Scientific, Wilmington, DE, USA) based on optical density. No patient was excluded based on insufficient DNA concentration. Samples from Quebec and France were transferred into 96-well plates and the DNA concentrations were adjusted to  $50 \pm 5$  ng/ $\mu$ L using TE buffer. The concentrations of the adjusted plates were confirmed by Quant-iT PicoGreen® dsDNA Assay.

### **Whole-genome genotyping and quality controls**

Standard genotyping quality controls were performed independently on the Quebec, France, and dbGaP cohorts. Each genotyping set was filtered for low-quality loci with 10<sup>th</sup> percentile of Illumina GenCall score  $\leq 0.1$ , call rate  $< 97\%$ , Hardy-Weinberg equilibrium  $P < 1 \times 10^{-7}$ , and minor allele frequency (MAF)  $< 1\%$ . Samples were excluded after consideration for the 10<sup>th</sup> percentile of Illumina GenCall score  $\leq 0.2$ , genotype completion rate  $< 95\%$ , genotypic and phenotypic gender mismatch, unexpected duplicates and genetic relatedness, and genetic background outliers detected by STRUCTURE[3] ( $k = 4$ ) with HapMap subjects as internal controls. A summary of genotyping quality controls on SNPs and samples for the all cohorts is provided in **S4** and **S5 Tables**, respectively.

### **Imputation and quality controls**

To increase whole-genome coverage, additional SNPs were inferred using the SHAPEIT[4] v2.release727 / IMPUTE2[5] v2.3.1 pipeline. The reference set consisted of the known phased haplotypes of 500 unrelated individuals from Africa, America, Asia, and Europe from the 1,000 Genomes Phase I interim variant set release (June 2011) in NCBI build 37 (hg19) coordinates downloaded from [http://mathgen.stats.ox.ac.uk/impute/data\\_download\\_1000G\\_phase1\\_integrated.html](http://mathgen.stats.ox.ac.uk/impute/data_download_1000G_phase1_integrated.html). SNPs with genotype call rate lower than 90%, genotype distribution deviating from that expected by Hardy-Weinberg equilibrium ( $P < 1 \times 10^{-7}$ ), monomorphic or with MAF  $< 1\%$ , and a certainty score  $< 0.9$  were also excluded. Imputation was conducted separately for all cohorts.

## Valve eQTL study

Aortic valves were explanted from 24 white male patients. A leaflet of the valves was cut into small pieces and then snap-frozen in liquid nitrogen, whereas another leaflet of the same valve was stored in RNA-later solution prior to grinding (mortar and pestle) in liquid nitrogen. The samples were stored in a local biobank at  $-80^{\circ}\text{C}$  until DNA and RNA isolation. All patients underwent a comprehensive Doppler-echocardiographic examination prior to surgery. A physical examination was performed, previous and current medical history was collected as well as current medication. In addition, these patients were characterized for metabolic variables including lipid-, type 2 diabetes- and obesity-related variables. They also undergo blood pressure measurement.

DNA was extracted from 60-80 mg of frozen aortic valve tissue digested with Qiagen's proteinase K at  $56^{\circ}\text{C}$  for 16 hours, followed by column purification using QIAGEN QIAamp® DNA Mini kit. The DNA concentration was assessed by the UV ratio 260 nm/280 nm and fluorescence determination using Quant-iT PicoGreen® dsDNA Assay. The DNA concentrations were adjusted to  $50 \pm 5 \text{ ng}/\mu\text{L}$  using TE buffer. The adjusted concentrations were confirmed by PicoGreen® dsDNA Assay. The DNA was stored at  $-30^{\circ}\text{C}$  until genotyping assay.

Total RNA was extracted from 100 mg of tissue. Concentration was evaluated by UV measurement using the Nanovue spectrophotometer (GE Healthcare LifeScience, Piscataway, NJ, USA). RNA quality was assessed using the Agilent 2100 Bioanalyzer (Agilent Technologie, Santa Clara, CA, USA).

To increase whole-genome coverage, additional SNPs were inferred using the SHAPEIT v2.release790 / IMPUTE2 v2.3.1 pipeline. The reference set consisted of the known phased haplotypes of 2,504 unrelated individuals from Africa, America, Asia, and Europe from the 1,000 Genomes Phase 3 release (October 2014) in NCBI build 37 (hg19) coordinates downloaded from [https://mathgen.stats.ox.ac.uk/impute/1000GP\\_Phase3.tgz](https://mathgen.stats.ox.ac.uk/impute/1000GP_Phase3.tgz). SNPs with genotype call rate lower than 90%, genotype distribution deviating from that expected by Hardy-

Weinberg equilibrium ( $P < 1 \times 10^{-7}$ ), monomorphic or with MAF  $< 1\%$ , and a certainty score  $< 0.9$  were also excluded. After imputation, a total of 7,657,363 SNPs were available for analysis.

## **Acknowledgment for dbGAP cohorts**

**eMERGE.** Samples and data in this study were provided by the Geisinger MyCode® Project. Funding for the MyCode® Project was provided by a grant from Commonwealth of Pennsylvania and the Clinic Research Fund of Geisinger Clinic. Funding support for the genotyping of the MyCode® cohort was provided by a Geisinger Clinic operating funds and an award from the Clinic Research Fund. The datasets used for the is described in this manuscript were obtained from dbGaP at <http://www.ncbi.nlm.nih.gov/gap> through dbGaP accession number phs000381.v1.p1 eMERGE GWAS data March 28, 2012 version.

**KORA.** The datasets used for the is described in this manuscript were obtained from the NEI Refractive Error Collaboration (NEIREC) Database found at <http://www.ncbi.nlm.nih.gov/gap> through dbGaP accession number phs000303.v1.p1. Funding support for NEIREC Research Group was provided by the National Eye Institute. We would like to thank NEIREC participants and the NEIREC Research Group for their valuable contribution to this research.

**PCOS.** The datasets used for the is described in this manuscript were obtained from the database of Genotype and Phenotype (dbGaP) found at <http://www.ncbi.nlm.nih.gov/gap> through dbGaP accession number phs000368. Samples and associated phenotype data for the Genome-Wide Association Scan [GWAS] of Polycystic Ovary Syndrome Phenotypes were provided by Andrea Dunaif, M.D.

**STAMPEED:CHS.** The research reported in this article was supported by contract numbers N01-HC-85079, N01-HC-85080, N01-HC-85081, N01-HC-85082, N01-HC-85083, N01-HC-85084, N01-HC-85085, N01-HC-85086, N01-HC-35129, N01 HC-15103, N01 HC-55222, N01-HC-75150, N01-HC-45133, N01-HC-85239 and HHSN268201200036C; grant numbers U01 HL080295 from the National Heart, Lung, and Blood Institute and R01 AG-023629 from the National Institute on Aging, with additional contribution from the National Institute of Neurological Disorders and Stroke. A full list of principal CHS investigators and institutions can be found at <http://www.chs-nhlbi.org/pi.htm>. This manuscript was not prepared in collaboration

with CHS investigators and does not necessarily reflect the opinions or views of CHS, or the NHLBI.

Support for the Cardiovascular Health Study Whole Genome Study (STAMPEED: CHS) was provided by NHLBI grant HL087652. Additional support for infrastructure was provided by HL105756 and additional genotyping among the African-American cohort was supported in part by HL085251. DNA handling and genotyping at Cedars-Sinai Medical Center was supported in part by National Center for Research Resources grant UL1RR033176, now at the National Center for Advancing Translational Technologies CTSI grant UL1TR000124; in addition to the National Institute of Diabetes and Digestive and Kidney Diseases grant DK063491 to the Southern California Diabetes Endocrinology Research Center.

## Supplemental references

1. Mailman MD, Feolo M, Jin Y, Kimura M, Tryka K, et al. The NCBI dbGaP database of genotypes and phenotypes. *Nat Genet.* 2007;39: 1181-1186.
2. Lahiri DK, Schnabel B DNA isolation by a rapid method from human blood samples: effects of MgCl<sub>2</sub>, EDTA, storage time, and temperature on DNA yield and quality. *Biochem Genet.* 1993;31: 321-328.
3. Falush D, Stephens M, Pritchard JK Inference of population structure using multilocus genotype data: linked loci and correlated allele frequencies. *Genetics.* 2003;164: 1567-1587.
4. Delaneau O, Marchini J, Zagury JF A linear complexity phasing method for thousands of genomes. *Nat Methods.* 2012;9: 179-181.
5. Howie BN, Donnelly P, Marchini J A flexible and accurate genotype imputation method for the next generation of genome-wide association studies. *PLoS Genet.* 2009;5: e1000529.
6. Knez I, Renner W, Maier R, Rehak P, Rienmuller R, et al. Angiotensin-converting enzyme polymorphisms and their potential impact on left ventricular myocardial geometry after aortic valve surgery. *J Heart Valve Dis.* 2003;12: 687-695.
7. Ellis SG, Dushman-Ellis S, Luke MM, Murugesan G, Kottke-Marchant K, et al. Pilot candidate gene analysis of patients  $\geq 60$  years old with aortic stenosis involving a tricuspid aortic valve. *Am J Cardiol.* 2012;110: 88-92.
8. Avakian SD, Annicchino-Bizzacchi JM, Grinberg M, Ramires JA, Mansura AP Apolipoproteins AI, B, and E polymorphisms in severe aortic valve stenosis. *Clin Genet.* 2001;60: 381-384.
9. Gaudreault N, Ducharme V, Lamontagne M, Guauque-Olarte S, Mathieu P, et al. Replication of genetic association studies in aortic stenosis in adults. *Am J Cardiol.* 2011;108: 1305-1310.
10. Novaro GM, Sachar R, Pearce GL, Sprecher DL, Griffin BP Association between apolipoprotein E alleles and calcific valvular heart disease. *Circulation.* 2003;108: 1804-1808.
11. Ortlepp JR, Pillich M, Mevissen V, Krantz C, Kimmel M, et al. APOE alleles are not associated with calcific aortic stenosis. *Heart.* 2006;92: 1463-1466.

12. Turkmen F, Ozdemir A, Sevinc C, Eren PA, Demiral S. Calcium-sensing receptor gene polymorphisms and cardiac valvular calcification in patients with chronic renal failure: a pilot study. *Hemodial Int.* 2009;13: 176-180.
13. Ortlepp JR, Schmitz F, Mevissen V, Weiss S, Huster J, et al. The amount of calcium-deficient hexagonal hydroxyapatite in aortic valves is influenced by gender and associated with genetic polymorphisms in patients with severe calcific aortic stenosis. *Eur Heart J.* 2004;25: 514-522.
14. Nordstrom P, Glader CA, Dahlen G, Birgander LS, Lorentzon R, et al. Oestrogen receptor alpha gene polymorphism is related to aortic valve sclerosis in postmenopausal women. *J Intern Med.* 2003;254: 140-146.
15. Thanassoulis G, Campbell CY, Owens DS, Smith JG, Smith AV, et al. Genetic associations with valvular calcification and aortic stenosis. *N Engl J Med.* 2013;368: 503-512.
16. Arsenault BJ, Boekholdt SM, Dube MP, Rheume E, Wareham NJ, et al. Lipoprotein(a) levels, genotype, and incident aortic valve stenosis: a prospective mendelian randomization study and replication in a case-control cohort. *Circ Cardiovasc Genet.* 2014;7: 304-310.
17. Moura LM, Faria S, Brito M, Pinto FJ, Kristensen SD, et al. Relationship of PON1 192 and 55 gene polymorphisms to calcific valvular aortic stenosis. *Am J Cardiovasc Dis.* 2012;2: 123-132.
18. Schmitz F, Ewering S, Zerres K, Klomfass S, Hoffmann R, et al. Parathyroid hormone gene variant and calcific aortic stenosis. *J Heart Valve Dis.* 2009;18: 262-267.
19. Ortlepp JR, Hoffmann R, Ohme F, Lauscher J, Bleckmann F, et al. The vitamin D receptor genotype predisposes to the development of calcific aortic valve stenosis. *Heart.* 2001;85: 635-638.
20. Baumgartner H, Hung J, Bermejo J, Chambers JB, Evangelista A, et al. Echocardiographic assessment of valve stenosis: EAE/ASE recommendations for clinical practice. *J Am Soc Echocardiogr.* 2009;22: 1-23; quiz 101-102.
21. Lang RM, Bierig M, Devereux RB, Flachskampf FA, Foster E, et al. Recommendations for chamber quantification: a report from the American Society of Echocardiography's Guidelines and Standards Committee and the Chamber Quantification Writing Group, developed in conjunction with the European Association of Echocardiography, a branch of the European Society of Cardiology. *J Am Soc Echocardiogr.* 2005;18: 1440-1463.

## Supplemental Tables

**S1 Table.** Genes previously associated with calcific aortic valve stenosis.

Symbol	Gene Name	Reference	Nearest SNP Calcified vs normal valves (distance)	FC (P adjusted)
<i>ACE</i>	Angiotensin I converting enzyme  (peptidyl-dipeptidase A) 1	Knez et al. 2003[6]	NS	3.79 (0.001)
<i>AGTR1</i>	Angiotensin II receptor, type 1	Ellis et al. 2012[7]	NS	-6.86 (0.005)
<i>APOA1</i>	Apolipoprotein A-I	Avakian et al. 2001[8]	NS	-6.58 (0.001)
<i>APOB</i>	Apolipoprotein B	Avakian et al. 2001[8],  Gaudreault et al. 2011[9]	NS	NS
<i>APOE</i>	Apolipoprotein E	Avakian et al. 2001[8],	NS	NS



---

		Novaro et al. 2003[10],		
		Ortlepp et al. 2006[11]		
<i>CASR</i>	Calcium-sensing receptor	Turkmen et al. 2009[12]	NS	NS
<i>CCR5</i>	Chemokine (C-C motif) receptor 5	Ortlepp et al. 2004[13]	NS	1.99 (0.004)
<i>CTGF</i>	Connective tissue growth factor	Ortlepp et al. 2004[13]	NS	NS
<i>ELN</i>	Elastin	Ellis et al. 2012[7]	NS	NS
<i>ESR1</i>	Estrogen receptor 1	Nordström et al. 2003[14]	rs9371549	-1.82 (0.036)
			(-3.776kb)	
<i>IL10</i>	Interleukin 10	Gaudreault et al. 2011[9],		
		Ortlepp et al. 2004[13]		

---

<i>LPA</i>	Lipoprotein, Lp(a)	Thanassoulis et al. 2013[15], Arsenault et al. 2014[16]	rs4708867 (-109kb)	NS
<i>MYO7A</i>	Myosin VIIA	Ellis et al. 2012[7]	NS	-1.70 (0.026)
<i>PONI</i>	Paraoxonase 1	Moura et al. 2012[17]	NS	NS
<i>PTH</i>	Parathyroid hormone	Schmitz et al. 2009[18], Gaudreault et al. 2011[9]	NS	NS
<i>TGFB1</i>	Transforming growth factor, beta 1	Nordström et al. 2003[14]	NS	NS
<i>VDR</i>	Vitamin D (1,25- dihydroxyvitamin D3) receptor	Ortlepp et al. 2001[19], Schmitz et al. 2009[18]	NS	2.08 (0.007)

NS: No SNP in the top GWAS results ( $P < 5 \times 10^{-6}$ ) 1Mb up or downstream the gene and/or gene not differentially expressed in calcified compared to normal aortic valves in the RNA-Seq experiment. FC: Fold Change.

**S2 Table.** Clinical characteristics of patients according to study stages.

	Meta-analysis		Valve specimens for RNA-Seq	
	Quebec <b>n = 474</b>	France <b>n = 486</b>	Tricuspid AS <b>n = 9</b>	Normal <b>n = 8</b>
Male gender	57%	59%	100%	100%
Age (years)	72.0 ± 8.8	77.2 ± 8.7	64.6 ± 4.3	59.1 ± 4.3
Weight (kg)	74.3 ± 15.0	76.8 ± 46.6	90.6 ± 16.3	87.3 ± 11.6
Waist circumference (cm)	100.7 ± 13.6	100.5 ± 13.3	110.4 ± 12.1	NA
Body surface area (m <sup>2</sup> )	1.8 ± 0.2	1.9 ± 0.7	2.0 ± 0.2	2.0 ± 0.1
Body mass index (kg/m <sup>2</sup> )	28.1 ± 5.2	27.8 ± 12.1	29.8 ± 4.5	28.5 ± 2.9

Mean gradient (mmHg)	41.5 ± 16.4	43.8 ± 21.7	40.4 ± 16.5	NA
Aortic valve area (cm <sup>2</sup> )	0.8 ± 0.2	1.0 ± 0.4	0.8 ± 0.2	NA
Indexed aortic valve area (cm <sup>2</sup> /m <sup>2</sup> )	0.4 ± 0.1	0.5 ± 0.2	0.4 ± 0.1	NA
Left ventricular hypertrophy	38.2%	89.9%	22%	0%
Mild aortic valve regurgitation	68.0%	63.4%	78%	20%
Coronary artery disease	63.9%	29.4%	50%	25%
Dyslipidemia/Hypercholesterolemia	79.3%	52.1%	100%	75%
Hypertension	70.7%	68.9%	78%	37.5%
Diabetes	29.9%	24.1%	0%	0%

Continuous variables are expressed as mean ± SD. Dichotomous variables are expressed as percentage. NA: Not available.

Clinical and echocardiographic definitions:

Coronary artery disease was defined as history of myocardial infarction, documented myocardial ischemia or coronary artery stenosis on coronary angiography.

Hypercholesterolemia was defined as total plasma cholesterol level  $> 6.2$  mmol/l or the use of cholesterol lowering medication.

Blood pressure was evaluated in a sitting position using a mercury sphygmomanometer. Hypertension was defined as blood pressure above 140/90 mmHg or the use of anti-hypertensive treatments.

Diabetes was defined as fasting glucose  $\geq 7$  mmol/l or the use of oral hypoglycemic or insulin medications.

Waist circumference was obtained using a measuring tape directly on the skin with the subject standing. Measurements were taken at the end of expiration at the level midway between the lower rib margin and the iliac crest.

Body surface area was obtained using the Dubois & Dubois formula. Body mass index (BMI) was calculated as weight (kg)/height<sup>2</sup> (m<sup>2</sup>).

The aortic valve area was calculated with the continuity equation and the mean transvalvular gradient was calculated with the Bernoulli equation[20].

The left ventricular mass was calculated following the modified formula of the American Society of Echocardiography criteria[21] and was indexed for body surface area. Left ventricular hypertrophy was defined as left ventricular mass index  $> 115$  g/m<sup>2</sup> in men and  $> 95$  g/m<sup>2</sup> in women.

**S3 Table.** Clinical characteristics of the control (dbGaP) cohorts.

	<b>PCOS n = 2,988</b>	<b>KORA n = 1,864</b>
Male gender	0%	49.7%
Age (years)	46.9 ± 15.2	55.6 ± 11.8
Weight (kg)	73.4 ± 20.6	NA
Body mass index (kg/m <sup>2</sup> )	26.9 ± 7.4	NA

Continuous variables are expressed as mean ± SD. NA: Not available.

**S4 Table.** Number of SNPs excluded at each quality control check.

<b>Quality control parameters</b>	<b>Quebec</b>	<b>France</b>	<b>PCOS</b>	<b>KORA</b>
Illumina GenCall	4343	0	NA	NA
Call rate	15,219	9,159	7,650	0
Hardy-Weinberg	987	1,187	3,305	209
Monomorphic	49,050	18,583	16,902	358,000
Minor allele frequency + No call	30,280	51,612	63,175	331,796
<b>Total unique SNPs excluded</b>	<b>94,150</b>	<b>78,839</b>	<b>86,004</b>	<b>689,952</b>
<b>Total initial SNPs number</b>	<b>733,202</b>	<b>733,202</b>	<b>731,442</b>	<b>2,182,680</b>
<b>Total SNPs remaining</b>	<b>639,052</b>	<b>654,363</b>	<b>645,438</b>	<b>1,492,728</b>

NA: Not available

**S5 Table.** Number of samples excluded at each quality control check.

<b>Quality control parameters</b>	<b>Quebec</b>	<b>France</b>	<b>PCOS</b>	<b>KORA</b>
Illumina GenCall	0	0	NA	NA
Call rate	0	2	0	0
Gender mismatch	3	4	6	3
Duplicates and genetic relatedness	2	2	51	0
Ethnicity	1	14	11	2
Total unique samples excluded	6	19	67	5
Total initial number of samples	480	505	3,056	1,869
Total samples remaining	474	486	2,988	1,864

NA: Not available



**S6 Table.** Clinical characteristics of patients used in the valve eQTL mapping study.

	<b>n = 22</b>
Male gender	22
Age (years)	62.5 ± 2.4
Mean gradient (mmHg)	41.0 ± 12
Aortic valve area (cm <sup>2</sup> )	0.848 ± 0.23
Fibrosis (light: moderate: NA)	3 : 11 : 8
Bicuspid (none : NA)	15 : 7
Insufficiency (trivial:light:moderate:NA)	4 : 8 : 9 : 1
Coronary artery bypass (yes:no)	12 : 10
Coronary artery disease (yes:no)	6 : 16

Continuous variables are expressed as mean ± SD. Dichotomous variables are expressed as n. Coronary artery disease was defined as history of myocardial infarction. The aortic valve area was calculated with the continuity equation. NA: Not available.

**S7 Table.** List of SNPs associated with aortic valve stenosis with a  $P < 5 \times 10^{-6}$  in the meta-analysis.

CHR	SNP	BP	A1 A2 allele	/ P fixed (OR)	P random	I <sup>2</sup> (%)	P (OR)	QC- P PCOS (OR)	FR- MAF KORA (OR)	MAF QC PCOS	/ FR KORA	MAF 1K / genomes†	Nearest gene (distance)
3	rs139795084	109,752,185	C/G	2.66x10 <sup>-7</sup> (7.48)	2.66x10 <sup>-7</sup>	0.0	1.48x10 <sup>-4</sup> (5.95)	3.81x10 <sup>-4</sup> (10.69)	0.013 0.011	/ 0.016 0.011	/ 0.010	<i>LINC01205</i> (+538.2kb)	
3	rs11715795	20,719,760	A/G	2.87x10 <sup>-7</sup> (3.33)	2.87x10 <sup>-7</sup>	0.0	2.19x10 <sup>-5</sup> (2.71)	2.55x10 <sup>-3</sup> (4.11)	0.101 0.079	/ 0.094 0.078	/ 0.093	<i>LOC101927829</i> (+327.3kb)	
3	rs11718740	20,750,665	T/A	6.00x10 <sup>-7</sup> (3.24)	3.31x10 <sup>-5</sup>	30.8	1.15x10 <sup>-5</sup> (2.44)	7.66x10 <sup>-3</sup> (4.30)	0.099 0.078	/ 0.091 0.078	/ 0.089	<i>LOC101927829</i> (+358.2kb)	
3	rs79874757	20,734,135	A/G	6.48x10 <sup>-7</sup> (3.24)	3.01x10 <sup>-5</sup>	29.7	1.29x10 <sup>-5</sup> (2.44)	7.52x10 <sup>-3</sup> (4.29)	0.097 0.079	/ 0.092 0.079	/ 0.094	<i>LOC101927829</i> (+341.7kb)	
3	rs112995365	20,751,951	G/A	6.81x10 <sup>-7</sup> (3.23)	2.96x10 <sup>-5</sup>	29.3	1.33x10 <sup>-5</sup> (2.44)	7.64x10 <sup>-3</sup> (4.27)	0.099 0.080	/ 0.092 0.079	/ 0.096	<i>LOC101927829</i> (+359.5kb)	

3	rs113299180	20,729,885	A/G	7.72x10 <sup>-7</sup> (3.21)	1.52x10 <sup>-5</sup>	23.4	1.68x10 <sup>-5</sup> (2.45)	7.25x10 <sup>-3</sup> (4.20)	0.097 0.079	/ 0.092 0.077	/ 0.093	<i>LOC101927829</i> (+337.5kb)
3	rs12491632*	20,744,029	C/T	8.08x10 <sup>-7</sup> (3.14)	8.08x10 <sup>-7</sup>	0.0	4.39x10 <sup>-5</sup> (2.59)	3.88x10 <sup>-3</sup> (3.81)	0.099 0.080	/ 0.094 0.079	/ 0.096	<i>LOC101927829</i> (+351.6kb)
21	rs10483012	33,869,748	T/C	1.11x10 <sup>-6</sup> (9.32)	6.24 x10 <sup>-4</sup>	48.9	5.37x10 <sup>-6</sup> (4.59)	2.54x10 <sup>-2</sup> (16.66)	0.026 0.015	/ 0.024 0.014	/ 0.025	<i>EVAIC</i> (intron)
19	rs17345014*	43,465,816	C/T	1.33x10 <sup>-6</sup> (2.77)	1.33x10 <sup>-6</sup>	0.0	2.63x10 <sup>-3</sup> (2.87)	1.50x10 <sup>-4</sup> (2.64)	0.171 0.111	/ 0.191 0.103	/ 0.124	<i>PSG7</i> (+24.49kb)
3	rs9857444	188,975,673	C/T	1.43x10 <sup>-6</sup> (4.03)	6.88x10 <sup>-6</sup>	13.3	5.41x10 <sup>-5</sup> (3.04)	4.44x10 <sup>-3</sup> (5.67)	0.068 0.054	/ 0.077 0.041	/ 0.067	<i>TPRG1</i> (intron)
17	rs75561073	5,745,812	G/T	1.69x10 <sup>-6</sup> (8.66)	1.69x10 <sup>-6</sup>	0.0	2.65x10 <sup>-3</sup> (10.75)	1.72x10 <sup>-4</sup> (6.92)	0.038 0.028	/ 0.028 0.013	/ 0.039	<i>LOC339166</i> (intron)
7	rs118040196	28,915,536	C/A	1.94x10 <sup>-6</sup> (7.32)	1.94x10 <sup>-6</sup>	0.0	1.81x10 <sup>-3</sup> (7.14)	3.25x10 <sup>-4</sup> (7.58)	0.024 0.018	/ 0.028 0.021	/ 0.021	<i>CREB5</i> (+50.02kb)

7	rs79158915	28,909,680	A/C	2.29x10 <sup>-6</sup> (7.83)	2.29x10 <sup>-6</sup>	0.0	8.95x10 <sup>-4</sup> (7.02)	7.41x10 <sup>-4</sup> (9.05)	0.021 0.016	/ 0.023 0.019	/ 0.022	<i>CREB5</i> (+44.17kb)
15	rs3894644*	34,718,594	T/C	2.36x10 <sup>-6</sup> (8.54)	4.97 x10 <sup>-2</sup>	68.1	4.33x10 <sup>-1</sup> (13.45)	6.40x10 <sup>-7</sup> (2.06)	0.012 0.011	/ 0.101 0.013	/ NFD	<i>GOLGA8A</i> (intron)
11	rs117752934	95,649,061	A/T	2.75x10 <sup>-6</sup> (6.89)	2.75x10 <sup>-6</sup>	0.0	8.91x10 <sup>-2</sup> (8.61)	8.29x10 <sup>-6</sup> (3.82)	0.012 0.015	/ 0.023 0.017	/ 0.012	<i>MTMR2</i> (intron)
3	rs9815491*	189,005,992	A/G	2.92x10 <sup>-6</sup> (4.03)	2.92x10 <sup>-6</sup>	0.0	2.68x10 <sup>-4</sup> (3.38)	2.70x10 <sup>-3</sup> (4.96)	0.068 0.053	/ 0.079 0.038	/ 0.065	<i>TPRGI</i> (intron)
3	rs7638684	189,001,604	G/A	2.97x10 <sup>-6</sup> (4.03)	2.97x10 <sup>-6</sup>	0.0	2.69x10 <sup>-4</sup> (3.37)	2.74x10 <sup>-3</sup> (4.96)	0.068 0.053	/ 0.079 0.039	/ 0.066	<i>TPRGI</i> (intron)
3	rs7614851	188,995,763	A/G	2.97x10 <sup>-6</sup> (4.03)	2.97x10 <sup>-6</sup>	0.0	2.69x10 <sup>-4</sup> (3.37)	2.73x10 <sup>-3</sup> (4.96)	0.068 0.053	/ 0.077 0.039	/ 0.065	<i>TPRGI</i> (intron)
3	rs16864172	188,999,966	C/T	2.97x10 <sup>-6</sup> (4.03)	2.97x10 <sup>-6</sup>	0.0	2.69x10 <sup>-4</sup> (3.37)	2.74x10 <sup>-3</sup> (4.96)	0.068 0.053	/ 0.079 0.039	/ 0.066	<i>TPRGI</i> (intron)

3	rs73055977	188,996,420	A/G	2.97x10 <sup>-6</sup> (4.03)	2.97x10 <sup>-6</sup>	0.0	2.69x10 <sup>-4</sup> (3.37)	2.73x10 <sup>-3</sup> (4.96)	0.068 0.053	/ 0.077 0.039	/ 0.065	<i>TPRG1</i> (intron)
3	rs138995217	189,002,601	A/G	3.01x10 <sup>-6</sup> (4.12)	3.01x10 <sup>-6</sup>	0.0	3.25x10 <sup>-4</sup> (3.47)	2.33x10 <sup>-3</sup> (5.08)	0.063 0.048	/ 0.076 0.036	/ 0.058	<i>TPRG1</i> (intron)
7	rs78850423	28,914,157	A/G	3.21x10 <sup>-6</sup> (7.53)	3.21x10 <sup>-6</sup>	0.0	1.51x10 <sup>-3</sup> (7.21)	6.47x10 <sup>-4</sup> (7.94)	0.022 0.017	/ 0.023 0.020	/ 0.021	<i>CREB5</i> (+48.65kb)
7	rs76323786	28,913,300	A/G	3.25x10 <sup>-6</sup> (7.53)	3.25x10 <sup>-6</sup>	0.0	1.53x10 <sup>-3</sup> (7.23)	6.48x10 <sup>-4</sup> (7.92)	0.022 0.017	/ 0.023 0.020	/ 0.021	<i>CREB5</i> (+47.79kb)
12	rs117740534	92,238,464	G/A	3.96x10 <sup>-6</sup> (7.51)	3.96x10 <sup>-6</sup>	0.0	6.28x10 <sup>-4</sup> (5.90)	1.50x10 <sup>-3</sup> (11.00)	0.019 0.015	/ 0.018 0.018	/ 0.022	<i>C12orf79</i> (- 140.3kb)
16	rs141826387	21,948,461	T/C	4.98x10 <sup>-6</sup> (6.94)	5.20 x10 <sup>-4</sup>	40.8	2.23x10 <sup>-5</sup> (3.81)	3.28x10 <sup>-2</sup> (11.52)	0.029 0.019	/ 0.023 0.019	/ 0.020	<i>UQCRC2</i> (- 16.15kb)

\*Genotyped SNP; A1: minor allele; A2: major allele; I<sup>2</sup>: Heterogeneity. QC: Quebec cases. FR: France cases. MAF: minor allele frequency. †Allele frequencies of Europeans from the 1000 genomes project. NDF: No frequency data. *C12orf79*: chromosome 12 open reading frame 79; *CREB5*: cAMP responsive element binding protein 5; *EVA1C*: eva-1 homolog C (*C. elegans*); *GOLGA8A*: golgin A8 family, member A; *LINC01205*: long intergenic non-protein coding RNA 1205; *LOC101927829*: uncharacterized LOC101927829; *LOC339166*: uncharacterized LOC339166; *MTMR2*: myotubularin related protein 2; *PSG7*: pregnancy specific beta-1-glycoprotein 7 (gene/pseudogene); *TPRG1*: tumor protein p63 regulated 1; *UQCRC2*: ubiquinol-cytochrome c reductase core protein II

**S8 Table.** Forty-six differentially expressed genes in calcified compared to normal valves located 1 Mb up- or down-stream of SNPs with GWAS  $P < 1 \times 10^{-4}$  in the meta-analysis.

Symbol	Name	SNPs with $P < 1 \times 10^{-4}$ (Distance from the gene)	Smallest $P$	FC (P adjusted)
<i>AMPD3</i>	murine retrovirus integration site 1 homolog	rs7947808 (+134.2 kb)	9.45E-05	2.69 (1.47E-03)
<i>APCDDIL</i>	phosphoenolpyruvate carboxykinase 1 (soluble)	rs6099674 (-883.9 kb), rs78547178 (-900.8 kb)	rs2865391 (-885.2 kb), 2.05E-05	4.08 (1.47E-03)
<i>APCDDIL-AS1</i>	phosphoenolpyruvate carboxykinase 1 (soluble)	rs6099674 (-939.9 kb), rs78547178 (-956.9 kb)	rs2865391 (-941.2 kb), 2.05E-05	3.65 (4.66E-02)
<i>ARL4C</i>	SH3-domain binding protein 4	rs140767021 (+429.1 kb), rs73124220 (+459.3 kb), rs73124221 (+460.8 kb), rs17868337 (-762 kb)	rs73124219 (+458.8 kb), 3.15E-05 rs7605644 (+459.6 kb),	2.77 (1.47E-03)

<i>BDKRB2</i>	small nucleolar RNA host gene 10 (non-protein coding)	rs141293055 (-690.6 kb)	5.51E-05	2.38 (6.00E-03)
<i>C8orf88</i>	long intergenic non-protein coding RNA 534	rs142390982 (-470.8 kb), rs6471103 (-472.2 kb),	rs7844905 (-472.1 kb), rs4734234 (-474.9 kb)	4.16E-05 -2.09 (1.47E-03)
<i>CD248</i>	D4, zinc and double PHD fingers family 2	rs603286 (-986.2 kb), rs630055 (-994.4 kb),	rs509303 (-988.8 kb), rs4149813 (-999.3 kb)	8.90E-05 1.96 (1.47E-03)
<i>COL4A1</i>	collagen, type IV, alpha 1	rs7983716 (-615.2 kb), rs1410422 (-634.7 kb)	rs4773061 (-623.9 kb)	9.43E-05 2.64 (1.47E-03)
<i>COL4A2</i>	collagen, type IV, alpha 2	rs7983716 (-773.5 kb)	9.43E-05	2.52 (1.47E-03)
<i>CST7</i>	synapse differentiation inducing 1	rs75976164 (-473.8 kb)	9.00E-05	2.20 (3.91E-03)
<i>ESR1</i>	estrogen receptor 1	rs9371549 (-3.776 kb), rs11155799 (-84.36 kb),	rs6557158 (-81.69 kb), rs4304175 (-87.65 kb)	7.47E-05 -1.82 (3.59E-02)

<i>FGFI</i>	Rho GTPase activating protein 26	rs9324897 (+90.82 kb)	2.62E-05	2.22 (1.47E-03)
<i>FXYDI</i>	succinate dehydrogenase complex assembly factor 1	rs4458134 (+855.4 kb)	6.59E-05	-1.55 (4.22E-02)
<i>FYB</i>	Dab, mitogen-responsive phosphoprotein, homolog (Drosophila)	rs62358400 (+118.8 kb), rs62358401 (+119.1 kb), rs62358402 (+119.6 kb), rs62358404 (+120.5 kb), rs62358405 (+120.8 kb), rs78092616 (+121.4 kb), rs62358406 (+121.6 kb), rs79185156 (+121.9 kb), rs79744831 (+121.9 kb), rs62358407 (+122.2 kb), rs62358408 (+122.3 kb), rs62358409 (+122.5 kb), rs62358410 (+122.8 kb), rs62358411 (+122.9 kb), rs76494922 (+122 kb), rs62358412 (+123.2 kb), rs34529705 (+123.6 kb), rs62358413 (+123.9 kb), rs62358414 (+124.3 kb), rs140023937 (+124.8 kb), rs62358416 (+125.2 kb), rs62358417 (+125.3 kb), rs2548565 (+125.4 kb), rs62358419 (+126.2 kb), rs62358418 (+126 kb), rs62358420 (+127.4 kb), rs62358421 (+127.4 kb), rs62358422 (+127.5 kb), rs115128266 (+127.6 kb), rs115861802 (+127.6 kb), rs79634545 (+127.6 kb), rs62358423 (+127.8 kb),	6.04E-05	1.84 (1.47E-03)



---

rs62358424 (+127.9 kb), rs62358425 (+127.9 kb),  
rs78127103 (+128.9 kb), rs62358426 (+129.2 kb),  
rs62358448 (+130.3 kb), rs62358449 (+130.5 kb),  
rs62358450 (+132.7 kb), rs62358451 (+132.8 kb),  
rs62358453 (+133.6 kb), rs182925183 (+133.8 kb),  
rs62358454 (+134.6 kb), rs115237520 (+138.3 kb),  
rs3849760 (+138.5 kb), rs143263623 (+138 kb),  
rs3849761 (+139.8 kb), rs3849762 (+139.9 kb),  
rs3909468 (+140.4 kb), rs3843909 (+140.5 kb),  
rs2367584 (+141.8 kb), rs3849763 (+141.9 kb),  
rs3849764 (+141.9 kb), rs3906413 (+142.5 kb),  
rs3849765 (+142 kb), rs3849766 (+145.1 kb),  
rs837085 (+145.5 kb), rs837086 (+145.6 kb),  
rs837087 (+146.8 kb), rs62358459 (+159.6 kb)

<i>GREM1</i>	formin 1	rs8038990 (+131.9 kb)	2.62E-05	8.15 (1.47E-03)
<i>GSC</i>	small nucleolar RNA host gene 10 (non-protein coding)	rs141293055 (+744.1 kb)	5.51E-05	2.64 (1.47E-03)

---

<i>GUCY1A3</i>	guanylate cyclase 1, soluble, beta 3	rs77169028 (+23.71 kb)	1.83E-05	1.86 (3.91E-03)
<i>GUCY1B3</i>	guanylate cyclase 1, soluble, beta 3	rs77169028 (0)	1.83E-05	1.79 (5.03E-03)
<i>HLA-DOA</i>	bromodomain containing 2	rs115221241 (-18.34 kb), rs116830522 (-20.99 kb), rs115382612 (-27.38 kb), rs150850682 (-28.85 kb), rs116194926 (-29.61 kb), rs138957550 (-33.1 kb), rs143892329 (-35.15 kb), rs115543507 (-38.06 kb), rs147983336 (-39.55 kb), rs114543582 (-39.88 kb)	5.02E-05	1.88 (1.47E-03)
<i>HLA-DPB2</i>	bromodomain containing 2	rs115221241 (-126.7 kb), rs116830522 (-129.3 kb), rs115382612 (-135.7 kb), rs150850682 (-137.2 kb), rs116194926 (-137.9 kb), rs138957550 (-141.4 kb), rs143892329 (-143.5 kb), rs115543507 (-146.4 kb), rs147983336 (-147.9 kb), rs114543582 (-148.2 kb)	5.02E-05	6.60 (1.47E-03)
<i>HLA-DQA1</i>	bromodomain containing 2	rs114543582 (+320.6 kb), rs147983336 (+321 kb), rs115543507 (+322.5 kb), rs143892329 (+325.4 kb), rs138957550 (+327.4 kb), rs116194926 (+330.9 kb),	8.02E-05	2.86 (1.47E-03)

---

		rs150850682 (+331.7 kb), rs115382612 (+333.1 kb), rs116830522 (+339.5 kb), rs115221241 (+342.2 kb)	
<i>HLA-DRA</i>	bromodomain containing 2	rs114543582 (+519.3 kb), rs147983336 (+519.6 kb), 8.02E-05 rs115543507 (+521.1 kb), rs143892329 (+524 kb), rs138957550 (+526 kb), rs116194926 (+529.5 kb), rs150850682 (+530.3 kb), rs115382612 (+531.7 kb), rs116830522 (+538.1 kb), rs115221241 (+540.8 kb)	2.42 (1.47E-03)
<i>HSD17B13</i>	dentin sialophosphoprotein	rs2627689 (+275.3 kb), rs1462361 (+277.4 kb), 8.73E-05 rs2615487 (+286.4 kb), rs2736979 (+287.3 kb), rs2627699 (+287.7 kb), rs2736980 (+287.8 kb), rs13131936 (+289.4 kb), rs2615490 (+296.1 kb), rs2627729 (+298.7 kb), rs2627731 (+300.2 kb), rs2627733 (+301 kb)	-4.03 (1.47E-03)
<i>IBSP</i>	dentin sialophosphoprotein	rs2627733 (-175.6 kb), rs2627731 (-176.5 kb), 4.74E-05 rs2627729 (-178 kb), rs2615490 (-180.5 kb), rs13131936 (-187.3 kb), rs2736980 (-188.8 kb), rs2627699 (-188.9 kb), rs2736979 (-189.3 kb), rs2615487 (-190.2 kb), rs1462361 (-199.3 kb),	145.49 (1.47E-03)

---

---

		rs2627689 (-201.3 kb)			
<i>IGSF11</i>	nuclear receptor subfamily 1, group I, member 2	rs72554015 (+652.6 kb),	7.37E-05	-3.79	(1.47E-03)
<i>IRS2</i>	insulin receptor substrate 2	rs7983716 (-220 kb), rs1410422 (-239.5 kb)	rs4773061 (-228.8 kb), 9.43E-05	-2.20	(1.47E-03)
<i>ITGB7</i>	single-strand-selective monofunctional uracil-DNA glycosylase 1	rs17109031 (+997.3 kb),	rs73114519 (+997.3 kb)	8.81E-05	2.81 (2.73E-03)
<i>KCNN4</i>	pregnancy specific beta-1-glycoprotein 7 (gene/pseudogene)	rs17345014 (-804.9 kb),	1.33E-06	2.85	(1.47E-03)
<i>LTB</i>	MHC class I polypeptide-related sequence A	rs114526672 (-182.8 kb),	1.51E-05	3.42	(1.47E-03)
<i>LUM</i>	chromosome 12 open reading frame 79	rs80043968 (+572.9 kb), rs117346209 (+576.2 kb), rs74359605 (+581.8 kb),	rs145430872 (+575.2 kb), rs117558304 (+581.1 kb), rs75938706 (+582.3 kb),	1.73E-05	2.84 (1.47E-03)

---

---

		rs142269906 (+583.9 kb), rs74544895 (+590.1 kb), rs140782786 (+590 kb), rs143135500 (+591.7 kb), rs191644194 (+591 kb), rs79989713 (+594.9 kb), rs75965246 (+595.1 kb), rs79006315 (+596.3 kb), rs144235028 (+598.4 kb), rs117655484 (+602.7 kb), rs78120715 (+602 kb), rs116885619 (+604.9 kb), rs76121582 (+609.5 kb), rs149715998 (+610.9 kb), rs185275685 (+611.3 kb), rs77367388 (+615.5 kb), rs75724249 (+615.7 kb), rs79913836 (+619.4 kb), rs76416906 (+619.8 kb)		
<i>PCDH1</i>	Rho GTPase activating protein 26	rs9324897 (+910.5 kb), rs9324897 (+910.5 kb)	2.62E-05	3.16 (1.47E-03)
<i>PCDH12</i>	Rho GTPase activating protein 26	rs9324897	2.62E-05	1.73 (1.47E-03)
<i>PKHD1L1</i>	potassium channel, subfamily V, member 1	rs62528148 (+843.2 kb),	6.76E-05	-3.62 (1.47E-03)

---

<i>PLAUR</i>	pregnancy specific beta-1-glycoprotein 7 (gene/pseudogene)	rs17345014 (-684.4 kb),	1.33E-06	2.45 (1.47E-03)
<i>PLEK2</i>	transmembrane protein 229B	rs57040446 (+77.87 kb), rs114651716 (+78.98 kb), rs78385101 (+86.03 kb), rs185427001 (+90.17 kb), rs117837736 (+91.36 kb), rs75234868 (+96.38 kb)	5.81E-06	2.83 (8.72E-03)
<i>PLEKHG1</i>	coiled-coil domain containing 170	rs4304175 (+759.2 kb), rs11155799 (+762.5 kb), rs6557158 (+765.1 kb), rs9371549 (+843.1 kb)	7.35E-05	1.91 (3.91E-03)
<i>PPMIH</i>	family with sequence similarity 19 (chemokine (C-C motif)-like), member A2	rs76408242 (-729.9 kb),	3.35E-05	-2.38 (1.47E-03)
<i>RFX8</i>	phosducin-like 3	rs112752332 (-768.9 kb),	1.25E-05	3.00 (4.46E-02)
<i>ROR2</i>	spleen tyrosine kinase	rs10993726 (-864.1 kb), rs12376537 (-864.8 kb), rs72729064 (-866.7 kb)	1.64E-05	2.32 (3.91E-03)

<i>RUNX2</i>	runt-related transcription factor 2	rs114193529 (0), rs144071310 (0)	5.33E-05	2.68 (1.47E-03)
<i>SCARA5</i>	adrenoceptor alpha 1A	rs117549674 (-981.4 kb),	5.11E-05	-2.05 (1.47E-03)
<i>SPP1</i>	dentin sialophosphoprotein	rs2627733 (-351.7 kb), rs2627731 (-352.6 kb), rs2627729 (-354.1 kb), rs2615490 (-356.6 kb), rs13131936 (-363.4 kb), rs2736980 (-364.9 kb), rs2736979 (-365.4 kb), rs2627699 (-365 kb), rs2615487 (-366.3 kb), rs1462361 (-375.4 kb), rs2627689 (-377.4 kb)	4.74E-05	15.39 (1.47E-03)
<i>TMEM51</i>	forkhead-associated phosphopeptide binding domain 1	rs112303425 (+98.22 kb),	6.58E-05	1.79 (1.74E-02)
<i>TRHDE</i>	thyrotropin-releasing degrading enzyme	hormone rs151310022 (+178.2 kb), rs146412572 (+326.2 kb)	1.72E-05	-2.82 (1.47E-03)
<i>TRHDE-AS1</i>	thyrotropin-releasing hormone	rs151310022 (+570.3 kb), rs146412572 (+718.3 kb)	1.72E-05	-3.18

---

	degrading enzyme		(1.87E-02)
<i>ZBPI</i>	phosphoenolpyruvate	rs6099674 (-28.38 kb), rs2865391 (-29.66 kb), 2.05E-05	2.90
	carboxykinase 1 (soluble)	rs78547178 (-45.32 kb)	(2.27E-02)

---

FC: Fold change.



**S9 Table.** Symbols and official names of genes included in **Fig. 5**.

<b>Symbol</b>	<b>Entrez Gene Name</b>
<i>ACAN</i>	Aggrecan
<i>ACE</i>	angiotensin I converting enzyme
<i>ADAM12</i>	ADAM metallopeptidase domain 12
<i>ADAM17</i>	ADAM metallopeptidase domain 17
<i>ADAMTS5</i>	ADAM metallopeptidase with thrombospondin type 1 motif, 5
<i>AGT</i>	angiotensinogen (serpin peptidase inhibitor, clade A, member 8)
<i>AGTR1</i>	angiotensin II receptor, type 1
<i>AGTR2</i>	angiotensin II receptor, type 2
<i>AHSG</i>	alpha-2-HS-glycoprotein
<i>ALPL</i>	alkaline phosphatase, liver/bone/kidney
<i>AMPD3</i>	adenosine monophosphate deaminase 3
<i>ANGPTL1</i>	angiopoietin-like 1

<i>ANGPTL2</i>	angiopoietin-like 2
<i>AOX1</i>	aldehyde oxidase 1
<i>APCDD1L</i>	adenomatosis polyposis coli down-regulated 1-like
<i>APCDD1L-AS1</i>	APCDD1L antisense RNA 1 (head to head)
<i>APOB</i>	apolipoprotein B
<i>APOBEC3B</i>	apolipoprotein B mRNA editing enzyme, catalytic polypeptide-like 3B
<i>APOC1</i>	apolipoprotein C-1
<i>APOE</i>	apolipoprotein E
<i>APOL6</i>	apolipoprotein L, 6
<i>ARL4C</i>	ADP-ribosylation factor-like 4C
<i>ARL4C</i>	ADP-ribosylation factor-like 4C
<i>BAI3</i>	brain-specific angiogenesis inhibitor 3
<i>BDKRB1</i>	bradykinin receptor B1
<i>BDKRB2</i>	bradykinin receptor B2

<i>BGLAP</i>	bone gamma-carboxyglutamate (gla) protein
<i>BGN</i>	Biglycan
<i>BMP2</i>	bone morphogenetic protein 2
<i>BMP4</i>	bone morphogenetic protein 4
<i>C8orf88</i>	chromosome 8 open reading frame 88
<i>CADM1</i>	cell adhesion molecule 1
<i>CADM2</i>	cell adhesion molecule 2
<i>CADM3</i>	cell adhesion molecule 3
<i>CCL18</i>	chemokine (C-C motif) ligand 18 (pulmonary and activation-regulated)
<i>CCL19</i>	chemokine (C-C motif) ligand 19
<i>CCL2</i>	chemokine (C-C motif) ligand 2
<i>CCL23</i>	chemokine (C-C motif) ligand 23
<i>CCL4</i>	chemokine (C-C motif) ligand 4
<i>CCL5</i>	chemokine (C-C motif) ligand 5

<i>CCL8</i>	chemokine (C-C motif) ligand 8
<i>CCR1</i>	chemokine (C-C motif) receptor 1
<i>CCR5</i>	chemokine (C-C motif) receptor 5 (gene/pseudogene)
<i>CCR7</i>	chemokine (C-C motif) receptor 7
<i>CD248</i>	CD248 molecule, endosialin
<i>CD34</i>	CD34 molecule
<i>CEACAM1</i>	carcinoembryonic antigen-related cell adhesion molecule 1 (biliary glycoprotein)
<i>CERCAM</i>	cerebral endothelial cell adhesion molecule
<i>CHI3L1</i>	chitinase 3-like 1 (cartilage glycoprotein-39)
<i>CMA1</i>	chymase 1, mast cell
<i>COL10A1</i>	collagen, type X, alpha 1
<i>COL11A1</i>	collagen, type XI, alpha 1
<i>COL12A1</i>	collagen, type XII, alpha 1

<i>COL15A1</i>	collagen, type XV, alpha 1
<i>COL18A1</i>	collagen, type XVIII, alpha 1
<i>COL1A1</i>	collagen, type I, alpha 1
<i>COL3A1</i>	collagen, type III, alpha 1
<i>COL4A1</i>	collagen, type IV, alpha 1
<i>COL4A2</i>	collagen, type IV, alpha 2
<i>COL4A3</i>	collagen, type IV, alpha 3 (Goodpasture antigen)
<i>COL4A4</i>	collagen, type IV, alpha 4
<i>COL5A1</i>	collagen, type V, alpha 1
<i>COL5A2</i>	collagen, type V, alpha 2
<i>COL6A2</i>	collagen, type VI, alpha 2
<i>COL9A3</i>	collagen, type IX, alpha 3
<i>CST3</i>	cystatin C
<i>CST7</i>	cystatin F (leukocystatin)

<i>CTGF</i>	connective tissue growth factor
<i>CTHRC1</i>	collagen triple helix repeat containing 1
<i>CTNNB1</i>	catenin (cadherin-associated protein), beta 1, 88kDa
<i>CTSB</i>	cathepsin B
<i>CTSC</i>	cathepsin C
<i>CTSD</i>	cathepsin D
<i>CTSG</i>	cathepsin G
<i>CTSK</i>	cathepsin K
<i>CTSL2</i>	cathepsin V
<i>CTSS</i>	cathepsin S
<i>CTSZ</i>	cathepsin Z
<i>CXCL1</i>	chemokine (C-X-C motif) ligand 1 (melanoma growth stimulating activity, alpha)
<i>CXCL12</i>	chemokine (C-X-C motif) ligand 12

<i>CXCL14</i>	chemokine (C-X-C motif) ligand 14
<i>CXCL16</i>	chemokine (C-X-C motif) ligand 16
<i>CXCL5</i>	chemokine (C-X-C motif) ligand 5
<i>CXCR3</i>	chemokine (C-X-C motif) receptor 3
<i>CXCR7</i>	atypical chemokine receptor 3
<i>DCN</i>	Decorin
<i>DKK2</i>	dickkopf WNT signaling pathway inhibitor 2
<i>DKK3</i>	dickkopf WNT signaling pathway inhibitor 3
<i>ELN</i>	Elastin
<i>ELOF1</i>	elongation factor 1 homolog (S. cerevisiae)
<i>EMILIN1</i>	elastin microfibril interfacier 1
<i>EMILIN3</i>	elastin microfibril interfacier 3
<i>ENG</i>	Endoglin
<i>ESR1</i>	estrogen receptor 1

<i>FGF1</i>	fibroblast growth factor 1 (acidic)
<i>FGF8</i>	fibroblast growth factor 8 (androgen-induced)
<i>FOS</i>	FBJ murine osteosarcoma viral oncogene homolog
<i>FOSB</i>	FBJ murine osteosarcoma viral oncogene homolog B
<i>FURIN</i>	furin (paired basic amino acid cleaving enzyme)
<i>FXYP1</i>	FXYP domain containing ion transport regulator 1
<i>FYB</i>	FYN binding protein
<i>GATA5</i>	GATA binding protein 5
<i>GPC5</i>	glypican 5
<i>GPR158</i>	G protein-coupled receptor 158
<i>GREM1</i>	gremlin 1, DAN family BMP antagonist
<i>GSC</i>	goosecoid homeobox
<i>GUCY1A3</i>	guanylate cyclase 1, soluble, alpha 3
<i>GUCY1B3</i>	guanylate cyclase 1, soluble, beta 3



<i>H19</i>	H19, imprinted maternally expressed transcript (non-protein coding)
<i>HBEGF</i>	heparin-binding EGF-like growth factor
<i>HEY1</i>	hes-related family bHLH transcription factor with YRPW motif 1
<i>HEY2</i>	hes-related family bHLH transcription factor with YRPW motif 2
<i>HIF3A</i>	hypoxia inducible factor 3, alpha subunit
<i>HLA-DOA</i>	major histocompatibility complex, class II, DO alpha
<i>HLA-DPB2</i>	major histocompatibility complex, class II, DP beta 2 (pseudogene)
<i>HLA-DQA1</i>	major histocompatibility complex, class II, DQ alpha 1
<i>HLA-DR</i>	major histocompatibility complex, class II, DR members
<i>HLA-DRA</i>	major histocompatibility complex, class II, DR alpha
<i>HMGCR</i>	3-hydroxy-3-methylglutaryl-CoA reductase
<i>HOXA3</i>	homeobox A3
<i>HSD17B13</i>	hydroxysteroid (17-beta) dehydrogenase 13
<i>HSPD1</i>	heat shock 60kDa protein 1 (chaperonin)

<i>HSPG2</i>	heparan sulfate proteoglycan 2
<i>HYAL1</i>	hyaluronoglucosaminidase 1
<i>IBSP</i>	integrin-binding sialoprotein
<i>ICAM1</i>	intercellular adhesion molecule 1
<i>IGSF11</i>	immunoglobulin superfamily, member 11
<i>IL10</i>	interleukin 10
<i>IL1B</i>	interleukin 1, beta
<i>IL1RN</i>	interleukin 1 receptor antagonist
<i>IL2RA</i>	interleukin 2 receptor, alpha
<i>IL2RB</i>	interleukin 2 receptor, beta
<i>IRS2</i>	insulin receptor substrate 2
<i>ITGB7</i>	integrin, beta 7
<i>JAK3</i>	Janus kinase 3
<i>KCNN4</i>	potassium intermediate/small conductance calcium-activated channel,

	subfamily N, member 4
<i>KDR</i>	kinase insert domain receptor
<i>LICAM</i>	L1 cell adhesion molecule
<i>LDLR</i>	low density lipoprotein receptor
<i>LECT1</i>	leukocyte cell derived chemotaxin 1
<i>LOXL2</i>	lysyl oxidase-like 2
<i>LPA</i>	lipoprotein, Lp(a)
<i>LRP1</i>	low density lipoprotein receptor-related protein 1
<i>LRP1B</i>	low density lipoprotein receptor-related protein 1B
<i>LRP5</i>	low density lipoprotein receptor-related protein 5
<i>LTB</i>	lymphotoxin beta (TNF superfamily, member 3)
<i>LUM</i>	Lumican
<i>MGP</i>	matrix Gla protein
<i>MGST1</i>	microsomal glutathione S-transferase 1

<i>MME</i>	membrane metallo-endopeptidase
<i>MMP1</i>	matrix metallopeptidase 1 (interstitial collagenase)
<i>MMP12</i>	matrix metallopeptidase 12 (macrophage elastase)
<i>MMP2</i>	matrix metallopeptidase 2 (gelatinase A, 72kDa gelatinase, 72kDa type IV collagenase)
<i>MMP3</i>	matrix metallopeptidase 3 (stromelysin 1, progelatinase)
<i>MMP7</i>	matrix metallopeptidase 7 (matrilysin, uterine)
<i>MMP9</i>	matrix metallopeptidase 9 (gelatinase B, 92kDa gelatinase, 92kDa type IV collagenase)
<i>MSX2</i>	msh homeobox 2
<i>NCAM1</i>	neural cell adhesion molecule 1
<i>NFATC1</i>	nuclear factor of activated T-cells, cytoplasmic, calcineurin-dependent 1
<i>NOS2</i>	nitric oxide synthase 2, inducible
<i>NOS3</i>	nitric oxide synthase 3 (endothelial cell)
<i>NOTCH1</i>	notch 1

<i>NRARP</i>	NOTCH-regulated ankyrin repeat protein
<i>PCDH1</i>	protocadherin 1
<i>PCDH12</i>	protocadherin 12
<i>PDGFB</i>	platelet-derived growth factor beta polypeptide
<i>PECAM1</i>	platelet/endothelial cell adhesion molecule 1
<i>PKHD1L1</i>	polycystic kidney and hepatic disease 1 (autosomal recessive)-like 1
<i>PLAU</i>	plasminogen activator, urokinase
<i>PLAUR</i>	plasminogen activator, urokinase receptor
<i>PLCE1</i>	phospholipase C, epsilon 1
<i>PLEK2</i>	pleckstrin 2
<i>PLEKHG1</i>	pleckstrin homology domain containing, family G (with RhoGef domain) member 1
<i>PLOD2</i>	procollagen-lysine, 2-oxoglutarate 5-dioxygenase 2
<i>PLTP</i>	phospholipid transfer protein

<i>POU1F1</i>	POU class 1 homeobox 1
<i>POU2AF1</i>	POU class 2 associating factor 1
<i>POU2F2</i>	POU class 2 homeobox 2
<i>PPARG</i>	peroxisome proliferator-activated receptor gamma
<i>PPM1H</i>	protein phosphatase, Mg <sup>2+</sup> /Mn <sup>2+</sup> dependent, 1H
<i>PROM1</i>	prominin 1
<i>RARA</i>	retinoic acid receptor, alpha
<i>RARG</i>	retinoic acid receptor, gamma
<i>RFX8</i>	RFX family member 8, lacking RFX DNA binding domain
<i>ROR2</i>	receptor tyrosine kinase-like orphan receptor 2
<i>RUNX1</i>	runt-related transcription factor 1
<i>RUNX2</i>	runt-related transcription factor 2
<i>RUNX3</i>	runt-related transcription factor 3
<i>SAMD1</i>	sterile alpha motif domain containing 1

<i>SCARA5</i>	scavenger receptor class A, member 5
<i>SELE</i>	selectin E
<i>SERPINA1</i>	serpin peptidase inhibitor, clade A (alpha-1 antiproteinase, antitrypsin), member 1
<i>SFRP1</i>	secreted frizzled-related protein 1
<i>SMAD6</i>	SMAD family member 6
<i>SMPD1</i>	sphingomyelin phosphodiesterase 1, acid lysosomal
<i>SOCS3</i>	suppressor of cytokine signaling 3
<i>SOD2</i>	superoxide dismutase 2, mitochondrial
<i>SOX9</i>	SRY (sex determining region Y)-box 9
<i>SPP1</i>	secreted phosphoprotein 1
<i>STAT4</i>	signal transducer and activator of transcription 4
<i>TGFA</i>	transforming growth factor, alpha
<i>TGFB1</i>	transforming growth factor, beta 1

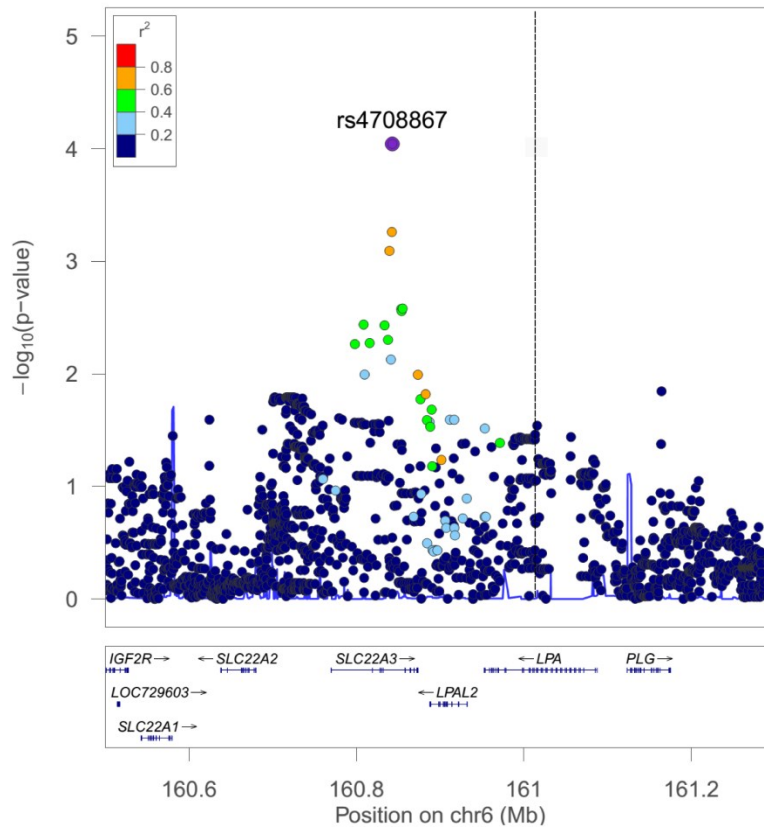
<i>TGFBR1</i>	transforming growth factor, beta receptor 1
<i>TGFBR2</i>	transforming growth factor, beta receptor II (70/80kDa)
<i>TIMP1</i>	TIMP metalloproteinase inhibitor 1
<i>TIMP2</i>	TIMP metalloproteinase inhibitor 2
<i>TIMP3</i>	TIMP metalloproteinase inhibitor 3
<i>TIMP4</i>	TIMP metalloproteinase inhibitor 4
<i>TMEM51</i>	transmembrane protein 51
<i>TNC</i>	tenascin C
<i>TNF</i>	tumor necrosis factor
<i>TNFAIP6</i>	tumor necrosis factor, alpha-induced protein 6
<i>TNFRSF11A</i>	tumor necrosis factor receptor superfamily, member 11a, NFkB activator
<i>TNFRSF11B</i>	tumor necrosis factor receptor superfamily, member 11b
<i>TNFRSF12A</i>	tumor necrosis factor receptor superfamily, member 12A



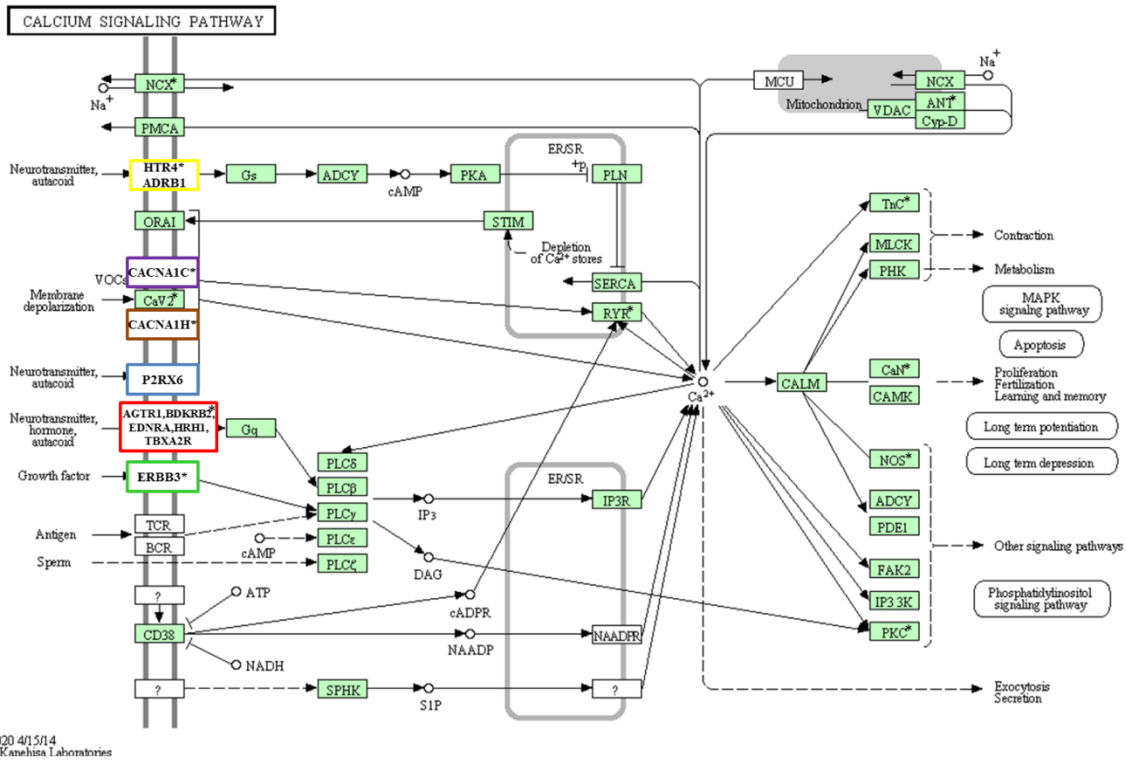
<i>TNFSF11</i>	tumor necrosis factor (ligand) superfamily, member 11
<i>TRHDE</i>	thyrotropin-releasing hormone degrading enzyme
<i>TRHDE-ASI</i>	TRHDE antisense RNA 1
<i>VCAM1</i>	vascular cell adhesion molecule 1
<i>VCAN</i>	Versican
<i>VDR</i>	vitamin D (1,25- dihydroxyvitamin D3) receptor
<i>VEGFA</i>	vascular endothelial growth factor A
<i>VWF</i>	von Willebrand factor
<i>WIF1</i>	WNT inhibitory factor 1
<i>WISP1</i>	WNT1 inducible signaling pathway protein 1
<i>WNT3</i>	wingless-type MMTV integration site family, member 3
<i>XCL2</i>	chemokine (C motif) ligand 2
<i>ZBP1</i>	Z-DNA binding protein 1

---

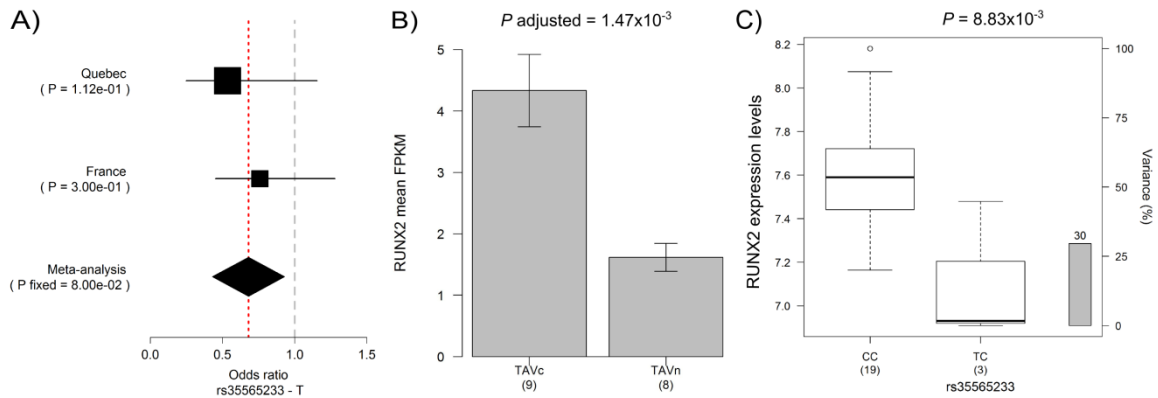
## Supplemental Figures



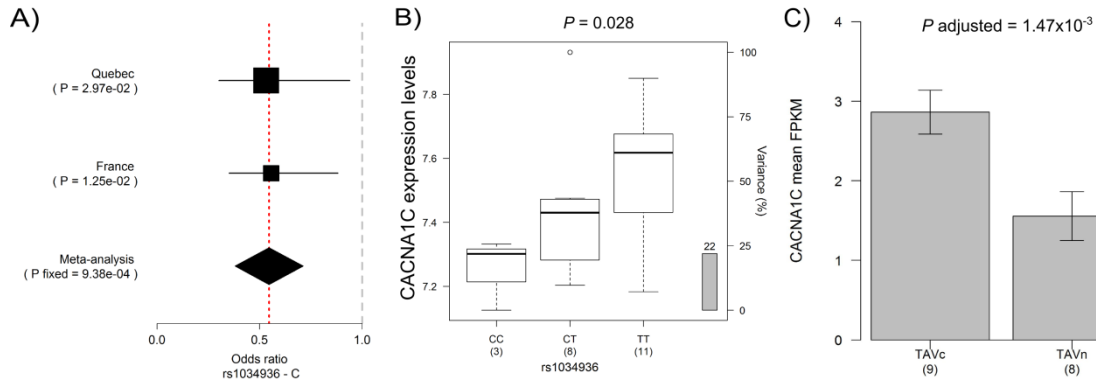
**S1 Figure.** Regional plot showing the results of the *LPA* locus in the GWAS meta-analysis. The y-axis shows the  $P$  values in  $-\log_{10}$  scale. The extent of LD ( $r^2$  values) between the most significant SNP in the region (rs4708867) and the remaining SNPs is indicated by colors. The significant SNP, rs10455872, in the study by Thanassoulis et al.[15] did not pass quality controls in the meta-analysis, but its location is indicated by a vertical dashed line. The LD ( $r^2$ ) between rs4708867 and rs10455872 is 0.045. The location of genes is shown at the bottom. SNPs are plotted based on their chromosomal position on build hg19.



**S2 Figure.** The KEGG calcium signaling pathway. The boxes in colors represent the differentially expressed genes in the RNA-Seq experiment. Yellow: *ADRB1* (adrenoceptor beta 1) and *HTR4* [5-hydroxytryptamine (serotonin) receptor 4, G protein-coupled]. Red: *AGTR1* (angiotensin II receptor, type 1), *BDKRB2* (bradykinin receptor B2), *EDNRA* (endothelin receptor type A), *HRH1* (histamine receptor H1), and *TBXA2R* (thromboxane A2 receptor). Violet: *CACNA1C* (calcium channel, voltage-dependent, L type, alpha 1C subunit). Brown: *CACNA1H* (calcium channel, voltage-dependent, T type, alpha 1H subunit). Green: *ERBB3* (v-erb-b2 avian erythroblastic leukemia viral oncogene homolog 3). Blue: *P2RX6* (purinergic receptor P2X, ligand-gated ion channel, 6). Asterisk indicates molecules in the pathway that are targets of clinical candidates or FDA approved drugs.



**S3 Figure.** A) Forest plot of overall effect size for rs35565233 in the two independent GWAS and meta-analysis. The black filled squares represent the odds ratio (OR) for each cohort, and are proportional to the study size. The horizontal lines represent the 95% confidence intervals of the OR. The dashed grey and the dotted red vertical lines represent an OR of 1.0 and the OR of the meta-analysis, respectively. B) Gene expression levels of *RUNX2* in human aortic valves measured by RNA-Seq and expressed as mean FPKM (fragments per kilobase of exon per million fragments mapped). The number of valves assessed per group is indicated in parenthesis. Error bars represent standard error. TAVn: normal tricuspid valve; TAVc: calcified tricuspid aortic valve. C) Boxplots of gene expression levels for *RUNX2* in human aortic valves according to genotyping groups for SNP rs35565233. The left y-axis presents the expression levels and the right y-axis presents the percent variance in gene expression explained by the genotype. Number of patients per genotype is presented in parenthesis.



**S4 Figure.** A) Forest plot of overall effect size for rs1034936 in the two independent GWAS and meta-analysis. The black filled squares represent the odds ratio (OR) for each cohort, and are proportional to the study size. The horizontal lines represent the 95% confidence intervals of the OR. The dashed grey and the dotted red vertical lines represent an OR of 1.0 and the OR of the meta-analysis, respectively. B) Boxplot of gene expression levels for *CACNA1C* in human aortic valves according to genotyping groups for SNP rs1034936. The left y-axis presents the expression levels and the right y-axis presents the percent variance in gene expression explained by the genotype. Number of patients per genotype is presented in parenthesis. C) Gene expression levels of *CACNA1C* in human aortic valves measured by RNA-Seq and expressed as mean FPKM (fragments per kilobase of exon per million fragments mapped). The number of valves assessed per group is indicated in parenthesis. Error bars represent the standard error. TAVn: normal tricuspid valve; TAVc: calcified tricuspid aortic valve.



## **Chapter 8. Article 3: Whole-genome expression profile of calcified bicuspid and tricuspid aortic valves from patients with severe aortic stenosis**

**Comparaison de l'expression des gènes dans des valves aortiques bicuspidales et tricuspides avec et sans calcification**

Sandra Guauque-Olarte, MSc<sup>1</sup>, Fayez Hadji<sup>1</sup>, Nathalie Gaudreault, BSc<sup>1</sup>, Philippe Pibarot, DVM, PhD<sup>1</sup>, Patrick Mathieu, MD<sup>1</sup>, Yohan Bossé, PhD<sup>1,2</sup>

1) Centre de recherche Institut universitaire de cardiologie et de pneumologie de Québec, Laval University, Quebec, Canada;

2) Department of Molecular Medicine, Laval University, Quebec, Canada.

**Short title:** Expression profile of bicuspid aortic valves

**Address all correspondence to:**

Yohan Bossé, Ph.D.

Associate Professor, Laval University

Institut universitaire de cardiologie et de pneumologie de Québec

Pavillon Marguerite-d'Youville, Y2106

2725, chemin Sainte-Foy

Québec (Québec)

Canada, G1V 4G5

Tel: 418-656-8711 ext. 3725

Fax: 418-656-4602

Email: [yohan.bosse@criucpq.ulaval.ca](mailto:yohan.bosse@criucpq.ulaval.ca)

## Résumé

**Objectif-** Le rétrécissement valvulaire aortique (RVA) est une maladie mortelle et sans traitement médical. Les symptômes du RVA apparaissent plus tôt chez les patients ayant une valve aortique bicuspide (BAV). Le but de ce projet était d'identifier les gènes différemment régulés entre les BAV et les valves tricuspides (TAV) avec et sans calcification.

**Méthodes et résultats-** Les BAV et TAV calcifiées ont été obtenues de 24 patients avec un RVA sévère. Toutes les valves présentaient le même degré de remodelage fibro-calcique. Douze valves TAV normales (contrôles) ont été obtenues de patients ayant subi une transplantation cardiaque. L'expression des gènes a été mesurée à l'aide de la plateforme de biopuce Illumina HumanHT-12v4. La normalisation et les contrôles de qualité ont été réalisés avec le logiciel R. La méthode « Significance Analysis of Microarrays » a été employée pour identifier les gènes différemment exprimés entre les trois groupes de valves (BAV, TAV, et contrôles). Les fonctions biologiques entre les gènes différemment régulés ont été identifiées avec « Ingenuity Pathway Analysis ». Deux gènes étaient exprimés à la hausse et deux étaient exprimés à la baisse dans les BAV comparativement aux TAV calcifiées. L'expression du gène *H19* était plus faible dans les contrôles par rapport aux BAV et TAV calcifiées. La comparaison BAV et contrôles a permis d'identifier 128 gènes différemment exprimés.

**Conclusion-** Les résultats montrent une grande similarité dans le profil d'expression des gènes entre les BAV et TAV calcifiées. Par contre, un gène biologiquement important, *H19*, était différemment exprimé entre les deux groupes. La calcification entraîne des changements importants au niveau du profil d'expression de plusieurs autres gènes. Les gènes identifiés nous permettent de mieux comprendre les bases moléculaires de la BAV et de trouver de nouvelles cibles thérapeutiques pour le RVA.



## **Abstract**

**Background**— Calcific aortic valve stenosis (AS) is a fatal disease with no medical treatment available. Patients with a bicuspid aortic valve (BAV) develop AS symptoms 20 years younger than patients with a tricuspid valve (TAV). The objective of this study was to identify genes differentially expressed between BAV and TAV.

**Methods and Results**— Twelve BAV and 12 TAV with calcification were explanted from white male patients who underwent aortic valve replacement surgery. The 24 valves had the same degree of fibro-calcific remodeling. Twelve non-stenotic TAV (controls) were taken from white males who underwent heart transplantation. Gene expression profiles were measured with the Illumina HumanHT-12v4 BeadChip. Gene expression levels were compared between the three groups of valves (BAV, TAV, and controls) using the Significance Analysis of Microarrays program. Pathway analysis was performed using Ingenuity Pathway Analysis. Comparing BAV and calcified TAV, 2 genes were up-regulated and 2 down-regulated in BAV. The genes differentially expressed were linked to pathways and functions related to AS including connective tissue disorders, inflammatory disease, and cell death and survival ( $P < 4.53E-2$ ). The expression of the gene *H19* [maternally imprinted transcript (non-protein coding)] was lower in controls compared to the other two tissues. Compared with controls, 128 genes were found differentially expressed in BAV.

**Conclusions**— The gene expression profiles of BAV and calcified TAV are highly similar but one biologically relevant candidate gene, *H19*, was found differentially expressed. The results of this study also increased our molecular understanding of early AS in BAV patients. Future outcomes are new therapeutic targets to prevent, slow the development or treat AS in patients with BAV.

**Key words:** Calcific aortic valve stenosis; valve stenosis; microarrays; gene expression

## Introduction

Calcific aortic valve stenosis (AS) is an age-related degenerative disease of the aortic valve that have been recently considered as an active process involving several risk factors, similar to coronary artery disease (CAD)<sup>1</sup>. AS affects 2%<sup>2</sup> and 4%<sup>3</sup> of people older than 65 and 85 years, respectively. Valve replacement surgery is the main treatment available for severe and/or symptomatic AS<sup>4</sup>. Consequently, AS is the principal cause for valvular replacement in the United States and Europe<sup>5</sup>. The disease has a mean incidence rate of 1.7% per year which increases significantly with age<sup>6</sup>. The symptoms of AS include angina, syncope, and heart failure<sup>7</sup>. Individuals who develop symptoms have a mortality rate of about 25% per year<sup>3</sup> and a 5-year risk of surgical valve replacement or clinical cardiovascular events of 80%<sup>8</sup>.

The aortic valve can be unicuspid, bicuspid (BAV), tricuspid (TAV) or quadricuspid<sup>4</sup>. 95% of individuals that undergo aortic valve replacement older than 75 years present TAV, while 75% of patients between 15 to 65 years have BAV<sup>9</sup>. Stenosis in patients with BAV progresses faster than those with TAV. In BAV patients, fibrosis and calcification starts at the second and fourth decade of life, respectively<sup>9</sup>, and 20 years earlier than in patients with a tricuspid aortic valve<sup>10</sup>.

Several histological and *in vitro* studies have identified potential pathways that contribute to AS development<sup>11-13</sup>. Specific polymorphisms in *NOTCH1* were detected in families affected with bicuspid AS<sup>14,15</sup>, in sporadic cases of bicuspid valve<sup>16</sup>, and in patients with tricuspid valve that underwent aortic valve replacement<sup>17</sup>. A recent GWAS identified lipoprotein(a) (*LPA*) as a susceptibility gene for aortic valve calcification<sup>18</sup>. Bossé *et al.*<sup>19</sup> performed a microarrays experiment to compare tricuspid valves from patients with and without AS. This latter study confirmed, refined, and comprehensively complemented prior research into the biological processes that are known to be involved in AS. The dataset also flagged two novel genes that are promising targets for the disease, namely, the matrix metalloproteinase 12 (*MMP12*) and the chitinase 3-like 1 (*CHI3LI*). The ectonucleotide pyrophosphatase/phosphodiesterase 1 (*ENPP1*) gene, also found differentially expressed in the gene expression dataset, was later demonstrated as a potential therapeutic target against AS<sup>20</sup>. So far, no study analyzed the whole genome expression profile of BAV. The objective of our study is to identify genes differentially expressed in BAV compared to calcified TAV, and normal TAV. In addition, we want to identify

220

molecular pathways among genes differentially expressed to understand the molecular processes involved in AS in the presence of bicuspid and tricuspid aortic valves.

## **Methods**

### **Ethics Statement**

A written informed consent was obtained from all participants. The study was approved by the ethics committee of the Institut universitaire de cardiologie et de pneumologie de Québec (IUCPQ).

### **Study population**

Aortic valves were explanted from 24 white male patients who underwent aortic valve replacement surgery for severe AS at the IUCPQ. Twelve samples were BAV and 12 were calcified TAV confirmed at surgery. All valves from AS patients had the same degree of fibro-calcific remodeling (Warren score of 3)<sup>21</sup>. In addition, 12 non-stenotic TAV (controls) were taken from white males who underwent heart transplantation at the IUCPQ. Control valves had no evidence of disease at post-explant examination and were explanted from patients with preoperative valve area  $> 2 \text{ cm}^2$  and no regurgitation (grade  $\leq 2$ ). The valves were collected during surgeries performed between March 2005 and May 2011. BAV, calcified TAV and control valves were match by age  $\pm 10$  years with to the controls. Exclusion criteria included smoking, type 2 diabetes, renal insufficiency (creatinine  $> 150 \text{ }\mu\text{mol/l}$ ), or ascending aorta replacement. Coronary artery disease (CAD) was considered if the patients presented a history of coronary artery bypass grafting. Doppler echocardiographic measurements were used to calculate transvalvular gradients using the modified Bernoulli equation<sup>22</sup> and the aortic valve area using the continuity equation<sup>23</sup>. Left ventricular hypertrophy was defined as left ventricular mass index  $> 115 \text{ g/m}^2$  in men and  $> 95 \text{ g/m}^2$  in women. The diagnosis of hypertension was based on a resting systolic or diastolic blood pressure  $> 140$  or  $> 90 \text{ mmHg}$ , respectively, or an actual hypertensive treatment. Dyslipidemia was defined as low-density lipoprotein cholesterol  $\geq 3 \text{ mmol/L}$  or the utilization of hypolipidemic agents. BMI was calculated as weight in kilograms divided by height in meters squared<sup>24</sup>. Waist circumference measurements were taken at the end of expiration at the level midway between the lower rib margin and the iliac crest using a measuring tape directly on the skin with the subject standing. Clinical characteristics of

patients between the three groups of valves were tested using t-tests, ANOVA, or Fisher's exact tests as appropriate. Table 1 shows the characteristics of the patients according to the three groups of valves.

### **RNA extraction**

The valves were snap-frozen in liquid nitrogen after extraction and stored in a local biobank at - 80°C until RNA isolation. RNA extraction from valve specimens was performed with 46-205 mg of tissue using a modification of a standard TRIzol protocol<sup>25</sup> followed by a purification step on QIAGEN RNeasy column (QIAGEN, Mississauga, Ontario). The RNA integrity score was obtained using the Agilent Bioanalyzer (Agilent technologies, Santa Clara, California) and ranged from 7.0 to 9.2.

### **Microarrays**

The gene expression profile of each valve was measured with the HumanHT-12 v4 Expression BeadChip (Illumina, San Diego, California), which targets 47,323 probes covering 28,688 coding transcripts with well-established annotation derived from the National Center for Biotechnology Information Reference Sequence release 38. RNA expression was measured by using the whole-genome gene expression direct hybridization assay system of Illumina, as previously described<sup>26</sup>, at the McGill University and Génome Québec Innovation Centre (<http://www.gqinnovationcenter.com>). The raw data, containing the signal values per probe, was generated using the GenomeStudio™ software. The complete data set will be deposited in the National Center for Biotechnology Information Gene Expression Omnibus repository<sup>27</sup>.

## **Microarray analysis**

The raw data was quantile normalized after log<sub>2</sub>-transformation using the lumi package in R version 2.14.1<sup>28,29</sup>. Three pairwise comparisons among the 3 tissues were performed (BAV vs. calcified TAV, BAV vs. normal TAV, and calcified vs. normal TAV). The differential expression analysis was carried-out with the Significance Analysis of Microarrays software<sup>30</sup>. The false discovery rate (FDR) and the fold change threshold were set at 5% and 2.0, respectively. The fold change was obtained by raising 2 to the power of the mean difference in expression between any two tissue compartments. Each probe was treated independently and transcripts interrogated by multiple probes were not summarized. The annotation of the significant probes to genes was performed by selecting the probe with the highest fold change to represent the gene.

## **Biological interpretation of microarrays**

Three lists of differentially expressed genes, one per pairwise comparison, were uploaded into IPA (Ingenuity Systems, [www.ingenuity.com](http://www.ingenuity.com)) to map the genes into biological pathways and functions. The lists contain all probes present in the microarrays, with their respective fold changes and the significant q-values obtained from SAM. The lists of genes were overlaid into the Ingenuity Knowledge Base to identify diseases, molecular or cellular functions, metabolic and cell signaling pathways that were enriched for genes claimed significant in the microarray experiment.

## Results

Patients with BAV present a smaller aortic valve area compared to patients with calcific TAV ( $P = 0.023$ ), which remains borderline significant after indexing for body surface ( $P = 0.056$ ). A significant higher percentage of patients with BAV (75%,  $P = 0.0003$ ) have left ventricular hypertrophy compared to 25% and 0% in patients with calcified and normal TAV, respectively.

## Microarrays

After gene expression normalization, the intrapair correlation coefficients for each set of tissues were calculated. The coefficients ranged between 0.98 and 0.99 for BAV and calcified TAV; and from 0.96 to 0.99 for TAVn (**Figure S1**). The global gene expression profiles of BAV and calcific TAV are more tightly clustered compared to normal TAV (**Figure 1**).

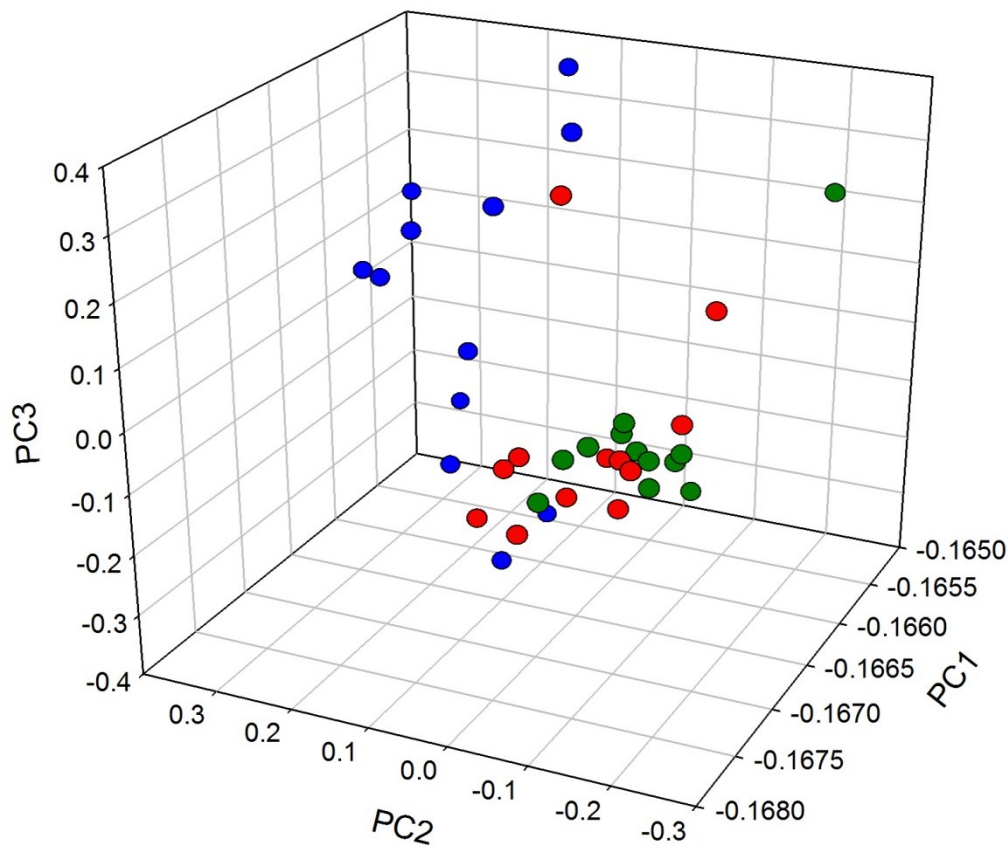


**Figure 1.** Principal components plot of the 36 aortic valves. BAV, calcific TAV, and normal TAV are shown in green, red, and blue, respectively.

Two up-regulated and two down-regulated genes were identified in the comparison BAV vs. calcific TAV (**Table 2**). The genes *H19* [imprinted maternally expressed transcript (non-protein coding)] and *CCL18* [chemokine (C-C motif) ligand 18 (pulmonary and activation-regulated)] were significantly up-regulated. The genes *FOS* (FBJ murine osteosarcoma viral oncogene homolog) and *FOSB* (FBJ murine osteosarcoma viral oncogene homolog B) were significantly down-regulated. **Table 3** indicates the biological and molecular functions of these genes, as well as the relevant IPA diseases or functions associated with them.

In the second comparison between BAV and normal TAV, 128 genes were differentially expressed. Finally, comparing calcific TAV and normal TAV 63 genes found differentially expressed (**Table 2**). **Figure 2** shows the heat maps of the top significant up- and down-regulated genes in the three pairwise comparisons.

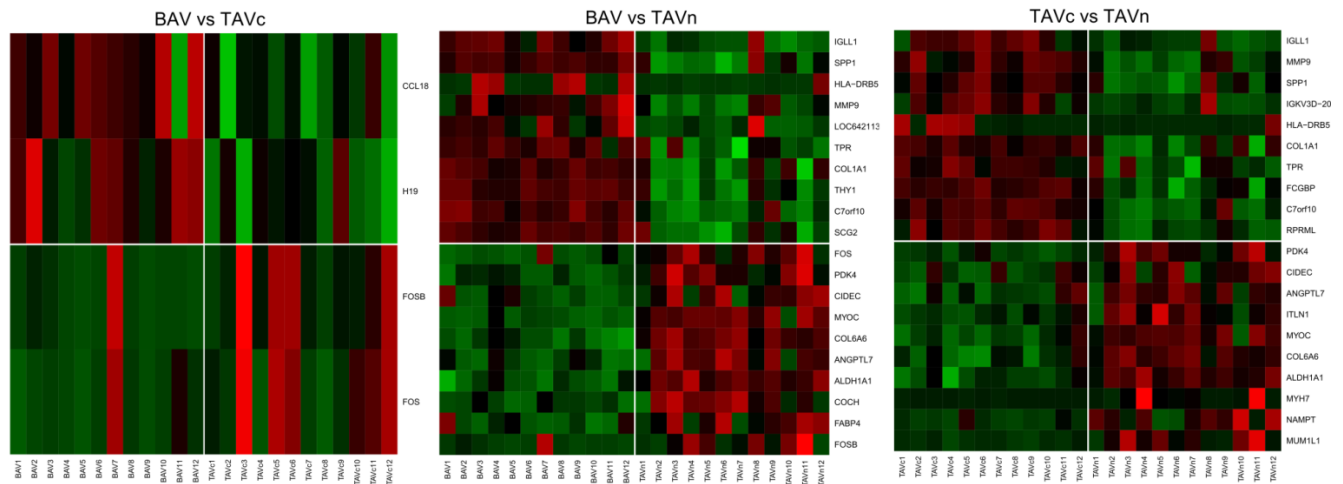


**Figure 2.** Heat maps of the top genes differentially up- and down-regulated for the three pairwise comparisons. The samples and genes are illustrated in columns and rows, respectively. Red and green represent high and low expression, respectively. These genes are described in **Table 3** and **Supplementary Tables 2** and **3**, respectively. BAV, bicuspid aortic valve; TAVc, calcific tricuspid aortic valve; TAVn, normal tricuspid aortic valve.

Among up-regulated genes, only *H19* was shared by the comparisons BAV vs. calcific TAV, and BAV vs. normal TAV. *FOS* and *FOSB* were down-regulated in BAV compared to the other two



tissues. Thirty-nine of the 42 (92.9%) up-regulated genes in calcific TAV vs. normal TAV were also up-regulated in BAV vs. normal TAV. Three up-regulated genes were not shared between the last comparisons: *FCN3* [ficolin (collagen/fibrinogen domain containing) 3], *LOC646723*, and *RGS5* [regulator of G-protein signaling 5]. Among down-regulated genes, 18 out of 21 (85.7%) genes were shared among the same two comparisons. The down-regulated genes were not in common, namely *MGST1* [microsomal glutathione S-transferase 1], *MYH7* [myosin, heavy chain 7, cardiac muscle, beta], and *MYL2* [myosin, light chain 2, regulatory, cardiac, slow] (**Figure S2**).

### **Mapping of differentially expressed genes to biological pathways**

In the comparison BAV vs. normal TAV, 71 bio-functions such as cellular growth and proliferation ( $P = 1.23E-8$ ), inflammatory disease ( $P = 1.83E-9$ ), and skeletal and muscular disorders ( $P = 2.69E-8$ ) were enriched. There were 196 enriched canonical pathways including the most significant granulocyte and agranulocyte adhesion and diapedesis, inhibition of matrix metalloproteases, and atherosclerosis signaling ( $p$  from  $2.09E-5$  to  $1.95E-4$ ). In the last comparison, calcific TAV vs. normal TAV, 74 bio-functions and 92 canonical pathways were enriched including 69 bio-functions and 84 canonical pathways enriched between BAV and normal TAV.

Additional results of IPA show that 21 and five significant genes in the BAV vs. normal TAV and calcific TAV vs. normal TAV comparisons, respectively, are targets of 47 potential drugs (IPA database from ClinicalTrials.gov) (**Supplementary Table 4**). These potential drugs act on cardiovascular disease, diabetes and cell proliferation.

## Discussion

The present study compares the whole-genome expression profile of calcified bicuspid and tricuspid aortic valves. Two genes were up-regulated (*H19* and *CCL18*) and two were down-regulated (*FOS* and *FOSB*) between the two valve morphologies. *H19* was the only transcript up-regulated in BAV compared to calcific TAV and normal TAV. *H19* is a non-coding RNA with biological functions that are just starting to be elucidated. *H19* is a maternally imprinted gene and only the copy inherited from the mother is expressed. *H19* is known to play a role in proliferation of cardiomyocytes<sup>31</sup>. Mice with a 13 kb deletion in chromosome 11 that includes *H19* had enlarged and thickened aortic and pulmonary valves<sup>31</sup>. *H19* is also known to bind *SOX9*<sup>32</sup>, which expression is regulated by *NOTCH1*. Deletion of the latter is known to cause valve malformation and calcification as well as ossification of the sternum in mice<sup>33</sup>. It is thus possible that *H19* has a role in early valve calcification observed in BAV patients through impaired *NOTCH1* signaling.

*CCL18*, *FOS*, and *FOSB* were differentially expressed in BAV valves compared to calcified and normal TAV. These three genes may be involved in AS development in BAV patients. *FOS* and *FOSB* were down-regulated in BAV compared to the other two tissues. *FOS* and *FOSB* are proteins implicated in regulation of cell proliferation, differentiation, and transformation, osteoclast differentiation and bone resorption<sup>34</sup>. The genes interact with proteins of the JUN family and act over matrix metalloproteinases to influence myocardial tissue remodeling<sup>35</sup>. *CCL18* was specifically up-regulated in BAV compared to calcific TAV, but not when compared to normal TAV. *CCL18* is a chemokine that can induce collagen deposition by fibroblast and has been involved in pulmonary fibrosis<sup>36</sup>. It is possible that fibrosis in BAV stenosis is induced through different mediators than in TAV.

The genes not shared between the comparison BAV vs. normal TAV and calcific TAV vs. normal TAV may also be specific to BAV or BAV-associated AS. The up-regulated genes *FCN3* and *RGS5* are involved in heart failure<sup>37</sup>, cardiac remodeling and fibrosis<sup>38</sup>. Although we observed higher mRNA of *FCN3* in stenotic valves, low levels of ficolin 3 protein in plasma was associated with advanced heart failure and possible action of the complement system<sup>37</sup>. More

studies are needed to clarify the role of *FCN3* in AS. The down-regulated genes *MGST1*, *MYH7*, and *MYL2* are part of the calcium signaling and cardiac hypertrophy canonical pathways.

Fifteen out of 21 down-regulated genes in the comparison calcific TAV vs. normal TAV were also up-regulated in our previous whole-genome gene expression study<sup>19</sup>. Similarly, 26 out of the 42 up-regulated genes were observed in our previous study. In addition, the orientation of effect was consistent for all genes. This level of concordance is interesting knowing that we have used different microarray platforms (Illumina BeadChips in this study vs. Affymetrix arrays in our previous study).

A large number of genes differentially expressed in calcified and normal aortic valves are targets for drug development. *In vitro* and *in vivo* studies of genes targeted by these chemicals are needed to identify drugs that may slow progression or reverse aortic valve stenosis.

The genes *BMP2*, *BMP6*, *MMP9*, *NOTCH1*, *RANKL/TNFSF11*, *RUNX2*, *SPPI/OPN*, and *TNFRSF11B/OPG* that are known to play a role in AS pathology<sup>39</sup> were not differentially expressed in BAV vs. calcific TAV. Additionally, only the genes *SPPI* and *TNFRSF11B* were significantly up-regulated in calcified BAV and TAV compared to normal aortic valves. These results are similar to the results of Bossé et al. where only *MMP9* and *SPPI* were significantly up-regulated in calcific TAV vs. normal TAV. It should be noted that we did not measure levels of the proteins coded by these genes. Our results indicate that the key genes implicated in the disease, especially in BAV, have not been discovered. Here we present novel candidate genes.

In the principal component analysis, the BAV and calcific TAV samples were tightly clustered compared to normal valves. All calcified aortic valves were selected to have the same degree of fibro-calcification remodeling in order to identify significant differences in gene expression due to the presence of AS and not because of morphological changes that occurs with disease severity. Normal aortic valves were visually inspected by a surgeon and a pathologist and matched with each stenotic valve. The age of individuals recruited in this study ranges from 46

to 67 years (mean  $\pm$  SD =  $58.5 \pm 5.5$ ). This may cause heterogeneity in valve composition due to the positive correlation observed between age and valve degeneration.

This study shows that, the transcriptome of BAV and calcified TAV are highly similar. However, some biologically relevant candidate genes were found differentially expressed. The results of this study also increased our molecular understanding of early AS in BAV patients. Future outcomes are new therapeutic targets to prevent, slow the development or treat AS in patients with BAV.

## **Acknowledgments**

The authors would like to thank the research team at the biobank of the Institut universitaire de cardiologie et de pneumologie de Québec for their valuable assistance. This study was supported by the Canadian Institutes of Health Research grants MOP 102481 (Y.B.) and MOP 79342 (P.P. and P.M.). This study was also funded by grants from the Heart and Stroke Foundation of Canada and the “Fondation de l’Institut universitaire de cardiologie et de pneumologie de Québec”. Y. Bossé is the recipient of a Junior 2 Research Scholar award from the Fonds de recherche Québec – Santé (FRQS). P. Mathieu is a research scholar from the FRQS. P. Pibarot holds the Canada Research Chair in Valvular Heart Diseases. S. Guauque-Olarte was a recipient of a studentship from the International Chair on Cardiometabolic Risk and she is now recipient of a doctoral scholarship from the “Centre de recherche Institut universitaire de cardiologie et de pneumologie de Québec”.

## References

1. Du X, Soon JL. Mild to moderate aortic stenosis and coronary bypass surgery. *J Cardiol.* 2011;57:31-35
2. Roger VL, Go AS, Lloyd-Jones DM, Adams RJ, Berry JD, Brown TM, Carnethon MR, Dai S, de Simone G, Ford ES, Fox CS, Fullerton HJ, Gillespie C, Greenlund KJ, Hailpern SM, Heit JA, Ho PM, Howard VJ, Kissela BM, Kittner SJ, Lackland DT, Lichtman JH, Lisabeth LD, Makuc DM, Marcus GM, Marelli A, Matchar DB, McDermott MM, Meigs JB, Moy CS, Mozaffarian D, Mussolino ME, Nichol G, Paynter NP, Rosamond WD, Sorlie PD, Stafford RS, Turan TN, Turner MB, Wong ND, Wylie-Rosett J. Heart disease and stroke statistics--2011 update: A report from the american heart association. *Circulation.* 2011;123:e18-e209
3. Carabello BA, Paulus WJ. Aortic stenosis. *Lancet.* 2009;373:956-966
4. Otto CM, Bonow RO. *Valvular heart disease: A companion to braunwald's heart disease.*: SAUNDERS Elsevier; 2009.
5. Salas MJ, Santana O, Escolar E, Lamas GA. Medical therapy for calcific aortic stenosis. *J Cardiovasc Pharmacol Ther.* 2012;17:133-138
6. Owens DS, Katz R, Takasu J, Kronmal R, Budoff MJ, O'Brien KD. Incidence and progression of aortic valve calcium in the multi-ethnic study of atherosclerosis (mesa). *Am J Cardiol.* 2010;105:701-708
7. Freeman RV, Otto CM. Spectrum of calcific aortic valve disease: Pathogenesis, disease progression, and treatment strategies. *Circulation.* 2005;111:3316-3326
8. Katz R, Budoff MJ, Takasu J, Shavelle DM, Bertoni A, Blumenthal RS, Ouyang P, Wong ND, O'Brien KD. Relationship of metabolic syndrome with incident aortic valve calcium and aortic valve calcium progression: The multi-ethnic study of atherosclerosis (mesa). *Diabetes.* 2009;58:813-819
9. Waller B, Howard J, Fess S. Pathology of aortic valve stenosis and pure aortic regurgitation. A clinical morphologic assessment--part i. *Clin Cardiol.* 1994;17:85-92
10. Waller BF, Howard J, Fess S. Pathology of aortic valve stenosis and pure aortic regurgitation: A clinical morphologic assessment--part ii. *Clin Cardiol.* 1994;17:150-156

11. Otto CM, Kuusisto J, Reichenbach DD, Gown AM, O'Brien KD. Characterization of the early lesion of 'degenerative' valvular aortic stenosis. Histological and immunohistochemical studies. *Circulation*. 1994;90:844-853
12. Mohty D, Pibarot P, Despres JP, Cote C, Arsenault B, Cartier A, Cosnay P, Couture C, Mathieu P. Association between plasma ldl particle size, valvular accumulation of oxidized ldl, and inflammation in patients with aortic stenosis. *Arterioscler Thromb Vasc Biol*. 2008;28:187-193
13. Akat K, Borggreffe M, Kaden JJ. Aortic valve calcification: Basic science to clinical practice. *Heart*. 2009;95:616-623
14. Garg V, Muth AN, Ransom JF, Schluterman MK, Barnes R, King IN, Grossfeld PD, Srivastava D. Mutations in notch1 cause aortic valve disease. *Nature*. 2005;437:270-274
15. Foffa I, Ait Ali L, Panesi P, Mariani M, Festa P, Botto N, Vecoli C, Andreassi MG. Sequencing of notch1, gata5, tgfr1 and tgfr2 genes in familial cases of bicuspid aortic valve. *BMC Med Genet*. 2013;14:44
16. Mohamed SA, Aherrahrou Z, Liptau H, Erasmi AW, Hagemann C, Wrobel S, Borzym K, Schunkert H, Sievers HH, Erdmann J. Novel missense mutations (p.T596m and p.P1797h) in notch1 in patients with bicuspid aortic valve. *Biochem Biophys Res Commun*. 2006;345:1460-1465
17. Ducharme V, Guauque-Olarte S, Gaudreault N, Pibarot P, Mathieu P, Bosse Y. Notch1 genetic variants in patients with tricuspid calcific aortic valve stenosis. *J Heart Valve Dis*. 2013;22:142-149
18. Thanassoulis G, Campbell CY, Owens DS, Smith JG, Smith AV, Peloso GM, Kerr KF, Pechlivanis S, Budoff MJ, Harris TB, Malhotra R, O'Brien KD, Kamstrup PR, Nordestgaard BG, Tybjaerg-Hansen A, Allison MA, Aspelund T, Criqui MH, Heckbert SR, Hwang SJ, Liu Y, Sjogren M, van der Pals J, Kalsch H, Muhleisen TW, Nothen MM, Cupples LA, Caslake M, Di Angelantonio E, Danesh J, Rotter JJ, Sigurdsson S, Wong Q, Erbel R, Kathiresan S, Melander O, Gudnason V, O'Donnell CJ, Post WS. Genetic associations with valvular calcification and aortic stenosis. *N Engl J Med*. 2013;368:503-512
19. Bosse Y, Miqdad A, Fournier D, Pepin A, Pibarot P, Mathieu P. Refining molecular pathways leading to calcific aortic valve stenosis by studying gene expression profile of normal and calcified stenotic human aortic valves. *Circ Cardiovasc Genet*. 2009;2:489-498

20. Cote N, El Husseini D, Pepin A, Guauque-Olarte S, Ducharme V, Bouchard-Cannon P, Audet A, Fournier D, Gaudreault N, Derbali H, McKee MD, Simard C, Despres JP, Pibarot P, Bosse Y, Mathieu P. Atp acts as a survival signal and prevents the mineralization of aortic valve. *J Mol Cell Cardiol.* 2012;52:1191-1202
21. Warren BA, Yong JL. Calcification of the aortic valve: Its progression and grading. *Pathology.* 1997;29:360-368
22. Baumgartner H, Hung J, Bermejo J, Chambers JB, Evangelista A, Griffin BP, Iung B, Otto CM, Pellikka PA, Quinones M. Echocardiographic assessment of valve stenosis: Eae/ase recommendations for clinical practice. *Eur J Echocardiogr.* 2009;10:1-25
23. Quinones MA, Otto CM, Stoddard M, Waggoner A, Zoghbi WA. Recommendations for quantification of doppler echocardiography: A report from the doppler quantification task force of the nomenclature and standards committee of the american society of echocardiography. *J Am Soc Echocardiogr.* 2002;15:167-184
24. Canoy D. Coronary heart disease and body fat distribution. *Curr Atheroscler Rep.* 2010;12:125-133
25. Lee JTY, Tsang WH, Chow KL. Simple modifications to standard trizol® protocol allow high-yield rna extraction from cells on resorbable materials. *Journal of biomaterials and nanobiotechnology. J Biomater Nanobiotechnol.* 2011;2:41-48
26. Guauque-Olarte S, Gaudreault N, Piche ME, Fournier D, Mauriege P, Mathieu P, Bosse Y. The transcriptome of human epicardial, mediastinal and subcutaneous adipose tissues in men with coronary artery disease. *PLoS One.* 2011;6:e19908
27. Edgar R, Domrachev M, Lash AE. Gene expression omnibus: Ncbi gene expression and hybridization array data repository. *Nucleic Acids Res.* 2002;30:207-210
28. Bolstad BM, Irizarry RA, Astrand M, Speed TP. A comparison of normalization methods for high density oligonucleotide array data based on variance and bias. *Bioinformatics.* 2003;19:185-193
29. Du P, Kibbe WA, Lin SM. Lumi: A pipeline for processing illumina microarray. *Bioinformatics.* 2008;24:1547-1548



30. Tusher VG, Tibshirani R, Chu G. Significance analysis of microarrays applied to the ionizing radiation response. *Proc Natl Acad Sci U S A*. 2001;98:5116-5121
31. Eggenschwiler J, Ludwig T, Fisher P, Leighton PA, Tilghman SM, Efstratiadis A. Mouse mutant embryos overexpressing igf-ii exhibit phenotypic features of the beckwith-wiedemann and simpson-golabi-behmel syndromes. *Genes Dev*. 1997;11:3128-3142
32. Wang G, Lunardi A, Zhang J, Chen Z, Ala U, Webster KA, Tay Y, Gonzalez-Billalabeitia E, Egia A, Shaffer DR, Carver B, Liu XS, Taulli R, Kuo WP, Nardella C, Signoretti S, Cordon-Cardo C, Gerald WL, Pandolfi PP. *Zbtb7a* suppresses prostate cancer through repression of a sox9-dependent pathway for cellular senescence bypass and tumor invasion. *Nat Genet*. 2013;45:739-746
33. Acharya A, Hans CP, Koenig SN, Nichols HA, Galindo CL, Garner HR, Merrill WH, Hinton RB, Garg V. Inhibitory role of *notch1* in calcific aortic valve disease. *PLoS One*. 2011;6:e27743
34. Kim WS, Kim HJ, Lee ZH, Lee Y, Kim HH. Apolipoprotein e inhibits osteoclast differentiation via regulation of *c-fos*, *nfatc1* and *nf-kappab*. *Exp Cell Res*. 2013;319:436-446
35. Windak R, Muller J, Felley A, Akhmedov A, Wagner EF, Pedrazzini T, Sumara G, Ricci R. The ap-1 transcription factor *c-jun* prevents stress-imposed maladaptive remodeling of the heart. *PLoS One*. 2013;8:e73294
36. Otto CM. Calcific aortic valve disease: Outflow obstruction is the end stage of a systemic disease process. *Eur Heart J*. 2009;30:1940-1942
37. Prohaszka Z, Munthe-Fog L, Ueland T, Gombos T, Yndestad A, Forhecz Z, Skjoedt MO, Pozsonyi Z, Gustavsen A, Janoskuti L, Karadi I, Gullestad L, Dahl CP, Askevold ET, Fust G, Aukrust P, Mollnes TE, Garred P. Association of *ficolin-3* with severity and outcome of chronic heart failure. *PLoS One*. 2013;8:e60976
38. Li H, He C, Feng J, Zhang Y, Tang Q, Bian Z, Bai X, Zhou H, Jiang H, Heximer SP, Qin M, Huang H, Liu PP, Huang C. Regulator of g protein signaling 5 protects against cardiac hypertrophy and fibrosis during biomechanical stress of pressure overload. *Proc Natl Acad Sci U S A*. 2010;107:13818-13823
39. Dweck MR, Boon NA, Newby DE. Calcific aortic stenosis: A disease of the valve and the myocardium. *J Am Coll Cardiol*. 2012;60:1854-1863

40. Grotenhuis HB, Ottenkamp J, Westenberg JJ, Bax JJ, Kroft LJ, de Roos A. Reduced aortic elasticity and dilatation are associated with aortic regurgitation and left ventricular hypertrophy in nonstenotic bicuspid aortic valve patients. *J Am Coll Cardiol.* 2007;49:1660-1665

## Tables and figures

**Table 1.** Clinical characteristics of the patients according to the three groups of aortic valves.

Characteristics	Bicuspid AS (n = 12)	Tricuspid AS (n = 12)	Normal (n = 12)	P
Age (years)	62.3 ± 6.9	64.0 ± 4.8	58.5 ± 5.5	0.073
Gender (% male)	100	100	100	1.000
Weight (kg)	81.7 ± 18.4	89.4 ± 15.5	84.8 ± 13.8	0.496
Body surface area (m <sup>2</sup> )	1.9 ± 0.2	2.0 ± 0.2	2.0 ± 0.2	0.264
Waist circumference (cm)	98.7 ± 12.5 [2]	108.1 ± 13.2 [3]	103.3 ± 11.4 [9]	0.127
Body mass index (kg/m <sup>2</sup> )	28.2 ± 5.5	29.3 ± 5.4	27.7 ± 3.7	0.706
Aortic valve area (cm <sup>2</sup> )	0.7 ± 0.1	0.8 ± 0.2	NA	0.023
Indexed aortic valve area (cm <sup>2</sup> /m <sup>2</sup> )	0.3 ± 0.1	0.4 ± 0.1	NA	0.056
Mean gradient (mmHg)	47.1 ± 20.9	37.7 ± 18.7	NA	0.272
History of CAD	2 [6]	4 [5]	2 [6]	0.611
Left ventricular hypertrophy	9	3	0	0.0003

---

Hypertension	6	9	3	0.061
Dyslipidemia	9	12	8	0.124

---

The number of missing values is shown in squared brackets. AS: calcific aortic valve stenosis. CAD: coronary artery disease. Continuous variables are expressed as mean  $\pm$  SD and tested using one-way ANOVA or t-test as appropriate. Dichotomous variables are expressed as percentage (n) and tested using Fisher's exact tests.

**Table 2.** Number of genes differentially up- and down-regulated in each pairwise comparison.

	<b>BAV vs. calcific TAV</b>		<b>BAV vs. normal TAV</b>		<b>Calcific TAV vs. normal TAV</b>	
	<b>Probes</b>	<b>Genes</b>	<b>Probes</b>	<b>Genes</b>	<b>Probes</b>	<b>Genes</b>
Up-regulated	2	2	89	80	48	42
Down-regulated	2	2	51	48	22	21
Total	4	4	140	128	70	63

**Table 3.** Genes differentially expressed in bicuspid compared to calcific tricuspid valves (Fold change  $\geq 2$ ).

Symbol	Gene name	Fold change	FDR	Biological function	Molecular function	IPA associated disease or function
H19	Imprinted maternally expressed transcript (non-protein coding)	2.13	0	Unknown	Putative tumor suppressor activity	Ossification of sternum; proliferation of cardiomyocytes, proliferation of muscle cells
CCL18	Chemokine (C-C motif) ligand 18 (pulmonary and activation-regulated)	2.09	0	Immune response; cell surface receptor linked signal transduction; cell-cell signaling; signal transduction; cell-cell signaling; response to stimulus	Receptor binding	Inflammatory reaction
FOS	FBJ murine osteosarcoma viral oncogene homolog B	-2.78	0	Immune system process; cell cycle; nucleobase, nucleoside, nucleotide and nucleic acid metabolic process; cell motion; cell cycle; mesoderm development; skeletal system development; response to stress; cellular defense response	DNA binding; transcription factor activity	Inflammatory reaction; Muscle cell proliferation, macrophage apoptosis; mineral density  Femur, osteopetrosis, coronary heart disease, atherosclerosis

---

FOSB	FBJ murine osteosarcoma viral -2.38 oncogene homolog	0	Immune system process; cell DNA binding; cycle; nucleobase, nucleoside, nucleotide and nucleic acid metabolic process; cell motion; cell cycle; mesoderm development; skeletal system development; response to stress; cellular defense response	Osteosclerosis, atherosclerosis
------	---	---	---	---------------------------------

---

FDR: False discovery rate.

## Supplementary material

**Supplementary Table 1.** Description of the top differentially expressed genes comparing BAV and normal TAV.

Gene Name	Entrez Gene Name	Location	Type(s)	Fold Change	q-value
IGLL1	Immunoglobulin lambda-like polypeptide 1	Plasma membrane	Other	9.50	0
SPP1	Secreted phosphoprotein 1	Extracellular space	Cytokine	6.32	0
HLA-DRB5	Major histocompatibility complex, class II, DR beta 5	Plasma Membrane	Transmembrane receptor	4.67	0.56
MMP9	Matrix metalloproteinase 9 (gelatinase B, 92kda gelatinase, 92kda type IV collagenase)	Extracellular Space	Peptidase	4.03	0



IGKV3D-20	immunoglobulin kappa variable 3D-20	Extracellular Space	Other	3.66	0
TPR	Translocated promoter region, nuclear basket protein	Nucleus	Transporter	3.59	0
COL1A1	Collagen, type I, alpha 1	Extracellular Space	Other	3.49	0
THY1	Thy-1 cell surface antigen	Plasma Membrane	Other	3.35	0
C7orf10	Chromosome 7 open reading frame 10	Cytoplasm	Other	3.29	0
SCG2	Secretogranin II	Extracellular Space	Cytokine	3.23	0
FOSB	FBJ murine osteosarcoma viral oncogene homolog B	Nucleus	Transcription regulator	-2.64	0.57
FABP4	Fatty acid binding protein 4, adipocyte	Cytoplasm	Transporter	-2.73	0

COCH	Cochlin	Extracellular space	Other	-2.80	0
ALDH1A1	Aldehyde dehydrogenase 1 family, member A1	Cytoplasm	Enzyme	-2.97	0
ANGPTL7	Angiopoietin-like 7	Extracellular space	Other	-3.00	0
COL6A6	Collagen, type VI, alpha 6	Extracellular Space	Other	-3.08	0
MYOC	Myocilin, trabecular meshwork inducible glucocorticoid response	Cytoplasm	Other	-3.22	0
CIDEA	Cell death-inducing DFFA-like effector c	Cytoplasm	Other	-3.39	0
PDK4	Pyruvate dehydrogenase kinase, isozyme 4	Cytoplasm	Kinase	-4.04	0
FOS	FBJ murine osteosarcoma viral oncogene homolog	Nucleus	Transcription	-4.27	0

regulator

---

**Supplementary Table 2.** Description of the top 10 differentially expressed genes comparing calcific TAV and normal TAV.

<b>Symbol</b>	<b>Entrez Gene Name</b>	<b>Location</b>	<b>Type(s)</b>	<b>Fold Change</b>	<b>q-value</b>
ALDH1A1	Aldehyde dehydrogenase 1 family, member A1	Cytoplasm	Enzyme	-2.35	0
COL6A6	Collagen, type VI, alpha 6	Extracellular Space	Other	-2.29	0
MYOC	Myocilin, trabecular meshwork inducible glucocorticoid response	Cytoplasm	Other	-2.42	0
MUM1L1	Melanoma associated antigen (mutated) 1-like 1	Other	Other	-2.20	0
NAMPT	Nicotinamide phosphoribosyltransferase	Extracellular Space	Cytokine	-2.23	0

PDK4	Pyruvate dehydrogenase kinase, isozyme 4	Cytoplasm	Kinase	-3.63	0
ITLN1	Intelectin 1 (galactofuranose binding)	Plasma Membrane	Other	-2.56	0
ANGPTL7	Angiopoietin-like 7	Extracellular Space	Other	-2.57	0
CIDEC	Cell death-inducing DFFA-like effector c	Cytoplasm	Other	-2.59	1.30
MYH7	Myosin, heavy chain 7, cardiac muscle, beta	Cytoplasm	Enzyme	-2.33	1.30
C7orf10	Chromosome 7 open reading frame 10	Cytoplasm	Other	2.85	0
COL1A1	Collagen, type I, alpha 1	Extracellular Space	Other	3.00	0
FCGBP	Fc fragment of IgG binding protein	Extracellular Space	Other	2.86	0
HLA-DRB5	Major histocompatibility complex, class II, DR beta 5	Plasma Membrane	Transmembrane	3.05	2.40

receptor

IGKV3D-20	Immunoglobulin kappa variable 3D-20	Extracellular Space	Other	4.37	0
IGLL1	Immunoglobulin lambda-like polypeptide 1	Plasma Membrane	Other	8.23	0
MMP9	Matrix metalloproteinase 9 (gelatinase B, 92kda gelatinase, 92kda type IV collagenase)	Extracellular Space	Peptidase	5.72	0
RPRML	Reprimo-like	Other	Other	2.78	0
SPP1	Secreted phosphoprotein 1	Extracellular Space	Cytokine	4.87	0
TPR	Translocated promoter region, nuclear basket protein	Nucleus	Transporter	2.87	0

---

**Supplementary Table 4.** Differentially expressed genes that are targets for known drug (IPA database from ClinicalTrials.gov).

BAV vs. TAVn				
Symbol	Entrez Name	Gene	Location	Drug(s)
ADH1A	alcohol dehydrogenase 1A (class I), alpha polypeptide		Cytoplasm	Fomepizole, ethanol
ADH1C	alcohol dehydrogenase 1C (class I), gamma polypeptide		Cytoplasm	Fomepizole, ethanol
ALDH1A1	aldehyde dehydrogenase 1 family,		Cytoplasm	Disulfiram, chlorpropamide

---

member A1

ATP1A2	ATPase, Na <sup>+</sup> /K <sup>+</sup> transporting, alpha 2 polypeptide	Plasma Membrane	Digoxin, omeprazole, ethacrynic acid, perphenazine
CD52	CD52 molecule	Plasma Membrane	Alemtuzumab
COL1A1	collagen, type I, alpha 1	Extracellular Space	Collagenase <i>Clostridium histolyticum</i>
COL1A2	collagen, type I, alpha 2	Extracellular Space	Collagenase <i>Clostridium histolyticum</i>
COL3A1	collagen, type III, alpha 1	Extracellular Space	Collagenase <i>Clostridium histolyticum</i>
COL4A3	collagen, type IV, alpha 3 (Goodpasture	Extracellular Space	Collagenase <i>Clostridium histolyticum</i>



---

antigen)

COL5A2	collagen, type V, alpha 2	Extracellular Space	Collagenase <i>Clostridium histolyticum</i>
COL6A2	collagen, type VI, alpha 2	Extracellular Space	Collagenase <i>Clostridium histolyticum</i>
COL8A1	collagen, type VIII, alpha 1	Extracellular Space	Collagenase <i>Clostridium histolyticum</i>
COL11A1	collagen, type XI, alpha 1	Extracellular Space	Collagenase <i>Clostridium histolyticum</i>
HMOX1	heme oxygenase (decycling) 1	Cytoplasm	Tin mesoporphyrin
IL7R	interleukin 7 receptor	Plasma Membrane	Recombinant human interleukin-7
LTB4R	leukotriene B4 receptor	Plasma Membrane	Etalocib

---

HLA-DRB1	major histocompatibility complex, class II, DR beta 1	Plasma Membrane	Apolizumab
MMP12	matrix metalloproteinase 12 (macrophage elastase)	Extracellular Space	Marimastat
PLA2G2A	phospholipase A2, group IIA (platelets, synovial fluid)	Cytoplasm	Varespladib methyl, varespladib, indomethacin
SERPINE1	serpin peptidase inhibitor, clade E (nexin, plasminogen activator inhibitor type 1), member 1	Extracellular Space	Drotrecogin alfa

---

TUBB3	tubulin, beta 3 class III	Cytoplasm	Epothilone B, ixabepilone, colchicine/probenecid, XRP9881, ABT-751, eribulin, MST-997, AL 108, EC145, NPI-2358, milataxel, TPI 287, TTI-237, brentuximab vedotin, cabazitaxel, gemcitabine/paclitaxel, docetaxel/prednisone, paclitaxel/trastuzumab, capecitabine/ixabepilone, BMS-275183, docetaxel, vinflunine, vinorelbine, vincristine, vinblastine, paclitaxel, podophyllotoxin, colchicine
-------	---------------------------	-----------	--

---

**Calcific TAV vs. normal TAV**

Symbol	Entrez Gene Name	Location	Drug(s)
ALDH1A1	aldehyde dehydrogenase 1 family, member A1	Cytoplasm	Disulfiram, chlorpropamide
COL1A1	collagen, type I, alpha 1	Extracellular Space	Collagenase <i>Clostridium histolyticum</i>
COL1A2	collagen, type I, alpha 2	Extracellular Space	Collagenase <i>Clostridium histolyticum</i>
COL8A1	collagen, type	Extracellular	Collagenase <i>Clostridium histolyticum</i>

---

VIII, alpha 1      Space

HLA-DRB1      major              Plasma              Apolizumab  
                  histocompatibili      Membrane  
                  ty      complex,  
                  class II, DR beta  
                  1

---

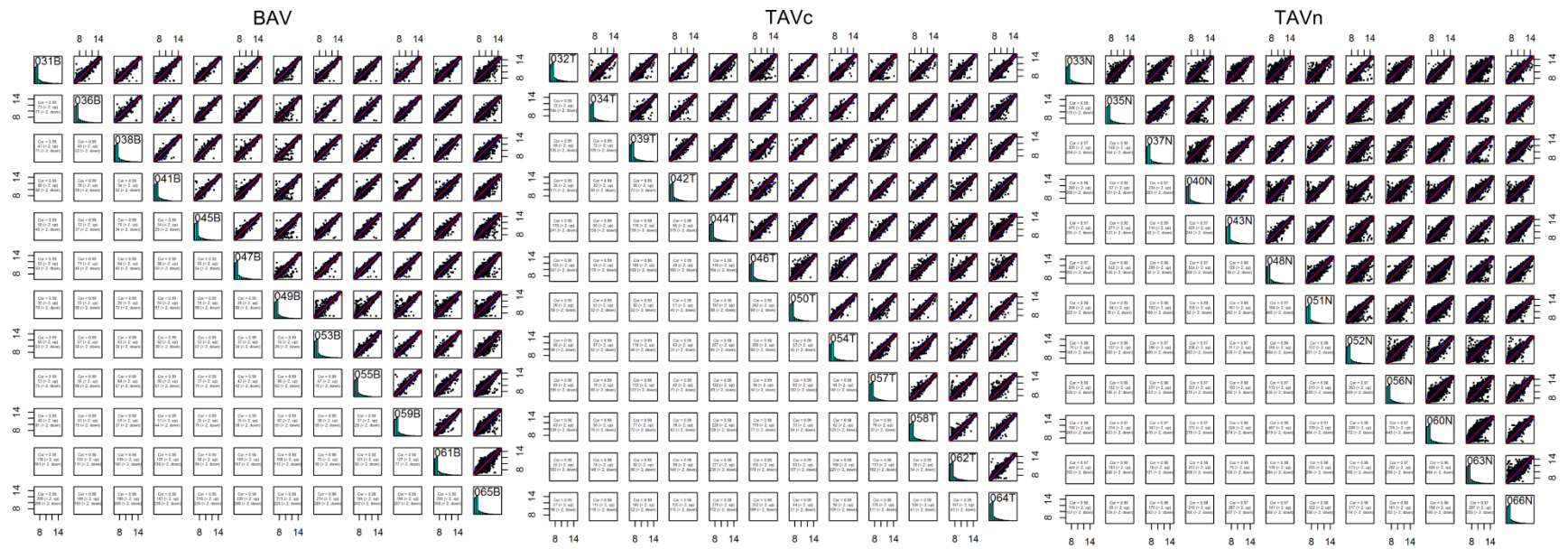


**Figure S1.** Intrapair correlation plots among samples of the same valve group.

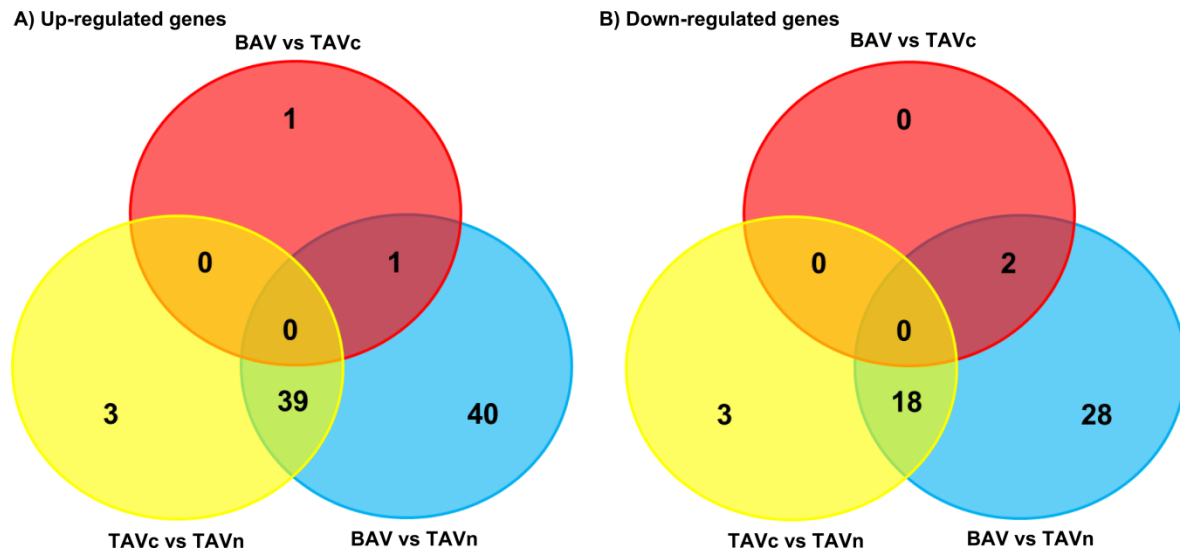


**Figure S2.** Venn diagrams showing the number of genes A) up-regulated and B) down-regulated in the three pairwise comparisons.

## **Chapter 9. Article 4: RNA expression profile of calcified bicuspid, tricuspid and normal human aortic valves by RNA sequencing**

**Séquençage d'ARN pour comparer l'expression des gènes dans des valves aortiques bicuspidales et tricuspides avec et sans calcification**

S. Guauque-Olarte<sup>1</sup>, A. Droit<sup>2</sup>, Joël Tremblay-Marchand<sup>1</sup>, N. Gaudreault<sup>1</sup>, J.G. Seidman<sup>3</sup>, S.C. Body<sup>3</sup>, P. Pibarot<sup>1</sup>, P. Mathieu<sup>1</sup>, Y. Bossé<sup>1,4</sup>.

- 1) Centre de recherche Institut universitaire de cardiologie et de pneumologie de Québec, Laval University, Quebec, Canada;
- 2) Centre de Recherche du CHU de Québec, Laval University, Quebec, Canada;
- 3) Harvard Medical School, Boston, Massachusetts, USA;
- 4) Department of Molecular Medicine, Laval University, Quebec, Canada

**Short title:** RNA sequencing on aortic valve stenosis

**Address correspondence to:**

Yohan Bossé, Ph.D.  
Associate Professor, Laval University  
Institut universitaire de cardiologie et de pneumologie de Québec  
Pavillon Marguerite-d'Youville, Y2106  
2725, chemin Sainte-Foy  
Québec (Québec)  
Canada, G1V 4G5  
Tel: 418-656-8711 ext. 3725  
Fax: 418-656-4602  
Email: yohan.bosse@criucpq.ulaval.ca

## Résumé

**Objectif-** Les mécanismes moléculaires impliqués dans le développement prématuré du rétrécissement valvulaire aortique (RVA) chez des individus avec une valve aortique bicuspidie (BAV) restent inconnus. Le but de cette étude était d'identifier les gènes différemment exprimés entre les BAV et les valves tricuspides avec (TAVc) et sans calcification (TAVn) par la méthode de séquençage d'ARN à haut débit.

**Méthodes et résultats-** Dix BAV calcifiées et neuf TAVc ont été obtenues de patients avec un RVA sévère. Toutes les valves présentaient le même degré de remodelage fibro-calcique. Dix valves TAVn ont été obtenues de patients ayant subi une transplantation cardiaque. L'expression des gènes a été mesurée avec le système de séquençage de nouvelle génération Illumina HiSeq 2000. L'alignement des séquences a été réalisé avec TopHat. Les outils Cufflinks, DESeq, edgeR, et SAMSeq ont été utilisés pour identifier les gènes différemment exprimés entre les trois groupes de valves, i.e. BAV, TAVc, et TAVn. L'outil bio-informatique «Ingenuity Pathway Analysis» a été utilisé afin d'identifier les principales fonctions biologiques des gènes différemment exprimés. Deux gènes étaient exprimés à la hausse et aucun n'était exprimé à la baisse dans les BAV comparativement aux TAVc. Par rapport aux TAVn, 462 gènes étaient exprimés à la hausse et 282 à la baisse dans les BAV. Un total de 329 et 170 gènes étaient exprimés à la hausse et à la baisse, respectivement, pour la comparaison entre les TAVc et les TAVn.

**Conclusion-** Les valves bicuspidies calcifiées présentent un profil d'expression similaire à celui des valves tricuspides calcifiées. L'analyse des gènes différemment exprimés nous permet de mieux comprendre les bases moléculaires de la BAV et de la calcification associée, et ainsi d'identifier de nouvelles cibles thérapeutiques pour le RVA.



## **Abstract**

**Objective-** The molecular mechanisms leading to premature development of aortic valve stenosis (AS) in individuals with a bicuspid aortic valve (BAV) are unknown. The objective of this study was to identify genes differentially expressed between calcified BAV and tricuspid valves with (TAVc) and without (TAVn) calcification using RNA sequencing (RNA-Seq).

**Methods and Results-** Ten human calcified BAV and nine TAVc were collected from men who underwent aortic valve replacement at the IUCPQ. Ten TAVn were obtained from men who underwent heart transplantation. mRNA levels were measured using the Illumina HiSeq 2000 system. Reads were aligned with TopHat. Cuffdiff, DESeq, edgeR, and SAMSeq were used to compare gene expression between valves. Genes with adjusted  $P < 0.05$  in the four methods were called differentially expressed. Pathway analysis was performed with IPA. Two genes were up-regulated and none were down-regulated in BAV compared to TAVc. There were 462 up-regulated and 282 down-regulated genes in BAV compared to TAVn. Compared to TAVn, 329 genes were up- and 170 were down-regulated in TAVc.

**Conclusion-** This is the first transcriptome study on calcified and normal aortic valves using RNA-Seq. BAV and TAVc have a highly similar expression profile. These results contribute to the identification of new therapeutic targets that may prevent, slow the development or treat AS in patients with bicuspid and tricuspid valves.

**Key words:** Calcific aortic valve disease, RNA sequencing, RNA-Seq, RNA expression.

## Introduction

Calcific aortic valve stenosis (AS) is an age-related degenerative disease of the aortic valve, impairing the blood flow between the left ventricle and aorta<sup>1,2</sup>. 2%<sup>3</sup> and 4%<sup>4</sup> of individuals of European descent older than 65 and 85 years are afflicted with AS, respectively. Surgical and transcatheter valve replacement are the only clinical treatments available for severe and/or symptomatic AS<sup>5</sup>. No therapeutic treatment exists<sup>6</sup>. The symptoms of AS include angina, syncope, and heart failure<sup>7</sup>. Individuals who develop symptoms have a mortality rate of about 25% per year<sup>4</sup> and a 5-year risk of surgical valve replacement or clinical cardiovascular event of 80%<sup>8</sup>. The aortic valve can be unicuspid, bicuspid (BAV), tricuspid (TAV) or quadricuspid<sup>5</sup>. BAV is the most common congenital valvular heart disease affecting 0.4 to 2.25% of adults, with the best single estimate at 1.37%<sup>9</sup>. 95% of individuals older than 75 years who developed AS present a TAV<sup>10</sup> while 75% of patients who underwent aortic valve replacement between 15 to 65 years present a BAV. In general, 49% of severe AS patients requiring surgery have BAV<sup>11</sup>. In BAV patients, fibrosis begins during the second decade of life and calcification at the fourth decade<sup>10</sup>, while valve replacement is required 5 to 10 years earlier than patients with tricuspid AS<sup>7</sup>.

Histological and *in vitro* studies have identified potential pathways that contribute to AS development<sup>12-14</sup>. Specific polymorphisms in *NOTCH1* were detected in families affected with bicuspid AS<sup>15,16</sup>. A microarray experiment comparing tricuspid valves from patients with AS and controls<sup>17</sup> identified nearly 1,000 genes differentially expressed between calcified and normal aortic valves, including genes involved in bone formation and calcium regulation, several matrix metalloproteinases, chemokines, and collagen genes. The molecular mechanisms leading to the premature development of AS in BAV individuals are still unknown. RNA sequencing (RNA-Seq), a potential successor to microarrays for the study of the transcriptome<sup>18</sup>, could provide insights into these mechanisms. The objective of this study was to identify genes differentially expressed between calcified BAV and tricuspid valves with (TAVc) or without (TAVn) calcification using RNA-Seq. In addition, we aimed to identify molecular pathways linking differentially expressed genes in order to understand the molecular processes involved in AS in the presence of bicuspid and tricuspid aortic valves. This is the first transcriptome study on calcified and normal aortic valves using RNA-Seq. We demonstrated that BAV and TAVc have

a highly similar expression profile and that several AS relevant pathways were enriched in differentially expressed genes. These results contribute to the search of new therapeutic targets that may prevent or slow the development of AS or treat it.

## **Methods**

### **Ethics Statement**

A written informed consent was obtained from all participants. The study was approved by the ethics committee of the Institut universitaire de cardiologie et de pneumologie de Québec (IUCPQ).

### **Study population**

Thirty men were included in this study. Ten BAV and ten TAV cases presented severe calcific aortic valve stenosis with a fibro-calcific remodeling score of 3<sup>19</sup>. Ten individuals undergoing heart replacement surgery without evidence of aortic valve disease were selected as controls. Patients were recruited at the IUCPQ during surgeries performed between March 2005 and May 2011. The patients were matched by age  $\pm$  10 years with respect to the controls. Only non-smoker individuals without type 2 diabetes, renal insufficiency (creatinine > 150  $\mu$ mol/l) or ascending aorta replacement were considered. Coronary artery disease (CAD) was defined as patients presenting a history of coronary artery bypass grafting, myocardial infarction, documented myocardial ischemia or coronary artery stenosis on coronary angiography. The mean transvalvular gradient was calculated using the modified Bernoulli equation<sup>20</sup> and the aortic valve area with the continuity equation<sup>21</sup>, both based on Doppler echocardiographic measurements. Left ventricular hypertrophy (LVH) was diagnosed by electrocardiography or electrocardiogram and was defined as a left ventricular mass index > 115 g/m<sup>2</sup> in men and > 95 g/m<sup>2</sup> in women. Body surface area was obtained using the Dubois & Dubois formula<sup>22</sup>. Body mass index (BMI) was calculated as weight (kg)/height<sup>2</sup>(m<sup>2</sup>). Waist circumference measurements were collected on standing subjects at the end of expiration, midway between the lower rib margin and the iliac crest using a measuring tape directly on the skin. Blood pressure was evaluated in a sitting position using a mercury sphygmomanometer. Hypertension was defined as blood pressure above 140/90 mmHg or the use of anti-hypertensive medication. Hypercholesterolemia was defined as total plasma cholesterol levels > 6.2 mmol/l or the use of cholesterol lowering medication. Diabetes was defined as fasting glucose  $\geq$  7 mmol/l or the use

of oral hypoglycemic or insulin medication. Clinical characteristics of patients were compared using t-tests, ANOVA or Fisher's exact tests as appropriate. **Table 1** describes the patient characteristics according to the three groups of valves.

### **Tissue description and RNA extraction**

Valve leaflets were snap-frozen in liquid nitrogen after surgical extraction and stored in a local biobank at -80°C until RNA isolation. RNA extraction was performed using 45 to 100 mg and 82 to 192 mg of tissue from one leaflet of normal and calcified valves, respectively, under a modified TRIzol protocol<sup>23</sup> followed by a purification step on QIAGEN RNeasy columns (QIAGEN, Mississauga, Ontario). The RNA integrity score ranged from 7.0 to 9.2 and was obtained using the Agilent Bioanalyzer (Agilent technologies, Santa Clara, California).

### **RNA sequencing**

Polyadenylated (coding pre and mature) RNAs were selected using oligodT beads (Dynabeads mRNA DIRECT kit, Invitrogen) to isolate the mRNA from the rRNA and tRNA. mRNA was fragmented into small pieces using divalent cations under elevated temperature. cDNA synthesis was carried out using the SuperScript III cDNA synthesis kit (Invitrogen) which contains random hexamers. cDNA ends were repaired using the End-It DNA End-Repair kit (Epicentre Biotechnologies). dATPs were added to the end of cDNAs using Roche dATP and Klenow DNA polymerase [Klenow Fragment (3' to 5' exo-), New England Biolabs]. Adapters were ligated to the cDNA to prepare hybridization in a single read flow cell (Quick Ligation kit, New England BioLabs). cDNA fragments of 150-300 bases were selected using a PippinPrep (Sage Science) followed by manual gel extraction and purification using Qiagen PCR columns. Phusion High-Fidelity DNA Polymerase (New England Biolabs) was used to amplify the cDNA library. Size, purity, and concentration of the libraries were verified using the Agilent TapeStation. One calcified tricuspid valve sample failed library preparation and was discarded. cDNA libraries were clustered using the Illumina cBOT automated clonal cluster generator and occurred within Illumina flow cells. 50 bp length paired-end sequencing was performed starting

with 2 ug of cDNA in an Illumina HiSeq 2000 sequencing system. Sequencing runs were set up based on the HiSeq 2000 user guide using Illumina TruSeq Reagents.

The quality of the fastq data was verified using FastQC version 0.11.2 ([www.bioinformatics.babraham.ac.uk/projects/fastqc](http://www.bioinformatics.babraham.ac.uk/projects/fastqc)). TopHat<sup>24</sup> was used to align reads of each sample to the UCSC Hg19 reference using these parameters: -r150 -mate-std-dev 100. Cufflinks was used to assemble reads and estimate their abundances. Transcriptomes were quantified and gene expression levels were compared between calcified and normal valves with Cuffdiff<sup>24</sup>. Genes with FPKM < 1 in more than 80% of the samples were excluded. In addition, HTSeq<sup>25</sup> was used to count reads aligned by TopHat. Genes with counts per million < 1 in more than 80% of the samples were excluded. Three other softwares were used to examine differential expression of count data between groups of valves: DESeq<sup>26</sup> version 1.16.0, edgeR<sup>27</sup> version 3.6.8, and SAMSeq version 4.01. The functions nbinomTest in DESeq and exactTest in edgeR were applied. Multidimensional scaling (MDS) plots generated with cummeRbund and edgeR identified two outliers in the normal valve group which were excluded from further analysis. Genes with adjusted  $P < 0.05$  using the four softwares were considered as differentially expressed. The RNA-Seq data have been deposited in NCBI Gene Expression Omnibus<sup>28</sup> (accession number GSE55492).

### **Mapping of genes to biological pathways**

IPA was used to integrate differentially expressed genes in biological processes as described before<sup>29</sup>. Pathways with Benjamini and Hochberg corrected  $P$  values lower than 0.05 were called significant. **Figure 1** summarizes the analysis pipeline followed for RNA-Seq analysis.

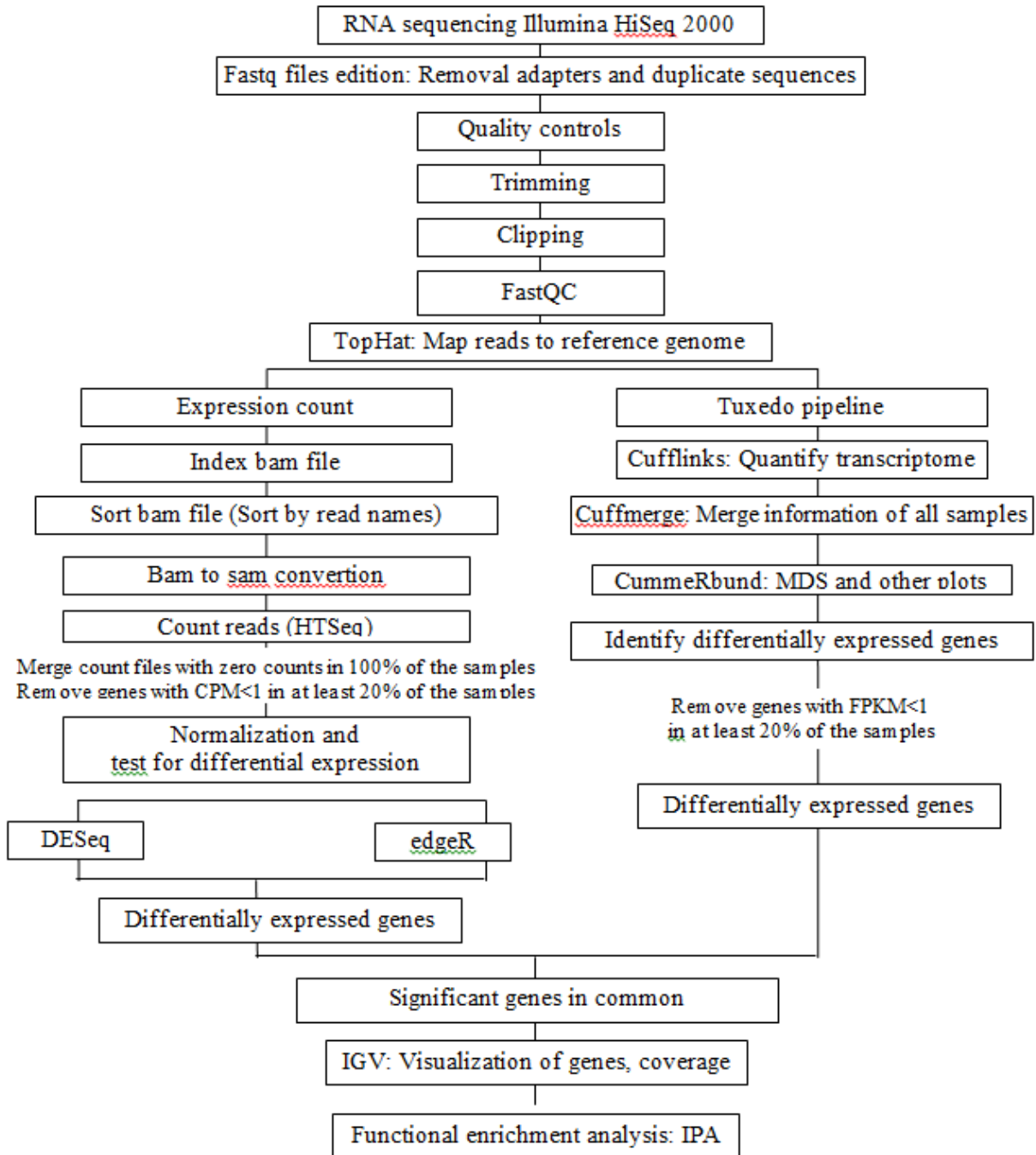


**Figure 1.** Summary of the RNA sequencing pipeline. CMP: counts per million. MDS: Multidimensional scaling. FPKM: fragments per kilobase of transcript per million mapped reads. IGV: Integrative Genomics Viewer. IPA: Ingenuity Pathway Analysis.

## Results

**Supplemental Figure 1** presents the multidimensional scaling (MDS) plot for the comparison between TAVc and TAVn. One TAVn sample was outside the two main clusters for calcified and normal valves. One TAVn sample clustered within the TAVc group. These two TAVn samples were discarded.

### Differential expression and pathway analysis

Four tools, Cuffdiff, DESeq, EdgeR, and SAMSeq, were used to identify differentially expressed genes in three pairwise comparisons between BAV, TAVc, and TAVn. The number of transcripts available for differential expression analysis after quality controls is shown in **Supplemental Table 1**. The number of differentially expressed genes in common for the four tools is shown in **Table 2** and **Figure 2**. The number of differentially expressed genes per bioinformatic tool is shown in **Supplemental Table 2**. Volcano plots based on the results of cuffdiff are shown in **Figure 3**. Three heat maps showing the top up- and down-regulated genes per comparison are shown in **Figure 4**.

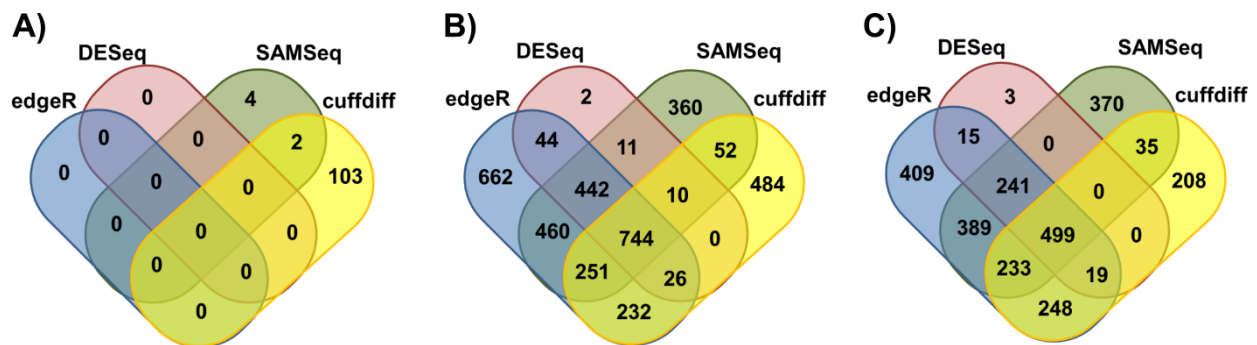


**Figure 2.** Venn diagrams showing the number of genes differentially expressed in common among cuffdiff, DESeq, edgeR, and SAMSeq. A) BAV vs. TAVc. B) BAV vs. TAVn. C) TAVc vs. TAVn.



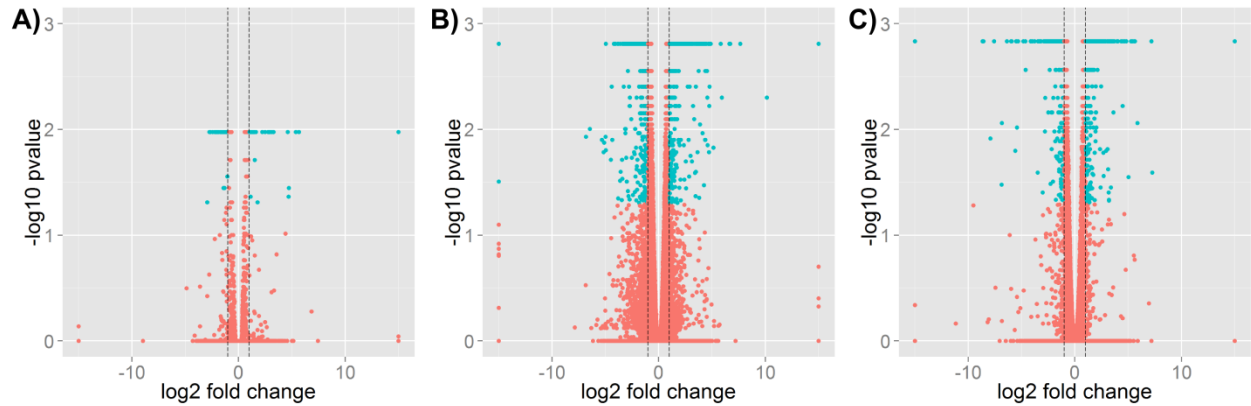


**Figure 3.** Volcano plots of the three pairwise comparisons based on the results of cuffdiff. A) BAV vs. TAVc, B) BAV vs. TAVn, and C) TAVc vs. TAVn. The x axis is the log<sub>2</sub> fold change between groups. The -log<sub>10</sub>(p-value) is plotted on the y axis. Each point represents a gene. Only genes that passed quality controls were plotted. Vertical dashed lines at -log<sub>2</sub> fold changes of -1 and 1 are plotted. Blue points indicate significant genes with q-values (*P* corrected for multiple testing) < 0.05 and absolute fold change > 2.

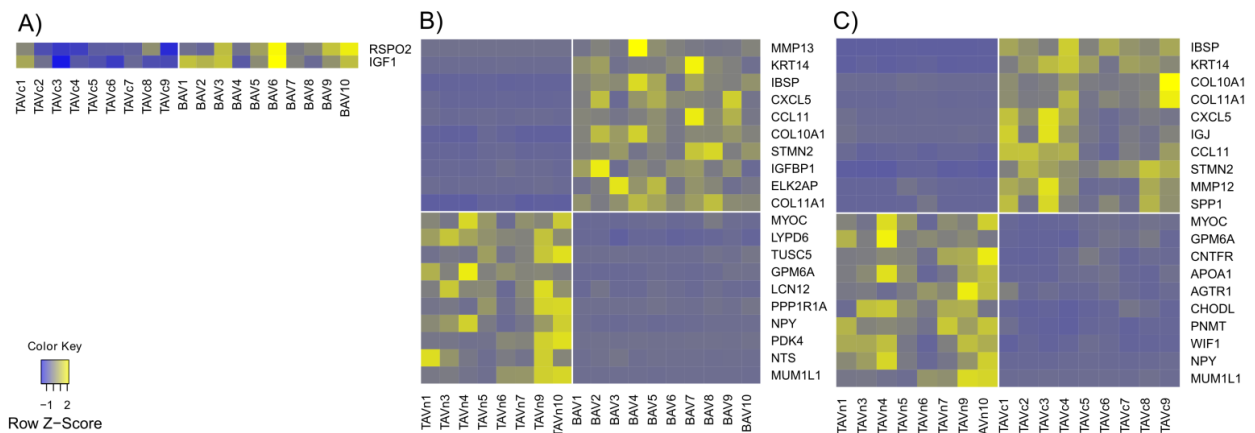


**Figure 4.** Heat maps presenting the gene expression of the top 10 up- and down-regulated annotated genes for each pairwise comparison. Yellow and blue indicate a high and low level of expression, respectively. The vertical white line separates the valve groups.

Two genes were up-regulated and none were down-regulated in BAV compared to TAVc. The up-regulated genes are *IGF1* [insulin-like growth factor 1 (somatomedin C)] and *RSPO2* (R-spondin 2) with fold changes of 1.64 (q-value = 0.11) and 2.03 (q-value = 0.011), respectively (**Table 3**).

In BAV, 462 genes were up-regulated and 282 were down-regulated when compared to TAVn; 516 genes had fold changes higher than 2.0 (**Table 2**). The smallest absolute fold change was 1.45. The top up-regulated genes (q-value  $\leq$  0.016) included *MMP13* [matrix metalloproteinase 13 (collagenase 3)], *KRT14* (keratin 14), *IBSP* (integrin-binding sialoprotein) and the chemokines *CXCL5* (chemokine (C-X-C motif) ligand 5) and *CCL11* (chemokine (C-C motif) ligand 11). The top down-regulated genes (q-value  $\leq$  0.004) included *MUMILI1* [melanoma associated antigen (mutated) 1-like 1], *PPP1RIA* [(protein phosphatase 1, regulatory (inhibitor) subunit 1A)], and *NPY* (neuropeptide Y) (**Table 3**). Among these up- and down-regulated genes, 50 (6.7%) are transcription regulators including *RUNX2* (runt-related transcription factor 2) and *VDR* [vitamin D (1,25- dihydroxyvitamin D3] receptor), 49 (6.6%) are transmembrane receptors, 31 (4.2%) are kinases such as *JAK3* (Janus kinase 3), and 13 (1.75%) are cytokines such as *SPPI* (secreted phosphoprotein 1, osteopontin) (**Supplemental Table 3**).

Thirty-one canonical pathways were significantly enriched in genes differentially expressed between BAV vs. TAVn. Pathways contained 4 to 37 differentially expressed genes. **Table 4** presents the top 10 enriched pathways for this comparison and pathways relevant to AS are highlighted. Other AS relevant pathways not in the top are inhibition of matrix metalloproteases ( $P = 0.034$ ) and cAMP-mediated signaling ( $P = 0.032$ ) pathways.

In the last pairwise comparison, 329 and 170 genes were up- and down-regulated in TAVc when compared to TAVn, respectively. 366 genes had absolute fold changes higher than 2.0 (**Table 2**). The minimum absolute fold change was 1.53. The top up-regulated genes (q-value  $<$  0.028) included *IBSP*, *KRT14* and *CXCL5*. The top down-regulated gene (q-value  $<$  0.005) was *MUMILI1*. Other top down-regulated genes were *WIF1* (WNT inhibitory factor 1) and *PNMT* (phenylethanolamine N-methyltransferase) (**Table 3**). Among differentially expressed genes, 32 (6.4%) are transcription regulators including *RUNX2* and *VDR*, 34 (6.8%) are transmembrane

receptors, 17 (3.4%) are kinases such as *JAK3*, 14 (2.8%) are ion channels such as *CACNA1C* (calcium channel, voltage-dependent, L type, alpha 1C subunit), and 9 (1.8%) are cytokines such as *SPPI* (secreted phosphoprotein 1, osteopontin) (**Supplemental Table 3**).

For the comparison of TAVc and TAVn, 28 canonical pathways were significantly enriched. The top 10 pathways are presented in **Table 5**. The significant pathways contained 3 to 27 differentially expressed genes. Twenty pathways, including the top five, were in common with the BAV vs. TAVn comparison. Genes in these common pathways are important to understand the process of valve calcification independently of valve configuration. Canonical pathways enriched only in the TAVc vs. TAVn comparison included atherosclerosis signaling ( $P = 0.035$ ), VDR/RXR activation ( $P = 0.035$ ), and the role of JAK1 and JAK3 in  $\gamma$ c cytokine signaling ( $P = 0.047$ ) pathways. These findings indicate a more important role of calcium and phosphorus in TAV patients with AS.

The canonical pathway hepatic fibrosis/hepatic stellate cell activation was enriched in the comparisons BAV vs. TAVn and TAVc vs. TAVn. Hepatic fibrosis is characterized by an accumulation of extracellular matrix (ECM) proteins in the liver (**Supplemental Figure 2**). The entire list of significant pathways in these comparisons is show in **Supplemental Table 4**.

In the comparison of BAV vs. TAVn, 85 differentially genes are targets of existing drugs (**Supplemental Table 5**). In the comparison TAVc vs. TAVn, 77 differentially expressed genes are targets of drugs (**Supplemental Table 6**) (IPA database from ClinicalTrials.gov).

## Discussion

We present the first RNA-Seq experiment comparing calcified bicuspid and tricuspid valves with normal aortic valves. Two genes were differentially expressed in BAV compared to TAVc. Higher differences in gene expression were found between the BAV and TAVc groups with respect to the normal group. This indicates that aortic stenosis in individuals with bicuspid and tricuspid valves alter gene expression in a similar way. Increased shear stress in BAV patients may help to initiate the process of calcification earlier<sup>30</sup>. However, two genes enriched in inflammatory response and apoptosis pathways were differentially expressed in BAV compared to TAVc. This finding can be important because inflammation is one of the first stages in AS development processes<sup>17</sup>.

The osteopontin coding gene and *RUNX2* were up-regulated in BAV and TAVc compared to TAVn. *RUNX2*, the master osteogenic regulator for which expression is mediated by *NOTCH1*<sup>31</sup>, regulates the expression of osteopontin. Upregulation of both osteopontin and Runx2 proteins have been observed in calcified valves<sup>15</sup>. Circulating and valve tissue levels of *RUNX2* significantly correlated with valve stenosis severity<sup>32</sup>. In our recent GWAS study, two SNPs, rs114193529 and rs144071310, in *RUNX2* were associated with AS. Furthermore, the mRNA expression of *RUNX2* measured by RNA-Seq was associated with three valve eQTL-SNPs. Those results support the importance of *RUNX2* in AS development in BAV and TAVc.

The hepatic fibrosis canonical pathway was enriched in significant genes from two pairwise comparisons. This pathway shares several biological processes and molecules that have been implicated with AS. Hepatic fibrosis is characterized by endothelial dysfunction, inflammation, neovascularization, and accumulation of ECM proteins that degrade collagen<sup>33</sup>. Those processes lead to fibrosis and liver cirrhosis. Causative agents include excess of hepatotoxins such as ethanol, bile acids, glucose, and free fatty acids. The analysis of this pathway may lead to the identification of the best candidate genes of biomarkers for treating AS.

This study has limitations. Patients were matched by aged (+/- 10 years). However, after removing outliers, there was a significant difference in age between BAV and TAVc groups

compared to the normal group. This could cause heterogeneity in valve composition due to the positive correlation observed between age and valve degeneration. Normal aortic valves were visually inspected by a surgeon and a pathologist. All calcified valves had degree 3 of fibrocalcific remodeling. This limits the effects on differential gene expression caused by the stage of valve calcification and/or age. The mRNA levels of the significant genes in this study must be confirmed by qPCR. Finally, it is important to mention that the protein levels of significant genes were not measured.

This is the first transcriptome study on calcified and normal aortic valves using RNA-Seq. The expression profile of BAV and TAVc is highly similar but two genes were up-regulated in BAV. Functional studies of these genes are important to reveal the mechanisms involved in BAV calcification. These results contribute to the identification of new therapeutic targets which could prevent, slow the development of, or treat AS in TAV and BAV patients.

## **Acknowledgments**

The authors would like to thank the research team at the biobank of the Institut universitaire de cardiologie et de pneumologie de Québec for their valuable assistance. This study was supported by the Canadian Institutes of Health Research grants MOP 102481 (Y.B.) and MOP 79342 (P.P. and P.M.). This study was also funded by grants from the Heart and Stroke Foundation of Canada and the “Fondation de l’Institut universitaire de cardiologie et de pneumologie de Québec”. Y. Bossé is the recipient of a Junior 2 Research Scholar award from the Fonds de recherche Québec – Santé (FRQS). P. Mathieu is a research scholar from the FRQS. P. Pibarot holds the Canada Research Chair in Valvular Heart Diseases. S. Guauque-Olarte was a recipient of a studentship from the International Chair on Cardiometabolic Risk and she is now recipient of a doctoral scholarship from the “Centre de recherche Institut universitaire de cardiologie et de pneumologie de Québec”.

## References

1. Du X, Soon JL. Mild to moderate aortic stenosis and coronary bypass surgery. *J. Cardiol.* 2011;57:31-35
2. Balachandran K, Sucusky P, Yoganathan AP. Hemodynamics and mechanobiology of aortic valve inflammation and calcification. *Int J Inflam.* 2011;2011:263870
3. Roger VL, Go AS, Lloyd-Jones DM, Adams RJ, Berry JD, Brown TM, Carnethon MR, Dai S, de Simone G, Ford ES, Fox CS, Fullerton HJ, Gillespie C, Greenlund KJ, Hailpern SM, Heit JA, Ho PM, Howard VJ, Kissela BM, Kittner SJ, Lackland DT, Lichtman JH, Lisabeth LD, Makuc DM, Marcus GM, Marelli A, Matchar DB, McDermott MM, Meigs JB, Moy CS, Mozaffarian D, Mussolino ME, Nichol G, Paynter NP, Rosamond WD, Sorlie PD, Stafford RS, Turan TN, Turner MB, Wong ND, Wylie-Rosett J. Heart disease and stroke statistics--2011 update: A report from the american heart association. *Circulation.* 2011;123:e18-e209
4. Carabello BA, Paulus WJ. Aortic stenosis. *Lancet.* 2009;373:956-966
5. Otto CM, Bonow RO. *Valvular heart disease: A companion to braunwald's heart disease.*: SAUNDERS Elsevier; 2009.
6. Mathieu P, Boulanger MC, Bouchareb R. Molecular biology of calcific aortic valve disease: Towards new pharmacological therapies. *Expert Rev Cardiovasc Ther.* 2014;12:851-862
7. Freeman RV, Otto CM. Spectrum of calcific aortic valve disease: Pathogenesis, disease progression, and treatment strategies. *Circulation.* 2005;111:3316-3326
8. Otto CM, Burwash IG, Legget ME, Munt BI, Fujioka M, Healy NL, Kraft CD, Miyake-Hull CY, Schwaegler RG. Prospective study of asymptomatic valvular aortic stenosis. Clinical, echocardiographic, and exercise predictors of outcome. *Circulation.* 1997;95:2262-2270
9. Hoffman JI, Kaplan S. The incidence of congenital heart disease. *J Am Coll Cardiol.* 2002;39:1890-1900
10. Waller B, Howard J, Fess S. Pathology of aortic valve stenosis and pure aortic regurgitation. A clinical morphologic assessment--part i. *Clin. Cardiol.* 1994;17:85-92

11. Roberts WC, Ko JM. Frequency by decades of unicuspid, bicuspid, and tricuspid aortic valves in adults having isolated aortic valve replacement for aortic stenosis, with or without associated aortic regurgitation. *Circulation*. 2005;111:920-925
12. Otto CM, Kuusisto J, Reichenbach DD, Gown AM, O'Brien KD. Characterization of the early lesion of 'degenerative' valvular aortic stenosis. Histological and immunohistochemical studies. *Circulation*. 1994;90:844-853
13. Mohty D, Pibarot P, Despres JP, Cote C, Arsenault B, Cartier A, Cosnay P, Couture C, Mathieu P. Association between plasma ldl particle size, valvular accumulation of oxidized ldl, and inflammation in patients with aortic stenosis. *Arterioscler. Thromb. Vasc. Biol.* 2008;28:187-193
14. Akat K, Borggrefe M, Kaden JJ. Aortic valve calcification: Basic science to clinical practice. *Heart*. 2009;95:616-623
15. Garg V, Muth AN, Ransom JF, Schluterman MK, Barnes R, King IN, Grossfeld PD, Srivastava D. Mutations in notch1 cause aortic valve disease. *Nature*. 2005;437:270-274
16. Foffa I, Ait Ali L, Panesi P, Mariani M, Festa P, Botto N, Vecoli C, Andreassi MG. Sequencing of notch1, gata5, tgfr1 and tgfr2 genes in familial cases of bicuspid aortic valve. *BMC Med Genet*. 2013;14:44
17. Bosse Y, Miqdad A, Fournier D, Pepin A, Pibarot P, Mathieu P. Refining molecular pathways leading to calcific aortic valve stenosis by studying gene expression profile of normal and calcified stenotic human aortic valves. *Circ Cardiovasc Genet*. 2009;2:489-498
18. Wang Z, Gerstein M, Snyder M. RNA-Seq: A revolutionary tool for transcriptomics. *Nat Rev Genet*. 2009;10:57-63
19. Warren BA, Yong JL. Calcification of the aortic valve: Its progression and grading. *Pathology (Phila)*. 1997;29:360-368
20. Baumgartner H, Hung J, Bermejo J, Chambers JB, Evangelista A, Griffin BP, Iung B, Otto CM, Pellikka PA, Quinones M. Echocardiographic assessment of valve stenosis: Eae/ase recommendations for clinical practice. *Eur J Echocardiogr*. 2009;10:1-25
21. Quinones MA, Otto CM, Stoddard M, Waggoner A, Zoghbi WA. Recommendations for quantification of doppler echocardiography: A report from the doppler quantification task force



of the nomenclature and standards committee of the american society of echocardiography. *J Am Soc Echocardiogr*. 2002;15:167-184

22. Du Bois D, Du Bois EF. A formula to estimate the approximate surface area if height and weight be known. 1916. *Nutrition*. 1989;5:303-311; discussion 312-303

23. Lee JTY, Tsang WH, Chow KL. Simple modifications to standard trizol® protocol allow high-yield rna extraction from cells on resorbable materials. *Journal of biomaterials and nanobiotechnology*. *J Biomater Nanobiotechnol*. 2011;2:41-48

24. Trapnell C, Roberts A, Goff L, Pertea G, Kim D, Kelley DR, Pimentel H, Salzberg SL, Rinn JL, Pachter L. Differential gene and transcript expression analysis of RNA-Seq experiments with tophat and cufflinks. *Nat Protoc*. 2012;7:562-578

25. Anders S, Pyl PT, Huber W. Htseq-a python framework to work with high-throughput sequencing data. *Bioinformatics*. 2014

26. Anders S, Huber W. Differential expression analysis for sequence count data. *Genome Biol*. 2010;11:R106

27. Robinson MD, McCarthy DJ, Smyth GK. Edger: A bioconductor package for differential expression analysis of digital gene expression data. *Bioinformatics*. 2010;26:139-140

28. Edgar R, Domrachev M, Lash AE. Gene expression omnibus: Ncbi gene expression and hybridization array data repository. *Nucleic. Acids. Res*. 2002;30:207-210

29. Guauque-Olarte S, Gaudreault N, Piche ME, Fournier D, Mauriege P, Mathieu P, Bosse Y. The transcriptome of human epicardial, mediastinal and subcutaneous adipose tissues in men with coronary artery disease. *PLoS One*. 2011;6:e19908

30. Bouchareb R, Boulanger MC, Fournier D, Pibarot P, Messaddeq Y, Mathieu P. Mechanical strain induces the production of spheroid mineralized microparticles in the aortic valve through a rhoa/rock-dependent mechanism. *J Mol Cell Cardiol*. 2014;67:49-59

31. Yang X, Meng X, Su X, Mauchley DC, Ao L, Cleveland JC, Jr., Fullerton DA. Bone morphogenic protein 2 induces runx2 and osteopontin expression in human aortic valve interstitial cells: Role of smad1 and extracellular signal-regulated kinase 1/2. *J Thorac Cardiovasc Surg*. 2009;138:1008-1015

32. Nagy E, Eriksson P, Yousry M, Caidahl K, Ingelsson E, Hansson GK, Franco-Cereceda A, Back M. Valvular osteoclasts in calcification and aortic valve stenosis severity. *Int J Cardiol.* 2013;168:2264-2271
33. Skeoch S, Bruce IN. Atherosclerosis in rheumatoid arthritis: Is it all about inflammation? *Nat Rev Rheumatol.* 2015
34. Grotenhuis HB, Ottenkamp J, Westenberg JJ, Bax JJ, Kroft LJ, de Roos A. Reduced aortic elasticity and dilatation are associated with aortic regurgitation and left ventricular hypertrophy in nonstenotic bicuspid aortic valve patients. *J Am Coll Cardiol.* 2007;49:1660-1665
35. Katz R, Budoff MJ, Takasu J, Shavelle DM, Bertoni A, Blumenthal RS, Ouyang P, Wong ND, O'Brien KD. Relationship of metabolic syndrome with incident aortic valve calcium and aortic valve calcium progression: The multi-ethnic study of atherosclerosis (mesa). *Diabetes.* 2009;58:813-819

## Tables and figures

**Table 1.** Clinical characteristics of patients according to the three groups of valves.

	<b>Bicuspid AS</b>	<b>Tricuspid AS</b>	<b>Normal</b>	<b><i>P</i></b>
	<b>(n = 10)</b>	<b>(n = 9)</b>	<b>(n = 8)</b>	
Male gender	100%	100%	100%	1.000
Age (years)	63.10 ± 4.33	64.55 ± 4.28	59.13 ± 4.32	0.044*
Weight (kg)	75.95 ± 13.72	90.57 ± 16.27	87.3 ± 11.58	0.078
Waist circumference (cm)	93.81 ± 8.09 [2]	110.4 ± 12.05 [1]	NA	0.007
Body surface area (m <sup>2</sup> )	1.87 ± 0.18	2.05 ± 0.18	2.03 ± 0.14	0.058
Body mass index (kg/m <sup>2</sup> )	26.32 ± 3.65	29.80 ± 4.53	28.47 ± 2.89	0.150
Mean gradient (mmHg)	46.90 ± 23.08	40.37 ± 16.47 [1]	NA	0.495
Aortic valve area (cm <sup>2</sup> )	0.66 ± 0.16	0.76 ± 0.17	NA	0.168
Indexed aortic valve area (cm <sup>2</sup> /m <sup>2</sup> )	0.35 ± 0.06	0.37 ± 0.08	NA	0.450
Left ventricular hypertrophy	70%	22%	0%	0.005†
Mild aortic valve regurgitation	80%	78%	20% [5]	0.061

Coronary artery disease	50% [6]	50%	25% [4]	0.820
Dyslipidemia/Hypercholesterolemia	70%	100%	75%	0.221
Hypertension	50%	78%	37.5%	0.241
Diabetes	0%	0%	0%	1.000

Continuous variables are expressed as mean  $\pm$  SD. Dichotomous variables are expressed as percentage. Missing data is shown inside brackets. NA: Not available. \*Different between tricuspid AS and normal valves ( $P = 0.041$ ). †Different between bicuspid AS and normal valves ( $P = 0.004$ ).

**Table 2.** The number of differentially expressed genes in common between cuffdiff, DESeq, edgeR, and SAMSeq.

	<b># of up-regulated genes</b>	<b># of up-regulated genes with absolute FC &gt; 2</b>	<b># of down-regulated genes</b>	<b># of down-regulated genes with absolute FC &gt; 2</b>
BAV vs. TAVc	0	0	0	0
BAV vs. TAVn	462	324	282	192
TAVc vs. TAVn	329	245	170	121

FC: Fold change.

**Table 3.** Top up- and down-regulated genes in the three pairwise comparisons.

Symbol	Gene name	Mean FPKM	Mean FPKM	FC	q-value
		TAVc	BAV		
<b>BAV vs. TAVc</b>					
<i>IGF1</i>	insulin-like growth factor 1 (somatomedin C)	40.03	65.48	1.64	0.011
<i>RSPO2</i>	R-spondin 2	2.23	4.51	2.03	0.011
<b>BAV vs. TAVn</b>					
<i>MMP13</i>	matrix metalloproteinase 13 (collagenase 3)	0.00	2.44	32768	0.002
<i>KRT14</i>	keratin 14	0.11	11.52	105.08	0.002
<i>IBSP</i>	integrin-binding sialoprotein	0.25	24.45	99.67	0.002
<i>CXCL5</i>	chemokine (C-X-C motif) ligand 5	0.28	8.12	29.48	0.002

<i>CCL11</i>	chemokine (C-C motif) ligand 11	0.19	5.04	26.68	0.006
<i>COL10A1</i>	collagen, type X, alpha 1	0.16	4.15	26.11	0.016
<i>STMN2</i>	stathmin-like 2	0.73	18.35	25.21	0.002
<i>IGFBP1</i>	insulin-like growth factor binding protein 1	0.10	2.11	22.04	0.002
<i>ELK2AP</i>	ELK2A, member of ETS oncogene family, pseudogene	27.79	609.28	21.92	0.002
<i>COL11A1</i>	collagen, type XI, alpha 1	0.21	4.10	19.25	0.002
<i>MYOC</i>	myocilin, trabecular meshwork inducible glucocorticoid response	96.52	10.17	-9.49	0.002
<i>LYPD6</i>	LY6/PLAUR domain containing 6	0.88	0.09	-9.70	0.004
<i>TUSC5</i>	tumor suppressor candidate 5	2.03	0.20	-10.18	0.002
<i>GPM6A</i>	glycoprotein M6A	3.79	0.37	-10.38	0.002

<i>LCN12</i>	lipocalin 12	2.47	0.23	-10.66	0.002
<i>PPP1R1A</i>	protein phosphatase 1, regulatory (inhibitor) subunit 1A	2.96	0.24	-12.44	0.002
<i>NPY</i>	neuropeptide Y	5.48	0.31	-17.56	0.002
<i>PDK4</i>	pyruvate dehydrogenase kinase, isozyme 4	124.09	6.74	-18.40	0.002
<i>NTS</i>	neurotensin	6.76	0.32	-21.28	0.004
<i>MUM1L1</i>	melanoma associated antigen (mutated) 1-like 1	7.66	0.25	-31.18	0.002

---

**TAVc vs. TAVn**

<i>IBSP</i>	integrin-binding sialoprotein	0.26	37.26	145.49	0.001
<i>KRT14</i>	keratin 14	0.12	4.47	38.34	0.001
<i>COL10A1</i>	collagen, type X, alpha 1	0.17	5.66	32.85	0.028



<i>COL11A1</i>	collagen, type XI, alpha 1	0.22	6.17	28.17	0.001
<i>CXCL5</i>	chemokine (C-X-C motif) ligand 5	0.28	7.10	25.16	0.001
<i>IGJ</i>	immunoglobulin J polypeptide, linker protein for 4.92 immunoglobulin  $\alpha$ and $\mu$ polypeptides		112.36	22.83	0.001
<i>CCL11</i>	chemokine (C-C motif) ligand 11	0.20	4.39	22.41	0.006
<i>STMN2</i>	stathmin-like 2	0.72	14.55	20.25	0.001
<i>MMP12</i>	matrix metalloproteinase 12 (macrophage elastase)	0.54	8.81	16.38	0.001
<i>SPPI</i>	secreted phosphoprotein 1	115.18	1772.64	15.39	0.001
<i>MYOC</i>	myocilin, trabecular meshwork inducible glucocorticoid response	99.26	18.66	-5.32	0.001

<i>GPM6A</i>	glycoprotein M6A	3.88	0.72	-5.39	0.001
<i>CNTFR</i>	ciliary neurotrophic factor receptor	14.11	2.30	-6.14	0.001
<i>APOA1</i>	apolipoprotein A-I	13.87	2.11	-6.58	0.001
<i>AGTR1</i>	angiotensin II receptor, type 1	1.04	0.15	-6.86	0.005
<i>CHODL</i>	chondrolectin	2.00	0.27	-7.36	0.001
<i>PNMT</i>	phenylethanolamine N-methyltransferase	2.84	0.28	-10.20	0.001
<i>WIF1</i>	WNT inhibitory factor 1	9.07	0.83	-10.98	0.001
<i>NPY</i>	neuropeptide Y	5.45	0.22	-24.62	0.003
<i>MUMILI1</i>	melanoma associated antigen (mutated) 1-like 1	8.45	0.30	-28.33	0.001

---

FC: Fold change. FPKM: fragments per kilobase of exon per million fragments mapped.

**Table 4.** Top 10 pathways enriched for differentially expressed genes in BAV compared to TAVn.

<b>Ingenuity Canonical Pathways</b>	<b>% significant</b>	<b>p BAV vs. TAVn</b>
	<b>molecules</b>	<b>(# significant</b>
	<b>in pathway</b>	<b>molecules)</b>
Hepatic Fibrosis / Hepatic Stellate Cell Activation*	18.78	1.58E-14 (37)
iCOS-iCOSL Signaling in T Helper Cells	14.81	2.29E-04 (16)
Type I Diabetes Mellitus Signaling	13.64	9.33E-04 (15)
Role of NFAT in Regulation of the Immune Response*	11.11	9.55E-04 (19)
CD28 Signaling in T Helper Cells	12.71	1.12E-03 (15)
PKCθ Signaling in T Lymphocytes	12.71	1.12E-03 (15)
Calcium-induced T Lymphocyte Apoptosis*	15.63	4.27E-03 (10)
T Cell Receptor Signaling	12.37	7.59E-03 (12)
Role of Osteoblasts, Osteoclasts and Chondrocytes in RA*	8.68	1.15E-02 (19)

---

OX40 Signaling Pathway

12.36

1.15E-02 (11)

---

\*: Relevant pathways to AS. q: Benjamini-Hochberg Multiple Testing Correction *P* value. RA: rheumatoid arthritis.

**Table 5.** Top 10 pathways enriched for differentially expressed genes in TAVc compared to TAVn.

<b>Ingenuity Canonical Pathways</b>	<b>% significant</b>	<b>p TAVc vs. TAVn</b>
	<b>molecules</b>	<b>(# significant</b>
	<b>in pathway</b>	<b>molecules)</b>
Hepatic Fibrosis / Hepatic Stellate Cell Activation*	18.78	5.01E-11 (27)
iCOS-iCOSL Signaling in T Helper Cells	14.81	2.75E-04 (13)
Type I Diabetes Mellitus Signaling	13.64	2.88E-03 (11)
Role of NFAT in Regulation of the Immune Response*	11.11	1.32E-03 (15)
CD28 Signaling in T Helper Cells	12.71	1.32E-03 (12)
PKCθ Signaling in T Lymphocytes	12.71	1.32E-03 (12)
Calcium-induced T Lymphocyte Apoptosis*	15.63	1.32E-03 (9)
T Cell Receptor Signaling	12.37	4.27E-03 (10)
Role of Osteoblasts, Osteoclasts and Chondrocytes in RA*	8.68	NS

---

OX40 Signaling Pathway

12.36

2.24E-02 (8)

---

q: Benjamini-Hochberg Multiple Testing Correction  $P$  value.

## Supplemental information

**Supplemental Table 1.** Number of transcripts available for differential expression analysis.

	<b>BAV vs. TAVc</b>	<b>BAV vs. TAVn</b>	<b>TAVc vs. TAVn</b>
edgeR, DESeq, and SAMSeq	19,973	19,998	19,969
Cuffdiff	16,956	24,751	17,402

\*The results of edgeR, DESeq, and SAMSeq are based on counts obtained from HTSeq.

**Supplemental Table 2.** The number of differentially expressed genes per bioinformatics tool.

	<b>BAV vs. TAVc</b>	<b>BAV vs. TAVn</b>	<b>TAVc vs. TAVn</b>
<b>Tool</b>	<b># of unique genes</b>	<b># of unique genes</b>	<b># of unique genes</b>
DESeq	0	1279	777
cuffdiff	0	1799	1242
edgeR	105	2861	2053
SAMSeq	6	2330	1767
Number of unique genes	109	3780	2669



**Supplemental Table 3.** Classification of differentially expressed genes in each pairwise comparison.

Type*	BAV vs. TAVc	BAV vs. TAVn	TAVc vs. TAVn
Other	1 (50%)	387 (52.0%)	256 (51.3%)
Enzyme	0	88 (11.8%)	54 (10.8%)
Transmembrane receptor	0	49 (6.6%)	34 (6.8%)
Transcription regulator	0	50 (6.7%)	32 (6.4%)
Transporter	0	37 (5.0%)	25 (5.0%)
Peptidase	0	32 (4.3%)	23 (4.6%)
GPCR	0	24 (3.2%)	17 (3.4%)
Kinase	0	31 (4.2%)	17 (3.4%)
Ion channel	0	11 (1.5%)	14 (2.8%)
Cytokine	0	13 (1.7%)	9 (1.8%)
Growth factor	1 (50%)	10 (1.3%)	7 (1.4%)
Phosphatase	0	7 (0.9%)	7 (1.4%)

Ligand-dependent nuclear receptor	0	3 (0.4%)	3 (0.6%)
MicroRNA	0	1 (0.1%)	1 (0.2%)
Translation regulator	0	1 (0.1%)	0 (0.0%)
<b>Total molecules</b>	<b>2</b>	<b>499</b>	<b>744</b>

\*Based on IPA classification.

**Supplemental Table 4.** IPA canonical pathways enriched for differentially expressed genes in the two pairwise comparisons.

<b>Canonical Pathways</b>	<b># molecules in pathway</b>	<b>p BAV vs. TAVn (# significant molecules)</b>	<b>p TAVc vs. TAVn (# significant molecules)</b>
Acute phase response signaling	169	2.00E-02 (15)	NS
Adipogenesis pathway	127	1.41E-02 (13)	NS
Agranulocyte adhesion and diapedesis	189	2.09E-02 (16)	1.51E-02 (13)
Agranulocyte adhesion and diapedesis	189	2.09E-02 (16)	1.51E-02 (13)
Altered T cell and B cell signaling in RA	88	4.90E-02 (9)	2.24E-02 (8)
Altered T cell and B cell signaling in RA	88	4.90E-02 (9)	2.24E-02 (8)
Atherosclerosis signaling	123	NS	3.55E-02 (9)
Axonal guidance signaling	433	1.20E-02 (30)	NS
Axonal guidance signaling	433	1.20E-02 (30)	NS
B cell development	34	2.09E-02 (6)	NS

---

Calcium-induced T lymphocyte apoptosis	64	4.27E-03 (10)	1.32E-03 (9)
Calcium-induced T lymphocyte apoptosis	64	4.27E-03 (10)	1.32E-03 (9)
Camp-mediated signaling	219	3.16E-02 (17)	3.47E-02 (13)
Camp-mediated signaling	219	3.16E-02 (17)	3.47E-02 (13)
CD28 signaling in T helper cells	118	1.12E-03 (15)	1.32E-03 (12)
CD28 signaling in T helper cells	118	1.12E-03 (15)	1.32E-03 (12)
Coagulation system	35	2.34E-02 (6)	NS
Crosstalk between dendritic cells and natural killer cells	89	NS	2.24E-02 (8)
Cytotoxic T lymphocyte-mediated apoptosis of target cells	32	NS	2.19E-02 (5)
Dendritic cell maturation	179	1.41E-02 (16)	2.24E-02 (12)
Dendritic cell maturation	179	1.41E-02 (16)	2.24E-02 (12)
Glioma invasiveness signaling	57	NS	3.47E-02 (6)
Glucocorticoid receptor signaling	261	3.39E-02 (19)	6.31E-03 (17)
Glucocorticoid receptor signaling	261	3.39E-02 (19)	6.31E-03 (17)

---

---

G-protein coupled receptor signaling	256	3.09E-02 (19)	1.17E-02 (16)
G-protein coupled receptor signaling	256	3.09E-02 (19)	1.17E-02 (16)
Granulocyte adhesion and diapedesis	177	1.41E-02 (16)	2.24E-02 (12)
Granulocyte adhesion and diapedesis	177	1.41E-02 (16)	2.24E-02 (12)
Hepatic fibrosis / hepatic stellate cell activation	197	1.58E-14 (37)	5.01E-11 (27)
Hepatic fibrosis / hepatic stellate cell activation	197	1.58E-14 (37)	5.01E-11 (27)
Hepatic fibrosis / hepatic stellate cell activation	197	1.58E-14 (37)	5.01E-11 (27)
Histamine degradation	13	NS	4.17E-02 (3)
iCOS-iCOSL signaling in T helper cells	108	2.29E-04 (16)	2.75E-04 (13)
iCOS-iCOSL signaling in T helper cells	108	2.29E-04 (16)	2.75E-04 (13)
Inhibition of matrix metalloproteases	39	3.39E-02 (6)	3.47E-02 (5)
Inhibition of matrix metalloproteases	39	3.39E-02 (6)	3.47E-02 (5)
Nur77 signaling in t lymphocytes	57	1.82E-02 (8)	1.17E-02 (7)
Nur77 signaling in t lymphocytes	57	1.82E-02 (8)	1.17E-02 (7)

---

---

OX40 signaling pathway	89	1.15E-02 (11)	2.24E-02 (8)
OX40 signaling pathway	89	1.15E-02 (11)	2.24E-02 (8)
PKCθ signaling in T lymphocytes	118	1.12E-03 (15)	1.32E-03 (12)
PKCθ signaling in T lymphocytes	118	1.12E-03 (15)	1.32E-03 (12)
Primary immunodeficiency signaling	52	1.35E-02 (8)	7.41E-03 (7)
Primary immunodeficiency signaling	52	1.35E-02 (8)	7.41E-03 (7)
Putrescine degradation III	17	3.72E-02 (4)	NS
Regulation of IL-2 expression in activated and anergic T lymphocytes	79	3.09E-02 (9)	3.55E-02 (7)
Regulation of IL-2 expression in activated and anergic T lymphocytes	79	3.09E-02 (9)	3.55E-02 (7)
Role of IL-17A in arthritis	54	1.41E-02 (8)	NS
Role of JAK1 and JAK3 in γc cytokine signaling	63	NS	4.68E-02 (6)
Role of macrophages, fibroblasts and endothelial cells in RA	298	1.23E-02 (23)	NS
Role of NFAT in regulation of the immune response	171	9.55E-04 (19)	1.32E-03 (15)

---

Role of NFAT in regulation of the immune response	171	9.55E-04 (19)	1.32E-03 (15)
Role of osteoblasts, osteoclasts and chondrocytes in RA	219	1.15E-02 (19)	NS
Role of osteoblasts, osteoclasts and chondrocytes in RA	219	1.15E-02 (19)	NS
Systemic lupus erythematosus signaling	220	NS	3.47E-02 (13)
T Cell receptor signaling	97	7.59E-03 (12)	4.27E-03 (10)
T Cell receptor signaling	97	7.59E-03 (12)	4.27E-03 (10)
T helper cell differentiation	71	4.57E-02 (8)	NS
Tryptophan degradation X (mammalian, via tryptamine)	18	4.47E-02 (4)	NS
Type I diabetes mellitus signaling	110	9.33E-04 (15)	2.88E-03 (11)
Type I diabetes mellitus signaling	110	9.33E-04 (15)	2.88E-03 (11)
VDR/RXR activation	78	NS	3.55E-02 (7)

q: Benjamini-Hochberg Multiple Testing Correction *P* value. RA: rheumatoid arthritis.

**Supplemental Table 5.** Potential targets for drug development among differentially expressed genes in the comparison BAV vs. TAVn (IPA database from ClinicalTrials.gov).

<b>Symbol</b>	<b>Entrez Gene Name</b>	<b>Drug(s)</b>
ACE	angiotensin I converting enzyme	Pentopril and others
ADRB1	adrenoceptor beta 1	Articaine/epinephrine and others
AGTR1	angiotensin II receptor, type 1	Amlodipine/olmesartan and others
ALDH1A1	aldehyde dehydrogenase 1 family, member A1	Disulfiram, chlorpropamide
ALDH2	aldehyde dehydrogenase 2 family (mitochondrial)	Disulfiram, chlorpropamide
AR	androgen receptor	Estradiol valerate/testosterone enanthate, and others
ATP1A2	ATPase, Na <sup>+</sup> /K <sup>+</sup> transporting, alpha 2 polypeptide	Digoxin, ethacrynic acid, perphenazine
BDKRB2	bradykinin receptor B2	Anatibant, icatibant
CA12	carbonic anhydrase XII	Methazolamide and others
CD2	CD2 molecule	Alefacept, siplizumab
CD22	CD22 molecule	Epratuzumab and others



CD247	CD247 molecule	Blinatumomab	
CD3D	CD3d molecule, delta (CD3-TCR complex)	Blinatumomab	
CD3E	CD3e molecule, epsilon (CD3-TCR complex)	Blinatumomab, muromonab-CD3	
CD3G	CD3g molecule, gamma (CD3-TCR complex)	Blinatumomab	
CD52	CD52 molecule	Phosphate/rituximab and others	
COL10A1	collagen, type X, alpha 1	Collagenase <i>histolyticum</i>	<i>Clostridium</i>
COL11A1	collagen, type XI, alpha 1	Collagenase <i>histolyticum</i>	<i>Clostridium</i>
COL12A1	collagen, type XII, alpha 1	Collagenase <i>histolyticum</i>	<i>Clostridium</i>
COL15A1	collagen, type XV, alpha 1	Collagenase <i>histolyticum</i>	<i>Clostridium</i>
COL4A1	collagen, type IV, alpha 1	Collagenase <i>histolyticum</i>	<i>Clostridium</i>
COL4A2	collagen, type IV, alpha 2	Collagenase <i>histolyticum</i>	<i>Clostridium</i>
COL4A3	collagen, type IV, alpha 3 (Goodpasture antigen)	Collagenase	<i>Clostridium</i>

		<i>histolyticum</i>	
COL4A4	collagen, type IV, alpha 4	Collagenase <i>histolyticum</i>	<i>Clostridium</i>
COL4A5	collagen, type IV, alpha 5	Collagenase <i>histolyticum</i>	<i>Clostridium</i>
COL5A1	collagen, type V, alpha 1	Collagenase <i>histolyticum</i>	<i>Clostridium</i>
COL5A2	collagen, type V, alpha 2	Collagenase <i>histolyticum</i>	<i>Clostridium</i>
COL8A1	collagen, type VIII, alpha 1	Collagenase <i>histolyticum</i>	<i>Clostridium</i>
COL9A1	collagen, type IX, alpha 1	Collagenase <i>histolyticum</i>	<i>Clostridium</i>
DLL4	delta-like 4 (Drosophila)	Omp-21m18, regn421	
DPP4	dipeptidyl-peptidase 4	Alogliptin/pioglitazone and others	
EDNRA	endothelin receptor type A	Bosentan and others	
EDNRB	endothelin receptor type B	Bosentan, sitaxsentan, macitentan, atrasentan	

ERBB3	v-erb-b2 avian erythroblastic leukemia viral oncogene homolog 3	Sapitinib
F2R	coagulation factor II (thrombin) receptor	Chrysalin, argatroban, bivalirudin
FCGR1A	Fc fragment of IgG, high affinity Ia, receptor (CD64)	IgG
FCGR1B	Fc fragment of IgG, high affinity Ib, receptor (CD64)	IgG
FCGR2A	Fc fragment of IgG, low affinity IIa, receptor (CD32)	IgG
FCGR3A	Fc fragment of IgG, low affinity IIIa, receptor (CD16a)	IgG
FCGR3B	Fc fragment of IgG, low affinity IIIa, receptor (CD16a)	IgG
FGF1	fibroblast growth factor 1 (acidic)	Pentosan polysulfate
FLT4	fms-related tyrosine kinase 4	Sunitinib and others
FOLH1	folate hydrolase (prostate-specific membrane antigen) 1	Capromab pendetide
GUCY1A3	guanylate cyclase 1, soluble, alpha 3	Nitroglycerin, isosorbide-5-mononitrate and others
HMOX1	heme oxygenase (decycling) 1	Tin mesoporphyrin

HTR4	5-hydroxytryptamine (serotonin) receptor 4, protein-coupled	G PRX-03140 and others
IFNGR2	interferon gamma receptor 2 (interferon gamma transducer 1)	Interferon gamma-1b
IL2RB	interleukin 2 receptor, beta	Monoclonal antibody Mik-Beta-1, daclizumab, and others
IL2RG	interleukin 2 receptor, gamma	Aldesleukin, denileukin diftitox
IL7R	interleukin 7 receptor	Recombinant human interleukin-7
ITGAL	integrin, alpha L (antigen CD11A (p180), function-associated antigen 1; alpha polypeptide)	Efalizumab
JAK3	janus kinase 3	Tofacitinib, R-348
KCNN4	potassium intermediate/small conductance activated channel, subfamily N, member 4	Betamethasone, clotrimazole, clotrimazole, senicapoc
KDR	kinase insert domain receptor (a type III tyrosine kinase)	AEE 788, sunitinib, cediranib, and others
LCK	LCK proto-oncogene, Src family tyrosine kinase	Dasatinib, pazopanib, nintedanib
LEPR	leptin receptor	Recombinant-methionyl human leptin

LYN	LYN proto-oncogene, Src family tyrosine kinase	Nintedanib, bosutinib
MAOA	monoamine oxidase A	Ladostigil, 1-ethylphenoxathiin 10 and others
MAPK13	mitogen-activated protein kinase 13	Talmapimod
MMP11	matrix metalloproteinase 11 (stromelysin 3)	Marimastat
MMP12	matrix metalloproteinase 12 (macrophage elastase)	Marimastat
MMP13	matrix metalloproteinase 13 (collagenase 3)	Marimastat
NCAM1	neural cell adhesion molecule 1	Bb-10901
NPR1	natriuretic peptide receptor 1	Nitroglycerin and others
P2RY1	purinergic receptor P2Y, G-protein coupled, 1	Clopidogrel/telmisartan, clopidogrel
PDE3B	phosphodiesterase 3B, cGMP-inhibited	Nitroglycerin and others
PDE7B	phosphodiesterase 7B	Nitroglycerin and others
PGF	placental growth factor	Aflibercept, aflibercept/irinotecan
PNP	purine nucleoside phosphorylase	Forodesine, 9-deaza-9-(3-thienylmethyl)guanine

PRLR	prolactin receptor	Fluoxymesterone
PTGER2	prostaglandin E receptor 2 (subtype EP2), 53kDa	Misoprostol and others
PTGER4	prostaglandin E receptor 4 (subtype EP4)	Misoprostol and others
QPRT	quinolinate phosphoribosyltransferase	Atorvastatin/niacin and others
RXRG	retinoid X receptor, gamma	Etretinate and others
S1PR4	sphingosine-1-phosphate receptor 4	Fingolimod
SCN7A	sodium channel, voltage-gated, type VII, alpha subunit	Riluzole
SLC1A7	solute carrier family 1 (glutamate transporter), member 7	Riluzole
SLC6A4	solute carrier family 6 (neurotransmitter transporter), member 4	Acetaminophen/clemastine/pseudoephedrine and others
TBXA2R	thromboxane A2 receptor	S-18886, ridogrel, torsemide
TLR7	toll-like receptor 7	5-fluorouracil/imiquimod and others
TUBA1C	tubulin, alpha 1c	Epothilone B and others
TUBB3	tubulin, beta 3 class III	Epothilone B and others

TXNRD1      thioredoxin reductase 1      Arsenic trioxide/tretinoin and others

VDR      vitamin D (1,25- dihydroxyvitamin D3) receptor      Calcipotriene and others

---

**Supplemental Table 6.** Potential targets for drug development among differentially expressed genes in the comparison TAVc vs. TAVn (IPA database from ClinicalTrials.gov).

<b>Symbol</b>	<b>Entrez Gene Name</b>	<b>Drug(s)</b>
ACE	angiotensin I converting enzyme	Pentopril and others
ADRB1	adrenoceptor beta 1	Articaine/epinephrine and others
AGTR1	angiotensin II receptor, type 1	Amlodipine/olmesartan medoxomil and others
ALAD	aminolevulinate dehydratase	Delta-aminolevulinic acid
ALDH1A1	aldehyde dehydrogenase 1 family, member A1	Disulfiram, chlorpropamide
ALDH2	aldehyde dehydrogenase 2 family (mitochondrial)	Disulfiram, chlorpropamide
AR	androgen receptor	Estradiol valerate/testosterone enanthate and others
ATP1A2	ATPase, Na <sup>+</sup> /K <sup>+</sup> transporting, alpha 2 polypeptide	Digoxin, ethacrynic acid, perphenazine
BDKRB2	bradykinin receptor B2	Anatibant, icatibant
CA12	carbonic anhydrase XII	Methazolamide and others



CACNA1C	calcium channel, voltage-dependent, Cinnarizine and others L type, alpha 1C subunit	
CACNA1H	calcium channel, voltage-dependent, Cinnarizine, T type, alpha 1H subunit	flunarizine, mibefradil, bepridil, zonisamide, isradipine
CACNA2D4	calcium channel, voltage-dependent, Pregabalin alpha 2/delta subunit 4	
CCR5	chemokine (C-C motif) receptor 5 (gene/pseudogene)	Maraviroc, vicriviroc, ancriviroc
CD2	CD2 molecule	Alefacept, sipilizumab
CD247	CD247 molecule	Blinatumomab
CD3D	CD3d molecule, delta (CD3-TCR complex)	Blinatumomab
CD3E	CD3e molecule, epsilon (CD3-TCR complex)	Blinatumomab, muromonab-CD3
CD3G	CD3g molecule, gamma (CD3-TCR complex)	Blinatumomab
CD52	CD52 molecule	Alemtuzumab and others
COL10A1	collagen, type X, alpha 1	Collagenase <i>Clostridium histolyticum</i>

COL11A1	collagen, type XI, alpha 1	Collagenase <i>Clostridium histolyticum</i>
COL12A1	collagen, type XII, alpha 1	Collagenase <i>Clostridium histolyticum</i>
COL18A1	collagen, type XVIII, alpha 1	Collagenase <i>Clostridium histolyticum</i>
COL4A1	collagen, type IV, alpha 1	Collagenase <i>Clostridium histolyticum</i>
COL4A2	collagen, type IV, alpha 2	Collagenase <i>Clostridium histolyticum</i>
COL4A3	collagen, type IV, alpha 3 (Goodpasture antigen)	Collagenase <i>Clostridium histolyticum</i>
COL4A4	collagen, type IV, alpha 4	Collagenase <i>Clostridium histolyticum</i>
COL5A1	collagen, type V, alpha 1	Collagenase <i>Clostridium histolyticum</i>
COL5A2	collagen, type V, alpha 2	Collagenase <i>Clostridium histolyticum</i>
COL8A1	collagen, type VIII, alpha 1	Collagenase <i>Clostridium histolyticum</i>
COL9A1	collagen, type IX, alpha 1	Collagenase <i>Clostridium histolyticum</i>
DPP4	dipeptidyl-peptidase 4	Saxagliptin and others
EDNRA	endothelin receptor type A	Bosentan and others
ERBB3	v-erb-b2 avian erythroblastic	Sapitinib

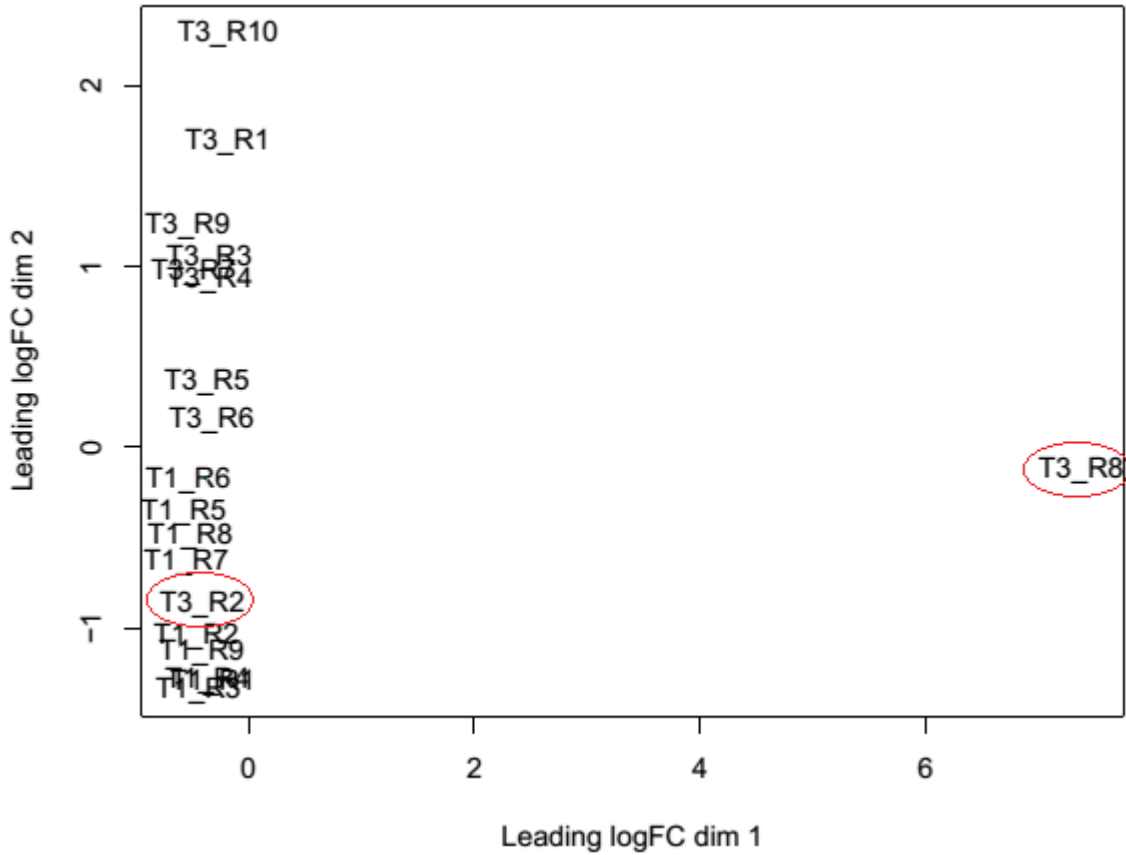
leukemia viral oncogene homolog 3

ESR1	estrogen receptor 1	17-alpha-ethinylestradiol and others
FCGR1A	Fc fragment of IgG, high affinity Ia, IgG receptor (CD64)	
FCGR1B	Fc fragment of IgG, high affinity Ib, IgG receptor (CD64)	
FCGR3A	Fc fragment of IgG, low affinity IIIa, IgG receptor (CD16a)	
FCGR3B	Fc fragment of IgG, low affinity IIIa, IgG receptor (CD16a)	
FGF1	fibroblast growth factor 1 (acidic)	Pentosan polysulfate
FOLH1	folate hydrolase (prostate-specific membrane antigen) 1	Capromab pendetide
GUCY1A3	guanylate cyclase 1, soluble, alpha 3	Nitroglycerin, isosorbide-5-mononitrate, isosorbide dinitrate, nitroprusside
GUCY1B3	guanylate cyclase 1, soluble, beta 3	Nitroglycerin, isosorbide-5-mononitrate, isosorbide dinitrate, nitroprusside
HPD	4-hydroxyphenylpyruvate dioxygenase	Nitisinone

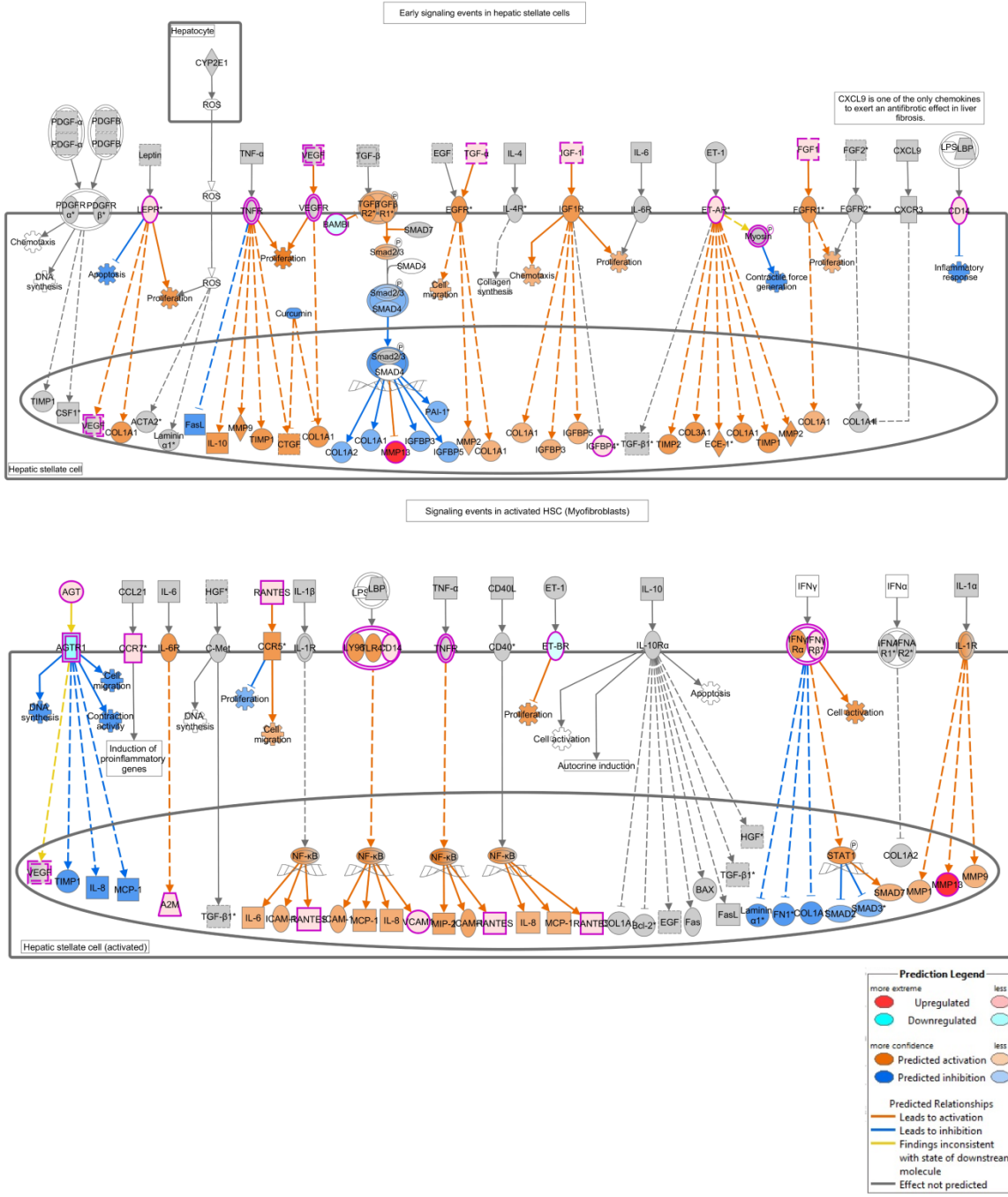
HRH1	histamine receptor H1	Paliperidone
HTR4	5-hydroxytryptamine (serotonin) receptor 4, G protein-coupled	PRX-03140, cisapride, renzapride, fenfluramine, tegaserod, ergotamine
IL2RB	interleukin 2 receptor, beta	Monoclonal antibody Mik-Beta-1, daclizumab, aldesleukin, denileukin diftitox
IL2RG	interleukin 2 receptor, gamma	Aldesleukin, denileukin diftitox
IL7R	interleukin 7 receptor	Recombinant human interleukin-7
ITGAL	integrin, alpha L (antigen CD11A (p180), lymphocyte function-associated antigen 1; alpha polypeptide)	Efalizumab
JAK3	janus kinase 3	Tofacitinib, R-348
KCNN4	potassium intermediate/small conductance calcium-activated channel, subfamily N, member 4	Betamethasone/clotrimazole, clotrimazole, senicapoc
LCK	LCK proto-oncogene, Src family tyrosine kinase	Dasatinib, pazopanib, nintedanib
LYN	LYN proto-oncogene, Src family tyrosine kinase	Nintedanib, bosutinib

MAPK13	mitogen-activated protein kinase 13	Talmapimod
MMP11	matrix metalloproteinase (stromelysin 3)	11 Marimastat
MMP12	matrix metalloproteinase (macrophage elastase)	12 Marimastat
NCAM1	neural cell adhesion molecule 1	Bb-10901
NPR1	natriuretic peptide receptor 1	Nitroglycerin and others
PDE3B	phosphodiesterase 3B, inhibited	cGMP- Nitroglycerin and others
PDE4D	phosphodiesterase 4D, specific	cAMP- Nitroglycerin and others
PLA2G5	phospholipase A2, group V	Varespladib methyl, varespladib
PNP	purine nucleoside phosphorylase	Forodesine, 9-deaza-9-(3-thienylmethyl) guanine
PRLR	prolactin receptor	Fluoxymesterone
PTGER4	prostaglandin E receptor 4 (subtype EP4)	Prostaglandin E2 and others
QPRT	quinolinate	Atorvastatin/niacin, acid/pioglitazone, nicotinic acid, nicotinic acid,

	phosphoribosyltransferase	lovastatin/niacin
S1PR4	sphingosine-1-phosphate receptor 4	Fingolimod
SLC1A7	solute carrier family 1 (glutamate transporter), member 7	Riluzole
SLC6A4	solute carrier family 6 (neurotransmitter transporter), member 4	Acetaminophen/clemastine/pseudoephedrin and others
TBXA2R	thromboxane A2 receptor	S-18886, ridogrel, torsemide
TLR7	toll-like receptor 7	UC-1V150, 5-fluorouracil/imiquimod, resiquimod, hydroxychloroquine, imiquimod
TNFSF11	tumor necrosis factor (ligand) superfamily, member 11	Lenalidomide and others /levothyroxine
TUBA1C	tubulin, alpha 1c	Colchicine/probenecid and others
TUBB3	tubulin, beta 3 class III	Colchicine/probenecid and others
TUBB4A	tubulin, beta 4A class IVa	Colchicine/probenecid and others
VDR	vitamin D (1,25-dihydroxyvitamin D3) receptor	Calcipotriene and others



**Supplemental Figure 1.** Multidimensional scaling (MDS) plot of TAVc (T1) vs. TAVn (T3). Distances on the plot represent coefficient of variation in mRNA expression levels between samples for the top genes that best distinguish the samples. Excluded samples are circled in red. FC: Fold change.



**Supplemental Figure 2.** Hepatic fibrosis/hepatic stellate cell activation canonical pathway. Hepatic fibrosis shares similarities with AS such as increased collagen synthesis, apoptosis, inflammation, and cell proliferation. Differentially expressed genes and other genes that are regulated by them as predicted by the Molecule Activity Predictor (MAP) are indicated. See legend for explanation of the colors.



# Chapter 10. Discussion, perspectives, and conclusion

## 10.1 Discussion

The sequencing of the human genome has been useful for life science, biotechnology, and medicine. One important goal of the application of omics in medicine is to develop personalized medicine. The susceptibility of a person to a disease and the way a person responds to medications can be mediated by the composition and regulation of its genome. The identification of an individual's genetic variations, along with the analysis of gene expression, can help determine the risk for developing a disease, select the best medication for treatment, inform screening, diagnose during the initiation of disease, and develop prevention strategies (Figure 10-1).

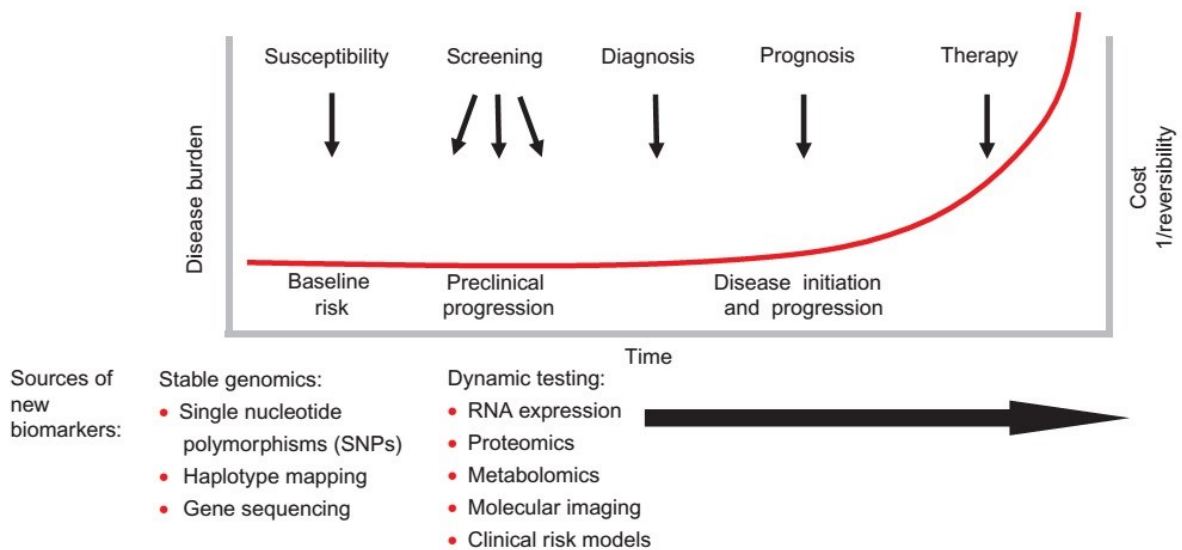


**Figure 10-1.** The role of genome-based information across the continuum of health to disease. Natural history of disease is represented by the red line. Genomic medicine is useful to identify base-line risk and early diagnosis methods that benefit the patients. When treatment occurs at the end of the disease process, it is most costly. Figure taken from Ginsburg & Willard<sup>8</sup>, license number 3627140058405).

The risk of CAVD increases with age. Due to the increase in life expectancy, CAVD is becoming a major public health problem. CAVD can be fatal in the absence of medical treatment. Currently, surgery is the only option for treating the severe stages of the disease, but in nearly 50% of individuals with CAVD, surgery is denied. Thus, it is urgent to discover the causal genes for CAVD, which will in turn, help to identify individuals at risk

of developing the disease. In addition, the identification of biomarkers and gene targets for medication development aiming to reverse or slow the progression of the disease are necessary.

The main objective of this thesis was to identify susceptibility genes for CAVD and to identify candidate genes for future development of medical therapies and/or earlier diagnostic methods for the disease. In the first article, we reported two rare mutations, p.R1279H and p.V2285I (rs61751489), in *NOTCH1* in patients with tricuspid aortic valves and CAVD. The non-sense mutation p.R1107X was also identified in a relatively young male. In addition, we found the association of a common polymorphism, rs13290979, with CAVD. *NOTCH1* is a transmembrane receptor and acts as a repressor of pro-osteogenic pathways and may prevent osteoblastogenic differentiation<sup>253</sup>. The inhibition of *NOTCH1* promotes activation of *RUNX2*<sup>33</sup> and *BMP2* in aortic valves, which then promotes calcium nodules formation in VICs<sup>253,254</sup>. Some mutations in *NOTCH1* were identified in patients with bicuspid and tricuspid aortic valves with and without CAVD<sup>33,142-144</sup>. However, no study was performed before in a large cohort of individuals with severe CAVD to search for common and rare polymorphisms in *NOTCH1*.

The results of the genotyping of 14 variants in *NOTCH1* in a cohort of 457 CAVD patients are presented. The mutation p.R1107X was identified in a relatively young male patient and confirmed by sequencing. This patient underwent aortic valve replacement for severe CAVD at 58 years old suggesting that the presence of p.R1107X variation might be associated with premature development of CAVD. The non-sense mutation p.R1107X was identified by Garg *et al.* in a genome-wide linkage scan of a five-generation family of European ancestry with 11 cases of congenital heart disease<sup>33</sup>. Seven affected individuals presented CAVD and three of them had tricuspid aortic valves. The variant was present only in affected individuals. In the present study, there was also evidence of the association of a common polymorphism in *NOTCH1* with CAVD, thus variants with lower effect sizes but more frequent may predispose to the disease. These results support the potential involvement of *NOCTHI* in CAVD development.

The main outcome of the second article was the identification of a new susceptibility gene for CAVD (*CACNA1C*) and the confirmation of the role of *RUNX2* in the disease. *CACNA1C* and *RUNX2* were not only associated with CAVD but also several cis-eQTL-SNPs affecting the expression of these genes in human aortic valves were identified. *CACNA1C* belongs to the calcium signaling pathway, which was highly enriched in disease-associated SNPs using the gene-set association analysis.

In this study, *CACNA1C* was overexpressed in calcified valves. *CACNA1C* encodes the pore-forming alpha-1C subunit of the L-type  $\text{Ca}^{2+}$  channel<sup>307</sup>. Hypertension is a risk factor for CAVD and polymorphisms in *CACNA1C* have been associated with systolic and diastolic blood pressure and hypertension<sup>308</sup>. Enhanced L-type calcium channel expression and activity contributes to blood pressure increases associated with elevated Ang II. In cultured vascular smooth muscle from arteries, Ang II stimulates generation of activated oxygen species by the endothelium and increases activity of L-type calcium channel and release of  $\text{Ca}^{2+}$  from intracellular stores<sup>309</sup>. The angiotensinogen, indirect precursor of angiotensin II, was also overexpressed in calcified valves in our RNA-Seq study. In endothelial cells,  $\text{Ca}^{2+}$  influx stimulates the activation of calmodulin, generation of oxygen anions, and upregulation of proliferating cell nuclear antigen (*PCNA*) and VACM-1/cullin 5, which in turn, stimulate cell growth and inflammation (**Figure 10-2**)<sup>310</sup>. Several commercial calcium channel inhibitors/blockers have anti-inflammatory effects<sup>311</sup> and are used for treating hypertension, arrhythmias, and chronic angina pectoris (IPA database from ClinicalTrials.gov). The utilization of calcium channel blockers in CAVD patients could be a potential treatment against the disease by inhibiting inflammation and maintaining intracellular calcium homeostasis. Studies involving activation and inhibition of the calcium channel in valvular cells in animal models will be needed to understand the role of *CACNA1C* in CAVD and the relevance of the use of channel blockers to treat patients with the disease.

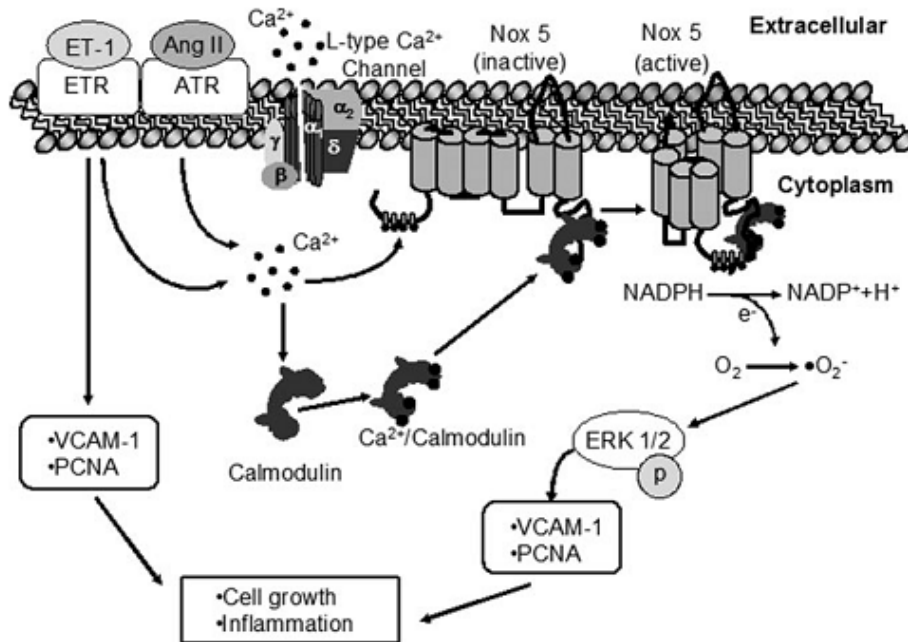


**Figure 10-2.** Interaction between Ang II and the L-type calcium channels. In human endothelial cells, binding of Ang II and endothelin (ET)-1 to their respective receptors (ATR and ETR) stimulates  $\text{Ca}^{2+}$  influx through L-type calcium channels. This causes activation of calmodulin, which then interacts with  $\text{Ca}^{2+}$ /calmodulin binding domains to activate Nox5. Activation of Nox5 results in generation of superoxide anions ( $\text{O}_2^-$ ) and phosphorylation of ERK1/2. Stimulation with Ang II induces up-regulation of PCNA and VACM-1, which are important in cell growth and inflammation, respectively. Whether a similar mechanism occurs in valvular endothelial cells must be studied. Figure taken from Montezano *et al.*<sup>310</sup>, license number 3614950274613.

As stated in section 4.1, *RUNX2* is an osteogenic regulator repressed by the action of *NOTCH1*<sup>312</sup>. Garg *et al.*<sup>33</sup> proposed a mechanism for valvular calcification in CAVD through the actions of osteoblast-like cells and elevated production of SPP1/OPN. *RUNX2* regulates the expression of SPP1/OPN and is up-regulated in mice and rabbits models of CAVD<sup>33</sup>. Circulating and valve tissue levels of *RUNX2* significantly correlate with valve stenosis severity<sup>313</sup>. In vascular smooth muscle cells and vascular myofibroblasts, *RUNX2* is activated by hydrogen peroxide which promotes mineralization<sup>312</sup>. Increased levels of reactive oxygen species are mediated by Ang II through the L-type calcium channel. In summary, CAVD might be associated with a dysregulation of the renin-angiotensin system caused by the dysfunction of genes such as *CACNA1C* and *RUNX2*. Our results confirm the importance of studying the use of ACE inhibitors and angiotensin II receptor blockers for the treatment of CAVD. MiRNA-30b represses *BMP2* in human VICs through direct

targeting of *RUNX2*, *SMAD1*, and caspase-3<sup>264</sup>. The later suggests another mechanism that may be an effective target for treatment of CAVD. A mechanism by which Ang II and *RUNX2* mediate aortic valve calcification is shown in **Figure 10-3**.

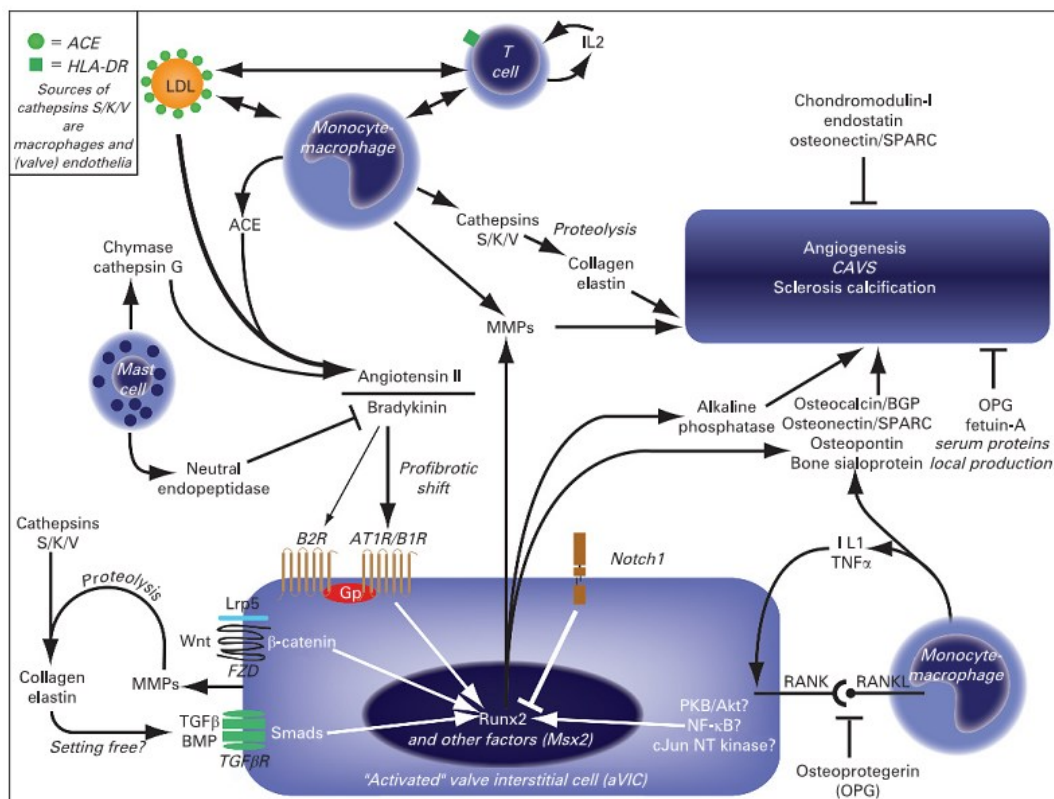


**Figure 10-3.** Ang II, *RUNX2*, and *NOTCH1* mediate aortic valve calcification. Overview of most of the discussed pathways in the development of CAVD. Non-collagenous matrix proteins (NMPs) are not shown. Not all NMPs favour calcification (e.g. *SPPI/OPN*). It is still unknown which of the many tissue-dependent intracellular proteins are used to propagate the message to the osteoblastic genes. This knowledge could help the development of more CAVD-specific therapeutic options. ACE: angiotensin-converting enzyme. AT1R: Ang II receptor type 1. B1R and B2R: bradykinin receptors. Figure taken from Akat *et al.*<sup>230</sup>, license number 3615031462834.

Thanassoulis *et al.*<sup>210</sup> reported the association of rs10455872 with aortic valve calcification. The SNP, located in the *LPA* gene, was not present in our genotyping array and was excluded after imputation based on a call rate < 90%. In the GWAS meta-analysis, the SNP rs4708867 located in exon 5 of solute carrier family 22 (organic cation transporter), member 3) (*SLC22A3*) and 109 kb of the *LPA* gene was found modestly associated with CAVD. In our study, *LPA* was not differentially expressed in aortic valves, neither was

*SLC22A3*. A large-scale meta-analysis of the *SLC22A3-LPA* gene cluster is needed to understand the contribution of SNPs in the region to CAVD. Other potential candidate genes identified in the present study are shown in **Figure 10-4**.

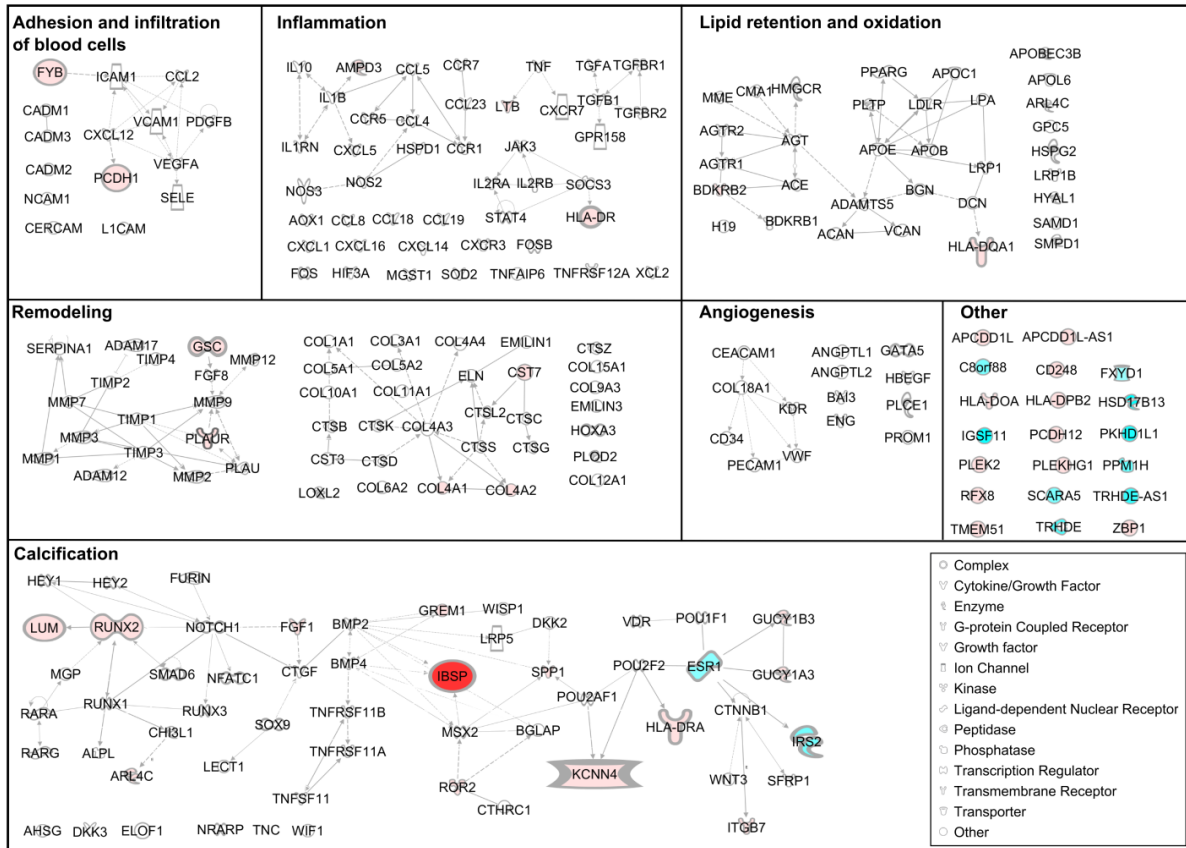


**Figure 10-4.** Integration of the GWAS and RNA-Seq results with known CAVD-related biological processes. Integration of genes differentially expressed between calcified and normal valves and with/near SNPs with  $P < 1 \times 10^{-4}$  in biological processes known to be implicated in CAVD development and progression. Cyan: down-regulated gene. Red: up-regulated genes. Some genes can belong to more than one biological process. Taken from Guauque-Olarte *et al.* (unpublished).

A limitation of GWAS is that most variants identified by this approach only explain a small proportion of heritability and usually have low associated risk<sup>30,314</sup>. In addition, more than 90% of variations identified in GWAS are located in non-coding regions of the genome, which makes it more difficult to understand their function<sup>81,82</sup>. To decrease the number of false positive results and to reduce costs of replication studies, a severe  $P$  value threshold ( $< 5 \times 10^{-8}$ ) for multiple testing correction has been set<sup>41,48</sup>. However, moderately significant

SNPs can nevertheless be truly associated with the disease and thus be missed if the prioritization strategy (very stringent p-value threshold) excludes them.

Several approaches have been proposed to identify true associations in the grey zone of GWAS. Gene-set association analysis can identify coordinated association patterns for genes involved in the same pathway. Significant pathways will be the ones with the highest number of moderate to high disease-associated SNPs. Most SNPs that are part of significant pathways may not be individually associated with the disease using a classical genome-wide significant cut-off. However, altogether, members of significant pathways can show an enrichment of small  $P$  values beyond what is expected by chance. In our study, 25 pathways were enriched for CAVD-associated SNPs; several of them are biologically relevant for CAVD such as the calcium signaling pathway and the extracellular matrix receptor interaction pathway. Genes in these significant pathways and the genetic variants located in these genes deserve to be further studied.

eQTL mapping studies also help prioritize genes and variants implicated in the disease under study. Disease-associated SNPs that are also associated with gene expression are the strongest candidates to reveal function of the associated SNP with the disease and candidate genes. Between 50 to 80% of eQTLs are cell- and tissue-type dependent<sup>84,85</sup>. In this regard, a strong point of the present doctoral work is that the transcriptome was measured in the most relevant tissue for CAVD, i.e. aortic valves with and without calcification. Three SNPs were significantly associated with the mRNA expression of *RUNX2* and 268 were associated with the expression levels of *CACNA1C*. The most significant eQTL-SNPs protective alleles in *RUNX2* and *CACNA1C* were associated with decreased mRNA expression levels of the genes. The mRNA levels of both genes were up-regulated in calcified aortic valves, thus, the eQTL-SNPs increased susceptibility to CAVD through up-regulation of the genes in valve tissues, an observation that is concordant with the literature.

The presence of a bicuspid valve is a main risk factor for the development of CAVD in patients younger than 65 years old. In the second and third articles, the transcriptome of

calcified bicuspid aortic valves was compared to that of calcified and normal tricuspid aortic valves. A large number of genes differentially expressed in calcified and normal aortic valves are targets of commercial drugs or drugs under development. *In vitro* and *in vivo* studies of genes targeted by these chemicals are needed to identify drugs that may slow progression or reverse aortic valve stenosis.

The third and fourth articles compare the gene expression profile of not only calcified and normal tricuspid valves (as in the second article) but also the one of calcified bicuspid aortic valves using microarrays and RNA-Seq technologies.

In the third article based on microarray data, two up-regulated and two down-regulated genes were identified in the comparison between calcified bicuspid and tricuspid aortic valves. Compared to normal valves, 128 genes were differentially expressed in calcified bicuspid valves. Finally, comparing calcific tricuspid and normal valves, 63 genes were found to be differentially expressed. The microarrays experiment led to the identification of imprinted maternally expressed transcript (non-protein coding) (*H19*) as a potential candidate gene for CAVD development in patients with bicuspid aortic valves. *H19* was differentially expressed in bicuspid compared to calcified and normal tricuspid aortic valves. *H19* is an lncRNA with functions not completely understood. *H19* is an imprinted gene and only the copy inherited from the mother is expressed. *H19* plays a role in the proliferation of cardiomyocytes<sup>315</sup> and aortic and pulmonary valve thickening<sup>315</sup>. *H19* targets *SOX9*<sup>316</sup>, a chondriogenic transcription factor regulated by *BMP2* and *NOTCH1*. It is thus possible that *H19* has a role in early valve calcification observed in patients with a bicuspid aortic valve through impaired *NOTCH1* signaling which is supported by the identification of *NOTCH1* variants in CAVD patients in the first article of this thesis.

In the fourth article based on RNA-Seq data, two genes were up-regulated and none were down-regulated in calcified bicuspid compared to calcified tricuspid aortic valves. There were 462 up-regulated and 282 down-regulated genes between calcified bicuspid and normal tricuspid valves. Compared to normal valves, 329 genes were up- and 170 were down-regulated in calcified tricuspid valves. *SPP1/OPN* and *RUNX2* were up-regulated in



calcified bicuspid and tricuspid valves compared to normal valves. *RUNX2* regulates the expression of *SPPI/OPN*. This supports the results of the GWAS meta-analysis where *RUNX2* was moderately associated with CAVD and highlights the importance of *RUNX2* for CAVD development in patients with a bicuspid or tricuspid aortic valve.

In general, RNA-Seq (Chapter 9) identified a higher number of up- and down-regulated genes in each comparison compared to microarrays (Chapter 8). Almost half of the differentially expressed genes by microarrays were also differentially expressed by RNA-Seq. Interestingly, the direction of fold change is consistent between the two methodologies for the common differentially expressed genes (Figure 10-5).

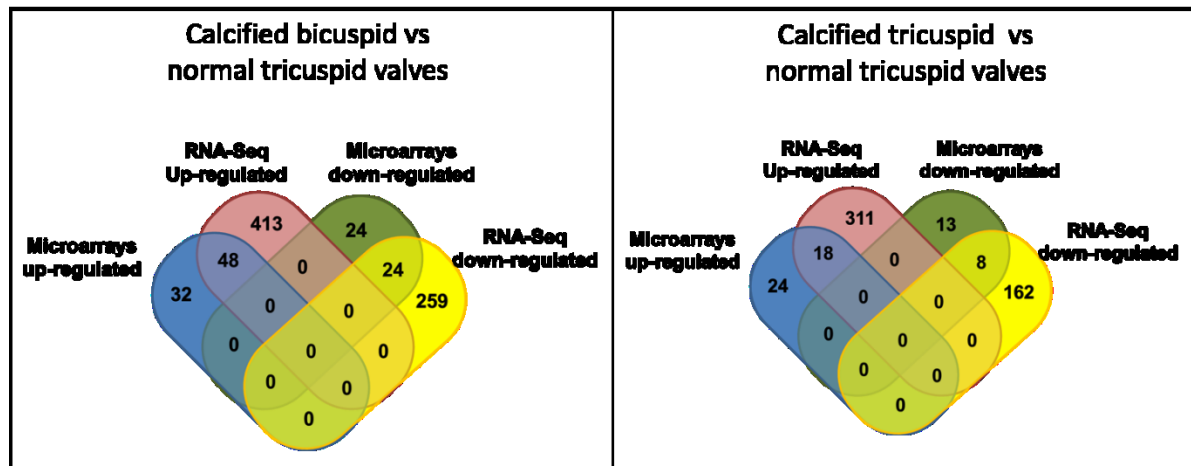


**Figure 10-5.** Venn diagrams showing the number of genes up- and down-regulated in common between RNA-Seq and microarrays results. The RNA-Seq differentially expressed genes include genes in common identified by cuffdiff, DESeq, edgeR, and SAMSeq. Figure by Guauque-Olarte.

In 2009, Bossé *et al.*<sup>231</sup> compare the expression profile of calcified and normal tricuspid valves from patients with severe CAVD using microarrays. A total of 409 and 306 genes were significantly up- and down-regulated, respectively. No bicuspid valves were included in that study. In the present microarrays study (Chapter 8), 15 out of 21 down-regulated genes and 26 out of 42 up-regulated genes comparing calcified tricuspid and normal valves were also observed in the study of Bossé *et al.* In addition, the orientation of effect was consistent for all of the common genes. This level of concordance is interesting knowing

that different microarray platforms were used (Illumina BeadChips in this study vs. Affymetrix arrays in our previous study).

Comparing the results of Bossé *et al.* with the RNA-Seq results (Chapter 9) for the same comparison, a total of 105 and 69 genes were found consistently up- and down-regulated in the two datasets (**Figure 10-6**). The direction of mRNA expression changes between stenotic and normal valves was also concordant between the two methodologies. Based on our experience with whole-genome gene expression data, this represents substantial overlap between the two experiments, especially because they were performed using different technologies.

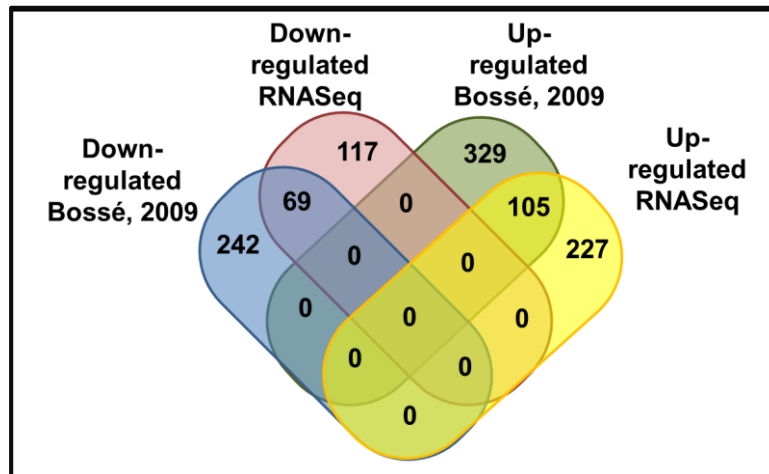


**Figure 10-6.** Venn diagrams showing the number of genes up- and down-regulated in common between RNA-Seq and microarrays results from Bossé *et al.*, 2009. The RNA-Seq differentially expressed genes include genes in common identified by cuffdiff, DESeq, edgeR, and SAMSeq. Figure by Guauque-Olarte.

Considering only genes differentially expressed using the four algorithms (i.e. cuffdiff, DESeq, edgeR, and SAMSeq), no genes were in common between calcified bicuspid and tricuspid aortic valves. However, two genes were in common between cuffdiff and SAMSeq. *IGF1* [insulin-like growth factor 1 (somatomedin C)] and *RSPO2* (R-spondin 2). *IGF1* has a similar function and structure than proinsulin and members of this family of proteins are involved in mediating growth and development<sup>317</sup>. Defects in *IGF1*

causes insulin-like growth factor I deficiency. *RSPO2* regulates  $\beta$ -catenin, which is translocated to the nucleus to activate *BMP2*.

*H19* and *CCL18*, the two up-regulated genes in the microarrays experiment were also significantly up-regulated according to the results of Cuffdiff, but not by the other three algorithms. Intragroup variability may explain why tools like DESeq, which is more conservative, did not call differentially expressed genes. For susceptibility genes identified in the GWAS meta-analysis, *CACNA1C* was up-regulated in calcified bicuspid and tricuspid valves compared to normal valves using Cuffdiff, DESeq, and EdgeR. *RUNX2* was also up-regulated in the same comparisons with the four algorithms.

## 10.2 Perspectives

In the short term, it is important to replicate the top disease-associated SNPs identified in our GWAS meta-analysis. This replication can be performed by genotyping tag SNPs in the best candidate genes or sequencing them using high-throughput DNA sequencing. Performing additional studies in animal models and VIC cultures lacking expression of *CACNA1C* will help better understand the role of this gene in aortic valve calcification. The expression of the differentially expressed genes in the microarrays and RNA-Seq experiment must be confirmed by qPCR. If possible, the protein levels of the most biologically important genes should be measured to confirm their involvement in CAVD and CAVD-related pathways.

In the long term, to increase the power to discover candidate genes for CAVD, it would be important to perform a meta-analysis that includes thousands of patients with the disease. In addition to our Quebec cohort of CAVD, other cohorts of CAVD were built in Montreal, Vancouver, France, Sweden, and Denmark. Thus, it is feasible to perform a large GWAS meta-analysis on CAVD.

A limitation of GWAS studies of CAVD is that the control cohorts have not been phenotyped to exclude the presence of CAVD or aortic sclerosis specifically. Furthermore, control cohorts include younger patients than the case cohorts. Thus, 2.5% of control

individuals may develop CAVD in the future considering the prevalence of the disease in the general population. This does not introduce a major bias in GWAS. If 5% of controls meet the definition of cases and are misclassified, the loss of power would be approximately the same as that due to a reduction of the sample size by 10%<sup>318</sup>. However, it would be important to build a cohort of controls for CAVD to eliminate most bias, help increase the power and reproducibility of GWAS, and in turn, identify the causal genes for the disease.

To identify biomarkers and causal genes for CAVD it is also recommended to analyze individuals in different stages of the disease: from mild to severe. This is important because not all patients with mild disease progress to the severe stage. Identifying genes that are associated with every step is important to detect biomarkers of disease progression and to develop screening methods.

Because the bicuspid aortic valve phenotype is highly heritable, it could be possible to perform family-based association studies using unaffected parents or siblings as controls to identify new susceptibility genes implicated in bicuspid aortic valve development. Recently, the Bicuspid Aortic Valve Consortium (BAVCon), an international consortium of 26 institutions with cohorts of bicuspid aortic valve patients, was created<sup>319,320</sup>. Members of the group have collected around 10,000 individuals including more than 5,000 patients with bicuspid aortic valves plus a similar number of controls. The goal of the consortium is to perform genomic and clinical studies in a large cohort of patients with a bicuspid aortic valve to identify the genetic basis of bicuspid aortic valve and new clinical diagnostic and prognostic tools.

So far, the field of epigenomics has not been explored for CAVD. Recent studies have shown that some miRNAs and lncRNAs are involved and can target genes that have been associated with calcification of the aortic valve. Analyzing miRNA and lncRNA at the genome levels will give more insight about dysregulation of gene expression in CAVD, and may help to identify biomarkers and drug targets. Whole-genome bisulfite sequencing is now available and could be performed to determine the influence of methylation in CAVD

development and progression. Those analyses remain expensive, even though the cost of omics studies have decreased, and may be restricted due to funding.

The goal of personalized medicine is not only to treat the patients but to prevent the development and progression of a disease by identifying genetic and environmental risk factors specific to each individual. This is beneficial for each person and also for communities because it can help reduce the societal and economic burden of common diseases. The translation from gene discovery to clinical application can take several years and involves different methods and resources summarized by Prakash *et al.*<sup>320</sup> (**Figure 10-7**). This thesis, which integrates genomics and transcriptomics, is one step forward to the goal of personalized medicine for CAVD patients.

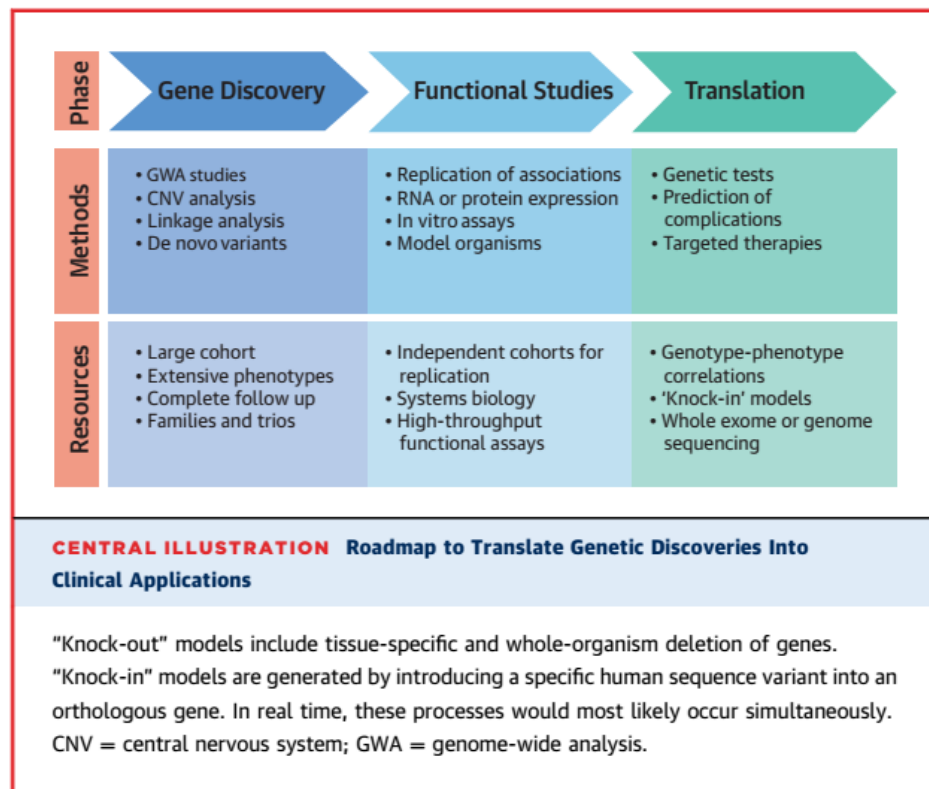


**Figure 10-7.** Gene discovery to clinical application. Figure taken from Prakash *et al.*<sup>320</sup>, license number 3615040164514.

### 10.3 Conclusion

CAVD is a common disease that causes the narrowing of the aortic valve due to fibrosis and calcification of the valve leaflets. Although several molecular pathways have been associated with the disease, the specific cell signaling pathways and genes implicated in CAVD development and progression are yet to be discovered.

In this project, we performed the first GWAS meta-analysis on CAVD. In addition, we performed the first whole-genome gene expression study comparing calcified bicuspid and tricuspid aortic valves with normal aortic valves. The integration of different whole-genome approaches such as GWAS, RNA-Seq, and eQTLs were important to reveal a new candidate gene for CAVD, *CACNA1C*. Furthermore, this work identified new genes differentially expressed in calcified compared to normal aortic valves that have functions in biological processes involved in the disease. This new information is important to better understand altered functions implicated in aortic valve calcification. This work also confirmed the potential involvement of *NOTCH1* and *RUNX2* in CAVD development and the importance of the renin-angiotensin system dysfunction of the disease.

In addition, several genes differentially expressed in calcified compared to normal valves that are targets of existing and emerging drugs have been identified. The only treatment available for severe stages of the disease is surgery. It is imperative to identify molecules that can be used as biomarkers or drug targets. In general, the present project has increased the knowledge about the etiology of aortic stenosis in patients with bicuspid and tricuspid aortic valves. The data generated is the base for future important discoveries that will improve the quality of life of patients with CAVD.

## References

1. Iung B, Vahanian A. Epidemiology of acquired valvular heart disease. *Can J Cardiol.* 2014;30:962-970
2. Waller B, Howard J, Fess S. Pathology of aortic valve stenosis and pure aortic regurgitation. A clinical morphologic assessment--part i. *Clin. Cardiol.* 1994;17:85-92
3. Watson JD, Baker TA, Bell SP, Gann A, Levine MS, Losick R, Harrison SC. *Molecular biology of the gene.* 2014
4. The ENCODE Project Consortium. An integrated encyclopedia of DNA elements in the human genome. *Nature.* 2012;489:57-74
5. Hahn S. Structure and mechanism of the rna polymerase ii transcription machinery. *Nat Struct Mol Biol.* 2004;11:394-403
6. Viktorovskaya OV, Schneider DA. Functional divergence of eukaryotic rna polymerases: Unique properties of rna polymerase i suit its cellular role. *Gene.* 2015;556:19-26
7. Schwartz SI, Brunnicardi FC, Andersen DK, Billiar TR, Dunn DL, Hunter JG, Matthews JB, Pollock RE, Alarcon LH, Angelos P, Angood PB, Ashley SW, Awad SS, Barbul A, Bauman JA, Bechara C, Beilman SW, Bell RH, Bell RL, Beldegrun A, Ben-Galim P, Berger DH, Biffi WL, Bland KI, Brandt ML, Bullocks J, Cagiannos C, Cain JM, Chandra RK, Chen CL, Chen CJ, Clark OH, Cole P, Copeland EM, Cormier JN, Coselli JS, Cothren CC, Crooke GA, Dempsey DT, Dorian RS, Dunn KMB, Efron DE, ElMasri WM, Endorf FW, Feng X-H, Fisher WE, Ford HR, Galloway AC, Gannon FH, Geller DA, Gibran NS, Gimbel M, Godinez CD, Gonzalez EA, Goss JA, Grady MS, Gregory T, Grikscheit TC, Grossi EA, Hackam DJ, Hall DE, Hardin RE, Heggeness MH, Heller L, Hinshaw DB, Holcomb JB, Hollier LH, Hunt KK, Huynh TT, Jaffe BM, Jan BV, Jastrow KM, Jobe BA, Karamlou TB, Kohn EC, Kougiass P, Kozar RA, La Rochelle J, Geeta L, Lee THL, LeMaire SA, Liem TK, Lifchez SD, Lin PH, Lin X, Losee JE, Lowry SF, Luketich JD, Macho JR, Maddaus MA, Makary MA, Meric-Bernstam F, Moneta GL, Moore EE, Nason KS, Newman K, Newman LA, Oddsdottir M, Park AE, Pawlik TM, Peitzman AB, Peters JH, Pham TH, Rothenberger DA, Rubin JP, Saluja AK, Schauer PR, Schirmer BD, Schwartz CF, Sen SK, Seymour NE, Shapiro ML, Sharma K, Sherman V, Shires GT, Shuch B, Smith ML, Stal S, Tavakkolizadeh A, Tsung A, Ungerleider RM, Wallace CG, Wang KS, Weber RS, Wei F-C, Wein RO, Weinberg J, Welke KF, Whang EE, Young DM, Zenilman ME, Zinner MJ, Zuckerbraun BS. Schwartz's principles of surgery. *McGraw-Hill's AccessMedicine Clinical library.* 2010

8. Ginsburg GS, Willard HF. *Genomic and personalized medicine*. London ; Waltham, MA: Elsevier/Academic Press; 2013
9. Djebali S, Davis CA, Merkel A, Dobin A, Lassmann T, Mortazavi A, Tanzer A, Lagarde J, Lin W, Schlesinger F, Xue C, Marinov GK, Khatun J, Williams BA, Zaleski C, Rozowsky J, Roder M, Kokocinski F, Abdelhamid RF, Alioto T, Antoshechkin I, Baer MT, Bar NS, Batut P, Bell K, Bell I, Chakraborty S, Chen X, Chrast J, Curado J, Derrien T, Drenkow J, Dumais E, Dumais J, Duttagupta R, Falconnet E, Fastuca M, Fejes-Toth K, Ferreira P, Foissac S, Fullwood MJ, Gao H, Gonzalez D, Gordon A, Gunawardena H, Howald C, Jha S, Johnson R, Kapranov P, King B, Kingswood C, Luo OJ, Park E, Persaud K, Preall JB, Ribeca P, Risk B, Robyr D, Sammeth M, Schaffer L, See LH, Shahab A, Skancke J, Suzuki AM, Takahashi H, Tilgner H, Trout D, Walters N, Wang H, Wrobel J, Yu Y, Ruan X, Hayashizaki Y, Harrow J, Gerstein M, Hubbard T, Reymond A, Antonarakis SE, Hannon G, Giddings MC, Ruan Y, Wold B, Carninci P, Guigo R, Gingeras TR. Landscape of transcription in human cells. *Nature*. 2012;489:101-108
10. Uchida S, Dimmeler S. Long noncoding rnas in cardiovascular diseases. *Circ Res*. 2015;116:737-750
11. Venter JC, Adams MD, Myers EW, Li PW, Mural RJ, Sutton GG, Smith HO, Yandell M, Evans CA, Holt RA, Gocayne JD, Amanatides P, Ballew RM, Huson DH, Wortman JR, Zhang Q, Kodira CD, Zheng XH, Chen L, Skupski M, Subramanian G, Thomas PD, Zhang J, Gabor Miklos GL, Nelson C, Broder S, Clark AG, Nadeau J, McKusick VA, Zinder N, Levine AJ, Roberts RJ, Simon M, Slayman C, Hunkapiller M, Bolanos R, Delcher A, Dew I, Fasulo D, Flanigan M, Florea L, Halpern A, Hannenhalli S, Kravitz S, Levy S, Mobarry C, Reinert K, Remington K, Abu-Threideh J, Beasley E, Biddick K, Bonazzi V, Brandon R, Cargill M, Chandramouliswaran I, Charlab R, Chaturvedi K, Deng Z, Di Francesco V, Dunn P, Eilbeck K, Evangelista C, Gabrielian AE, Gan W, Ge W, Gong F, Gu Z, Guan P, Heiman TJ, Higgins ME, Ji RR, Ke Z, Ketchum KA, Lai Z, Lei Y, Li Z, Li J, Liang Y, Lin X, Lu F, Merkulov GV, Milshina N, Moore HM, Naik AK, Narayan VA, Neelam B, Nusskern D, Rusch DB, Salzberg S, Shao W, Shue B, Sun J, Wang Z, Wang A, Wang X, Wang J, Wei M, Wides R, Xiao C, Yan C, Yao A, Ye J, Zhan M, Zhang W, Zhang H, Zhao Q, Zheng L, Zhong F, Zhong W, Zhu S, Zhao S, Gilbert D, Baumhueter S, Spier G, Carter C, Cravchik A, Woodage T, Ali F, An H, Awe A, Baldwin D, Baden H, Barnstead M, Barrow I, Beeson K, Busam D, Carver A, Center A, Cheng ML, Curry L, Danaher S, Davenport L, Desilets R, Dietz S, Dodson K, Doup L, Ferriera S, Garg N, Gluecksmann A, Hart B, Haynes J, Haynes C, Heiner C, Hladun S, Hostin D, Houck J, Howland T, Ibegwam C, Johnson J, Kalush F,



- Kline L, Koduru S, Love A, Mann F, May D, McCawley S, McIntosh T, McMullen I, Moy M, Moy L, Murphy B, Nelson K, Pfannkoch C, Pratts E, Puri V, Qureshi H, Reardon M, Rodriguez R, Rogers YH, Romblad D, Ruhfel B, Scott R, Sitter C, Smallwood M, Stewart E, Strong R, Suh E, Thomas R, Tint NN, Tse S, Vech C, Wang G, Wetter J, Williams S, Williams M, Windsor S, Winn-Deen E, Wolfe K, Zaveri J, Zaveri K, Abril JF, Guigo R, Campbell MJ, Sjolander KV, Karlak B, Kejariwal A, Mi H, Lazareva B, Hatton T, Narechania A, Diemer K, Muruganujan A, Guo N, Sato S, Bafna V, Istrail S, Lippert R, Schwartz R, Walenz B, Yooseph S, Allen D, Basu A, Baxendale J, Blick L, Caminha M, Carnes-Stine J, Caulk P, Chiang YH, Coyne M, Dahlke C, Mays A, Dombroski M, Donnelly M, Ely D, Esparham S, Fosler C, Gire H, Glanowski S, Glasser K, Glodek A, Gorokhov M, Graham K, Gropman B, Harris M, Heil J, Henderson S, Hoover J, Jennings D, Jordan C, Jordan J, Kasha J, Kagan L, Kraft C, Levitsky A, Lewis M, Liu X, Lopez J, Ma D, Majoros W, McDaniel J, Murphy S, Newman M, Nguyen T, Nguyen N, Nodell M, Pan S, Peck J, Peterson M, Rowe W, Sanders R, Scott J, Simpson M, Smith T, Sprague A, Stockwell T, Turner R, Venter E, Wang M, Wen M, Wu D, Wu M, Xia A, Zandieh A, Zhu X. The sequence of the human genome. *Science*. 2001;291:1304-1351
12. LaFramboise T. Single nucleotide polymorphism arrays: A decade of biological, computational and technological advances. *Nucleic Acids Res*. 2009;37:4181-4193
  13. Abecasis GR, Auton A, Brooks LD, DePristo MA, Durbin RM, Handsaker RE, Kang HM, Marth GT, McVean GA. An integrated map of genetic variation from 1,092 human genomes. *Nature*. 2012;491:56-65
  14. Ke X, Taylor MS, Cardon LR. Singleton snps in the human genome and implications for genome-wide association studies. *Eur J Hum Genet*. 2008;16:506-515
  15. Koboldt DC, Miller RD, Kwok PY. Distribution of human snps and its effect on high-throughput genotyping. *Hum Mutat*. 2006;27:249-254
  16. Eilbeck K, Lewis SE, Mungall CJ, Yandell M, Stein L, Durbin R, Ashburner M. The sequence ontology: A tool for the unification of genome annotations. *Genome Biol*. 2005;6:R44
  17. Lee W, Yue P, Zhang Z. Analytical methods for inferring functional effects of single base pair substitutions in human cancers. *Hum Genet*. 2009;126:481-498
  18. Ho E, Bhindi R, Ashley EA, Figtree GA. Genetic analysis in cardiovascular disease: A clinical perspective. *Cardiol. Rev*. 2011;19:81-89
  19. International Human Genome Sequencing Consortium. Finishing the euchromatic sequence of the human genome. *Nature*. 2004;431:931-945

20. Altshuler DM, Gibbs RA, Peltonen L, Dermitzakis E, Schaffner SF, Yu F, Bonnen PE, de Bakker PI, Deloukas P, Gabriel SB, Gwilliam R, Hunt S, Inouye M, Jia X, Palotie A, Parkin M, Whittaker P, Chang K, Hawes A, Lewis LR, Ren Y, Wheeler D, Muzny DM, Barnes C, Darvishi K, Hurler M, Korn JM, Kristiansson K, Lee C, McCarroll SA, Nemesh J, Keinan A, Montgomery SB, Pollack S, Price AL, Soranzo N, Gonzaga-Jauregui C, Anttila V, Brodeur W, Daly MJ, Leslie S, McVean G, Moutsianas L, Nguyen H, Zhang Q, Ghorji MJ, McGinnis R, McLaren W, Takeuchi F, Grossman SR, Shlyakhter I, Hostetter EB, Sabeti PC, Adebamowo CA, Foster MW, Gordon DR, Licinio J, Manca MC, Marshall PA, Matsuda I, Ngare D, Wang VO, Reddy D, Rotimi CN, Royal CD, Sharp RR, Zeng C, Brooks LD, McEwen JE. Integrating common and rare genetic variation in diverse human populations. *Nature*. 2010;467:52-58
21. The International HapMap Consortium. A haplotype map of the human genome. *Nature*. 2005;437:1299-1320
22. Kundaje A, Meuleman W, Ernst J, Bilenky M, Yen A, Heravi-Moussavi A, Kheradpour P, Zhang Z, Wang J, Ziller MJ, Amin V, Whitaker JW, Schultz MD, Ward LD, Sarkar A, Quon G, Sandstrom RS, Eaton ML, Wu YC, Pfenning AR, Wang X, Claussnitzer M, Liu Y, Coarfa C, Harris RA, Shores N, Epstein CB, Gjoneska E, Leung D, Xie W, Hawkins RD, Lister R, Hong C, Gascard P, Mungall AJ, Moore R, Chuah E, Tam A, Canfield TK, Hansen RS, Kaul R, Sabo PJ, Bansal MS, Carles A, Dixon JR, Farh KH, Feizi S, Karlic R, Kim AR, Kulkarni A, Li D, Lowdon R, Elliott G, Mercer TR, Neph SJ, Onuchic V, Polak P, Rajagopal N, Ray P, Sallari RC, Siebenthal KT, Sinnott-Armstrong NA, Stevens M, Thurman RE, Wu J, Zhang B, Zhou X, Beaudet AE, Boyer LA, De Jager PL, Farnham PJ, Fisher SJ, Haussler D, Jones SJ, Li W, Marra MA, McManus MT, Sunyaev S, Thomson JA, Tlsty TD, Tsai LH, Wang W, Waterland RA, Zhang MQ, Chadwick LH, Bernstein BE, Costello JF, Ecker JR, Hirst M, Meissner A, Milosavljevic A, Ren B, Stamatoyannopoulos JA, Wang T, Kellis M. Integrative analysis of 111 reference human epigenomes. *Nature*. 2015;518:317-330
23. The GTEx Consortium. The genotype-tissue expression (gtex) project. *Nat Genet*. 2013;45:580-585
24. Sherry ST, Ward MH, Kholodov M, Baker J, Phan L, Smigielski EM, Sirotkin K. Dbsnp: The ncbi database of genetic variation. *Nucleic Acids Res*. 2001;29:308-311
25. Mailman MD, Feolo M, Jin Y, Kimura M, Tryka K, Bagoutdinov R, Hao L, Kiang A, Paschall J, Phan L, Popova N, Pretel S, Ziyabari L, Lee M, Shao Y, Wang ZY, Sirotkin K, Ward M, Kholodov M, Zbicz K, Beck J, Kimelman M, Shevelev S, Preuss D, Yaschenko E, Graeff A, Ostell J, Sherry ST. The ncbi dbgap database of genotypes and phenotypes. *Nat Genet*. 2007;39:1181-1186

26. Welter D, MacArthur J, Morales J, Burdett T, Hall P, Junkins H, Klemm A, Flicek P, Manolio T, Hindorff L, Parkinson H. The nhgri gwas catalog, a curated resource of snp-trait associations. *Nucleic Acids Res.* 2014;42:D1001-1006
27. Barrett T, Wilhite SE, Ledoux P, Evangelista C, Kim IF, Tomashevsky M, Marshall KA, Phillippy KH, Sherman PM, Holko M, Yefanov A, Lee H, Zhang N, Robertson CL, Serova N, Davis S, Soboleva A. Ncbi geo: Archive for functional genomics data sets--update. *Nucleic Acids Res.* 2013;41:D991-995
28. Huntington's Disease Collaborative Research Group. A novel gene containing a trinucleotide repeat that is expanded and unstable on huntington's disease chromosomes. The huntington's disease collaborative research group. *Cell.* 1993;72:971-983
29. Riordan JR, Rommens JM, Kerem B, Alon N, Rozmahel R, Grzelczak Z, Zielenski J, Lok S, Plavsic N, Chou JL, et al. Identification of the cystic fibrosis gene: Cloning and characterization of complementary DNA. *Science.* 1989;245:1066-1073
30. Manolio TA, Collins FS, Cox NJ, Goldstein DB, Hindorff LA, Hunter DJ, McCarthy MI, Ramos EM, Cardon LR, Chakravarti A, Cho JH, Guttmacher AE, Kong A, Kruglyak L, Mardis E, Rotimi CN, Slatkin M, Valle D, Whittemore AS, Boehnke M, Clark AG, Eichler EE, Gibson G, Haines JL, Mackay TF, McCarroll SA, Visscher PM. Finding the missing heritability of complex diseases. *Nature.* 2009;461:747-753
31. Zondervan KT, Cardon LR. Designing candidate gene and genome-wide case-control association studies. *Nat Protoc.* 2007;2:2492-2501
32. McCarthy MI, Abecasis GR, Cardon LR, Goldstein DB, Little J, Ioannidis JP, Hirschhorn JN. Genome-wide association studies for complex traits: Consensus, uncertainty and challenges. *Nat Rev Genet.* 2008;9:356-369
33. Garg V, Muth AN, Ransom JF, Schluterman MK, Barnes R, King IN, Grossfeld PD, Srivastava D. Mutations in notch1 cause aortic valve disease. *Nature.* 2005;437:270-274
34. Kwon JM, Goate AM. The candidate gene approach. *Alcohol Res Health.* 2000;24:164-168
35. Longo DL, Harrison TR. Harrison's principles of internal medicine. 2012
36. Gauderman WJ, Witte JS, Thomas DC. Family-based association studies. *J Natl Cancer Inst Monogr.* 1999:31-37
37. Kebede MA, Attie AD. Insights into obesity and diabetes at the intersection of mouse and human genetics. *Trends Endocrinol Metab.* 2014;25:493-501
38. Avakian SD, Annicchino-Bizzacchi JM, Grinberg M, Ramires JA, Mansura AP. Apolipoproteins ai, b, and e polymorphisms in severe aortic valve stenosis. *Clin. Genet.* 2001;60:381-384

39. Frazer KA, Ballinger DG, Cox DR, Hinds DA, Stuve LL, Gibbs RA, Belmont JW, Boudreau A, Hardenbol P, Leal SM, Pasternak S, Wheeler DA, Willis TD, Yu F, Yang H, Zeng C, Gao Y, Hu H, Hu W, Li C, Lin W, Liu S, Pan H, Tang X, Wang J, Wang W, Yu J, Zhang B, Zhang Q, Zhao H, Zhou J, Gabriel SB, Barry R, Blumenstiel B, Camargo A, Defelice M, Faggart M, Goyette M, Gupta S, Moore J, Nguyen H, Onofrio RC, Parkin M, Roy J, Stahl E, Winchester E, Ziaugra L, Altshuler D, Shen Y, Yao Z, Huang W, Chu X, He Y, Jin L, Liu Y, Sun W, Wang H, Wang Y, Xiong X, Xu L, Waye MM, Tsui SK, Xue H, Wong JT, Galver LM, Fan JB, Gunderson K, Murray SS, Oliphant AR, Chee MS, Montpetit A, Chagnon F, Ferretti V, Leboeuf M, Olivier JF, Phillips MS, Roumy S, Sallee C, Verner A, Hudson TJ, Kwok PY, Cai D, Koboldt DC, Miller RD, Pawlikowska L, Taillon-Miller P, Xiao M, Tsui LC, Mak W, Song YQ, Tam PK, Nakamura Y, Kawaguchi T, Kitamoto T, Morizono T, Nagashima A, Ohnishi Y, Sekine A, Tanaka T, Tsunoda T, Deloukas P, Bird CP, Delgado M, Dermitzakis ET, Gwilliam R, Hunt S, Morrison J, Powell D, Stranger BE, Whittaker P, Bentley DR, Daly MJ, de Bakker PI, Barrett J, Chretien YR, Maller J, McCarroll S, Patterson N, Pe'er I, Price A, Purcell S, Richter DJ, Sabeti P, Saxena R, Schaffner SF, Sham PC, Varilly P, Stein LD, Krishnan L, Smith AV, Tello-Ruiz MK, Thorisson GA, Chakravarti A, Chen PE, Cutler DJ, Kashuk CS, Lin S, Abecasis GR, Guan W, Li Y, Munro HM, Qin ZS, Thomas DJ, McVean G, Auton A, Bottolo L, Cardin N, Eyheramendy S, Freeman C, Marchini J, Myers S, Spencer C, Stephens M, Donnelly P, Cardon LR, Clarke G, Evans DM, Morris AP, Weir BS, Mullikin JC, Sherry ST, Feolo M, Skol A, Zhang H, Matsuda I, Fukushima Y, Macer DR, Suda E, Rotimi CN, Adebamowo CA, Ajayi I, Aniagwu T, Marshall PA, Nkwodimmah C, Royal CD, Leppert MF, Dixon M, Peiffer A, Qiu R, Kent A, Kato K, Niikawa N, Adewole IF, Knoppers BM, Foster MW, Clayton EW, Watkin J, Muzny D, Nazareth L, Sodergren E, Weinstock GM, Yakub I, Birren BW, Wilson RK, Fulton LL, Rogers J, Burton J, Carter NP, Clee CM, Griffiths M, Jones MC, McLay K, Plumb RW, Ross MT, Sims SK, Willey DL, Chen Z, Han H, Kang L, Godbout M, Wallenburg JC, L'Archeveque P, Bellemare G, Saeki K, An D, Fu H, Li Q, Wang Z, Wang R, Holden AL, Brooks LD, McEwen JE, Guyer MS, Wang VO, Peterson JL, Shi M, Spiegel J, Sung LM, Zacharia LF, Collins FS, Kennedy K, Jamieson R, Stewart J. A second generation human haplotype map of over 3.1 million snps. *Nature*. 2007;449:851-861
40. Bush WS, Moore JH. Chapter 11: Genome-wide association studies. *PLoS Comput Biol*. 2012;8:e1002822
41. Manolio TA. Genomewide association studies and assessment of the risk of disease. *N. Engl. J. Med*. 2010;363:166-176

42. Newton-Cheh C, Johnson T, Gateva V, Tobin MD, Bochud M, Coin L, Najjar SS, Zhao JH, Heath SC, Eyheramendy S, Papadakis K, Voight BF, Scott LJ, Zhang F, Farrall M, Tanaka T, Wallace C, Chambers JC, Khaw KT, Nilsson P, van der Harst P, Polidoro S, Grobbee DE, Onland-Moret NC, Bots ML, Wain LV, Elliott KS, Teumer A, Luan J, Lucas G, Kuusisto J, Burton PR, Hadley D, McArdle WL, Brown M, Dominiczak A, Newhouse SJ, Samani NJ, Webster J, Zeggini E, Beckmann JS, Bergmann S, Lim N, Song K, Vollenweider P, Waeber G, Waterworth DM, Yuan X, Groop L, Orho-Melander M, Allione A, Di Gregorio A, Guarrera S, Panico S, Ricceri F, Romanazzi V, Sacerdote C, Vineis P, Barroso I, Sandhu MS, Luben RN, Crawford GJ, Jousilahti P, Perola M, Boehnke M, Bonnycastle LL, Collins FS, Jackson AU, Mohlke KL, Stringham HM, Valle TT, Willer CJ, Bergman RN, Morken MA, Doring A, Gieger C, Illig T, Meitinger T, Org E, Pfeufer A, Wichmann HE, Kathiresan S, Marrugat J, O'Donnell CJ, Schwartz SM, Siscovick DS, Subirana I, Freimer NB, Hartikainen AL, McCarthy MI, O'Reilly PF, Peltonen L, Pouta A, de Jong PE, Snieder H, van Gilst WH, Clarke R, Goel A, Hamsten A, Peden JF, Seedorf U, Syvanen AC, Tognoni G, Lakatta EG, Sanna S, Scheet P, Schlessinger D, Scuteri A, Dorr M, Ernst F, Felix SB, Homuth G, Lorbeer R, Reffellmann T, Rettig R, Volker U, Galan P, Gut IG, Herberg S, Lathrop GM, Zelenika D, Deloukas P, Soranzo N, Williams FM, Zhai G, Salomaa V, Laakso M, Elosua R, Forouhi NG, Volzke H, Uiterwaal CS, van der Schouw YT, Numans ME, Matullo G, Navis G, Berglund G, Bingham SA, Kooner JS, Connell JM, Bandinelli S, Ferrucci L, Watkins H, Spector TD, Tuomilehto J, Altshuler D, Strachan DP, Laan M, Meneton P, Wareham NJ, Uda M, Jarvelin MR, Mooser V, Melander O, Loos RJ, Elliott P, Abecasis GR, Caulfield M, Munroe PB. Genome-wide association study identifies eight loci associated with blood pressure. *Nat. Genet.* 2009;41:666-676
43. Reich DE, Cargill M, Bolk S, Ireland J, Sabeti PC, Richter DJ, Lavery T, Kouyoumjian R, Farhadian SF, Ward R, Lander ES. Linkage disequilibrium in the human genome. *Nature.* 2001;411:199-204
44. Ardlie KG, Kruglyak L, Seielstad M. Patterns of linkage disequilibrium in the human genome. *Nat Rev Genet.* 2002;3:299-309
45. Charles BA, Shriner D, Rotimi CN. Accounting for linkage disequilibrium in association analysis of diverse populations. *Genet Epidemiol.* 2014;38:265-273
46. Anderson CA, Pettersson FH, Clarke GM, Cardon LR, Morris AP, Zondervan KT. Data quality control in genetic case-control association studies. *Nat Protoc.* 2010;5:1564-1573
47. Clarke GM, Anderson CA, Pettersson FH, Cardon LR, Morris AP, Zondervan KT. Basic statistical analysis in genetic case-control studies. *Nat Protoc.* 2011;6:121-133

48. Panagiotou OA, Ioannidis JP. What should the genome-wide significance threshold be? Empirical replication of borderline genetic associations. *Int J Epidemiol.* 2012;41:273-286
49. Schunkert H, Erdmann J, Samani NJ. Genetics of myocardial infarction: A progress report. *European heart journal.* 2010;31:918-925
50. Turner S, Armstrong LL, Bradford Y, Carlson CS, Crawford DC, Crenshaw AT, de Andrade M, Doheny KF, Haines JL, Hayes G, Jarvik G, Jiang L, Kullo IJ, Li R, Ling H, Manolio TA, Matsumoto M, McCarty CA, McDavid AN, Mirel DB, Paschall JE, Pugh EW, Rasmussen LV, Wilke RA, Zuvich RL, Ritchie MD. Quality control procedures for genome-wide association studies. *Curr Protoc Hum Genet.* 2011;Chapter 1:Unit1 19
51. Wigginton JE, Cutler DJ, Abecasis GR. A note on exact tests of hardy-weinberg equilibrium. *Am J Hum Genet.* 2005;76:887-893
52. Hirschhorn JN, Lohmueller K, Byrne E, Hirschhorn K. A comprehensive review of genetic association studies. *Genet Med.* 2002;4:45-61
53. Falush D, Stephens M, Pritchard JK. Inference of population structure using multilocus genotype data: Linked loci and correlated allele frequencies. *Genetics.* 2003;164:1567-1587
54. Delaneau O, Marchini J. Integrating sequence and array data to create an improved 1000 genomes project haplotype reference panel. *Nat Commun.* 2014;5:3934
55. Howie BN, Donnelly P, Marchini J. A flexible and accurate genotype imputation method for the next generation of genome-wide association studies. *PLoS Genet.* 2009;5:e1000529
56. Li Y, Willer C, Sanna S, Abecasis G. Genotype imputation. *Annu Rev Genomics Hum Genet.* 2009;10:387-406
57. Browning BL, Browning SR. A unified approach to genotype imputation and haplotype-phase inference for large data sets of trios and unrelated individuals. *Am J Hum Genet.* 2009;84:210-223
58. Hong EP, Park JW. Sample size and statistical power calculation in genetic association studies. *Genomics Inform.* 2012;10:117-122
59. Evangelou E, Ioannidis JP. Meta-analysis methods for genome-wide association studies and beyond. *Nat Rev Genet.* 2013;14:379-389
60. Begum F, Ghosh D, Tseng GC, Feingold E. Comprehensive literature review and statistical considerations for gwas meta-analysis. *Nucleic Acids Res.* 2012;40:3777-3784
61. Wang K, Li M, Hakonarson H. Analysing biological pathways in genome-wide association studies. *Nat Rev Genet.* 2010;11:843-854

62. Cantor RM, Lange K, Sinsheimer JS. Prioritizing gwas results: A review of statistical methods and recommendations for their application. *Am J Hum Genet.* 2010;86:6-22
63. Edwards SL, Beesley J, French JD, Dunning AM. Beyond gwas: Illuminating the dark road from association to function. *Am J Hum Genet.* 2013;93:779-797
64. Nam D, Kim J, Kim SY, Kim S. Gsa-snp: A general approach for gene set analysis of polymorphisms. *Nucleic Acids Res.* 2010;38:W749-754
65. Pastinen T. Genome-wide allele-specific analysis: Insights into regulatory variation. *Nat Rev Genet.* 2010;11:533-538
66. Tarca AL, Romero R, Draghici S. Analysis of microarray experiments of gene expression profiling. *American journal of obstetrics and gynecology.* 2006;195:373-388
67. Wang Z, Gerstein M, Snyder M. Rna-seq: A revolutionary tool for transcriptomics. *Nat Rev Genet.* 2009;10:57-63
68. Ballman KV. Genetics and genomics: Gene expression microarrays. *Circulation.* 2008;118:1593-1597
69. Tusher VG, Tibshirani R, Chu G. Significance analysis of microarrays applied to the ionizing radiation response. *Proc. Natl. Acad. Sci. U. S. A.* 2001;98:5116-5121
70. Huang da W, Sherman BT, Lempicki RA. Systematic and integrative analysis of large gene lists using david bioinformatics resources. *Nat Protoc.* 2009;4:44-57
71. Huang da W, Sherman BT, Lempicki RA. Bioinformatics enrichment tools: Paths toward the comprehensive functional analysis of large gene lists. *Nucleic Acids Res.* 2009;37:1-13
72. Subramanian A, Tamayo P, Mootha VK, Mukherjee S, Ebert BL, Gillette MA, Paulovich A, Pomeroy SL, Golub TR, Lander ES, Mesirov JP. Gene set enrichment analysis: A knowledge-based approach for interpreting genome-wide expression profiles. *Proc Natl Acad Sci U S A.* 2005;102:15545-15550
73. Nagalakshmi U, Waern K, Snyder M. Rna-seq: A method for comprehensive transcriptome analysis. *Curr Protoc Mol Biol.* 2010;Chapter 4:Unit 4 11 11-13
74. Trapnell C, Hendrickson DG, Sauvageau M, Goff L, Rinn JL, Pachter L. Differential analysis of gene regulation at transcript resolution with rna-seq. *Nat. Biotechnol.* 2013;31:46-53
75. Garber M, Grabherr MG, Guttman M, Trapnell C. Computational methods for transcriptome annotation and quantification using rna-seq. *Nat Methods.* 2011;8:469-477
76. Sonesson C, Delorenzi M. A comparison of methods for differential expression analysis of rna-seq data. *BMC Bioinformatics.* 2013;14:91

77. Anders S, Huber W. Differential expression analysis for sequence count data. *Genome Biol.* 2010;11:R106
78. Robinson MD, McCarthy DJ, Smyth GK. Edger: A bioconductor package for differential expression analysis of digital gene expression data. *Bioinformatics.* 2010;26:139-140
79. Li J, Tibshirani R. Finding consistent patterns: A nonparametric approach for identifying differential expression in rna-seq data. *Stat Methods Med Res.* 2013;22:519-536
80. Anders S, Pyl PT, Huber W. Htseq--a python framework to work with high-throughput sequencing data. *Bioinformatics.* 2015;31:166-169
81. Kumar V, Westra HJ, Karjalainen J, Zhernakova DV, Esko T, Hrdlickova B, Almeida R, Zhernakova A, Reinmaa E, Vosa U, Hofker MH, Fehrmann RS, Fu J, Withoff S, Metspalu A, Franke L, Wijmenga C. Human disease-associated genetic variation impacts large intergenic non-coding rna expression. *PLoS Genet.* 2013;9:e1003201
82. Cookson W, Liang L, Abecasis G, Moffatt M, Lathrop M. Mapping complex disease traits with global gene expression. *Nat Rev Genet.* 2009;10:184-194
83. Cheung VG, Spielman RS. Genetics of human gene expression: Mapping DNA variants that influence gene expression. *Nat Rev Genet.* 2009;10:595-604
84. Albert FW, Kruglyak L. The role of regulatory variation in complex traits and disease. *Nat Rev Genet.* 2015;16:197-212
85. Hao K, Bosse Y, Nickle DC, Pare PD, Postma DS, Laviolette M, Sandford A, Hackett TL, Daley D, Hogg JC, Elliott WM, Couture C, Lamontagne M, Brandsma CA, van den Berge M, Koppelman G, Reicin AS, Nicholson DW, Malkov V, Derry JM, Suver C, Tsou JA, Kulkarni A, Zhang C, Vessey R, Opiteck GJ, Curtis SP, Timens W, Sin DD. Lung eqtls to help reveal the molecular underpinnings of asthma. *PLoS Genet.* 2012;8:e1003029
86. Koopmann TT, Adriaens ME, Moerland PD, Marsman RF, Westerveld ML, Lal S, Zhang T, Simmons CQ, Baczko I, dos Remedios C, Bishopric NH, Varro A, George AL, Jr., Lodder EM, Bezzina CR. Genome-wide identification of expression quantitative trait loci (eqtls) in human heart. *PLoS One.* 2014;9:e97380
87. Goring HH. Tissue specificity of genetic regulation of gene expression. *Nat Genet.* 2012;44:1077-1078
88. Dimas AS, Deutsch S, Stranger BE, Montgomery SB, Borel C, Attar-Cohen H, Ingle C, Beazley C, Gutierrez Arcelus M, Sekowska M, Gagnebin M, Nisbett J,



- Deloukas P, Dermitzakis ET, Antonarakis SE. Common regulatory variation impacts gene expression in a cell type-dependent manner. *Science*. 2009;325:1246-1250
89. Fuster V, Walsh RA, Harrington RA. *Hurst's the heart. Volume one*. New York: McGraw-Hill Medical; 2011
  90. Levy MN, Pappano AJ, Berne RM. *Cardiovascular physiology*. Philadelphia, PA: Mosby Elsevier; 2007
  91. Lilly LS, Harvard Medical School. *Pathophysiology of heart disease : A collaborative project of medical students and faculty*. Baltimore: Williams & Wilkins; 1998
  92. Alché E-Pd. *Comprendre la physiologie cardiovasculaire*. Paris: Médecine-Sciences Flammarion; 2008
  93. Ho SY, Nihoyannopoulos P. Anatomy, echocardiography, and normal right ventricular dimensions. *Heart*. 2006;92 Suppl 1:i2-13
  94. Steven D, Roberts-Thomson KC, Seiler J, Inada K, Tedrow UB, Mitchell RN, Sobieszczyk PS, Eisenhauer AC, Couper GS, Stevenson WG. Ventricular tachycardia arising from the aortomitral continuity in structural heart disease: Characteristics and therapeutic considerations for an anatomically challenging area of origin. *Circ Arrhythm Electrophysiol*. 2009;2:660-666
  95. Rozeik M, Wheatley D, Gourlay T. The aortic valve: Structure, complications and implications for transcatheter aortic valve replacement. *Perfusion*. 2014;29:285-300
  96. Butcher JT, Mahler GJ, Hockaday LA. Aortic valve disease and treatment: The need for naturally engineered solutions. *Adv Drug Deliv Rev*. 2011;63:242-268
  97. Tao G, Kotick JD, Lincoln J. Heart valve development, maintenance, and disease: The role of endothelial cells. *Curr Top Dev Biol*. 2012;100:203-232
  98. Bateman MG, Quill JL, Hill AJ, Iaizzo PA. The clinical anatomy and pathology of the human atrioventricular valves: Implications for repair or replacement. *J Cardiovasc Transl Res*. 2013;6:155-165
  99. Misfeld M, Sievers HH. Heart valve macro- and microstructure. *Philos Trans R Soc Lond B Biol Sci*. 2007;362:1421-1436
  100. Otto CM. Timing of surgery in mitral regurgitation. *Heart*. 2003;89:100-105
  101. Taramasso M, Vanermen H, Maisano F, Guidotti A, La Canna G, Alfieri O. The growing clinical importance of secondary tricuspid regurgitation. *J Am Coll Cardiol*. 2012;59:703-710
  102. Stephens EH, Kearney DL, Grande-Allen KJ. Insight into pathologic abnormalities in congenital semilunar valve disease based on advances in understanding normal valve microstructure and extracellular matrix. *Cardiovasc Pathol*. 2012;21:46-58

103. Underwood MJ, El Khoury G, Deronck D, Glineur D, Dion R. The aortic root: Structure, function, and surgical reconstruction. *Heart*. 2000;83:376-380
104. Sutton JP, 3rd, Ho SY, Anderson RH. The forgotten interleaflet triangles: A review of the surgical anatomy of the aortic valve. *Ann Thorac Surg*. 1995;59:419-427
105. Charitos EI, Sievers HH. Anatomy of the aortic root: Implications for valve-sparing surgery. *Ann Cardiothorac Surg*. 2013;2:53-56
106. Otto CM, Bonow RO. Valvular heart disease a companion to braunwald's heart disease. 2014
107. Dweck MR, Boon NA, Newby DE. Calcific aortic stenosis: A disease of the valve and the myocardium. *J Am Coll Cardiol*. 2012;60:1854-1863
108. Ho SY. Structure and anatomy of the aortic root. *Eur J Echocardiogr*. 2009;10:i3-10
109. Chester AH, El-Hamamsy I, Butcher JT, Latif N, Bertazzo S, Yacoub MH. The living aortic valve: From molecules to function. *Glob Cardiol Sci Pract*. 2014;2014:52-77
110. Hasan A, Ragaert K, Swieszkowski W, Selimovic S, Paul A, Camci-Unal G, Mofrad MR, Khademhosseini A. Biomechanical properties of native and tissue engineered heart valve constructs. *J Biomech*. 2014;47:1949-1963
111. Mol A, Bouten CV, Baaijens FP, Zund G, Turina MI, Hoerstrup SP. Review article: Tissue engineering of semilunar heart valves: Current status and future developments. *J Heart Valve Dis*. 2004;13:272-280
112. Puceat M. Embryological origin of the endocardium and derived valve progenitor cells: From developmental biology to stem cell-based valve repair. *Biochim Biophys Acta*. 2013;1833:917-922
113. Quinlan AM, Billiar KL. Investigating the role of substrate stiffness in the persistence of valvular interstitial cell activation. *J Biomed Mater Res A*. 2012;100:2474-2482
114. Yang Y, Sun W, Wu SM, Xiao J, Kong X. Telocytes in human heart valves. *J Cell Mol Med*. 2014;18:759-765
115. Liu AC, Joag VR, Gotlieb AI. The emerging role of valve interstitial cell phenotypes in regulating heart valve pathobiology. *Am J Pathol*. 2007;171:1407-1418
116. Akerstrom F, Barderas MG, Rodriguez-Padial L. Aortic stenosis: A general overview of clinical, pathophysiological and therapeutic aspects. *Expert Rev Cardiovasc Ther*. 2013;11:239-250
117. Garg V. Molecular genetics of aortic valve disease. *Curr Opin Cardiol*. 2006;21:180-184

118. LaHaye S, Lincoln J, Garg V. Genetics of valvular heart disease. *Curr Cardiol Rep.* 2014;16:487
119. Thomas PS, Sridurongrit S, Ruiz-Lozano P, Kaartinen V. Deficient signaling via *alk2* (*acvr1*) leads to bicuspid aortic valve development. *PLoS One.* 2012;7:e35539
120. Lin CJ, Lin CY, Chen CH, Zhou B, Chang CP. Partitioning the heart: Mechanisms of cardiac septation and valve development. *Development.* 2012;139:3277-3299
121. Wirrig EE, Yutzey KE. Conserved transcriptional regulatory mechanisms in aortic valve development and disease. *Arterioscler Thromb Vasc Biol.* 2014;34:737-741
122. McPhee SJ, Hammer GD, Aagaard EM, Barsh G, Bauer DC, Bloch KC, Bunnett NW, Davoren JB, Else T, Fode M, Fuchs JD, Funk JL, Gelber AC, Ix JH, Khalili M, Kishiyama JL, Kusumoto FM, Kwok Y, Levine SM, Liao CE, Lomen-Hoerth C, McCalmont TH, Messing RO, Mills JC, Mitrovic I, Moasser MM, Nguyen TT, Ohl DA, Parker BD, Prendergast TJ, Purcell KJ, Rosen A, Ruoss SJ, Seeley EJ, Sellmeyer DE, Shoback DM, Simeone DM, Snksen J, Sonnenday CJ, Stappenbeck TS, Taylor RN, Wang S. Pathophysiology of disease an introduction to clinical medicine. *McGraw-Hill's AccessMedicine Lange educational library.* 2010
123. Mozaffarian D, Benjamin EJ, Go AS, Arnett DK, Blaha MJ, Cushman M, de Ferranti S, Despres JP, Fullerton HJ, Howard VJ, Huffman MD, Judd SE, Kissela BM, Lackland DT, Lichtman JH, Lisabeth LD, Liu S, Mackey RH, Matchar DB, McGuire DK, Mohler ER, 3rd, Moy CS, Muntner P, Mussolino ME, Nasir K, Neumar RW, Nichol G, Palaniappan L, Pandey DK, Reeves MJ, Rodriguez CJ, Sorlie PD, Stein J, Towfighi A, Turan TN, Virani SS, Willey JZ, Woo D, Yeh RW, Turner MB. Heart disease and stroke statistics-2015 update: A report from the american heart association. *Circulation.* 2015;131:e29-e322
124. Supino PG, Borer JS, Preibisz J, Bornstein A. The epidemiology of valvular heart disease: A growing public health problem. *Heart Fail Clin.* 2006;2:379-393
125. Nkomo VT, Gardin JM, Skelton TN, Gottdiener JS, Scott CG, Enriquez-Sarano M. Burden of valvular heart diseases: A population-based study. *Lancet.* 2006;368:1005-1011
126. Public Health Agency of Canada. 2009 tracking heart disease and stroke in canada. 2009:viii, 118 p.
127. Sehatzadeh S, Doble B, Xie F, Blackhouse G, Campbell K, Kaulback K, Chandra K, Goeree R. Transcatheter aortic valve implantation (tavi) for treatment of aortic valve stenosis: An evidence update. *Ont Health Technol Assess Ser.* 2013;13:1-40

128. Moraes RCSd, Katz M, Tarasoutchi F. Clinical and epidemiological profile of patients with valvular heart disease admitted to the emergency department. *Einstein (São Paulo) [online]*. 2014;12:154-158
129. Lindroos M, Kupari M, Heikkila J, Tilvis R. Prevalence of aortic valve abnormalities in the elderly: An echocardiographic study of a random population sample. *J Am Coll Cardiol*. 1993;21:1220-1225
130. Eveborn GW, Schirmer H, Heggelund G, Lunde P, Rasmussen K. The evolving epidemiology of valvular aortic stenosis. The tromso study. *Heart*. 2013;99:396-400
131. Stewart BF, Siscovick D, Lind BK, Gardin JM, Gottdiener JS, Smith VE, Kitzman DW, Otto CM. Clinical factors associated with calcific aortic valve disease. Cardiovascular health study. *J. Am. Coll. Cardiol*. 1997;29:630-634
132. Iung B, Baron G, Butchart EG, Delahaye F, Gohlke-Barwolf C, Levang OW, Tornos P, Vanoverschelde JL, Vermeer F, Boersma E, Ravaud P, Vahanian A. A prospective survey of patients with valvular heart disease in europe: The euro heart survey on valvular heart disease. *Eur. Heart J*. 2003;24:1231-1243
133. Rose AG. Etiology of valvular heart disease. *Curr Opin Cardiol*. 1996;11:98-113
134. Rajamannan NM, Bonow RO, Rahimtoola SH. Calcific aortic stenosis: An update. *Nat. Clin. Pract. Cardiovasc. Med*. 2007;4:254-262
135. Roberts WC, Ko JM. Frequency by decades of unicuspid, bicuspid, and tricuspid aortic valves in adults having isolated aortic valve replacement for aortic stenosis, with or without associated aortic regurgitation. *Circulation*. 2005;111:920-925
136. Otto CM, Bonow RO. *Valvular heart disease: A companion to braunwald's heart disease.*: SAUNDERS Elsevier; 2009
137. Sievers HH, Schmidtke C. A classification system for the bicuspid aortic valve from 304 surgical specimens. *J Thorac Cardiovasc Surg*. 2007;133:1226-1233
138. Yutzey KE, Demer LL, Body SC, Huggins GS, Towler DA, Giachelli CM, Hofmann-Bowman MA, Mortlock DP, Rogers MB, Sadeghi MM, Aikawa E. Calcific aortic valve disease: A consensus summary from the alliance of investigators on calcific aortic valve disease. *Arterioscler Thromb Vasc Biol*. 2014;34:2387-2393
139. Fernandes SM, Sanders SP, Khairy P, Jenkins KJ, Gauvreau K, Lang P, Simonds H, Colan SD. Morphology of bicuspid aortic valve in children and adolescents. *J Am Coll Cardiol*. 2004;44:1648-1651
140. Clementi M, Notari L, Borghi A, Tenconi R. Familial congenital bicuspid aortic valve: A disorder of uncertain inheritance. *Am J Med Genet*. 1996;62:336-338

141. Huntington K, Hunter AG, Chan KL. A prospective study to assess the frequency of familial clustering of congenital bicuspid aortic valve. *J Am Coll Cardiol.* 1997;30:1809-1812
142. Foffa I, Ait Ali L, Panesi P, Mariani M, Festa P, Botto N, Vecoli C, Andreassi MG. Sequencing of notch1, gata5, tgfr1 and tgfr2 genes in familial cases of bicuspid aortic valve. *BMC Med Genet.* 2013;14:44
143. Mohamed SA, Aherrahrou Z, Liptau H, Erasmi AW, Hagemann C, Wrobel S, Borzym K, Schunkert H, Sievers HH, Erdmann J. Novel missense mutations (p.T596m and p.P1797h) in notch1 in patients with bicuspid aortic valve. *Biochem Biophys Res Commun.* 2006;345:1460-1465
144. McKellar SH, Tester DJ, Yagubyan M, Majumdar R, Ackerman MJ, Sundt TM, 3rd. Novel notch1 mutations in patients with bicuspid aortic valve disease and thoracic aortic aneurysms. *J Thorac Cardiovasc Surg.* 2007;134:290-296
145. Siu SC, Silversides CK. Bicuspid aortic valve disease. *J Am Coll Cardiol.* 2010;55:2789-2800
146. Loey s BL, Chen J, Neptune ER, Judge DP, Podowski M, Holm T, Meyers J, Leitch CC, Katsanis N, Sharifi N, Xu FL, Myers LA, Spevak PJ, Cameron DE, De Backer J, Hellems J, Chen Y, Davis EC, Webb CL, Kress W, Coucke P, Rifkin DB, De Paepe AM, Dietz HC. A syndrome of altered cardiovascular, craniofacial, neurocognitive and skeletal development caused by mutations in tgfr1 or tgfr2. *Nat Genet.* 2005;37:275-281
147. Martin LJ, Ramachandran V, Cripe LH, Hinton RB, Andelfinger G, Tabangin M, Shoener K, Keddache M, Benson DW. Evidence in favor of linkage to human chromosomal regions 18q, 5q and 13q for bicuspid aortic valve and associated cardiovascular malformations. *Hum. Genet.* 2007;121:275-284
148. Guo DC, Pannu H, Tran-Fadulu V, Papke CL, Yu RK, Avidan N, Bourgeois S, Estrera AL, Safi HJ, Sparks E, Amor D, Ades L, McConnell V, Willoughby CE, Abuelo D, Willing M, Lewis RA, Kim DH, Scherer S, Tung PP, Ahn C, Buja LM, Raman CS, Shete SS, Milewicz DM. Mutations in smooth muscle alpha-actin (acta2) lead to thoracic aortic aneurysms and dissections. *Nat Genet.* 2007;39:1488-1493
149. Guo DC, Gong L, Regalado ES, Santos-Cortez RL, Zhao R, Cai B, Veeraghavan S, Prakash SK, Johnson RJ, Muilenburg A, Willing M, Jondeau G, Boileau C, Pannu H, Moran R, Debacker J, Bamshad MJ, Shendure J, Nickerson DA, Leal SM, Raman CS, Swindell EC, Milewicz DM. Mat2a mutations predispose individuals to thoracic aortic aneurysms. *Am J Hum Genet.* 2015;96:170-177

150. Laforest B, Andelfinger G, Nemer M. Loss of gata5 in mice leads to bicuspid aortic valve. *J Clin Invest*. 2011;121:2876-2887
151. Makki N, Capecchi MR. Cardiovascular defects in a mouse model of hoax1 syndrome. *Hum Mol Genet*. 2012;21:26-31
152. Lee TC, Zhao YD, Courtman DW, Stewart DJ. Abnormal aortic valve development in mice lacking endothelial nitric oxide synthase. *Circulation*. 2000;101:2345-2348
153. Du X, Soon JL. Mild to moderate aortic stenosis and coronary bypass surgery. *J. Cardiol*. 2011;57:31-35
154. Wyss K, Yip CY, Mirzaei Z, Jin X, Chen JH, Simmons CA. The elastic properties of valve interstitial cells undergoing pathological differentiation. *J. Biomech*. 2012;45:882-887
155. Carabello BA, Paulus WJ. Aortic stenosis. *Lancet*. 2009;373:956-966
156. Beckmann E, Grau JB, Sainger R, Poggio P, Ferrari G. Insights into the use of biomarkers in calcific aortic valve disease. *J Heart Valve Dis*. 2010;19:441-452
157. Boon NA, Bloomfield P. The medical management of valvular heart disease. *Heart*. 2002;87:395-400
158. Roger VL, Go AS, Lloyd-Jones DM, Adams RJ, Berry JD, Brown TM, Carnethon MR, Dai S, de Simone G, Ford ES, Fox CS, Fullerton HJ, Gillespie C, Greenlund KJ, Hailpern SM, Heit JA, Ho PM, Howard VJ, Kissela BM, Kittner SJ, Lackland DT, Lichtman JH, Lisabeth LD, Makuc DM, Marcus GM, Marelli A, Matchar DB, McDermott MM, Meigs JB, Moy CS, Mozaffarian D, Mussolino ME, Nichol G, Paynter NP, Rosamond WD, Sorlie PD, Stafford RS, Turan TN, Turner MB, Wong ND, Wylie-Rosett J. Heart disease and stroke statistics--2011 update: A report from the American Heart Association. *Circulation*. 2011;123:e18-e209
159. Davies MJ, Treasure T, Parker DJ. Demographic characteristics of patients undergoing aortic valve replacement for stenosis: Relation to valve morphology. *Heart*. 1996;75:174-178
160. Owens DS, Katz R, Takasu J, Kronmal R, Budoff MJ, O'Brien KD. Incidence and progression of aortic valve calcium in the multi-ethnic study of atherosclerosis (MESA). *The American journal of cardiology*. 2010;105:701-708
161. Messika-Zeitoun D, Bielak LF, Peyser PA, Sheedy PF, Turner ST, Nkomo VT, Breen JF, Maalouf J, Scott C, Tajik AJ, Enriquez-Sarano M. Aortic valve calcification: Determinants and progression in the population. *Arterioscler Thromb Vasc Biol*. 2007;27:642-648

162. Patel DK, Green KD, Fudim M, Harrell FE, Wang TJ, Robbins MA. Racial differences in the prevalence of severe aortic stenosis. *J Am Heart Assoc.* 2014;3:e000879
163. Freeman RV, Otto CM. Spectrum of calcific aortic valve disease: Pathogenesis, disease progression, and treatment strategies. *Circulation.* 2005;111:3316-3326
164. Bonow RO, Carabello BA, Chatterjee K, de Leon AC, Jr., Faxon DP, Freed MD, Gaasch WH, Lytle BW, Nishimura RA, O'Gara PT, O'Rourke RA, Otto CM, Shah PM, Shanewise JS. 2008 focused update incorporated into the acc/aha 2006 guidelines for the management of patients with valvular heart disease: A report of the american college of cardiology/american heart association task force on practice guidelines (writing committee to revise the 1998 guidelines for the management of patients with valvular heart disease). Endorsed by the society of cardiovascular anesthesiologists, society for cardiovascular angiography and interventions, and society of thoracic surgeons. *J Am Coll Cardiol.* 2008;52:e1-142
165. Grimard BH, Larson JM. Aortic stenosis: Diagnosis and treatment. *Am Fam Physician.* 2008;78:717-724
166. Balachandran K, Sucusky P, Yoganathan AP. Hemodynamics and mechanobiology of aortic valve inflammation and calcification. *Int J Inflamm.* 2011;2011:263870
167. Bach DS. Echo/doppler evaluation of hemodynamics after aortic valve replacement: Principles of interrogation and evaluation of high gradients. *JACC Cardiovasc Imaging.* 2010;3:296-304
168. Baumgartner H, Hung J, Bermejo J, Chambers JB, Evangelista A, Griffin BP, Iung B, Otto CM, Pellikka PA, Quinones M. Echocardiographic assessment of valve stenosis: Eae/ase recommendations for clinical practice. *Eur J Echocardiogr.* 2009;10:1-25
169. Garcia D, Kadem L. What do you mean by aortic valve area: Geometric orifice area, effective orifice area, or gorlin area? *J Heart Valve Dis.* 2006;15:601-608
170. Bax JJ, Delgado V, Bapat V, Baumgartner H, Collet JP, Erbel R, Hamm C, Kappetein AP, Leipsic J, Leon MB, MacCarthy P, Piazza N, Pibarot P, Roberts WC, Rodes-Cabau J, Serruys PW, Thomas M, Vahanian A, Webb J, Zamorano JL, Windecker S. Open issues in transcatheter aortic valve implantation. Part 1: Patient selection and treatment strategy for transcatheter aortic valve implantation. *European heart journal.* 2014;35:2627-2638
171. Le Ven F, Tizon-Marcos H, Fuchs C, Mathieu P, Pibarot P, Larose E. Valve tissue characterization by magnetic resonance imaging in calcific aortic valve disease. *Can J Cardiol.* 2014;30:1676-1683

172. Bergler-Klein J, Gyongyosi M, Maurer G. The role of biomarkers in valvular heart disease: Focus on natriuretic peptides. *Can J Cardiol.* 2014;30:1027-1034
173. Ferrari G, Sainger R, Beckmann E, Keller G, Yu PJ, Monti MC, Galloway AC, Weiss RL, Vernick W, Grau JB. Validation of plasma biomarkers in degenerative calcific aortic stenosis. *J. Surg. Res.* 2010;163:12-17
174. Capoulade R, Cote N, Mathieu P, Chan KL, Clavel MA, Dumesnil JG, Teo KK, Tam JW, Fournier D, Despres JP, Pibarot P. Circulating levels of matrix gla protein and progression of aortic stenosis: A substudy of the aortic stenosis progression observation: Measuring effects of rosuvastatin (astronomer) trial. *Can J Cardiol.* 2014;30:1088-1095
175. Smith JG, Luk K, Schulz CA, Engert JC, Do R, Hindy G, Rukh G, Dufresne L, Almgren P, Owens DS, Harris TB, Peloso GM, Kerr KF, Wong Q, Smith AV, Budoff MJ, Rotter JJ, Cupples LA, Rich S, Kathiresan S, Orho-Melander M, Gudnason V, O'Donnell CJ, Post WS, Thanassoulis G. Association of low-density lipoprotein cholesterol-related genetic variants with aortic valve calcium and incident aortic stenosis. *JAMA.* 2014;312:1764-1771
176. Cosmi JE, Kort S, Tunick PA, Rosenzweig BP, Freedberg RS, Katz ES, Applebaum RM, Kronzon I. The risk of the development of aortic stenosis in patients with "benign" aortic valve thickening. *Arch Intern Med.* 2002;162:2345-2347
177. Otto CM, Burwash IG, Legget ME, Munt BI, Fujioka M, Healy NL, Kraft CD, Miyake-Hull CY, Schwaegler RG. Prospective study of asymptomatic valvular aortic stenosis. Clinical, echocardiographic, and exercise predictors of outcome. *Circulation.* 1997;95:2262-2270
178. Coffey S, Cox B, Williams MJ. The prevalence, incidence, progression, and risks of aortic valve sclerosis: A systematic review and meta-analysis. *J Am Coll Cardiol.* 2014;63:2852-2861
179. Bonow RO, Greenland P. Population-wide trends in aortic stenosis incidence and outcomes. *Circulation.* 2015
180. Ross J, Jr., Braunwald E. Aortic stenosis. *Circulation.* 1968;38:61-67
181. Thanassoulis G, Massaro JM, Cury R, Manders E, Benjamin EJ, Vasani RS, Cupples LA, Hoffmann U, O'Donnell CJ, Kathiresan S. Associations of long-term and early adult atherosclerosis risk factors with aortic and mitral valve calcium. *J Am Coll Cardiol.* 2010;55:2491-2498
182. Kamstrup PR, Tybjaerg-Hansen A, Nordestgaard BG. Elevated lipoprotein(a) and risk of aortic valve stenosis in the general population. *J Am Coll Cardiol.* 2014;63:470-477



183. Katz R, Budoff MJ, Takasu J, Shavelle DM, Bertoni A, Blumenthal RS, Ouyang P, Wong ND, O'Brien KD. Relationship of metabolic syndrome with incident aortic valve calcium and aortic valve calcium progression: The multi-ethnic study of atherosclerosis (mesa). *Diabetes*. 2009;58:813-819
184. Linefsky JP, O'Brien KD, Katz R, de Boer IH, Barasch E, Jenny NS, Siscovick DS, Kestenbaum B. Association of serum phosphate levels with aortic valve sclerosis and annular calcification: The cardiovascular health study. *J Am Coll Cardiol*. 2011;58:291-297
185. Michelena HI, Desjardins VA, Avierinos JF, Russo A, Nkomo VT, Sundt TM, Pellikka PA, Tajik AJ, Enriquez-Sarano M. Natural history of asymptomatic patients with normally functioning or minimally dysfunctional bicuspid aortic valve in the community. *Circulation*. 2008;117:2776-2784
186. Mathieu P, Boulanger MC. Basic mechanisms of calcific aortic valve disease. *Can J Cardiol*. 2014;30:982-993
187. Braunwald E. Aortic valve replacement: An update at the turn of the millennium. *European heart journal*. 2000;21:1032-1033
188. Bach DS, Cimino N, Deeb GM. Unoperated patients with severe aortic stenosis. *J Am Coll Cardiol*. 2007;50:2018-2019
189. Iung B. Interface between valve disease and ischaemic heart disease. *Heart*. 2000;84:347-352
190. Pibarot P, Dumesnil JG. Prosthetic heart valves: Selection of the optimal prosthesis and long-term management. *Circulation*. 2009;119:1034-1048
191. Bax JJ, Delgado V, Bapat V, Baumgartner H, Collet JP, Erbel R, Hamm C, Kappetein AP, Leipsic J, Leon MB, MacCarthy P, Piazza N, Pibarot P, Roberts WC, Rodes-Cabau J, Serruys PW, Thomas M, Vahanian A, Webb J, Zamorano JL, Windecker S. Open issues in transcatheter aortic valve implantation. Part 2: Procedural issues and outcomes after transcatheter aortic valve implantation. *European heart journal*. 2014;35:2639-2654
192. Kodali SK, Williams MR, Smith CR, Svensson LG, Webb JG, Makkar RR, Fontana GP, Dewey TM, Thourani VH, Pichard AD, Fischbein M, Szeto WY, Lim S, Greason KL, Teirstein PS, Malaisrie SC, Douglas PS, Hahn RT, Whisenant B, Zajarias A, Wang D, Akin JJ, Anderson WN, Leon MB. Two-year outcomes after transcatheter or surgical aortic-valve replacement. *The New England journal of medicine*. 2012;366:1686-1695
193. Makkar RR, Fontana GP, Jilaihawi H, Kapadia S, Pichard AD, Douglas PS, Thourani VH, Babaliaros VC, Webb JG, Herrmann HC, Bavaria JE, Kodali S, Brown DL, Bowers B, Dewey TM, Svensson LG, Tuzcu M, Moses JW, Williams MR, Siegel

- RJ, Akin JJ, Anderson WN, Pocock S, Smith CR, Leon MB. Transcatheter aortic-valve replacement for inoperable severe aortic stenosis. *The New England journal of medicine*. 2012;366:1696-1704
194. Ngo DT, Sverdlov AL, Horowitz JD. Prevention of aortic valve stenosis: A realistic therapeutic target? *Pharmacol Ther*. 2012;135:78-93
195. Liebe V, Brueckmann M, Borggrefe M, Kaden JJ. Statin therapy of calcific aortic stenosis: Hype or hope? *European heart journal*. 2006;27:773-778
196. Bellamy MF, Pellikka PA, Klarich KW, Tajik AJ, Enriquez-Sarano M. Association of cholesterol levels, hydroxymethylglutaryl coenzyme-a reductase inhibitor treatment, and progression of aortic stenosis in the community. *J Am Coll Cardiol*. 2002;40:1723-1730
197. Rajamannan NM, Subramaniam M, Caira F, Stock SR, Spelsberg TC. Atorvastatin inhibits hypercholesterolemia-induced calcification in the aortic valves via the lrp5 receptor pathway. *Circulation*. 2005;112:I229-234
198. Teo KK, Corsi DJ, Tam JW, Dumesnil JG, Chan KL. Lipid lowering on progression of mild to moderate aortic stenosis: Meta-analysis of the randomized placebo-controlled clinical trials on 2344 patients. *Can J Cardiol*. 2011;27:800-808
199. Moura LM, Ramos SF, Zamorano JL, Barros IM, Azevedo LF, Rocha-Goncalves F, Rajamannan NM. Rosuvastatin affecting aortic valve endothelium to slow the progression of aortic stenosis. *J. Am. Coll. Cardiol*. 2007;49:554-561
200. Mohty D, Pibarot P, Despres JP, Cote C, Arsenault B, Cartier A, Cosnay P, Couture C, Mathieu P. Association between plasma ldl particle size, valvular accumulation of oxidized ldl, and inflammation in patients with aortic stenosis. *Arterioscler. Thromb. Vasc. Biol*. 2008;28:187-193
201. Cote N, Mahmut A, Fournier D, Boulanger MC, Couture C, Despres JP, Trahan S, Bosse Y, Page S, Pibarot P, Mathieu P. Angiotensin receptor blockers are associated with reduced fibrosis and interleukin-6 expression in calcific aortic valve disease. *Pathobiology*. 2014;81:15-24
202. Nishimura RA, Otto C. 2014 acc/aha valve guidelines: Earlier intervention for chronic mitral regurgitation. *Heart*. 2014;100:905-907
203. Cowell SJ, Newby DE, Prescott RJ, Bloomfield P, Reid J, Northridge DB, Boon NA. A randomized trial of intensive lipid-lowering therapy in calcific aortic stenosis. *N. Engl. J. Med*. 2005;352:2389-2397
204. Chan KL, Teo K, Dumesnil JG, Ni A, Tam J. Effect of lipid lowering with rosuvastatin on progression of aortic stenosis: Results of the aortic stenosis progression

- observation: Measuring effects of rosuvastatin (astronomer) trial. *Circulation*. 2010;121:306-314
205. Rossebo AB, Pedersen TR, Boman K, Brudi P, Chambers JB, Egstrup K, Gerds E, Gohlke-Barwolf C, Holme I, Kesaniemi YA, Malbecq W, Nienaber CA, Ray S, Skjaerpe T, Wachtell K, Willenheimer R. Intensive lipid lowering with simvastatin and ezetimibe in aortic stenosis. *N. Engl. J. Med.* 2008;359:1343-1356
206. Nagy L, Tontonoz P, Alvarez JG, Chen H, Evans RM. Oxidized ldl regulates macrophage gene expression through ligand activation of ppargamma. *Cell*. 1998;93:229-240
207. Li F, Cai Z, Chen F, Shi X, Zhang Q, Chen S, Shi J, Wang DW, Dong N. Pioglitazone attenuates progression of aortic valve calcification via down-regulating receptor for advanced glycation end products. *Basic Res Cardiol*. 2012;107:306
208. Chu Y, Lund DD, Weiss RM, Brooks RM, Doshi H, Hajj GP, Sigmund CD, Heistad DD. Pioglitazone attenuates valvular calcification induced by hypercholesterolemia. *Arterioscler Thromb Vasc Biol*. 2013;33:523-532
209. Kronenberg F, Utermann G. Lipoprotein(a): Resurrected by genetics. *Journal of internal medicine*. 2013;273:6-30
210. Thanassoulis G, Campbell CY, Owens DS, Smith JG, Smith AV, Peloso GM, Kerr KF, Pechlivanis S, Budoff MJ, Harris TB, Malhotra R, O'Brien KD, Kamstrup PR, Nordestgaard BG, Tybjaerg-Hansen A, Allison MA, Aspelund T, Criqui MH, Heckbert SR, Hwang SJ, Liu Y, Sjogren M, van der Pals J, Kalsch H, Muhleisen TW, Nothen MM, Cupples LA, Caslake M, Di Angelantonio E, Danesh J, Rotter JI, Sigurdsson S, Wong Q, Erbel R, Kathiresan S, Melander O, Gudnason V, O'Donnell CJ, Post WS. Genetic associations with valvular calcification and aortic stenosis. *N. Engl. J. Med.* 2013;368:503-512
211. Arsenault BJ, Boekholdt SM, Dube MP, Rheume E, Wareham NJ, Khaw KT, Sandhu MS, Tardif JC. Lipoprotein(a) levels, genotype, and incident aortic valve stenosis: A prospective mendelian randomization study and replication in a case-control cohort. *Circ. Cardiovasc. Genet*. 2014;7:304-310
212. Helmbold AF, Slim JN, Morgan J, Castillo-Rojas LM, Shry EA, Slim AM. The effects of extended release niacin in combination with omega 3 fatty acid supplements in the treatment of elevated lipoprotein (a). *Cholesterol*. 2010;2010:306147
213. Mahmut A, Boulanger MC, El Hussein D, Fournier D, Bouchareb R, Despres JP, Pibarot P, Bosse Y, Mathieu P. Elevated expression of lipoprotein-associated phospholipase a2 in calcific aortic valve disease: Implications for valve mineralization. *J Am Coll Cardiol*. 2014;63:460-469

214. Hung MY, Witztum JL, Tsimikas S. New therapeutic targets for calcific aortic valve stenosis: The lipoprotein(a)-lipoprotein-associated phospholipase a<sub>2</sub>-oxidized phospholipid axis. *J Am Coll Cardiol*. 2014;63:478-480
215. Capoulade R, Clavel MA, Mathieu P, Cote N, Dumesnil JG, Arsenault M, Bedard E, Pibarot P. Impact of hypertension and renin-angiotensin system inhibitors in aortic stenosis. *Eur J Clin Invest*. 2013;43:1262-1272
216. Fontana V, Luizon MR, Sandrim VC. An update on the pharmacogenetics of treating hypertension. *J Hum Hypertens*. 2014
217. Cote N, Pibarot P, Pepin A, Fournier D, Audet A, Arsenault B, Couture C, Poirier P, Despres JP, Mathieu P. Oxidized low-density lipoprotein, angiotensin ii and increased waist circumference are associated with valve inflammation in prehypertensive patients with aortic stenosis. *Int J Cardiol*. 2010;145:444-449
218. Salas MJ, Santana O, Escolar E, Lamas GA. Medical therapy for calcific aortic stenosis. *J Cardiovasc Pharmacol Ther*. 2012;17:133-138
219. Cote N, Couture C, Pibarot P, Despres JP, Mathieu P. Angiotensin receptor blockers are associated with a lower remodelling score of stenotic aortic valves. *Eur J Clin Invest*. 2011;41:1172-1179
220. Urata H, Boehm KD, Philip A, Kinoshita A, Gabrovsek J, Bumpus FM, Husain A. Cellular localization and regional distribution of an angiotensin ii-forming chymase in the heart. *J Clin Invest*. 1993;91:1269-1281
221. Mohler ER, 3rd, Gannon F, Reynolds C, Zimmerman R, Keane MG, Kaplan FS. Bone formation and inflammation in cardiac valves. *Circulation*. 2001;103:1522-1528
222. Skolnick AH, Osranek M, Formica P, Kronzon I. Osteoporosis treatment and progression of aortic stenosis. *The American journal of cardiology*. 2009;104:122-124
223. Innasimuthu AL, Katz WE. Effect of bisphosphonates on the progression of degenerative aortic stenosis. *Echocardiography*. 2011;28:1-7
224. Yip CY, Simmons CA. The aortic valve microenvironment and its role in calcific aortic valve disease. *Cardiovasc Pathol*. 2011;20:177-182
225. Kaden JJ, Bickelhaupt S, Grobholz R, Haase KK, Sarikoc A, Kilic R, Brueckmann M, Lang S, Zahn I, Vahl C, Hagl S, Dempfle CE, Borggrefe M. Receptor activator of nuclear factor kappa b ligand and osteoprotegerin regulate aortic valve calcification. *J Mol Cell Cardiol*. 2004;36:57-66
226. Collin-Osdoby P, Rothe L, Anderson F, Nelson M, Maloney W, Osdoby P. Receptor activator of nf-kappa b and osteoprotegerin expression by human microvascular endothelial cells, regulation by inflammatory cytokines, and role in human osteoclastogenesis. *The Journal of biological chemistry*. 2001;276:20659-20672

227. Kaden JJ, Dempfle CE, Kilic R, Sarikoc A, Hagl S, Lang S, Brueckmann M, Borggreffe M. Influence of receptor activator of nuclear factor kappa b on human aortic valve myofibroblasts. *Exp Mol Pathol*. 2005;78:36-40
228. Le Gal G, Bertault V, Bezon E, Cornily JC, Barra JA, Blanc JJ. Heterogeneous geographic distribution of patients with aortic valve stenosis: Arguments for new aetiological hypothesis. *Heart*. 2005;91:247-249
229. Otto CM, Kuusisto J, Reichenbach DD, Gown AM, O'Brien KD. Characterization of the early lesion of 'degenerative' valvular aortic stenosis. Histological and immunohistochemical studies. *Circulation*. 1994;90:844-853
230. Akat K, Borggreffe M, Kaden JJ. Aortic valve calcification: Basic science to clinical practice. *Heart*. 2009;95:616-623
231. Bosse Y, Miqdad A, Fournier D, Pepin A, Pibarot P, Mathieu P. Refining molecular pathways leading to calcific aortic valve stenosis by studying gene expression profile of normal and calcified stenotic human aortic valves. *Circ Cardiovasc Genet*. 2009;2:489-498
232. Yutzey KE, Demer LL, Body SC, Huggins GS, Towler DA, Giachelli CM, Hofmann-Bowman MA, Mortlock DP, Rogers MB, Sadeghi MM, Aikawa E. Calcific aortic valve disease: A consensus summary from the alliance of investigators on calcific aortic valve disease. *Arterioscler Thromb Vasc Biol*. 2014;34:2387-2393
233. Bouchareb R, Boulanger MC, Fournier D, Pibarot P, Messaddeq Y, Mathieu P. Mechanical strain induces the production of spheroid mineralized microparticles in the aortic valve through a rhoa/rock-dependent mechanism. *J Mol Cell Cardiol*. 2014;67:49-59
234. Holliday CJ, Ankeny RF, Jo H, Nerem RM. Discovery of shear- and side-specific mrnas and mirnas in human aortic valvular endothelial cells. *Am J Physiol Heart Circ Physiol*. 2011;301:H856-867
235. Drolet MC, Roussel E, Deshaies Y, Couet J, Arsenault M. A high fat/high carbohydrate diet induces aortic valve disease in c57bl/6j mice. *J Am Coll Cardiol*. 2006;47:850-855
236. Tanaka K, Sata M, Fukuda D, Suematsu Y, Motomura N, Takamoto S, Hirata Y, Nagai R. Age-associated aortic stenosis in apolipoprotein e-deficient mice. *J Am Coll Cardiol*. 2005;46:134-141
237. Ngo DT, Stafford I, Kelly DJ, Sverdlov AL, Wuttke RD, Weedon H, Nightingale AK, Rosenkranz AC, Smith MD, Chirkov YY, Kennedy JA, Horowitz JD. Vitamin d(2) supplementation induces the development of aortic stenosis in rabbits: Interactions with

endothelial function and thioredoxin-interacting protein. *Eur J Pharmacol.* 2008;590:290-296

238. Mathieu P, Pibarot P, Larose E, Poirier P, Marette A, Despres JP. Visceral obesity and the heart. *The international journal of biochemistry & cell biology.* 2008;40:821-836
239. Audet A, Cote N, Couture C, Bosse Y, Despres JP, Pibarot P, Mathieu P. Amyloid substance within stenotic aortic valves promotes mineralization. *Histopathology.* 2012;61:610-619
240. Miller JD, Chu Y, Brooks RM, Richenbacher WE, Pena-Silva R, Heistad DD. Dysregulation of antioxidant mechanisms contributes to increased oxidative stress in calcific aortic valvular stenosis in humans. *J Am Coll Cardiol.* 2008;52:843-850
241. Cote C, Pibarot P, Despres JP, Mohty D, Cartier A, Arsenault BJ, Couture C, Mathieu P. Association between circulating oxidised low-density lipoprotein and fibrocalcific remodelling of the aortic valve in aortic stenosis. *Heart.* 2008;94:1175-1180
242. Derbali H, Bosse Y, Cote N, Pibarot P, Audet A, Pepin A, Arsenault B, Couture C, Despres JP, Mathieu P. Increased biglycan in aortic valve stenosis leads to the overexpression of phospholipid transfer protein via toll-like receptor 2. *Am J Pathol.* 2010;176:2638-2645
243. El Husseini D, Boulanger MC, Mahmut A, Bouchareb R, Laflamme MH, Fournier D, Pibarot P, Bosse Y, Mathieu P. P2y2 receptor represses il-6 expression by valve interstitial cells through akt: Implication for calcific aortic valve disease. *J Mol Cell Cardiol.* 2014;72:146-156
244. Osman N, Grande-Allen KJ, Ballinger ML, Getachew R, Marasco S, O'Brien KD, Little PJ. Smad2-dependent glycosaminoglycan elongation in aortic valve interstitial cells enhances binding of ldl to proteoglycans. *Cardiovasc Pathol.* 2013;22:146-155
245. Le Quang K, Bouchareb R, Lachance D, Laplante MA, El Husseini D, Boulanger MC, Fournier D, Fang XP, Avramoglu RK, Pibarot P, Deshaies Y, Sweeney G, Mathieu P, Marette A. Early development of calcific aortic valve disease and left ventricular hypertrophy in a mouse model of combined dyslipidemia and type 2 diabetes mellitus. *Arterioscler Thromb Vasc Biol.* 2014;34:2283-2291
246. Cote N, Mahmut A, Bosse Y, Couture C, Page S, Trahan S, Boulanger MC, Fournier D, Pibarot P, Mathieu P. Inflammation is associated with the remodeling of calcific aortic valve disease. *Inflammation.* 2013;36:573-581
247. Kaden JJ, Dempfle CE, Grobholz R, Tran HT, Kilic R, Sarikoc A, Brueckmann M, Vahl C, Hagl S, Haase KK, Borggreffe M. Interleukin-1 beta promotes matrix

- metalloproteinase expression and cell proliferation in calcific aortic valve stenosis. *Atherosclerosis*. 2003;170:205-211
248. Charest A, Pepin A, Shetty R, Cote C, Voisine P, Dagenais F, Pibarot P, Mathieu P. Distribution of sparc during neovascularisation of degenerative aortic stenosis. *Heart*. 2006;92:1844-1849
249. Soini Y, Satta J, Maatta M, Autio-Harminen H. Expression of mmp2, mmp9, mt1-mmp, timp1, and timp2 mrna in valvular lesions of the heart. *J Pathol*. 2001;194:225-231
250. Chalajour F, Treede H, Gehling UM, Ebrahimnejad A, Boehm DH, Riemer RK, Ergun S, Reichenspurner H. Identification and characterization of cells with high angiogenic potential and transitional phenotype in calcific aortic valve. *Exp Cell Res*. 2007;313:2326-2335
251. Weiss RM, Ohashi M, Miller JD, Young SG, Heistad DD. Calcific aortic valve stenosis in old hypercholesterolemic mice. *Circulation*. 2006;114:2065-2069
252. Aikawa E, Nahrendorf M, Sosnovik D, Lok VM, Jaffer FA, Aikawa M, Weissleder R. Multimodality molecular imaging identifies proteolytic and osteogenic activities in early aortic valve disease. *Circulation*. 2007;115:377-386
253. Yang X, Meng X, Su X, Mauchley DC, Ao L, Cleveland JC, Jr., Fullerton DA. Bone morphogenic protein 2 induces runx2 and osteopontin expression in human aortic valve interstitial cells: Role of smad1 and extracellular signal-regulated kinase 1/2. *J Thorac Cardiovasc Surg*. 2009;138:1008-1015
254. Nigam V, Srivastava D. Notch1 represses osteogenic pathways in aortic valve cells. *J Mol Cell Cardiol*. 2009;47:828-834
255. Acharya A, Hans CP, Koenig SN, Nichols HA, Galindo CL, Garner HR, Merrill WH, Hinton RB, Garg V. Inhibitory role of notch1 in calcific aortic valve disease. *PLoS One*. 2011;6:e27743
256. Miller JD, Weiss RM, Serrano KM, Castaneda LE, Brooks RM, Zimmerman K, Heistad DD. Evidence for active regulation of pro-osteogenic signaling in advanced aortic valve disease. *Arterioscler Thromb Vasc Biol*. 2010;30:2482-2486
257. Rajamannan NM. The role of lrp5/6 in cardiac valve disease: Experimental hypercholesterolemia in the apoe<sup>-/-</sup>/lrp5<sup>-/-</sup> mice. *J Cell Biochem*. 2011;112:2987-2991
258. Hartmann C. A wnt canon orchestrating osteoblastogenesis. *Trends Cell Biol*. 2006;16:151-158
259. Chen JH, Chen WL, Sider KL, Yip CY, Simmons CA. Beta-catenin mediates mechanically regulated, transforming growth factor-beta1-induced myofibroblast

differentiation of aortic valve interstitial cells. *Arterioscler Thromb Vasc Biol.* 2011;31:590-597

260. Liu AC, Gotlieb AI. Transforming growth factor-beta regulates in vitro heart valve repair by activated valve interstitial cells. *Am J Pathol.* 2008;173:1275-1285
261. Cote N, El Husseini D, Pepin A, Guauque-Olarte S, Ducharme V, Bouchard-Cannon P, Audet A, Fournier D, Gaudreault N, Derbali H, McKee MD, Simard C, Despres JP, Pibarot P, Bosse Y, Mathieu P. Atp acts as a survival signal and prevents the mineralization of aortic valve. *J. Mol. Cell. Cardiol.* 2012;52:1191-1202
262. Galeone A, Brunetti G, Oranger A, Greco G, Di Benedetto A, Mori G, Colucci S, Zallone A, Paparella D, Grano M. Aortic valvular interstitial cells apoptosis and calcification are mediated by tnf-related apoptosis-inducing ligand. *Int J Cardiol.* 2013;169:296-304
263. Thum T, Condorelli G. Long noncoding rnas and micrnas in cardiovascular pathophysiology. *Circ Res.* 2015;116:751-762
264. Zhang M, Liu X, Zhang X, Song Z, Han L, He Y, Xu Z. Microrna-30b is a multifunctional regulator of aortic valve interstitial cells. *J Thorac Cardiovasc Surg.* 2014;147:1073-1080 e1072
265. Lagendijk AK, Goumans MJ, Burkhard SB, Bakkers J. Microrna-23 restricts cardiac valve formation by inhibiting has2 and extracellular hyaluronic acid production. *Circ Res.* 2011;109:649-657
266. Vacchi-Suzzi C, Hahne F, Scheubel P, Marcellin M, Dubost V, Westphal M, Boeglen C, Buchmann-Moller S, Cheung MS, Cordier A, De Benedetto C, Deurinck M, Frei M, Moulin P, Oakeley E, Grenet O, Grevot A, Stull R, Theil D, Moggs JG, Marrer E, Couttet P. Heart structure-specific transcriptomic atlas reveals conserved microrna-mrna interactions. *PLoS One.* 2013;8:e52442
267. Yanagawa B, Lovren F, Pan Y, Garg V, Quan A, Tang G, Singh KK, Shukla PC, Kalra NP, Peterson MD, Verma S. Mirna-141 is a novel regulator of bmp-2-mediated calcification in aortic stenosis. *J Thorac Cardiovasc Surg.* 2012;144:256-262
268. Carrion K, Dyo J, Patel V, Sasik R, Mohamed SA, Hardiman G, Nigam V. The long non-coding hotair is modulated by cyclic stretch and wnt/beta-catenin in human aortic valve cells and is a novel repressor of calcification genes. *PLoS One.* 2014;9:e96577
269. Sider KL, Blaser MC, Simmons CA. Animal models of calcific aortic valve disease. *Int J Inflam.* 2011;2011:364310
270. Weiss RM, Miller JD, Heistad DD. Fibrocalcific aortic valve disease: Opportunity to understand disease mechanisms using mouse models. *Circ Res.* 2013;113:209-222



271. Yin W, Carballo-Jane E, McLaren DG, Mendoza VH, Gagen K, Geoghagen NS, McNamara LA, Gorski JN, Eiermann GJ, Petrov A, Wolff M, Tong X, Wilsie LC, Akiyama TE, Chen J, Thankappan A, Xue J, Ping X, Andrews G, Wickham LA, Gai CL, Trinh T, Kulick AA, Donnelly MJ, Voronin GO, Rosa R, Cumiskey AM, Bekkari K, Mitnaul LJ, Puig O, Chen F, Raubertas R, Wong PH, Hansen BC, Koblan KS, Roddy TP, Hubbard BK, Strack AM. Plasma lipid profiling across species for the identification of optimal animal models of human dyslipidemia. *J Lipid Res.* 2012;53:51-65
272. Veniant MM, Withycombe S, Young SG. Lipoprotein size and atherosclerosis susceptibility in apoe(-/-) and ldlr(-/-) mice. *Arterioscler Thromb Vasc Biol.* 2001;21:1567-1570
273. Chen B, Bronson RT, Klaman LD, Hampton TG, Wang JF, Green PJ, Magnuson T, Douglas PS, Morgan JP, Neel BG. Mice mutant for egfr and shp2 have defective cardiac semilunar valvulogenesis. *Nat Genet.* 2000;24:296-299
274. Barrick CJ, Roberts RB, Rojas M, Rajamannan NM, Suitt CB, O'Brien KD, Smyth SS, Threadgill DW. Reduced egfr causes abnormal valvular differentiation leading to calcific aortic stenosis and left ventricular hypertrophy in c57bl/6j but not 129s1/svimj mice. *Am J Physiol Heart Circ Physiol.* 2009;297:H65-75
275. Atochin DN, Huang PL. Endothelial nitric oxide synthase transgenic models of endothelial dysfunction. *Pflugers Arch.* 2010;460:965-974
276. Nus M, MacGrogan D, Martinez-Poveda B, Benito Y, Casanova JC, Fernandez-Aviles F, Bermejo J, de la Pompa JL. Diet-induced aortic valve disease in mice haploinsufficient for the notch pathway effector rbpjk/csl. *Arterioscler. Thromb. Vasc. Biol.* 2011;31:1580-1588
277. Tkatchenko TV, Moreno-Rodriguez RA, Conway SJ, Molkentin JD, Markwald RR, Tkatchenko AV. Lack of periostin leads to suppression of notch1 signaling and calcific aortic valve disease. *Physiol Genomics.* 2009;39:160-168
278. Hakuno D, Kimura N, Yoshioka M, Mukai M, Kimura T, Okada Y, Yozu R, Shukunami C, Hiraki Y, Kudo A, Ogawa S, Fukuda K. Periostin advances atherosclerotic and rheumatic cardiac valve degeneration by inducing angiogenesis and mmp production in humans and rodents. *J Clin Invest.* 2010;120:2292-2306
279. Luo G, Ducky P, McKee MD, Pinero GJ, Loyer E, Behringer RR, Karsenty G. Spontaneous calcification of arteries and cartilage in mice lacking matrix gla protein. *Nature.* 1997;386:78-81
280. Yukata K, Matsui Y, Shukunami C, Takimoto A, Goto T, Nishizaki Y, Nakamichi Y, Kubo T, Sano T, Kato S, Hiraki Y, Yasui N. Altered fracture callus formation in chondromodulin-i deficient mice. *Bone.* 2008;43:1047-1056

281. Yoshioka M, Yuasa S, Matsumura K, Kimura K, Shiomi T, Kimura N, Shukunami C, Okada Y, Mukai M, Shin H, Yozu R, Sata M, Ogawa S, Hiraki Y, Fukuda K. Chondromodulin-i maintains cardiac valvular function by preventing angiogenesis. *Nat Med.* 2006;12:1151-1159
282. Cuniberti LA, Stutzbach PG, Guevara E, Yannarelli GG, Laguens RP, Favaloro RR. Development of mild aortic valve stenosis in a rabbit model of hypertension. *J Am Coll Cardiol.* 2006;47:2303-2309
283. Shiomi M, Koike T, Ito T. Contribution of the whhl rabbit, an animal model of familial hypercholesterolemia, to elucidation of the anti-atherosclerotic effects of statins. *Atherosclerosis.* 2013;231:39-47
284. Guerraty MA, Grant GR, Karanian JW, Chiesa OA, Pritchard WF, Davies PF. Hypercholesterolemia induces side-specific phenotypic changes and peroxisome proliferator-activated receptor-gamma pathway activation in swine aortic valve endothelium. *Arterioscler Thromb Vasc Biol.* 2010;30:225-231
285. Simmons CA, Grant GR, Manduchi E, Davies PF. Spatial heterogeneity of endothelial phenotypes correlates with side-specific vulnerability to calcification in normal porcine aortic valves. *Circ Res.* 2005;96:792-799
286. Bosse Y, Mathieu P, Pibarot P. Genomics: The next step to elucidate the etiology of calcific aortic valve stenosis. *J. Am. Coll. Cardiol.* 2008;51:1327-1336
287. O'Brien KD. Epidemiology and genetics of calcific aortic valve disease. *J. Investig. Med.* 2007;55:284-291
288. Knez I, Renner W, Maier R, Rehak P, Rienmuller R, Pils M, Stanger O, Mircic A, Dacar D, Szalay Z, Martinovic I, Vogt PR, Rigler B. Angiotensin-converting enzyme polymorphisms and their potential impact on left ventricular myocardial geometry after aortic valve surgery. *J. Heart Valve Dis.* 2003;12:687-695
289. Ortlepp JR, Hoffmann R, Ohme F, Lauscher J, Bleckmann F, Hanrath P. The vitamin d receptor genotype predisposes to the development of calcific aortic valve stenosis. *Heart.* 2001;85:635-638
290. Novaro GM, Sachar R, Pearce GL, Sprecher DL, Griffin BP. Association between apolipoprotein e alleles and calcific valvular heart disease. *Circulation.* 2003;108:1804-1808
291. Nordstrom P, Glader CA, Dahlen G, Birgander LS, Lorentzon R, Waldenstrom A, Lorentzon M. Oestrogen receptor alpha gene polymorphism is related to aortic valve sclerosis in postmenopausal women. *J. Intern. Med.* 2003;254:140-146
292. Ortlepp JR, Schmitz F, Mevissen V, Weiss S, Huster J, Dronskowski R, Langebartels G, Autschbach R, Zerres K, Weber C, Hanrath P, Hoffmann R. The

- amount of calcium-deficient hexagonal hydroxyapatite in aortic valves is influenced by gender and associated with genetic polymorphisms in patients with severe calcific aortic stenosis. *Eur. Heart J.* 2004;25:514-522
293. Schmitz F, Ewering S, Zerres K, Klomfass S, Hoffmann R, Ortlepp JR. Parathyroid hormone gene variant and calcific aortic stenosis. *J. Heart Valve Dis.* 2009;18:262-267
294. Turkmen F, Ozdemir A, Sevinc C, Eren PA, Demiral S. Calcium-sensing receptor gene polymorphisms and cardiac valvular calcification in patients with chronic renal failure: A pilot study. *Hemodial Int.* 2009;13:176-180
295. Gaudreault N, Ducharme V, Lamontagne M, Guauque-Olarte S, Mathieu P, Pibarot P, Bosse Y. Replication of genetic association studies in aortic stenosis in adults. *The American journal of cardiology.* 2011;108:1305-1310
296. Moura LM, Faria S, Brito M, Pinto FJ, Kristensen SD, Barros IM, Rajamannan N, Rocha-Goncalves F. Relationship of pon1 192 and 55 gene polymorphisms to calcific valvular aortic stenosis. *Am J Cardiovasc Dis.* 2012;2:123-132
297. Ellis SG, Dushman-Ellis S, Luke MM, Murugesan G, Kottke-Marchant K, Ellis GM, Griffin B, Tuzcu EM, Hazen S. Pilot candidate gene analysis of patients  $\geq 60$  years old with aortic stenosis involving a tricuspid aortic valve. *The American journal of cardiology.* 2012;110:88-92
298. Arsenault BJ, Dube MP, Brodeur MR, de Oliveira Moraes AB, Lavoie V, Kernaleguen AE, Guauque-Olarte S, Mathieu P, Pibarot P, Messika-Zeitoun D, Bosse Y, Rhoads D, Rheume E, Tardif JC. Evaluation of links between high-density lipoprotein genetics, functionality, and aortic valve stenosis risk in humans. *Arterioscler Thromb Vasc Biol.* 2014;34:457-462
299. McCoy CM, Nicholas DQ, Masters KS. Sex-related differences in gene expression by porcine aortic valvular interstitial cells. *PLoS One.* 2012;7:e39980
300. Nigam V, Sievers HH, Jensen BC, Sier HA, Simpson PC, Srivastava D, Mohamed SA. Altered micrnas in bicuspid aortic valve: A comparison between stenotic and insufficient valves. *J Heart Valve Dis.* 2010;19:459-465
301. Patel V, Carrion K, Hollands A, Hinton A, Gallegos T, Dyo J, Sasik R, Leire E, Hardiman G, Mohamed SA, Nigam S, King CC, Nizet V, Nigam V. The stretch responsive microrna mir-148a-3p is a novel repressor of ikkbb, nf-kappab signaling, and inflammatory gene expression in human aortic valve cells. *FASEB journal : official publication of the Federation of American Societies for Experimental Biology.* 2015;29:1859-1868

302. Martin-Rojas T, Gil-Dones F, Lopez-Almodovar LF, Padial LR, Vivanco F, Barderas MG. Proteomic profile of human aortic stenosis: Insights into the degenerative process. *J Proteome Res.* 2012;11:1537-1550
303. Alvarez-Llamas G, Martin-Rojas T, de la Cuesta F, Calvo E, Gil-Dones F, Darde VM, Lopez-Almodovar LF, Padial LR, Lopez JA, Vivanco F, Barderas MG. Modification of the secretion pattern of proteases, inflammatory mediators, and extracellular matrix proteins by human aortic valve is key in severe aortic stenosis. *Mol Cell Proteomics.* 2013;12:2426-2439
304. Gil-Dones F, Darde VM, Alonso-Orgaz S, Lopez-Almodovar LF, Mourino-Alvarez L, Padial LR, Vivanco F, Barderas MG. Inside human aortic stenosis: A proteomic analysis of plasma. *J Proteomics.* 2012;75:1639-1653
305. Bertacco E, Million R, Arrigoni G, Faggini E, Iop L, Puato M, Pinna LA, Tessari P, Pauletto P, Rattazzi M. Proteomic analysis of clonal interstitial aortic valve cells acquiring a pro-calcific profile. *J Proteome Res.* 2010;9:5913-5921
306. Matsumoto K, Satoh K, Maniwa T, Araki A, Maruyama R, Oda T. Noticeable decreased expression of tenascin-x in calcific aortic valves. *Connect Tissue Res.* 2012;53:460-468
307. Hennessey JA, Boczek NJ, Jiang YH, Miller JD, Patrick W, Pfeiffer R, Sutphin BS, Tester DJ, Barajas-Martinez H, Ackerman MJ, Antzelevitch C, Kanter R, Pitt GS. A cacna1c variant associated with reduced voltage-dependent inactivation, increased cav1.2 channel window current, and arrhythmogenesis. *PLoS One.* 2014;9:e106982
308. Johnson AD, Newton-Cheh C, Chasman DI, Ehret GB, Johnson T, Rose L, Rice K, Verwoert GC, Launer LJ, Gudnason V, Larson MG, Chakravarti A, Psaty BM, Caulfield M, van Duijn CM, Ridker PM, Munroe PB, Levy D. Association of hypertension drug target genes with blood pressure and hypertension in 86,588 individuals. *Hypertension.* 2011;57:903-910
309. Wang W, Pang L, Palade P. Angiotensin ii upregulates ca(v)1.2 protein expression in cultured arteries via endothelial h(2)o(2) production. *J. Vasc. Res.* 2011;48:67-78
310. Montezano AC, Burger D, Paravicini TM, Chignalia AZ, Yusuf H, Almasri M, He Y, Callera GE, He G, Krause KH, Lambeth D, Quinn MT, Touyz RM. Nicotinamide adenine dinucleotide phosphate reduced oxidase 5 (nox5) regulation by angiotensin ii and endothelin-1 is mediated via calcium/calmodulin-dependent, rac-1-independent pathways in human endothelial cells. *Circ Res.* 2010;106:1363-1373
311. Das R, Burke T, Van Wagoner DR, Plow EF. L-type calcium channel blockers exert an antiinflammatory effect by suppressing expression of plasminogen receptors on macrophages. *Circ. Res.* 2009;105:167-175

312. Towler DA. Molecular and cellular aspects of calcific aortic valve disease. *Circ. Res.* 2013;113:198-208
313. Nagy E, Eriksson P, Yousry M, Caidahl K, Ingelsson E, Hansson GK, Franco-Cereceda A, Back M. Valvular osteoclasts in calcification and aortic valve stenosis severity. *Int J Cardiol.* 2013;168:2264-2271
314. Manolio TA. Bringing genome-wide association findings into clinical use. *Nat Rev Genet.* 2013;14:549-558
315. Eggenschwiler J, Ludwig T, Fisher P, Leighton PA, Tilghman SM, Efstratiadis A. Mouse mutant embryos overexpressing igf-ii exhibit phenotypic features of the beckwith-wiedemann and simpson-golabi-behmel syndromes. *Genes Dev.* 1997;11:3128-3142
316. Wang G, Lunardi A, Zhang J, Chen Z, Ala U, Webster KA, Tay Y, Gonzalez-Billalabeitia E, Egia A, Shaffer DR, Carver B, Liu XS, Tauli R, Kuo WP, Nardella C, Signoretti S, Cordon-Cardo C, Gerald WL, Pandolfi PP. *Zbtb7a* suppresses prostate cancer through repression of a sox9-dependent pathway for cellular senescence bypass and tumor invasion. *Nat Genet.* 2013;45:739-746
317. Cohen J, Blethen S, Kuntze J, Smith SL, Lomax KG, Mathew PM. Managing the child with severe primary insulin-like growth factor-1 deficiency (igfd): Igfd diagnosis and management. *Drugs in R&D.* 2014;14:25-29
318. Colhoun HM, McKeigue PM, Davey Smith G. Problems of reporting genetic associations with complex outcomes. *Lancet.* 2003;361:865-872
319. Michelena HI, Prakash SK, Della Corte A, Bissell MM, Anavekar N, Mathieu P, Bosse Y, Limongelli G, Bossone E, Benson DW, Lancellotti P, Isselbacher EM, Enriquez-Sarano M, Sundt TM, 3rd, Pibarot P, Evangelista A, Milewicz DM, Body SC. Bicuspid aortic valve: Identifying knowledge gaps and rising to the challenge from the international bicuspid aortic valve consortium (bavcon). *Circulation.* 2014;129:2691-2704
320. Prakash SK, Bosse Y, Muehlschlegel JD, Michelena HI, Limongelli G, Della Corte A, Pluchinotta FR, Russo MG, Evangelista A, Benson DW, Body SC, Milewicz DM. A roadmap to investigate the genetic basis of bicuspid aortic valve and its complications: Insights from the international bavcon (bicuspid aortic valve consortium). *J Am Coll Cardiol.* 2014;64:832-839